



University
of Glasgow

<https://theses.gla.ac.uk/>

Theses Digitisation:

<https://www.gla.ac.uk/myglasgow/research/enlighten/theses/digitisation/>

This is a digitised version of the original print thesis.

Copyright and moral rights for this work are retained by the author

A copy can be downloaded for personal non-commercial research or study,
without prior permission or charge

This work cannot be reproduced or quoted extensively from without first
obtaining permission in writing from the author

The content must not be changed in any way or sold commercially in any
format or medium without the formal permission of the author

When referring to this work, full bibliographic details including the author,
title, awarding institution and date of the thesis must be given

Enlighten: Theses

<https://theses.gla.ac.uk/>
research-enlighten@glasgow.ac.uk

The Response Spectral Density of a Nonlinear
System Under Broad Band Random Excitation.
A Numerical Simulation Approach.

Thesis presented for the degree of Doctor of
Philosophy in Mechanical Engineering of the
University of Glasgow.

Elias Michael A. Thaniotis B.Sc. (Eng)
Department of Mechanical Engineering.

September, 1982.

ProQuest Number: 10644232

All rights reserved

INFORMATION TO ALL USERS

The quality of this reproduction is dependent upon the quality of the copy submitted.

In the unlikely event that the author did not send a complete manuscript and there are missing pages, these will be noted. Also, if material had to be removed, a note will indicate the deletion.



ProQuest 10644232

Published by ProQuest LLC (2017). Copyright of the Dissertation is held by the Author.

All rights reserved.

This work is protected against unauthorized copying under Title 17, United States Code
Microform Edition © ProQuest LLC.

ProQuest LLC.
789 East Eisenhower Parkway
P.O. Box 1346
Ann Arbor, MI 48106 – 1346

C O N T E N T S

Summary

Chapter 1 Introduction.

Chapter 2 Analytical Prediction of Response Characteristics
for the Duffing System Under Random Excitation.

2.1 Response to White Noise Excitation. The
Fokker - Planck Equation.

2.2 Equivalent Linearization Technique.

2.3 Discussion.

Chapter 3 Numerical Simulation.

Introduction.

3.1 The Numerical Integration of the Duffing
Equation.

3.2 Spectrum of Excitation.

3.3 Testing the Numerical Simulation for Random
Excitation.

Chapter 4 The Non-Dimensional Form of the Duffing System.

Introduction.

4.1 The Deterministic System.

4.2 The Duffing System Under Broad Band
Excitation.

4.3 Discussion.

Chapter 5 Response Spectral Densities of the Duffing System
Under Broad Band Random Excitation.

Introduction

5.1 Spectra of Excitation. Broad Band Excitation
As An Approximation to White Noise.

5.2 Stationarity of Response. The Autocorrelation
Function.

- 5.3 Observations on the Response Spectra of the
Duffing System Under Broad Band Excitation.
- 5.4 Connection with Existing Theory.
- 5.5 Graphical Representation.

Chapter 6 Effects of Different Forms of Excitation Spectra.

Introduction

- 6.1 Response Spectra Under Band Limited
Excitation.
- 6.2 Response Spectra Under High Pass Excitation.
- 6.3 Discussion.

Chapter 7 Discussion.

REFERENCES

APPENDIX A

- A.1 The Duffing System Under Sinusoidal Excitation.
- A.2 Approximate Solutions Involving Third Harmonics
for the Duffing System Under Sinusoidal Excitation
- A.3 The Duffing System Under Modulated sinusoidal
Excitation.

APPENDIX B

- B.1 Notes on the Equivalent Linearization Technique.
- B.2 Perturbation Analysis.
- B.3 The Heuristic Approach.

APPENDIX C

- C.1 Theory of Numerical Integration Methods.
- C.2 Excitation.
- C.3 Generation of the Excitation Signal.
- C.4 Listings of the Simulation Programs.

ACKNOWLEDGEMENTS

This thesis reports on work carried out at Glasgow University during the academic years 1979 - 1982 in the Department of Mechanical Engineering.

The author gratefully acknowledges the help and encouragement given to him by Professor J.D.Robson, Dr. D.B.McVean and Dr. J.A.Fitzpatric.

The research was financed by a Glasgow University grant, to whom the author is indebted.

SUMMARY

The object of this study is to obtain the response spectra of the Duffing system excited by a Gaussian broad band random process, through the use of numerical simulations and to identify behavioural patterns of these spectra. The task was greatly simplified by the use of dimensional analysis. In Chapter 4 this method is applied to the Duffing system.

The products of this non-dimensionalisation of the system under Gaussian broad band random excitation are the non dimensional quantities $k^1 S_x(\omega)/S_i$, $\beta S_x(\omega)\sqrt{(k/m)}$, $\beta S_i/\sqrt{mk^3}$, $\beta \sigma_x^2$, $c/2\sqrt{km}$ (the first three were symbolized by the capital Greek letters A, B, Γ and ζ for $c/2 km$) where S_i is the excitation spectrum intensity, $S_x(\omega)$ the displacement response spectrum and σ_x^2 the response displacement variance. Of these quantities only two are sufficient to describe the system completely under the aforementioned excitation namely Γ and ζ . Simple examination of the above quantities revealed the possibility of direct relation of the quantities Γ/ζ and $\beta \sigma_x^2$. A parabolic relation was proved using the equivalent linearization technique and was verified by the findings of the simulation technique and the probabilistic information derived through the solution of the appropriate Fokker - Planck equation. Further it was found that the response spectra of the Duffing system under broad band excitation could be described with reasonable accuracy as functions of one variable, the ratio Γ/ζ .

Finally the applicability of the above findings and of the equivalent linearization technique for the Duffing system under band limited and high pass filtered random processes was investigated.

It is worth noting that the findings of this study apply equally to 'large' and 'small' nonlinearities and it is hoped that it will provide a better understanding of these terms as applied in different approaches to this problem.

1.1 General

A linear formulation or mathematical model of a structure is in general the least precise model and is normally regarded as a first approximation to the solution. However it can always be refined by the introduction of nonlinearity so that its range of application (in terms of large deflections for instance) is extended and that the precision of its predictions even within the less extended range is increased. Further, the nonlinear model may introduce the means of explaining or predicting phenomena which were outside the limits of the linear theory. Thus the question of whether a linear model is satisfactory depends on the sort of information and the precision that is being sought. As modern structures become more lightweight, linear modeling becomes less satisfactory because of membrane stresses and large deflections. As a consequence an increasing interest is being focused on nonlinear vibration problems.

The field of nonlinear vibration is in general much more extensive and complicated than that of linear vibrations. While many broad classes within the nonlinear vibration field have been described and in some cases investigated in detail, much still remains to be discovered.

In particular the problem of nonlinearity in the random vibration of structures has attracted much attention in recent years. Such problems can be recognised for example in the statistical description of measurements of the motion of ships in a confused sea or aircraft flying through turbulent air; in the severe vibration of aircraft or missile structure due to the random fluctuation of pressure fields generated by jet or rocket propulsion; in the severe vibration even failure of buildings and other structures excited by strong earthquakes.

1.2 Questions of Random Excitation

The theory of linear systems subjected to random excitation is well developed, and, though there still remain many unanswered questions, one can answer most of the questions of practical interest [1-7] . In the case of nonlinear systems, however, where the standard techniques of linear analysis cannot be applied, there is a lack of knowledge which is partially filled through mainly approximate methods, which have been developed to extend linear analysis to certain systems containing small nonlinearities. The method actually employed normally depends upon the desired information since none can provide a complete description of the system. However when response statistics of a probabilistic nature are required, the method of the Fokker - Planck equation seems to be the most promising one. (This is not an approximate method and its application depends on a special type of excitation).

There are a great number of response characteristics which are of interest in the study of nonlinear systems with random inputs, such as amplitude distributions, wave shapes, power spectre and average resonance frequencies, 'mean clump sizes'* etc. Most of these quantities vary with the type of excitation, (shape of excitation acceleration, velocity or displacement spectrum) and depend whether it is the response acceleration, velocity or displacement that is being studied. It is readily seen that even in the study of one particular nonlinear system the amount of data necessary to adequately describe the various response statistics is considerable.

*The expression 'mean clump size' was originally introduced by R.H.Lyon and describes the average number of cycles which exceed a predetermined level in one 'clump', i.e. where one cycle immediately succeeds the previous one.

1. 3 Various Approaches to the Response Problem

1.3.1 The Fokker-Planck Approach

Typically in seeking the probability density function of a Markovian diffusion process representing a system response, the associated Fokker-Planck equation is considered [8-16] This equation is a partial differential equation governing the evolution of the probability density function of the response. The broadest reported class of single-degree of freedom nonlinear systems for which the stationary or steady state solution of the associated Fokker-Planck equation can be determined requires that the coefficient of viscous damping is a function of the total energy of the structure. This restricts the use of the method to systems with stiffness nonlinearity only. Another restriction concerns the type of excitation. If the exciting forces do not exhibit white spectra, the solution is not Markovian hence the Fokker-Planck equation is not applicable. Further, although it is usually possible to solve the Fokker-Planck equation to obtain the stationary joint probability density function for the system response, the solution of the associated non-homogeneous equation to obtain the joint transition probability density function is in general extremely scarce. Without this transition probability law it is generally impossible to obtain the correlation function and spectral density (Section 2.1). Caughey and Dienes [11] however, have managed to solve a rather trivial first order problem in complete detail and obtain the spectral density. The techniques used in the solution of that problem do not appear to lend themselves to the solution of other nonlinear problems. Wolaver [12] was able to obtain an analytical closed form expression for the autocorrelation function for the nonlinear system,

$$\ddot{x} + 2c\dot{x} + \text{sgn}(x) = F(t) \text{ where } F(t) \text{ is white noise} \quad (1.1)$$

1.3.2 Numerical Simulation

The increasing availability of digital computers has presented the numerical simulation techniques as an attractive alternative method for estimating within almost any desired confidence level, the exact response statistics of randomly excited nonlinear structural systems, and allows one to drop

common artificial simplifying assumptions and to consider excitations that are more realistic than ideal white noise. The theoretical foundation of numerical simulation — based studies is associated with the fact that the differential equation governing the motion of the system under random excitation can be considered as an infinite collection of deterministic differential equations. The backbone of such a digital method is a subroutine (Chapter 3) which provides a set of pseudorandom numbers belonging to a population with a specified probability density function. Proper processing of the set of pseudorandom numbers can yield samples of random excitations of a desired spectral density. Upon generating a single realization of the random excitation the structural response is computed by any of the commonly available subroutines for numerical integration of differential equations. Then, another sample of the excitation is generated and the computed values of the structural response are used to update its statistics. Obviously this approach is applicable for the estimation of both stationary and non-stationary statistics of the response of structural systems. Unfortunately the number of sample records which are necessary for the estimation of the response statistics, within commonly acceptable engineering limits, is in most cases very large. This fact makes the cost of the simulation quite significant. However, the necessity of a large number of records can be reduced if interest is confined to stationary response statistics.

1.3.3 Approximate Methods

The scarcity or non availability of exact solutions, and in many cases the significant cost of numerical simulation have necessitated the development of methods of approximate analysis. They can be classified into two large categories.

[21] . One category includes methods which can be applied to the Fokker-Planck equation. In this class belong all the methods which yield approximate analytical or numerical solutions of partial differential equations. The other category comprises methods which are directly applicable to the differential equations which governs the motion of the randomly excited system. This latter class consists mainly of approximate methods (perturbation, heuristic, etc.)

which have been developed to extend linear analysis to certain systems containing small nonlinearities. Most of these techniques of approximate analysis are best suited for single-degree of freedom systems under stationary random excitation and 'weak' nonlinearities. [22 - 24]

The noticable exception in this class of approximate techniques is the method of equivalent linearization.

[17 - 21] The concept of this method is to replace the nonlinear structural system by an optimal (in some sense) linear substitute which lends itself to methods of analytical solution. The method was first introduced for deterministic systems by Krylov and Bogoliubov. [17] The extension of this technique to problems of random excitation was made independently and more or less simultaneously by Booton and Caughey in 1953. [18,19] Since then much attention has been concentrated on further development of the method. The method is outlined in its basic form in section 2.2 where it is applied to the Duffing system. Most of the efforts to improve on the technique attempt to disguise the rather embarrassing fact that the response of the equivalent linear system to a Gaussian excitation cannot be other than Gaussian. However, it must describe or approximate to a degree the non Gaussian response of the original nonlinear system. Nevertheless, it should be clearly understood that the method is an approximate one and indeed a very powerful one as such. Its power is derived from its wide and relatively inexpensive, compared to numerical simulation, application to almost any kind of nonlinear system under either stationary or nonstationary, broad band or narrow band random excitations. It is also true that it can provide some exact answers under special circumstances even for large nonlinearities (Chapter 5). On the other hand many problems to which it is applied do not lend themselves to any other reliable method of analysis. Hence, indiscriminate use of the method is inadvisable, especially for design purposes. Instead, it is recommended that a representative set of response statistics obtained through this method be verified by simulations, prior to an extensive use of the method. Alternatively these answers

should be used at best as indications of what might happen in the real system. It must also be noted that several stochastic linearization schemes which have proved quite reliable in predicting statistical movements of nonlinear structural responses, have been found not as reliable in predicting other useful response statistics, such as, the autocorrelation and the spectral density functions, and the average rate of a certain level crossing of a stationary response. This should not be surprising since the equivalent linear system can be optimised only in a limited sense, using a single criterion for optimisation (eg. optimising the mean square error of the response of the equivalent linear system with respect to the response of the nonlinear system). There is no reason therefore to expect the equivalent linear system to provide correct answers for properties of the response that bear no direct relation to the optimising criterion. In particular, as far as information on the frequency content of the response is considered, it is unreasonable to expect the equivalent linear system to provide anything more than an indication of shift in the resonant frequency of the system.

Finally, in the class of approximate techniques for nonlinear systems under random excitation some attention has been focused on H.R. Kraichman's 'Method of Stochastic Models', [25] which has been applied with success to the problem of isotropic turbulence (in that he was able to get a solution for the energy spectrum). Basically his approach is as follows. The coupled nonlinear equations of motion are written for the degrees of freedom of the system. For a turbulence field, these are the spatial Fourier amplitudes; for a nonlinear oscillator, they are the spectral amplitudes. The nonlinear interaction terms are replaced by statistical interactions of the mode with an infinite set of other modes. The statistics of the interaction terms are evaluated by making certain assumptions regarding sources of coherence in the interacting modes [25 - 28].

One finds that the 'zeroeth order approximation' is just the method of equivalent linearization. Moreover, Kraichman's method describes how to go beyond equivalent linearization.

It is not a small step, but the procedures are defined. For the nonlinear oscillator, this method could produce results for the spectrum changes due to nonlinearity beyond the mere shift in resonant frequency that one gets from equivalent linearization.

J.B. Morton and S. Corrsin [27] have used the above method to predict the response spectrum of the Duffing oscillator under white noise excitation, and small non linearity. Their work was critically reviewed by A.B. Budgor and co-workers [18] who concluded that for the particular case at least, better results were obtainable through the equivalent linearization method, when the effective frequency of the equivalent linear system was determined by the exact variance of the nonlinear response as calculated by the exact probability density (derived through the Fokker - Plank equation). Their results were compared with analogue computer experiments.

It should be stressed that the nonlinearities involved were very small and in a range where, the true nonlinear spectra are very similar to the linear (or equivalent linear) ones. Further the computational effort involved even for a 'first order approximation' is very large and probably not worthwhile for the small gain in accuracy obtained over the conventional equivalent linearization method. However, the method should be investigated further before its performance on stochastic structural nonlinear problems is finally judged.

1.4 Problems Considered in Present Work

This thesis explores the use that can be made of numerical simulation in describing the response of a single-degree of freedom nonlinear system, under random excitation. It also demonstrates how the task can be greatly simplified by a systematic approach to choosing ranges of parameters only possible as a result of dimensional analysis.

The system, whose spectral response behaviour under random excitation is to be investigated, is the Duffing system. It belongs to a class of nonlinear spring systems of the form

$$m\ddot{x} + 2c\dot{x} + g(x) = F(t) \quad (1-2)$$

Where $g(x)$ is a nonlinear function of displacement and $F(t)$ the excitation force.

When $F(t)$ is white noise equation (1-2) is usually referred to as Kramer's after H.A.Kramer who first considered them in 1940.

In particular when $g(x) = k(x+\beta x^3)$ (1-3)

the equation is known as Duffing's equation, irrespective of whether $F(t)$ is deterministic or random.

It should be noted that sometimes systems with

$$g(x) = \beta x^3 \quad (1-4)$$

$$\text{or} \quad g(x) = k \{ (1+\gamma)x - \gamma x_0 \} \quad (1-5)$$

with $\gamma = 0$ when $|x| < x_0$ and $x_0 = -x$ when $x < -x_0$

are also referred to as Duffing's equation [33]

Henceforth Duffing's system implies the one degree of freedom system governed by

$$m\ddot{x} + c\dot{x} + k(x+\beta x^3) = F(t) \quad (1-6)$$

where the symbols have their usual meaning and the non linearity constant, β , has dimensions L^{-2} .

The system with $g(x)$ of the type of equation (1-5) will be referred to as trilinear or piece-wise linear and will be the subject of a short discussion in the closing chapter of this thesis.

The Duffing equation arises when describing a single mode of vibration of a clamped-clamped beam with axial restraint, of flat panels fastened at their edges, shells etc. However, more important is the role that the Duffing equation plays in the study of nonlinear systems, since it is one of the simplest systems which can be treated in sufficient detail to investigate the usefulness of alternative methods.

The main body of this research will be concerned with the spectral response of the Duffing system to broad band Gaussian force excitation. Band limited and high pass filtered Gaussian excitations are also considered in Chapter 6 but the purpose of this chapter is to provide a better understanding of the response of the system to the broad band excitation. It will also indicate possible trouble spots of future research in this direction.

The selection of a broad band Gaussian random process as excitation is a natural start to describing the system.

In many random vibration problems which occur in practice where the response of a given system to a single random excitation is required, it is reasonable to assume that the excitation is Gaussian. If the system can be considered to be linear then the response to Gaussian excitation will itself be Gaussian, characterised by definition of its first and second order moments (mean value and spectral density).

Although this cannot be the case with a nonlinear system, the assumption of Gaussianity at least simplifies the description of the input. It is encouraging however to know through statistical information provided for the system in question, by the solution of the appropriate Fokker-Planck equation, that the velocity amplitude distribution under white noise excitation itself is Gaussian. Broad band excitation is usually an approximation to white noise and is seldomly encountered in reality with its box like spectrum. Knowledge of the response of a linear system to a sufficiently broad band excitation

provides complete description of the system. Although no such description is possible here, the work is expected to provide a means of predicting the response of the nonlinear system just to broad band excitation. Such excitation may be the response of another overdamped linear system which acts as excitation to the nonlinear system (providing there is no coupling) or maybe part of a more complicated spectrum such as is the case of sea spectra (Figure 1).

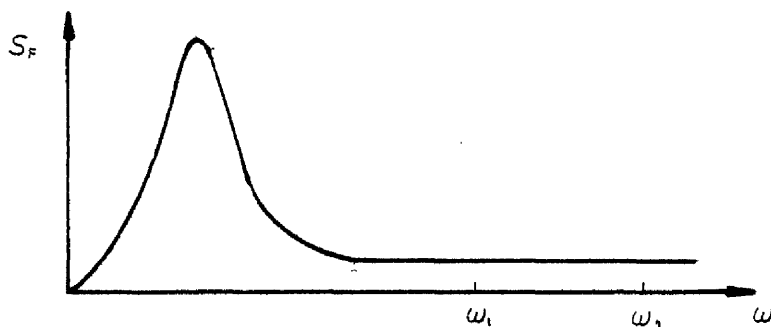


Figure 1

In the latter it is arguable whether the large energy concentration in the low frequency range will effect the response when the natural frequencies lie in a range ω_1 to ω_2 .

By describing the response spectra of the Duffing system to Gaussian random broad band excitation the description of the response is by no means complete since the output is non - Gaussian. It is however a useful and logical first step.

As mentioned earlier the Duffing system has been investigated extensively with varying degrees of success depending on the method of analysis. A certain amount of information is obtained through the solution of the appropriate Fokker - Plank equation. However only the stationary joint probability density of response displacement and velocity under white noise excitation is available. [8-14]

Wollaver [12] has proved that the method of equivalent linearization technique can under certain conditions provide the exact variance of response displacement and

velocity for the system under white noise excitation. This is a dubious advantage since one of the conditions assumes previous knowledge of the exact joint probability density function of response velocity and displacement.

Simulation methods (analog or digital) have not been used in general in their own right to describe the system. A number of experiments have been performed by researchers in the field who used simulations in order to confirm various theoretical predictions derived through their particular version of some approximate method. Since most approximate methods are applicable to systems with 'weak' nonlinearities the numerical results simply confirmed, with varying degree of success, the findings of particular approximate technique. J.B. Morton and S. Corrsin [27] for example have as mentioned earlier used Krainchman's 'Method of Stochastic Models', to predict the response spectrum of the Duffing system to white noise excitation. The spectra obtained using this method were compared with spectra obtained by analogue computer experiments and were in good agreement. However, the nonlinearity involved was 'weak'.

At this point an example to show the ambiguity behind the term 'weak' may not be out of place. For the Duffing system a measure of nonlinearity is the term $\beta \langle x^2 \rangle$. When the expression for the displacement variance of the system under white noise excitation, is obtained through the equivalent linearization technique, equation (1-7), and compared with a similar expression obtained through the perturbation technique, equation (1-8), it is seen that the results agree if $\beta \sigma_x^2$ is assumed much smaller than unity. [19,22]

$$\langle x^2 \rangle = \{ (1 + 12 \beta \sigma_x^2)^{1/2} - 1 \} / 6\beta \quad (1-7)$$

$$\text{if } \beta \sigma_x^2 \ll 1$$

$$\text{therefore } \langle x^2 \rangle \simeq \sigma_x^2 - 3\beta \sigma_x^4 \quad (1-8)$$

Where σ_x^2 in equation (1-7) is the variance of the equivalent linear system which in the form presented

provides an underestimated value for $\langle x^2 \rangle$ the mean square response displacement of the nonlinear system. Strictly speaking σ_x^2 in equation (1-8) has yet another meaning being the variance of the nonlinear system with $\beta = 0$. However, when $\beta\sigma_x^2 \ll 1$ the two variances are practically the same. This still does not define 'weak' nonlinearity even if the criterion $\beta\sigma_x^2 \ll 1$ is translated to $\beta\langle x^2 \rangle \ll 1$ since no definite value is given. Further it is obvious that this condition can be achieved by a number of combinations of input intensity (affecting x^2) and nonlinearity parameter (β). It is seen here that that the interpretation of results given by various methods present a certain difficulty, which is created on one hand from the lack of adequate knowledge, and on the other hand by the increase in the number of independent parameters in the nonlinear system as compared to the linear.

Numerical simulation methods on the other hand need not present the same problem. Each response record may be thought of as the outcome of a single (digital) experiment on a particular system with known parameters. A collection of these records will provide the characteristics of this unique combination of system parameters. Understandably the number of possible combinations can be overwhelming depending on the independent variables governing the system. As is the case with most experiments where a complete quantitative theory is lacking, the application of dimensional analysis [29-31] can simplify the problem significantly. By making use of the guidance provided by this analysis one can derive substantially complete information from a set of experiments, and with the greatest economy of effort, since in all cases the dimensional analysis substantially reduces the number of the functionally related quantities below the number of the relevant physical quantities. Provided that the indicial equations are linearly independent, this reduction in the number of independent variables is equal to the number of the relevant fundamental units (three in the case of mechanical systems). Consequently a great reduction in the number of experiments (simulations) may be expected for the adequate exploration

of the phenomenon. Although it is usually difficult to establish exact mathematical relations between the non dimensional quantities, empirical relations are almost the inevitable outcome of such experiments. Aside from their practical value these relations can prove invaluable 'clues' to a future mathematical analysis of the problem.

1.6 Arrangement of Chapters

The structure of the rest of this thesis is as follows.

In Chapter 2 the first order probabilistic information on the response of the system is obtained through the solution of the appropriate Fokker-Planck equation. This is preceded by a general outline of the appropriate theory. The general theory of the equivalent linearization technique follows in section 2 of this chapter along with its application to the Duffing system and a general discussion of the method.

In Chapter 3 the numerical simulation technique used is described in detail with reference to Appendices and tests to prove its accuracy.

Chapter 4 presents the non dimensional form of the Duffing system under both deterministic (sinusoidal) and random excitations and is followed by a discussion clarifying the apparent similarity of the two systems.

Chapter 5 contains the results of the numerical simulation which are compared where possible with the exact results obtained through the solution of the appropriate Fokker - Planck equation. The results are presented in convenient non dimensional form and a graphical representation of the response spectra useful for engineering application is suggested.

In Chapter 6 the response of the system to Gaussian band limited and high-pass filtered processes is briefly examined. The purpose of this work is to support the results of chapter 5 and suggests difficulties that may be encountered by further research in this direction.

Chapter 7 contains a discussion of various conclusions and also deals briefly with the piece-wise trilinear system.

CHAPTER 2

ANALYTICAL PREDICTION OF RESPONSE CHARACTERISTICS FOR THE DUFFING SYSTEM UNDER RANDOM EXCITATION

The alternatives to numerical simulation for the treatment of nonlinear systems under random excitation have already been reviewed in a general sense in the Introduction.

In this chapter two methods are used to obtain response characteristics of the Duffing system, namely the analytical method involving the solution of the Fokker-Planck equation and the equivalent linearization technique. In particular, in section 2.2, it is the conventional form of the equivalent linearization technique, that is used to obtain the variance of the response displacement of the system. This method is contrasted with a refined version in the discussion to this chapter.

2.1 Response to White Noise Excitation. The Fokker - Planck Equation

This solution is restricted to ideal stationary white noise excitation and in the first instance is capable of providing only probabilistic information regarding the response of the Duffing system.

In general it can be shown [10 - 14] that the behaviour of discrete dynamic systems subjected to white noise excitation are examples of continuous multidimensional Markoff processes. Such processes are completely characterised by their transitional - conditional probability law, which is obtained as fundamental solution to the Fokker - Planck equation appropriate to the dynamic system. Further it can be shown that exact stationary solutions may be constructed for a class of nonlinear problems in which the nonlinearity is a function only of displacements, and that if stationary solutions exist they are unique.

Consider the differential equation

$$\ddot{x} + 2\zeta\omega_n\dot{x} + \omega_n^2(1+\beta x^2)x = F(t) \quad (2-1)$$

If the subensemble of response, taking the values $x = x_0$ and $\dot{x} = \dot{x}_0$ at $t = 0$, are considered, the joint distribution of x and \dot{x} at time t is described by the transitional-joint-conditional density

$$\tilde{P}_t = P(x, \dot{x}, t / x_0, \dot{x}_0, 0) \quad (2-2)$$

This conditional density function diffuses in time from a Dirac delta function at (x_0, \dot{x}_0) and $t = 0$ towards the steady state, or stationary joint distribution density $P_s(x, \dot{x})$. The conditional density \tilde{P}_t is governed by the Fokker - Plank equation

$$\frac{\partial \tilde{P}_t}{\partial t} = - \dot{x} \frac{\partial \tilde{P}_t}{\partial x} + \frac{\partial}{\partial \dot{x}} (2\zeta\omega_n \dot{x} \tilde{P}_t) + \omega_n^2 (x + \beta x^3) \frac{\partial \tilde{P}_t}{\partial x} + 2\pi S_0 \frac{\partial^2 \tilde{P}_t}{\partial \dot{x}^2} \quad (2-3)$$

Where S_0 is the uniform spectral density of the ideal white noise acceleration excitation. Here a single sided spectrum is used with units of mean square excitation per unit of circular frequency. Note that equation (2-3) is linear in \tilde{P}_t although it does have variable coefficients. The stationary joint density $P_s(x, \dot{x})$ is the limit approached by \tilde{P}_t as $t \rightarrow \infty$ and is thus determined by the stationary equation

$$0 = - \dot{x} \frac{\partial P_s}{\partial x} + \frac{\partial}{\partial \dot{x}} (2\zeta\omega_n \dot{x} P_s) + \omega_n^2 (x + \beta x^3) \frac{\partial P_s}{\partial x} + 2\pi S_0 \frac{\partial^2 P_s}{\partial \dot{x}^2} \quad (2-4)$$

and the normalisation requirement

$$\int_{-\infty}^{+\infty} \int_{-\infty}^{+\infty} P_s(x, \dot{x}) dx d\dot{x} = 1 \quad (2-5)$$

It can be shown that the unique solution to equation (2-4) is

$$P_s(x, \dot{x}) = C \exp \left\{ - \frac{4\zeta\omega_n}{\pi S_0} \left(\frac{\dot{x}^2}{2} + G(x) \right) \right\} \quad (2-6)$$

Where $G(x) = \int_0^x \omega_n^2 (\eta + \beta \eta^3) d\eta$ is the potential energy function for the spring force. The integration constant C remains to be fixed by the normalisation requirement of equation (2-5). It can be seen that $P_s(x, \dot{x})$ has the form

$$P_s(x, \dot{x}) = P_x(x) \cdot P_{\dot{x}}(\dot{x}) \quad (2-7)$$

This implies that the response velocity and displacement of the Duffing equation under white noise excitation are

statistically independent. Indeed the probability distribution function of the response velocity is Gaussian and identical to what it would be if the system were linear (i.e. $\beta = 0$)

$$P_{\dot{x}}(\dot{x}) = C \exp \left\{ -\frac{2\zeta\omega_n}{\pi S_0} \dot{x}^2 \right\} \quad (2-8)$$

therefore

$$\sigma_{\dot{x}}^2 = \int_{-\infty}^{+\infty} \dot{x}^2 P_{\dot{x}}(\dot{x}) d\dot{x} = \frac{\pi S_0}{4\zeta\omega_n} \quad (2-9)$$

In general, displacement will not have a normal distribution except when the stiffness is linear. Clearly here the displacement has the form

$$\begin{aligned} P_x(x) &= C \exp \left\{ \frac{4\zeta\omega_n}{\pi S_0} G(x) \right\} \\ &= C \exp \left\{ -\frac{\zeta\omega_n^3}{\pi S_0} \left[2x^2 + \beta x^4 \right] \right\} \end{aligned} \quad (2-10)$$

R.H.Lyon [14] has produced exact expressions for the moments of the Duffing system using parabolic cylinder functions. The expression however is particularly easy to integrate numerically due to the decaying effect of x^4 .

Since the joint density is available it is an easy matter to compute various response statistics such as mean square response, expected number of crossings of the level $x = a$ etc.

Apart from the above probability functions there is great interest in the various correlation functions as a means of calculating the spectra. In order to see the problems involved in their determination consider for example the autocorrelation function of response displacement

$$R_{xx}(t) = \iiint_{-\infty}^{+\infty} x_0 x P(x_0, \dot{x}_0, 0; x, \dot{x}, t) dx d\dot{x} dx_0 d\dot{x}_0 \quad (2-11)$$

for $t \geq 0$

where $P(x_0, \dot{x}_0, 0; x, \dot{x}, t)$ is the transitional density function. Using the relation

$$P(x_0, \dot{x}_0, 0; x, \dot{x}, t) = P_s(x_0, \dot{x}_0) P_r(x, \dot{x}, t/x_0, \dot{x}_0, 0) \quad (2-12)$$

Equation (2-11) may be rewritten in the form

$$R_{xx}(t) = \int_{-\infty}^{+\infty} \int_{-\infty}^{+\infty} \int_{-\infty}^{+\infty} \int_{-\infty}^{+\infty} x_0 \dot{x}_0 P_s(x_0, \dot{x}_0) P_r(x, \dot{x}, t/x_0, \dot{x}_0, 0) dx d\dot{x} dx_0 d\dot{x}_0 \quad (2-13)$$

The function

$$v(x, \dot{x}, t) = \int_{-\infty}^{+\infty} \int_{-\infty}^{+\infty} x_0 P_s(x_0, \dot{x}_0) P_r(\dot{x}, x, t/x_0, x_0, 0) dx_0 d\dot{x}_0 \quad (2-14)$$

is a weighted average of P_r and is therefore a solution to the Fokker-Planck equation with appropriate boundary conditions i.e.

$$\frac{\partial v}{\partial t} = 2\pi S. \frac{\partial^2 v}{\partial \dot{x}^2} + \frac{\partial}{\partial \dot{x}} (2\zeta\omega_n \dot{x}v) + \omega_n^2 (x + \beta x^3) \frac{\partial v}{\partial x} - \dot{x} \frac{\partial v}{\partial x} \quad (2-15)$$

which must be solved for $v(x, \dot{x}, t)$ with finite boundary conditions.

$$v(x, \dot{x}, 0) = x P_s(x, \dot{x}) \quad (2-16)$$

The autocorrelation is then obtainable through

$$R_{xx}(t) = \int_{-\infty}^{+\infty} \int_{-\infty}^{+\infty} x v(x, \dot{x}, t) dx d\dot{x} \quad (2-17)$$

It is thus necessary to know $P_s(x, \dot{x})$ apriori as a boundary condition. Because of this any analytical approach for finding the autocorrelation function is restricted to Kramer's class (see introduction, [12]). Unfortunately all attempts to solve the above F.P. equation for the general class of Kramer's equations or indeed the Duffing system have been unsuccessful. The tools for solving partial differential equations are very meagre compared to those for ordinary differential equations. Even numerical solutions are beset with difficulty because of the boundary conditions. Further the path leading to spectral densities through this method is probably too indirect to be suitable for a numerical procedure. It is worth noting however that this method has successfully applied to certain mathematically 'convenient' nonlinearities [12].

2.2 Equivalent Linearization Technique

The method of equivalent linearization has proved, over the period of the last three decades, a useful approximate method for probabilistic analysis of nonlinear structural dynamic problems, as discussed in section 1.3. The technique of equivalent linearization was first introduced by Krylov and Bogoliubov [17] in connection with deterministic nonlinear problems. It was first applied to the problem of random oscillations by Booton [18] and Caughey [19] and later was used on several occasions by Crandall [20] and many others [21].

The underlying idea of this approach is that, given a nonlinear differential equation, an 'equivalent' linear equation is constructed so that the behaviour of the linear system approximates that of the nonlinear system in some sense. Once the equivalent linear equation is established, the properties of the solution process can be easily analysed by means of the linear theory and the results should be approximations to the solution properties of the original nonlinear equation. It is important to note that this technique is best suited for problems with 'small' nonlinearities, but under certain conditions may produce remarkable accuracy for 'large' nonlinearities. On the other hand, a number of difficulties develop in the process of derivation and they can be overcome satisfactorily only for a certain class of nonlinear problems.

For a single-degree of freedom system such as

$$\ddot{x} + g(x, \dot{x}) = F(t) \quad (2-18)$$

it is assumed that an approximate solution can be obtained from the linearised equation

$$\ddot{x}_1 + b_1 \dot{x}_1 + \omega_1^2 x_1 = F(t) \quad (2-19)$$

where the parameters b_1 and ω_1^2 are to be selected so that the linear equation above produces a solution which 'best' approximates (usually in least squares sense) that of the original nonlinear equation. Adding the terms $(\ddot{x}_1 + b_1 \dot{x}_1 + \omega_1^2 x_1)$ to both sides of equation (2-18) and rearranging

$$\ddot{x} + b_e \dot{x} + \omega_e^2 x = F(t) + N(t) \quad (2-20)$$

where

$$N(t) = b_e \dot{x} + \omega_e^2 x - g(x, \dot{x}) \quad (2-21)$$

Note the difference of equations (2-19) and (2-20). The quantity $N(t)$ is itself a random process and can be considered as the error term of the approximation procedure. In order to minimise the approximate error, a common criterion is to minimise the mean square value of the error process $N(t)$. Hence it is required that b_e and ω_e^2 are chosen such that

$$E(N^2(t)) = E([b_e \dot{x} + \omega_e^2 x - g(x, \dot{x})]^2) \quad (2-22)$$

is minimised for $t \in T$. The first and second derivatives of $E(N^2(t))$ with respect to b_e , ω_e^2 are

$$\frac{\partial}{\partial b_e} E(N^2) = 2E(b_e \dot{x}^2 + \omega_e^2 x \dot{x} - \dot{x}g(x, \dot{x}))$$

$$\frac{\partial}{\partial \omega_e^2} E(N^2) = 2E(\omega_e^2 x^2 + b_e x \dot{x} - xg(x, \dot{x}))$$

$$\frac{\partial^2}{\partial b_e^2} E(N^2) = 2E(\dot{x}^2) \geq 0$$

$$\frac{\partial^2}{\partial (\omega_e^2)^2} E(N^2) = 2E(x^2) \geq 0$$

$$\frac{\partial^2}{\partial b_e^2} E(N^2) \frac{\partial^2}{\partial (\omega_e^2)^2} E(N^2) - \left[\frac{\partial^2}{\partial b_e \partial \omega_e^2} E(N^2) \right]^2 =$$

$$4(E(\dot{x}^2)E(x^2) - E(x\dot{x})^2) \geq 0$$

From the above it is seen that the necessary conditions for minimising $E(N^2(t))$ are

$$\frac{\partial}{\partial b_e} E(N^2) = 0 \text{ and } \frac{\partial}{\partial \omega_e^2} E(N^2) = 0$$

Hence, b_e and ω_e^2 are the solutions of the equations

$$\begin{aligned} b_e E(\dot{x})^2 + \omega_e E(\dot{x}x) - E(\dot{x}g(x, \dot{x})) &= 0 \\ \omega_e^2 E(\dot{x})^2 + b_e E(\ddot{x}x) - E(xg(x, \dot{x})) &= 0 \end{aligned} \quad (2-23)$$

In this form, the solutions for b_e and ω_e^2 , requires the knowledge of the indicated expectations, which are obviously unknown. There are two possible approximations at this point. The joint density function $P(x, t; \dot{x}, t)$ may be replaced by the stationary density function $P(x, \dot{x})$ computed from the original nonlinear equation (for example solving the appropriate Fokker - Planck equation when possible); or $P(x, \dot{x})$ can be determined approximately using the linearized equation (2-19) (conventional equivalent linear technique).

The latter is now applied for the Duffing system excited by stationary Gaussian input with zero mean. A further assumption is made that x and \dot{x} are jointly stationary but not necessarily Gaussian. This implies

$$E(\dot{x}x) = E(\ddot{x}x) = 0$$

Hence for the system

$$\ddot{x} + b\dot{x} + \omega_n^2(x + \beta\dot{x}^3) = F(t) \quad (2-24)$$

equations (2-23) become

$$\begin{aligned} b_e E(\dot{x})^2 - E(b\dot{x}^2 + \omega_n^2(\dot{x}x + \beta\dot{x}\ddot{x})) &= 0 \\ \omega_e^2 E(\dot{x})^2 - E(bx\dot{x} + \omega_n^2(x^2 + \beta\dot{x}^4)) &= 0 \end{aligned} \quad (2-25)$$

or $b = b_e$

$$\omega_e^2 = \omega_n^2 \left(1 + \beta \frac{E(\dot{x}^4)}{E(\dot{x}^2)} \right) \quad (2-26)$$

Hence the equivalent linear equation becomes

$$\ddot{x}_e + b\dot{x}_e + \omega_e^2 \left(1 + \beta \frac{E(\dot{x}^4)}{E(\dot{x}^2)} \right) x_e = F(t) \quad (2-27)$$

Where both the expectations involved are unknown. If equation (2-19) is used to evaluate the unknown ratio

$$E(\dot{x}^4) / E(\dot{x}^2) = 3 \sigma_{\dot{x}}^2 \quad (2-28)$$

therefore

$$\omega_e^2 = \omega_n^2 (1 + 3\beta\sigma_{\dot{x}}^2) \quad (2-29)$$

thus

$$\ddot{x}_1 + b \dot{x}_1 + \omega_n^2 (1 + 3\beta \sigma_{x_1}^2) x_1 = F(t) \quad (2-30)$$

The variance $\sigma_{x_1}^2$ of the output displacement can be computed from the spectral density function $S_o(\omega)$ of $F(t)$ as

$$\sigma_{x_1}^2 = \int_0^\infty S_{x_1}(\omega) d\omega = \int_0^\infty |H(i\omega)|^2 S_o(\omega) d\omega$$

where

$$\begin{aligned} H(i\omega) &= (\omega_n^2 - \omega^2 + i b \omega)^{-1} \\ &= (\omega_n^2 - \omega^2 + i b \omega)^{-1} \end{aligned} \quad (2-31)$$

For ideal white noise acceleration input of intensity S_o

$$\sigma_{x_1}^2 = \frac{S_o \pi}{2b\omega_n^2} \quad (2-32)$$

Substituting equations (2-28) in equation (2-31) and rearranging

$$6\beta b \omega_n^2 \sigma_{x_1}^4 + 2b\omega_n^2 \sigma_{x_1}^2 = S_o \pi \quad (2-33)$$

It will be shown later that this equation provides an underestimation for the variance of the nonlinear response displacement.

2.3 Discussion

The analysis previously shown are consistent up to equations (2-26). If the values for b_e , ω_e^2 were to be evaluated precisely the expected values indicated in equations (1-25) should be calculated using the correct probabilities. These can only be obtained through the corresponding Fokker-Planck equation or the moments may be calculated by a simulation process as the one developed in this project. Wolaver [12] has shown that in the case of a system where only the stiffness law is nonlinear and where excitation is a Gaussian white noise process, the equivalent linearization method can lead to the exact mean square value for the stationary displacement regardless of the magnitude of the nonlinear term. He has also proved that in this case the MacLaurin series expansion of the approximate autocorrelation function $R_{xx}(\tau)$ of the stationary displacement obtained from the equivalent linearization agrees with that of the exact autocorrelation function up to the τ^3 term. (Appendix B1). It is unreasonable however to attempt to derive any more information about the nonlinear system through this technique. Further what might seem as an advantage of the method, i.e. the exact value for the mean square response displacement, loses its significance since that in order to obtain the correct mean square value, ω_e^2 should be evaluated using the correct ratio of $\frac{E(x^4)}{E(x^2)}$ which implies the previous knowledge of the moments, through some other method. Hence the only additional information that can be obtained through the technique is the approximate autocorrelation function. The usefulness of this knowledge will be investigated in Chapter 5.

In addition to the methods outlined in sections 1 and 2 of this chapter, the perturbation and heuristic methods are also presented in Appendices B.2 and B.3. These are only applicable for nearly linear systems. The perturbation technique is closely related to the classical perturbation methods used in the solution of differential equations [22-24]. The heuristic method, named thus by Crandall who devised it, is an early attempt to provide a simpler derivation of the results obtained by perturbation techniques [23].

NUMERICAL SIMULATION

Before proceeding to outline the details of the numerical simulation technique employed, it is appropriate to describe the general problem of response simulation for dynamic systems. The general simulation problem can be visualised in three separate stages:-

- a) Description of the input.
- b) Definition of the system in the form of differential equations.
- c) Numerical solution of the set of differential equations describing the system for the input defined.

Clearly for the particular problem of response simulation of the Duffing system, stage (b) is already defined. It was therefore towards the two other stages that particular attention was drawn.

In this chapter only essential features of the simulation technique will be outlined along with a list of tests of the technique. More details may be found in Appendix C.

3.1 The Numerical Integration

For the numerical integration of Duffing's equation, the main criterion for the selection of a particular technique, and the set up of the whole simulation procedure is the suitability of the process to cope with random input. Inevitably as it is the case with all computer work, economy of computer time is also important.

The simulation was performed on the ICL 2976 main frame computer at Glasgow University. The facilities available include a package of numerical integration routines which were supplied by NAG LTD., under the general title NAG FORTRAN Library Mark 7.

For simple problems with low accuracy requirements, that is problems on a short range of integration, with derivative functions which are inexpensive to calculate and where only a few correct figures are required, the best routines to use are likely to be the Runge - Kutta Merson routines. For large problems, over long ranges or with high accuracy requirements the variable-order, variable-step Adams routines should usually be preferred. For stiff equations, that is those with widely different natural frequencies, the Gear variable-order, variable-step routines are often superior.

All the NAG procedures are called in the user's program in the form of a subroutine. The problem is formulated as a set of first order ordinary differential equations is defined in an other subroutine as an external function (EF) Each call of the NAG, integrates the differential equations from t to $t + \Delta t$.

Hence if the solution of the initial value problem

$$\ddot{x} + 2\zeta\omega_n \dot{x} + g(x) = F(t), \quad x(0) = A; \quad \dot{x}(0) = B \quad (3-1)$$

is required, the EF should be defined as

$$\frac{dx}{dt} = z \quad (3-2)$$

$$\frac{dz}{dt} = F(t) - 2\zeta\omega_n z - g(x)$$

This subroutine should have some means of accessing information about $F(t)$. If $F(t)$ is deterministic then this information can be included in the EF. If however $F(t)$ is random and represented by a digital signal sampled at a given rate Δt , problems arise especially if a variable-step technique is used.

The way chosen to overcome this problem is as follows:-

Since the input would be sampled at regular intervals the step length should be set to a value smaller than the data spacing Δt , by the integration method automatic process depending on accuracy requirements, then values of excitation between the specified values will be taken to lie on the line joining the surrounding specified points. Alternatively, the integration should be performed only at times where the excitation is known i.e. at multiples of the data spacing, in which case only fixed step routines could be used. Unfortunately, variable step routines are desirable for reasons other than their variable step facility being generally of a higher order than the fixed step methods available in the packages, and much faster.

With the continuity of the input guaranteed by the linear interpolation, instead of proceeding to obtain the response of the system with the initial conditions for the complete input. the following 'segmentation' of the solution was proposed. The numerical integration routine would be called to integrate the system using the initial conditions at some point in time t_1 up to $t_2 = t_1 + \Delta t$ along the straight line segment from t_1 to t_2 at this point the routine would be reset to regard the values at t_1 as initial values to proceed to obtain the solution at $t_3 = t_2 + \Delta t = t_1 + 2\Delta t$. Again there is no justification for this method except that it allows the use of low accuracy requirements hence the less expensive Runge-Kutta-Merson routines. This technique is the easiest method of making certain that all the

excitation data points are used by the integration sub routine, since the integration steps of the routine are automatically set. The particular subroutine selected was a Runge-Kutta-Merson version, implemented by NAG under the code name D02BAF.

The idea was first tested using deterministic excitation. Two programs were used, identical in all respects the only difference being the definition of the excitation data. One used a deterministic definition of the input in the form of a function which provided the exact excitation at any required point, and the other the interpolation idea outlined above. The output was printed at the end of each interval. The first step was to find the most reasonable time interval in terms of accuracy and economy. The deterministic excitations used for these tests were:-

a) A sinusoidal signal defined as:-

$$F(t) = F_0 \sin(\omega t) \text{ of fixed frequency } \omega \text{ and}$$

b) A modulated sinusoidal signal defined as:-

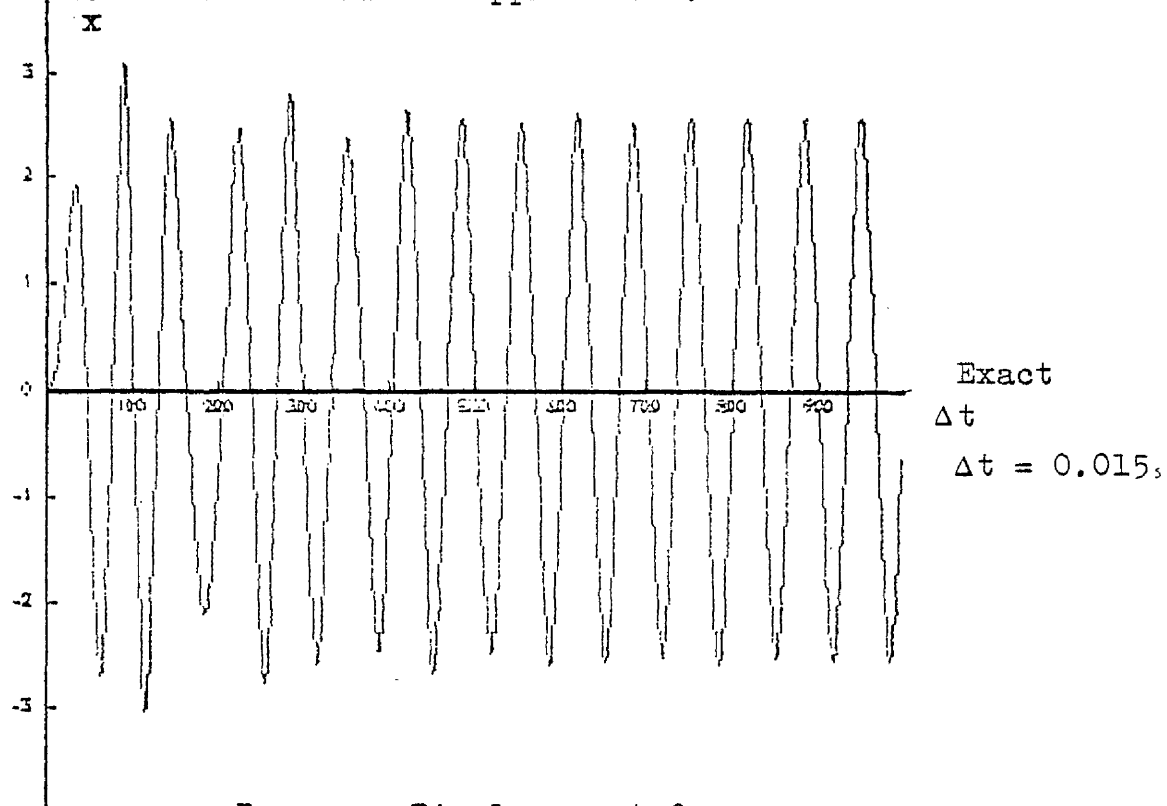
$F(t) = F_0 \cos(\omega_e t) \sin(\omega t)$ where ω_e is the modulation frequency. The system was defined by the differential equation:-

$$\ddot{x} + 2\zeta\omega_n\dot{x} + \omega_n^2(1 + \beta x^2)x = F(t) \quad (3-3)$$

with initial values $x = \dot{x} = 0$

It was observed that the substitution tends to underestimate the output as the interval increases. Although a sampling rate of eight points per cycle of input produced good results a sampling rate of twelve points per cycle was adopted. Typical response records are shown in figures 2.a-2.d. The tests were performed for a wide range of damping and non linearity constants. For high nonlinearity with typical values of $\beta = 10$, $F_0 = 40$, $\omega_n = \pi$ (i.e. γ in the range of 1600. Section 4.1 for significance of γ) the sampling process produced smoother shapes for the response velocity oscillations, than the process using a functional representation of excitation. Figure 2.d. This was taken into account when the simulation was modified to handle random excitation. Further, the investigation of the response

function representation of input are called exact and the results obtained by using the method of linear interpretation of the excitation are called approximate.



Response Displacement for

$$F(t) = 40 \sin \omega t \quad \omega = 2\pi$$

$$\gamma = 0.1$$

$$\omega_n = \pi$$

$$\beta = 1.0$$

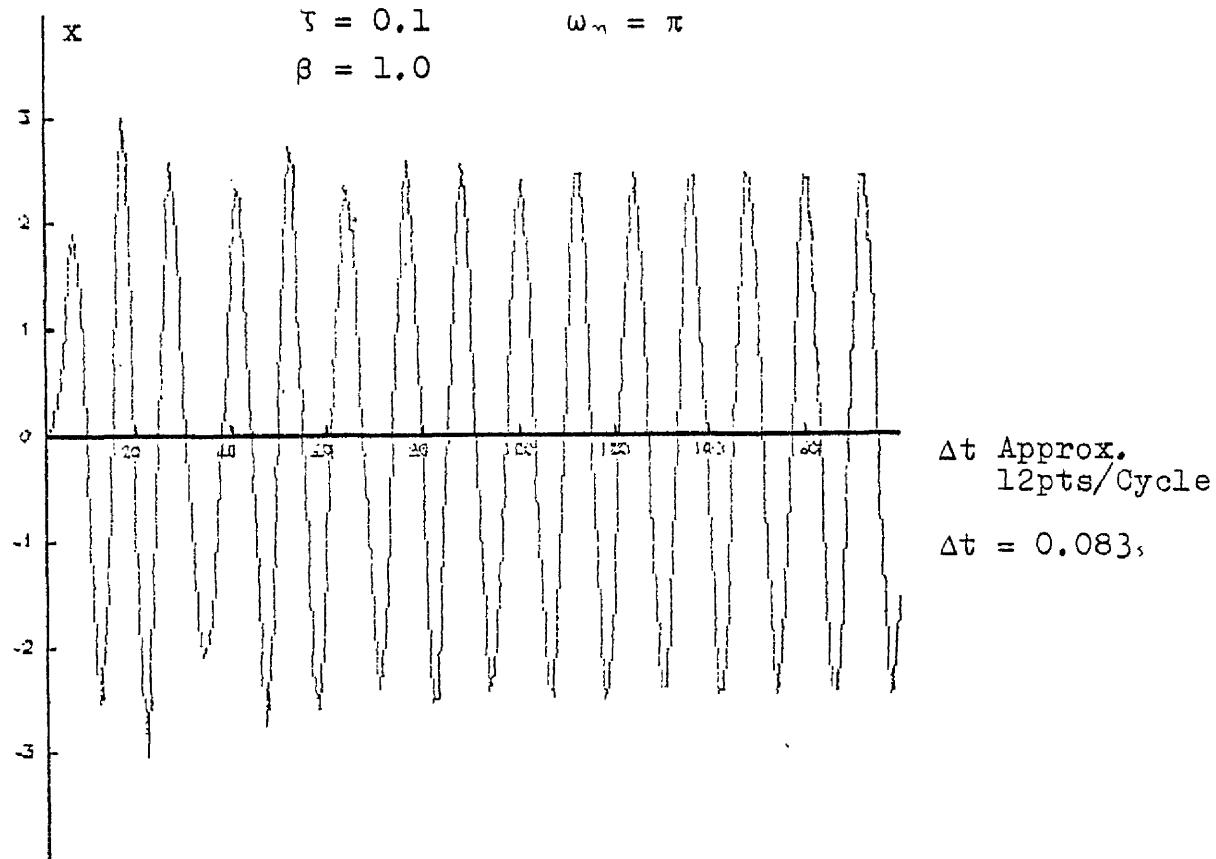
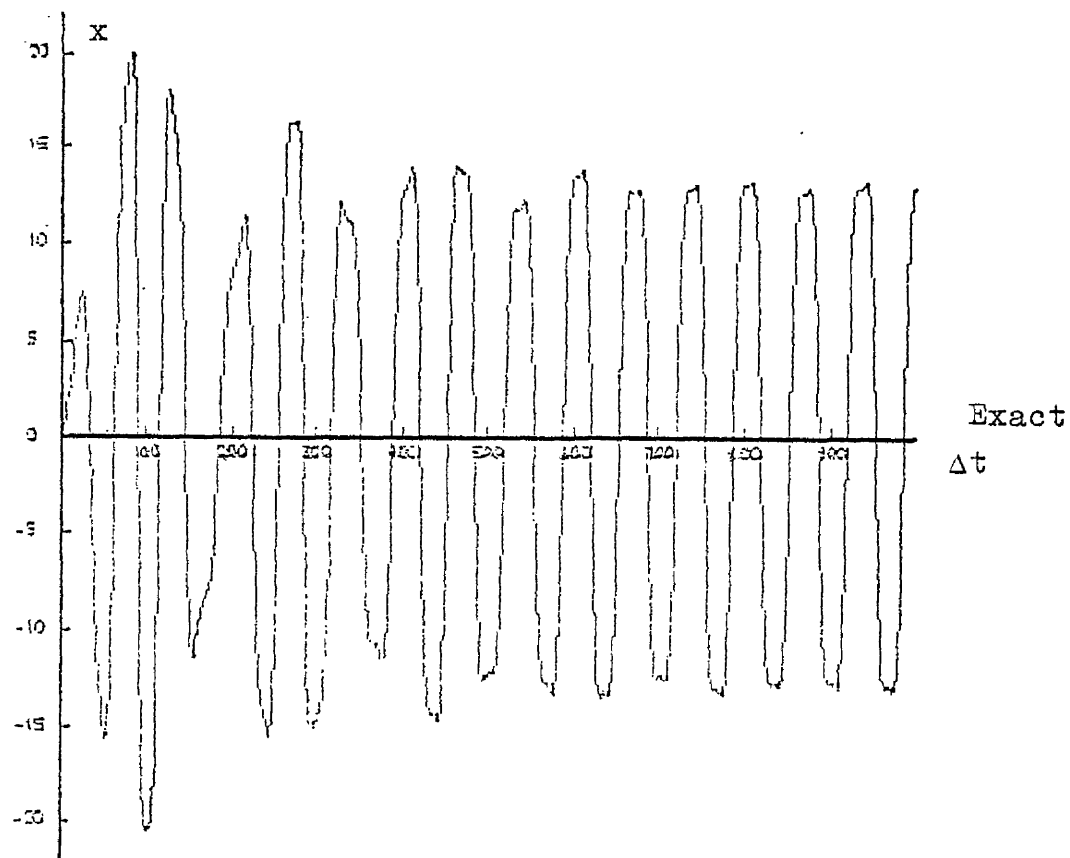


Figure 2a



Response velocity as for Figure 2a

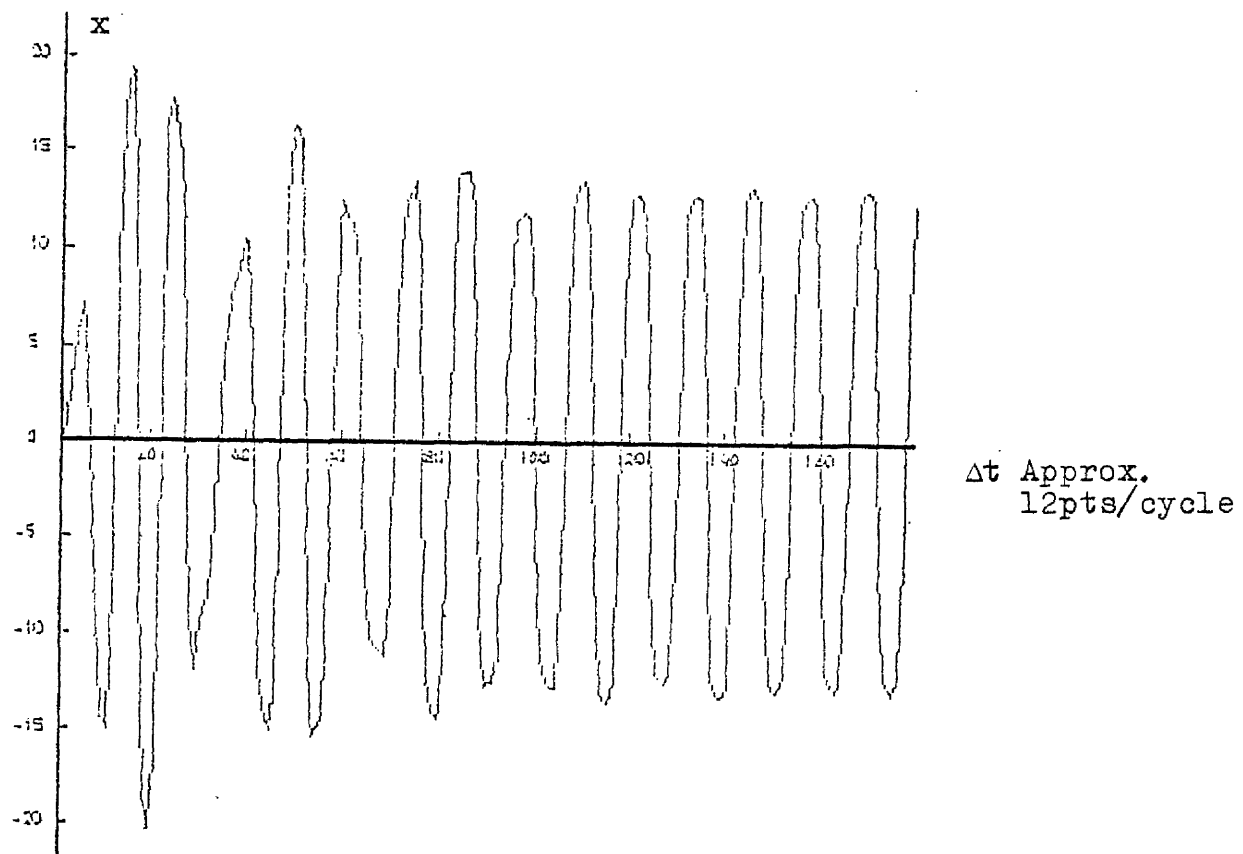


Figure 2.b

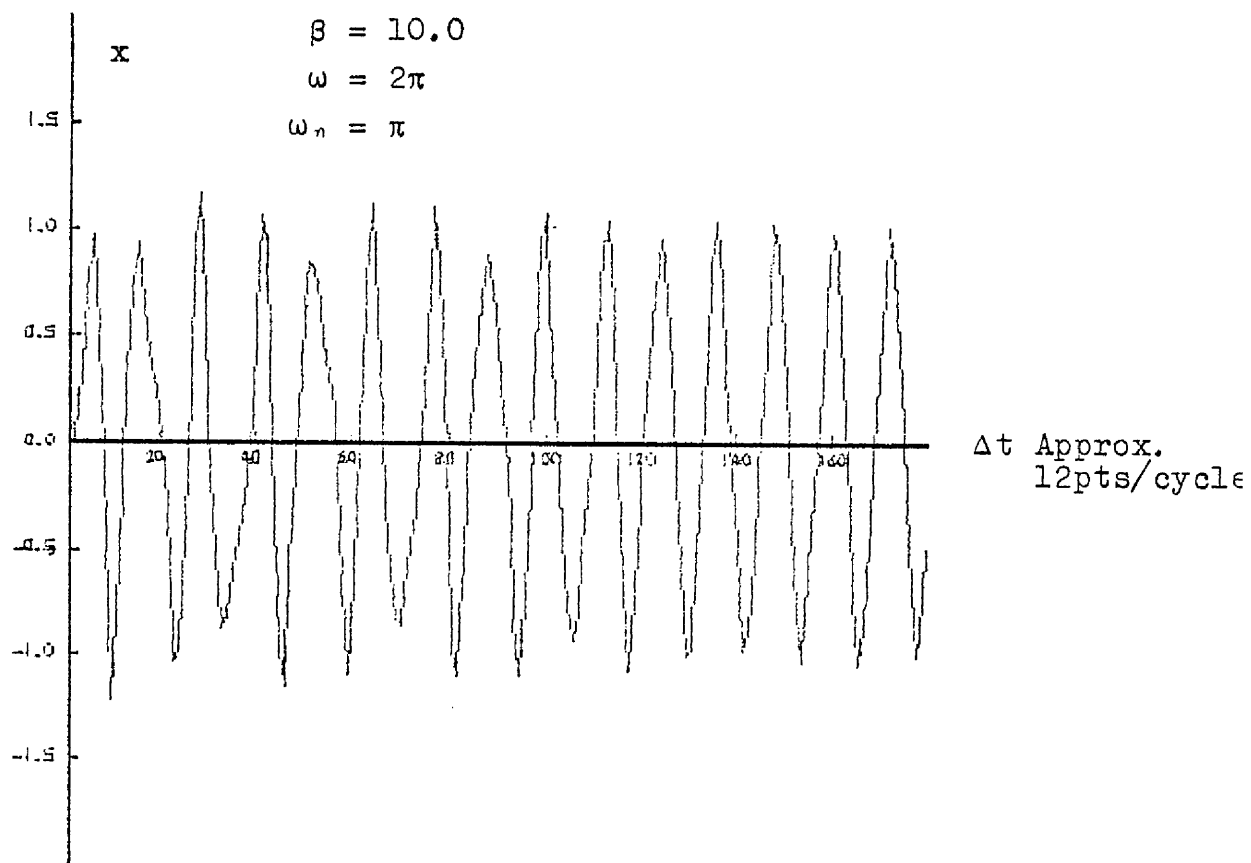
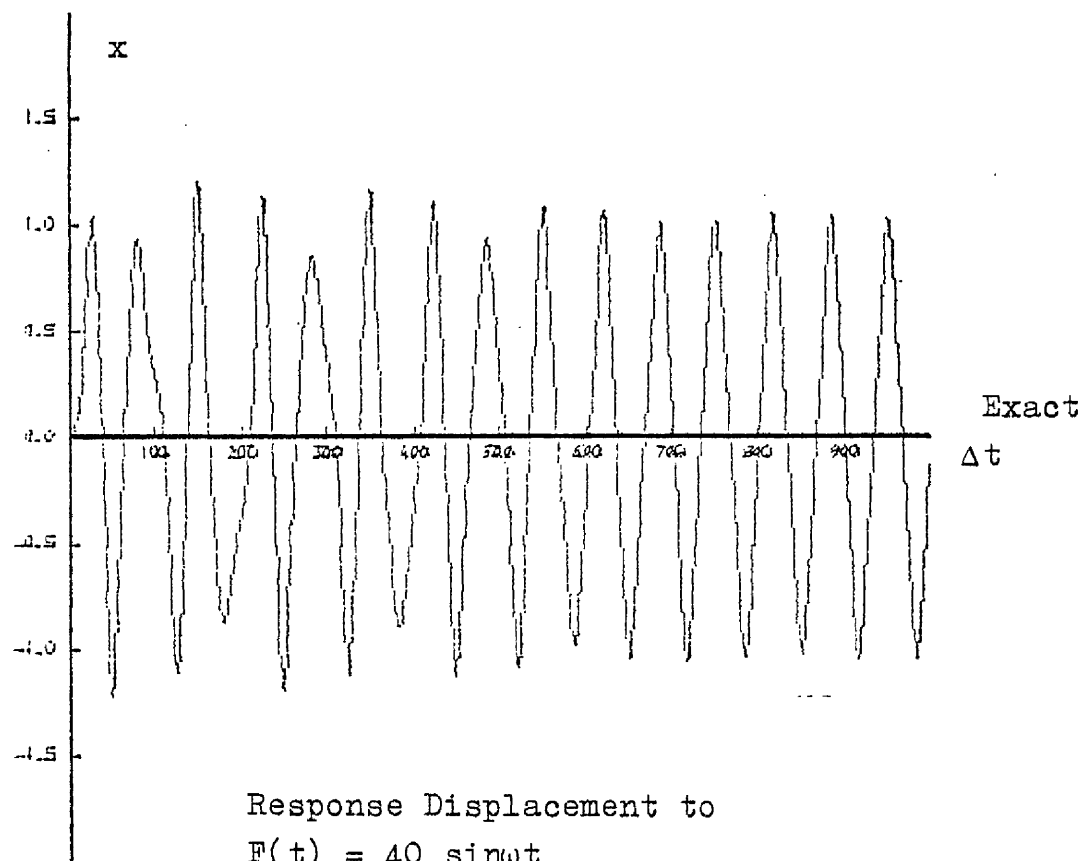
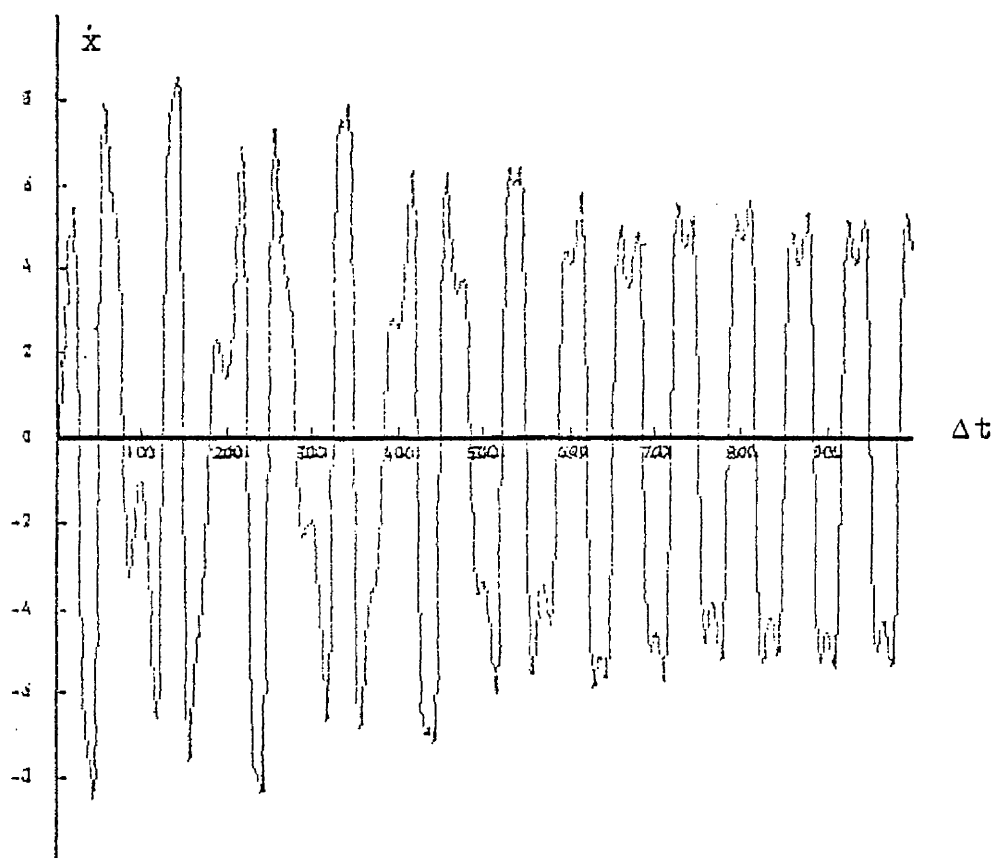
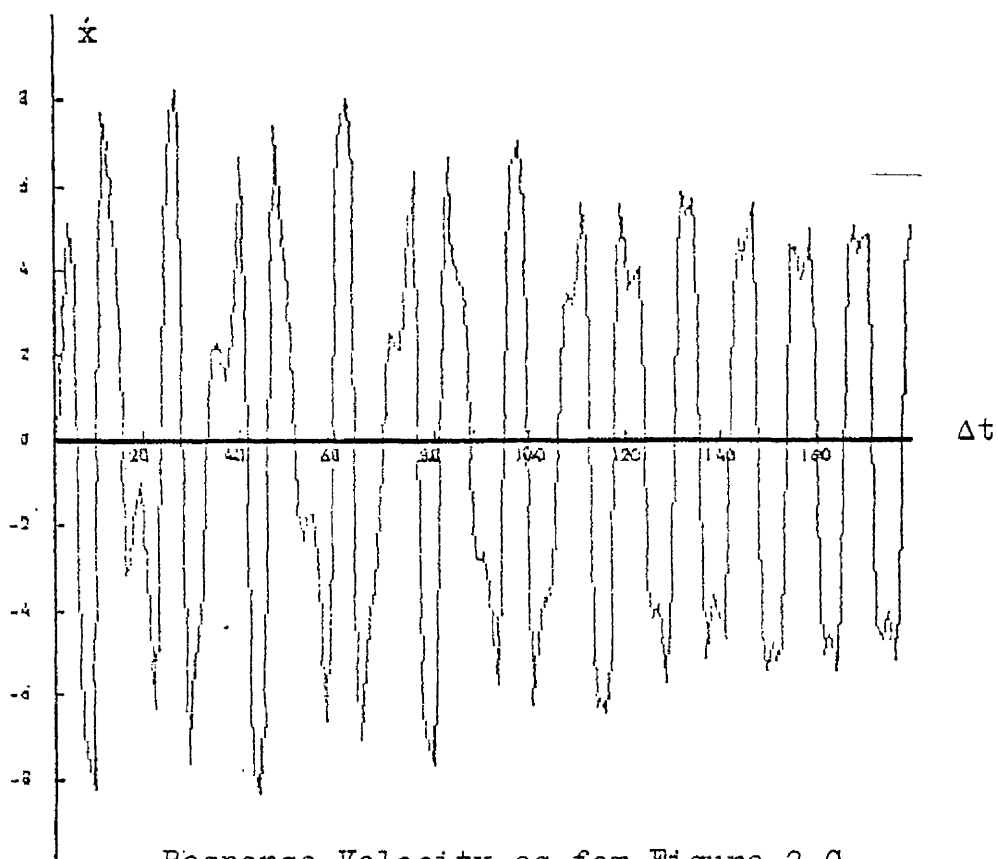


Figure 2.c



Response Velocity as for Figure 2.C



Response Velocity as for Figure 2.C

under sinusoidal excitation, also served the purpose of providing a behavioural pattern for the settling time of the system, to be used as an indication of the behaviour of the settling time under random excitation.

One of the most important deterministic manifestations of the nonlinearity of the Duffing system is the jump phenomenon (Appendix A.1). Although this phenomenon can not occur under broad band random excitation [32] it is almost certain to occur under narrow band excitation. The modulated sinusoidal excitation used to test the simulation process proved the ability of the method to cope with response jumps. A theoretical response prediction for such excitation is shown in Appendix A.3. Figure 3 shows a computer plot of the response obtained by the numerical simulation.

Having proved the ability of the simulation process to cope with the deterministic inputs and jump phenomena, the next step was to test the process for random excitation. The NAG library contains subroutines which can provide a set of pseudorandom numbers belonging to a population with a specified probability density function. The adjective 'pseudo' is included because the obtained numbers are perfectly reproducible and the only random element involved is associated with the fact that they are generated by means of a periodic sequence of integer numbers of extremely long periods, thus ensuring very small correlation of consecutive numbers. The first tests of the method were conducted using a subroutine (NAG subroutine G05DDF) that produced a set of random numbers with normal distribution and were defined mean and standard derivation. The numbers generated were set up in an array and a time interval Δt was assigned between them. Thus it could be assumed that these numbers represented sampled values of a random process $F(t)$ of given mean and standard deviation. The frequency scale of this process is determined by the number of points per record (2K) and the time interval Δt . A Fast Fourier Transformation algorithm may be used (NAG subroutine C06AAF) to obtain the power spectrum of the above process, over a

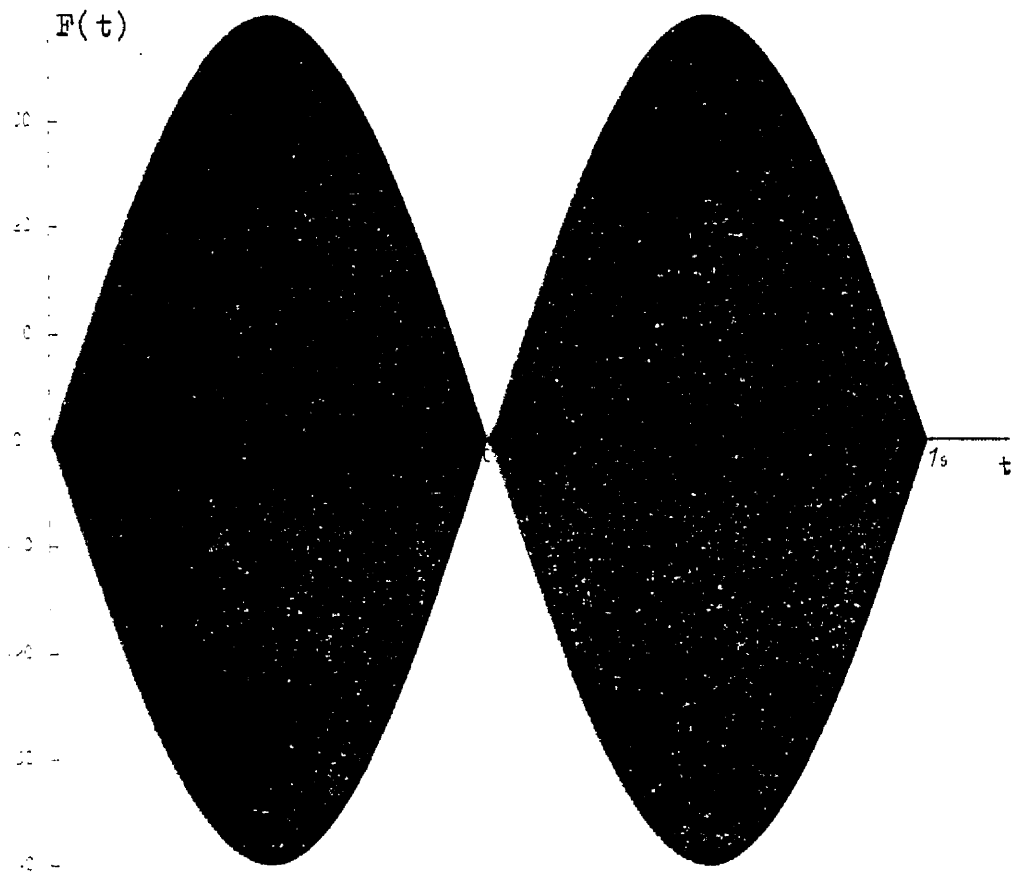


Figure 3.a

Excitation

$$F(t) = 40\sin(\omega t)\cos(\omega_e t) \text{ with } \omega = 2\pi, \omega_e/\omega = 0.001$$

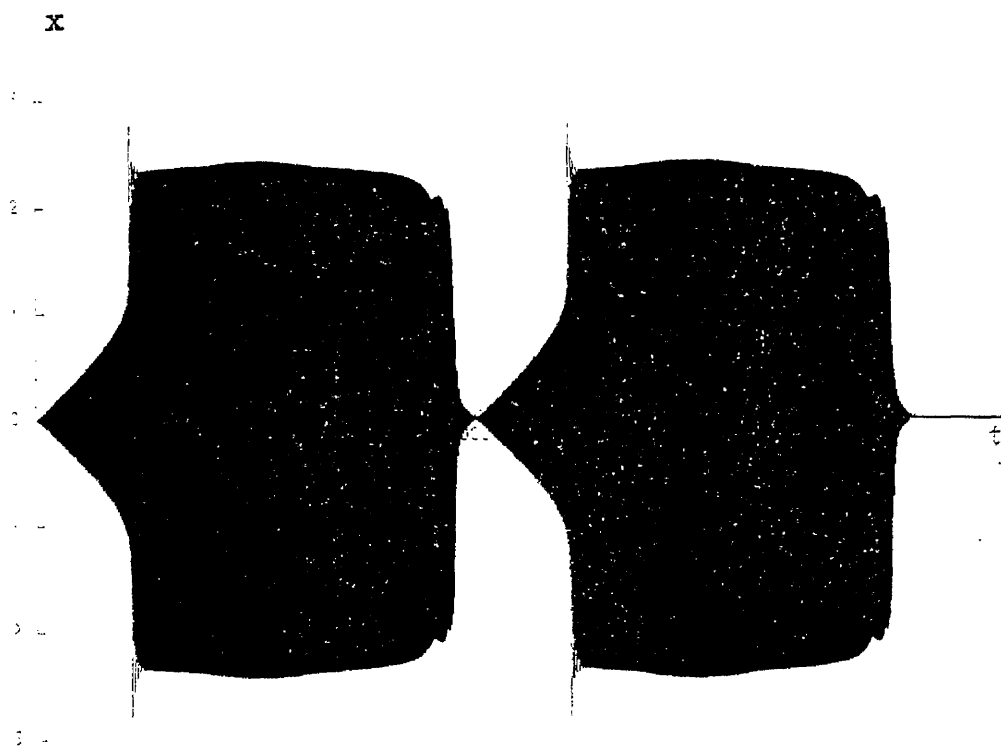


Figure 3.b

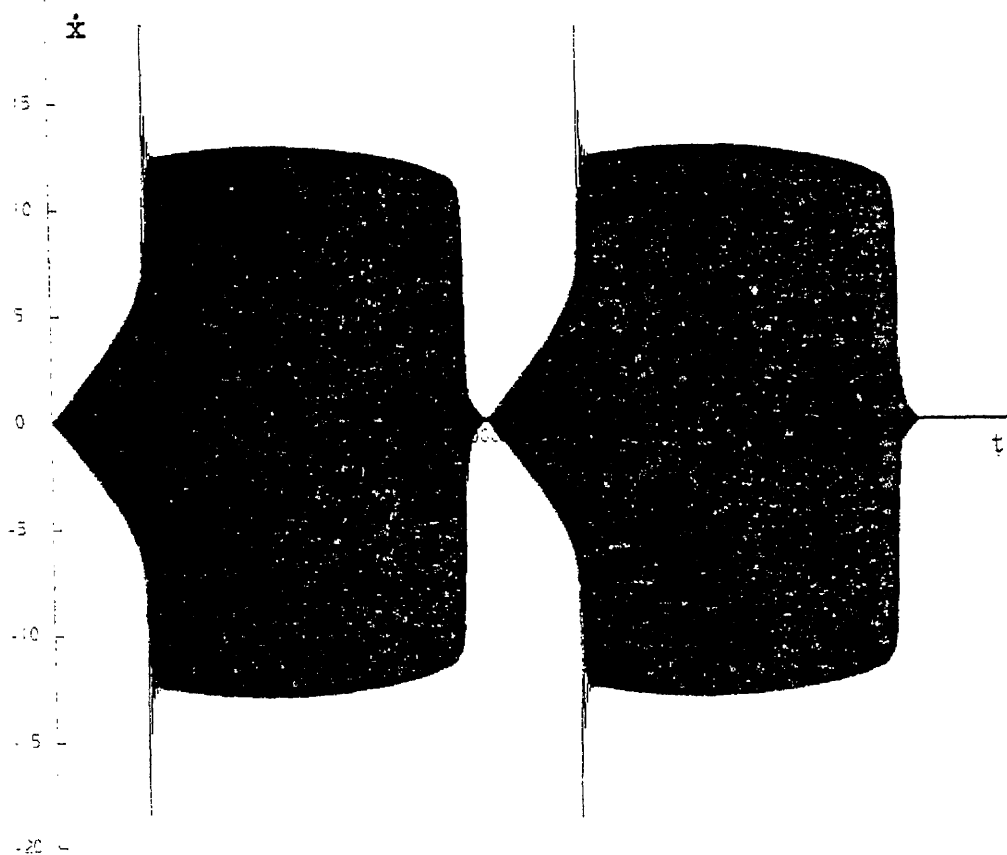


Figure 3.c

Response displacement and velocity of the Duffing equation

$\beta = 1.0$, $\omega_n = \pi$ and $\gamma = 0.1$

(Illustration of jump phenomenon)

number of sample records of $2K$ points each. The time duration of the records $T = 2K\Delta t$ determines the frequency resolution of the power spectrum, whereas the time interval Δt determines the highest frequency content of the signal.

The simulation process was tested for a linear system ($\beta = 0$) with the excitation data produced as described above. The response displacement and velocity records were processed and the response spectra obtained agreed with the linear theory.

However this method of producing excitation data was considered unsuitable for use in connection with the nonlinear system and an alternative method was devised. As it will be explained in the next section.

3.2 The excitation Spectrum

A random excitation signal may be thought of as composed of sinusoids of different frequencies. Such a signal will be used to obtain the response of the Duffing system through the numerical integration of equation (3-3). The discrete system tests showed that in order to obtain the correct output for a sinusoidal excitation, the input should be sampled at a rate of twelve points per cycle. If this rule is not observed then the input components which are under sampled, will be under estimated or even ignored by the integration. One of the reasons for this is the linear interpolation between input data points, which 'straightens the bends' and affects the r.m.s. of the signal. The excitation spectrum produced as described at the end of the previous section represents a signal whose highest frequency component is sampled at a rate of two points per cycle (Nyquist frequency). Thus the two processes (the FFT and the numerical integration) interpret the same signal in two different ways. In terms of power spectra, the FFT reproduces the true power spectrum Figure (4.a) whereas the numerical integration results would suggest an excitation spectrum as shown in Figure (4.b).

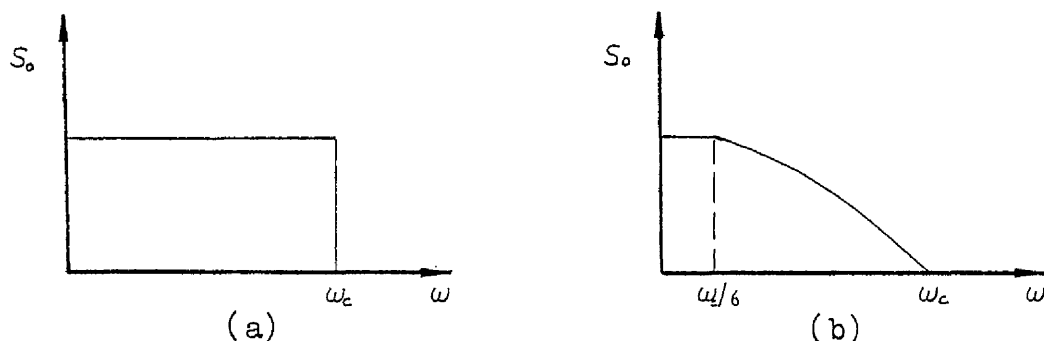


Figure 4

In the case of a linear system and for a constant number of data points per signal, Δt between points may be selected such that the frequencies of interest lay below $\omega_c/6$. In the case of the Duffing system however the frequencies of interest are not known precisely since the response spectrum shifts [10] with increased intensity of the input, and there is also the possibility of superharmonic resonance. One could use low pass filters to cut off the unwanted (under sampled) frequencies of the input, or use curve fitting techniques to increase the sampling rate. These are however

expensive techniques which also present their own problems. For a low pass filter, for example, a critically damped second order linear system would have to be integrated and its response used as excitation for the Duffing system. Instead it was decided to produce an input signal with a spectrum that could be 'seen' correctly by both the FFT and the numerical integration technique. This should produce an FFT spectrum which would look like Figure (4.c).



Figure 4c

Where ω_c is the Nyquist frequency (two points per cycle). It can be shown that by introducing a random phase angle $\varphi(\omega)$ with a uniform distribution between 0 to 2π to each term of a smoothed spectrum such as the one shown above an equivalent complex fourier transformation $F(\omega)$ can be calculated as follows

$$\begin{aligned} F(\omega_k) &= \frac{1}{2\pi} \sqrt{S(\omega_k)} e^{i\varphi_k} \\ &= \frac{1}{2\pi} (\sqrt{S(\omega_k)} \cos \varphi_k + i\sqrt{S(\omega_k)} \sin \varphi_k) \end{aligned}$$

from which (3-4)

$$F(t) = \frac{1}{2\pi} \int_{-\omega_c}^{\omega_c} F(\omega) e^{i\omega t} d\omega = \frac{1}{\pi} \int_0^{\omega_c} \sqrt{S(\omega)} \cos(\omega t + \varphi_k) d\omega$$

where $\varphi_k = \varphi(\omega)$ (3-5)

This is based on the concept that any random signal can be represented as an infinite series in the form

$$F(t) = \sum_n c_n \cos(\omega_n t + \varphi_n) \quad (3-6)$$

where the frequencies ω_n are distributed densely in the interval $(0, \infty)$, the phases φ_n are random and distributed uniformly between 0 and 2π , and the amplitudes c_n are such that in any small interval of frequency $d\omega$,

$$\sum_{\omega = \omega_n}^{\omega + d\omega} \frac{1}{2} c_n^2 = S(\omega) d\omega \quad (3-7)$$

where $S(\omega)$ is the energy spectrum of $F(t)$ and is a continuous function of frequency ω . S.O.Rice [1] has used this method to describe noise signal and obtain its statistical properties. There remains however the question of stationary and Gaussianity of this signal. These are answered in Appendix C, along with more details of the excitation signal production method and its properties.

3.3 Testing the Numerical Simulation for Random Excitation

The complete simulation, with the new input, was tested for a linear system and agreed with the theoretical predictions. The tests on the nonlinear output were the following.

A cross check of the displacement, velocity and acceleration spectra was made using the property of spectra

$$S\ddot{x}\ddot{x}(\omega) = \omega^2 S\dot{x}\dot{x}(\omega) = \omega^4 Sxx(\omega)$$

The acceleration spectrum was also calculated from data values using the relation

$$\ddot{x} = F(t) - 2\zeta\omega_n\dot{x} - \omega_n^2 (1+\beta x^2)x$$

An example of these comparisons may be seen in Figure 5.

The suitability of the Runge - Kutta - Merson numerical integration routine was compared with the more accurate (and more expensive) Adams routine, as follows. It can be seen from the previous section equation (3-6) that it is possible but very expensive, to represent the input in an exact continuous form and hence avoid the linear interpolation between the points and provide greater accuracy. The system was integrated using this form of input by both routines. The response values for the two methods agreed very well, (maximum recorded relative discrepancy 0.07%). Although the integration proceeded for only $1/40$ of the complete record normally used there is no reason why this argument should be affected for the complete record. The two routines were also used to integrate the system with the input in sampled form i.e. linear interpolation between points. As can be seen from Figures 6.a to 6.g., the Runge - Kutta - Merson routine agreed better with the previous integration of the same input in the continuous representation. A possible explanation for this is that the Adams routine being more accurate is also more sensitive to the linear interpolation between input points. It was not possible to obtain spectral estimations of the output obtained by integrating the system using the exact representation of input, because of the limited data obtained. As noted earlier the continuous representation of the input without the help of the linear interpolation between points is very expensive, this is due

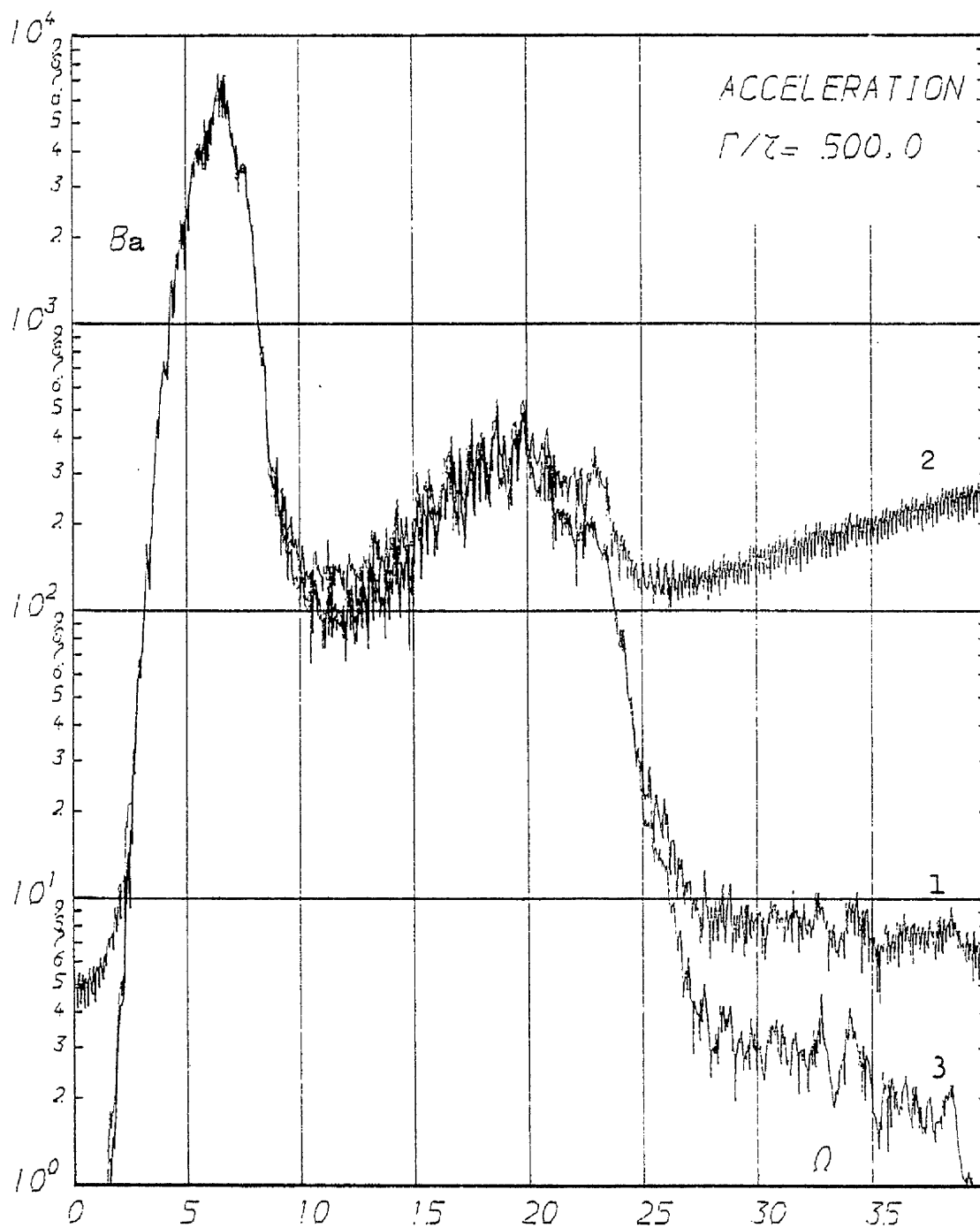


Figure 5

Response acceleration spectra of the
 Duffing system obtained through

$$S\ddot{x}\ddot{x}(\omega) = \omega^2 S\dot{x}\dot{x}(\omega) = \omega^4 Sxx(\omega)$$

and $\ddot{x} = F(t) - 2\zeta\omega_n \dot{x} - \omega_n^2(1+\beta x^2)x$

$$Ba = \beta S_{xx}(\Omega)/\omega_n^3$$

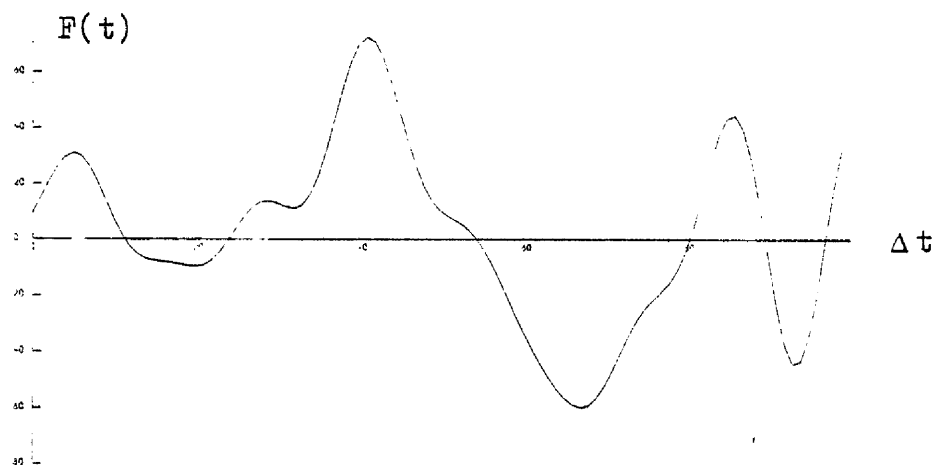
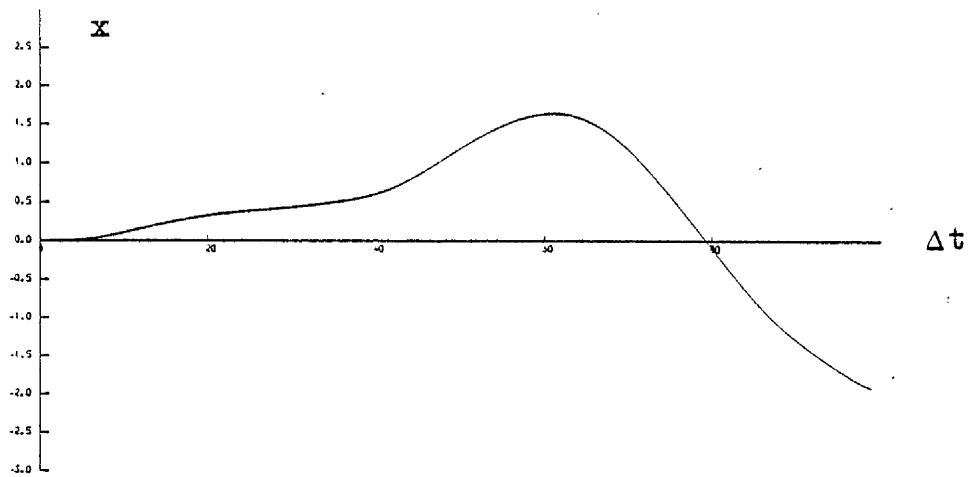


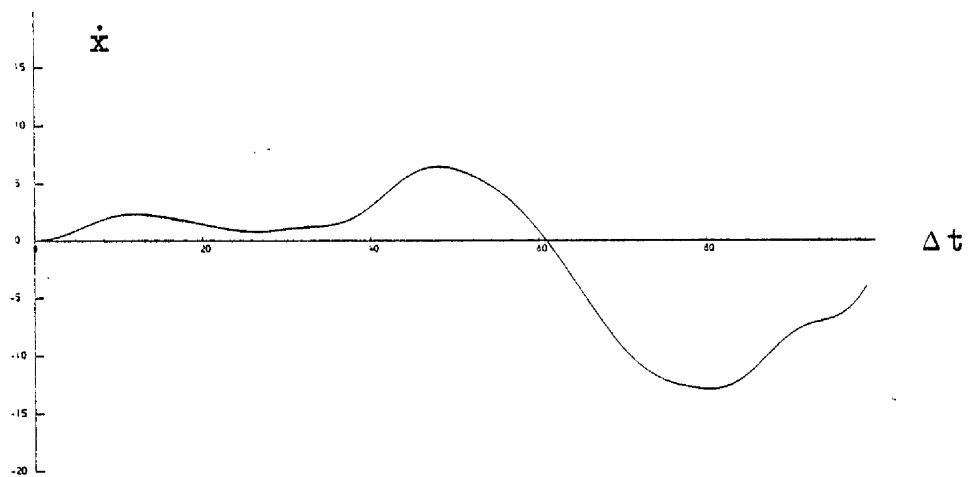
Figure 6a

Sample of excitation record (1/40 of T)

$$\Delta t = 0.01075$$



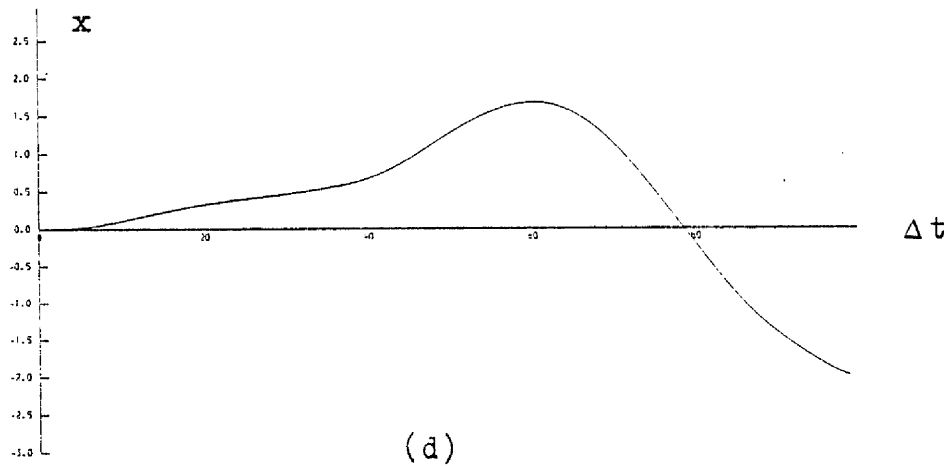
(b)



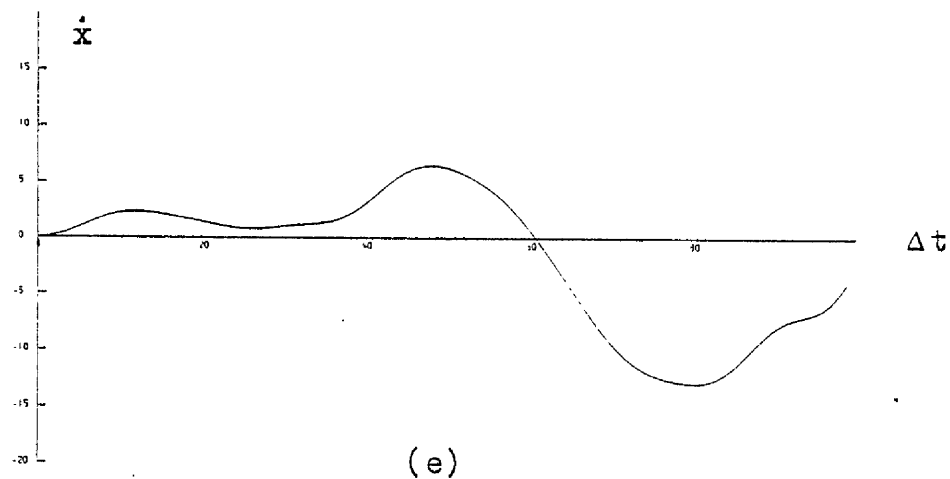
(c)

Figures 6b,c

Displacement and velocity response
using functional expression for
excitation data. Runge-Kutta-Merson
technique



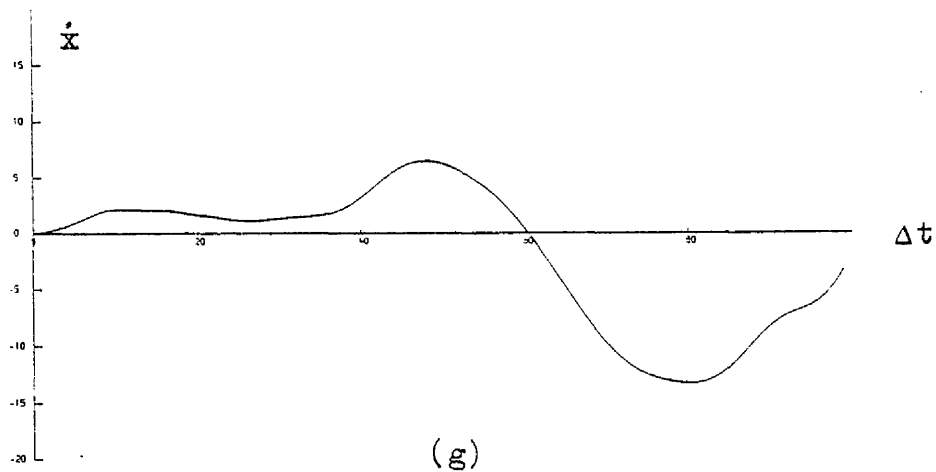
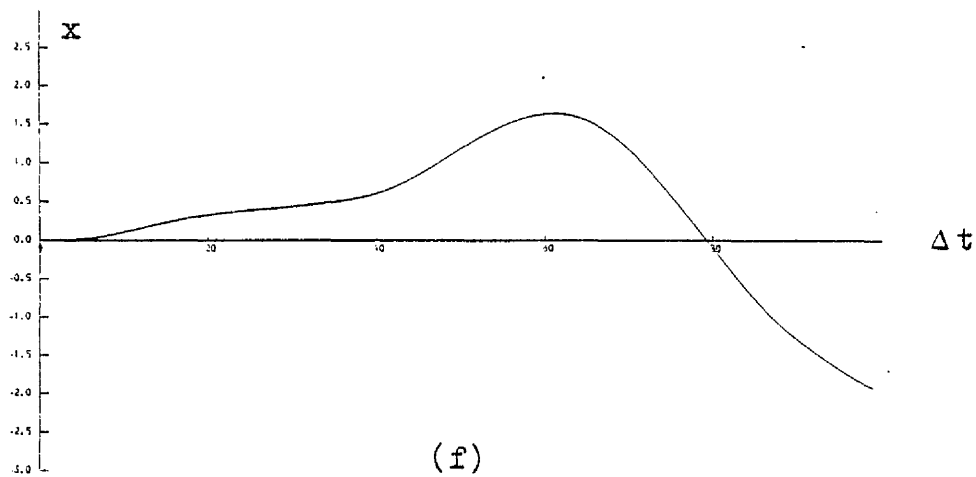
(d)



(e)

Figures 6d,e

Sampled excitation. Runge-Kutta
Merson integration technique



Figures 6f,g

As for Figures 8d,e. Adams
numerical integration technique

to the fact that sinusoidal values are relatively slow computer process and the number of evaluations is overwhelming (well over 340×4096 per realisation).

Finally, an important test was performed only after a certain amount of knowledge was obtained about the system using the simulation technique. It was established that there exists a maximum frequency of response (ω_c) which depends on the intensity of input, beyond which any input component is ineffective as far as the system is concerned. (Section 5.1). This implies that if ω_c is less than $\omega_c/6$ in Figure 4.b the response should not be affected by the curved part of the input spectrum since the system does not respond at these high frequencies ($>\omega_c$). The random number generating routine G05DD5 described in Section 3.1 was used to produce data that conformed with the above restrictions. The response of the system to this input agreed with the response obtained using input data produced with the method described in Section 3.2. This comparison proved that the two inputs are compatible under the conditions mentioned above and also to some extent the existence of the aforementioned frequency. (ω_c)

CHAPTER 4

THE NON - DIMENSIONAL FORM OF THE DUFFING SYSTEM

The existence of the well-known transfer function for the linear system makes it possible that one can visualise the behaviour of the linear response fairly accurately just by looking at the values of stiffness, damping, mass and the form of excitation for the particular system. On the other hand, in the case of the nonlinear system, even if one knew all the system parameters there is no simple way of obtaining the information on the nonlinear response. The description of the response is further complicated by the increase of the system parameters due to the nonlinear terms.

In this chapter the dimensional analysis technique will be applied to the Duffing system under sinusoidal and random excitations. The dimensional analysis promises to reduce the number of independent variables by three (Section 1.5). The advantages of being able to obtain even a rough guidance on the behaviour of a system by thinking in terms of two variables instead of five ($m, k, c, \beta, F(t)$) are self evident. It is hoped that the presentation of response properties of the system in non-dimensional form will provide a better understanding of the properties of the system and also make best use of the numerical simulation results by transforming them into more versatile general qualities whose effects will be more easily interpretable. Further it is always possible to revert to dimensional qualities if required.

4.1 The Deterministic System

Consider the response governed by the equation

$$m\ddot{x} + c\dot{x} + k(x + \beta x^3) = F_0 \cos(\omega t + \varphi) \quad (4-1)$$

The amplitude response x is given approximately by the relation (Appendix A)

$$\left[\left(1 + \frac{3}{4}\beta x_0^2 - \Omega^2\right)^2 + (2\zeta\Omega)^2 \right] x_0^2 = \bar{F}_0^2 \quad (4-2)$$

where $\Omega = \omega/\omega_n$, $\omega_n = \sqrt{k/m}$, $\bar{F}_0 = F_0/m\omega_n^2$ and $\zeta = c/2\sqrt{km}$

The non-dimensional form of equation (4-2) is simply

$$\left(1 + \frac{3}{4}\beta x_0^2 - \Omega^2\right)^2 + (2\zeta\Omega)^2 = \frac{\bar{F}_0^2}{x_0^2} = \frac{F_0^2}{m^2 \omega_n^4 x_0^2} = \frac{F_0^2}{k^2 x_0^2} \quad (4-3)$$

This provides the following independent non-dimensional groups

$$\beta x_0^2, \frac{\omega}{\omega_n}, \text{ and } k^2 x^2 / F_0^2$$

A further independent combination is also possible $\beta F_0^2 / k^2$. For fixed damping ratio ($\zeta = \text{constant}$) each of the quantities x_0, β, F_0 can be treated as an independent variable. Thus the non-dimensional group $\beta F_0^2 / k^2$ may be used as index either of F_0 or of β the other being assumed fixed. If for example this quantity is used as a measure of the effect of β on the response, the relation

$$k^2 x^2 / F_0^2 = \varphi \left[\beta F_0^2 / k^2, \omega/\omega_n, \zeta \right] \quad (4-4)$$

should be used (Figure 7). If on the other hand $\beta F_0^2 / k^2$ is used to show the effect of F_0 on the response, the relation

$$\beta x_0^2 = \phi \left[\beta F_0^2 / k^2, \omega/\omega_n, \zeta \right] \quad (4-5)$$

should be used (Figure 8). Thus it is possible to combine the non-dimensional groups in relations that will make the effects of changes in particular parameters of the system directly observable. It is emphasised that both the non dimensional plots Figures (7,8) and a dimensional one from which the former may be derived contain the same information, each being readily convertible in any other. The notable difference however being, in the case of the non-dimensional plots, the ease of interpretation. Equally important is the fact that the behaviour of the system can be completely

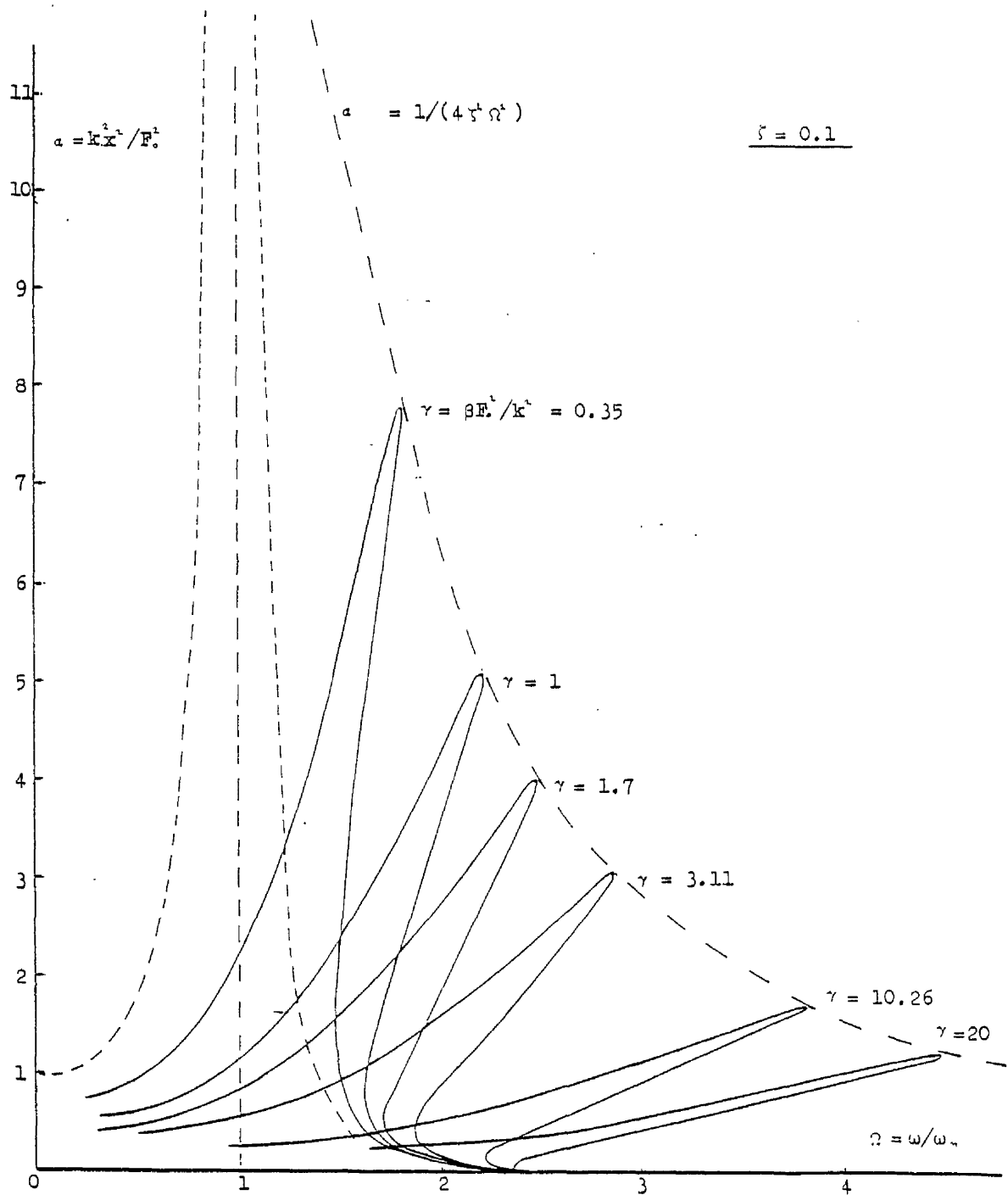
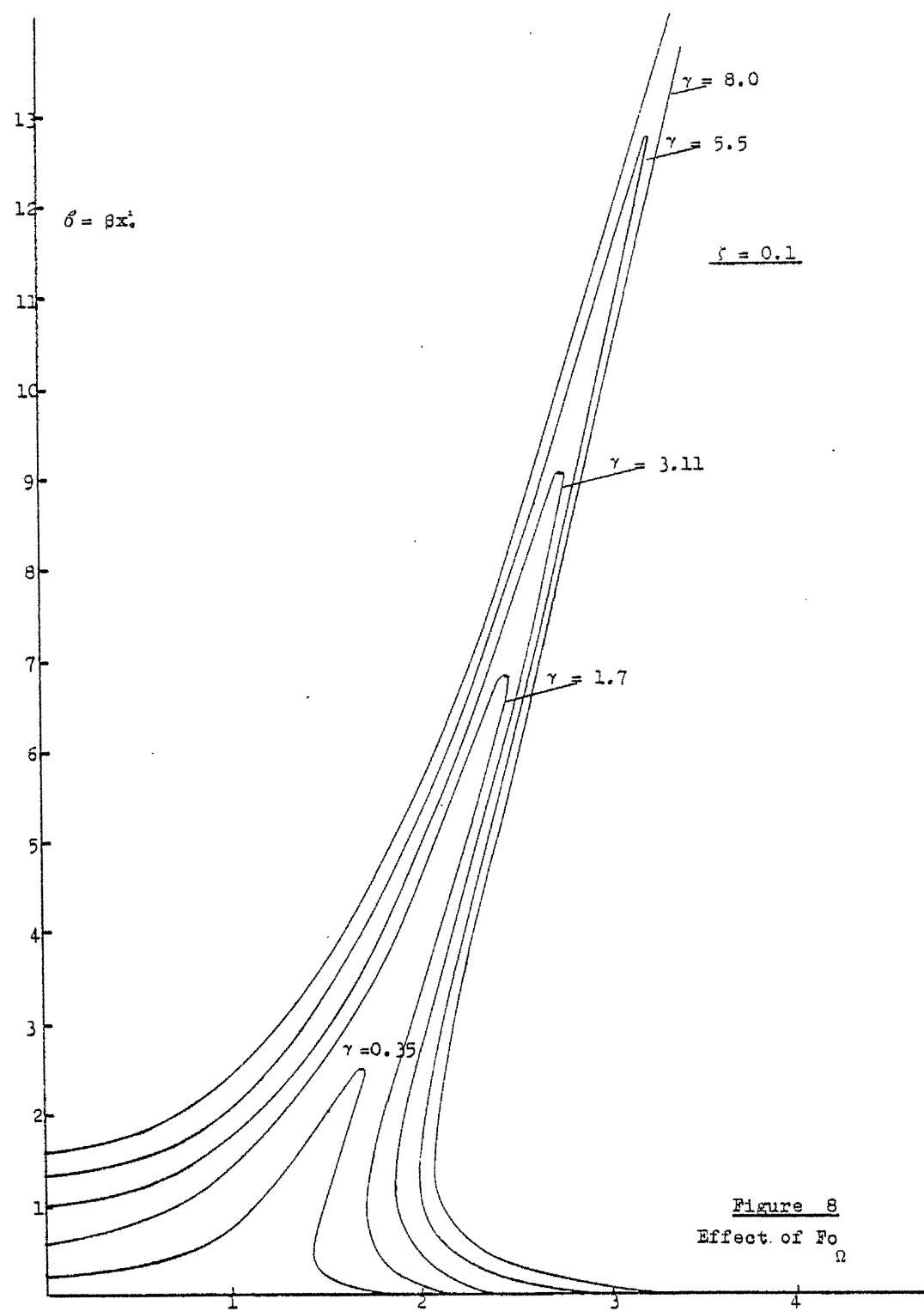


Figure 7
 Non-dimensional response displacement under sinusoidal excitation
 Effect of β



described through just two parameters $\beta F_0^2/k^2$ and ζ . For example, the quantity βx_0^2 which is a measure of the system nonlinearity, (i.e. the deviation from the linear stiffness law), has a unique relation with the quantity $\beta F_0^2/k^2$ expressed by equation (4-5), so does the resonant frequency and the frequencies where jumps may occur. Thus if the quantity $\beta F_0^2/k^2$ is kept constant in the system, while its individual parameters (with the exception of ζ) are changed, the system will exhibit the same nonlinear properties. An increase in the value of $\beta F_0^2/k^2$ implies an increase in nonlinear behaviour, provided that ζ is kept constant and the opposite is also true.

The following symbols will be reserved for the non dimensional quantities of the Duffing system under sinusoidal excitation.

$$a = k^2 x_0^2 / F_0^2$$

$$\delta = \beta x_0^2$$

$$\gamma = \beta F_0^2 / k^2$$

4.2 The Duffing System Under Broad Band Random Excitation

Consider the response governed by the equation

$$m\ddot{x} + c\dot{x} + k(x + \beta x^3) = F(t) \quad (4-6)$$

The excitation $F(t)$ at the first stage of this investigation is to be a Gaussian broad band stationary random process. Such an excitation is characterised by its spectral density $S_F(\omega)$, and its cut off frequency ω_c . Figure 9.

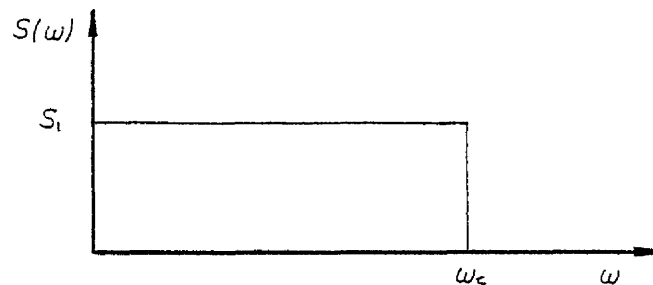


Figure 9

The spectral density of the response displacement $x(t)$ is to be investigated. Hence the parameters of interest are the following. (Their dimensions in brackets)

$$\left. \begin{array}{ll} S_x(\omega) & (L^2 T) \\ S_1 & (M^2 L^2 T^{-3}) \\ \omega & (T^{-1}) \\ \omega_c & (T^{-1}) \end{array} \right\} \begin{array}{ll} m & (M) \\ c & (MT^{-1}) \\ k & (MT^{-2}) \\ \beta & (L^{-1}) \end{array} \quad (4-7)$$

From these the following non-dimensional groups may be constructed.

$$\Omega = \omega \sqrt{k/m}, \quad \Omega_c = \omega_c \sqrt{k/m}, \quad \zeta = c/2\sqrt{mk}$$

and $A(\Omega) = k^2 S_x(\Omega) / S_1, \quad B(\Omega) = \beta S_x(\Omega) \sqrt{k/m}$

The group $\Gamma = \beta S_1 \sqrt{mk^3}$ will also be found useful. This may be thought of as an equivalent quantity to the non-dimensional group $F^2 \beta / k^2$ of the deterministic system. This similarity is however only apparent and will be discussed further in the discussion to this chapter.

The plot of response spectra and other statistical quantities is sought in a way which will bring out the influence of

changes in the nonlinearity parameter β , excitation intensity S , excitation band width ω , etc. As response parameters the non-dimensional groups of either $k^2 S_x / S_1$ or $\beta S_x \sqrt{k/m}$ can be used, where the choice will depend on the influence which is to be brought out and under the same considerations used in the deterministic case. Thus the following relationships of the form

$$k^2 S_x(\omega) / S_1 = \Phi(\beta S_1 / \sqrt{mk^3}, c/2\sqrt{km}, \omega_c / \sqrt{k/m}, \omega / \sqrt{k/m}) \quad (4-8)$$

$$\text{or} \quad A = \Phi(\Gamma, \zeta, \Omega_c, \Omega)$$

$$\text{and } \beta S_x(\omega) \sqrt{k/m} = \Psi(\beta S_1 / \sqrt{mk^3}, c/2\sqrt{km}, \omega_c / \sqrt{k/m}, \omega / \sqrt{k/m}) \quad (4-9)$$

$$\text{or} \quad B = \Psi(\Gamma, \zeta, \Omega_c, \Omega)$$

can be assumed. In equation (4-8) the group $k^2 S_x(\omega) / S_1$ is a convenient response parameter and variations of the group $\beta S_1 / \sqrt{mk^3}$ may be used to illustrate changes in β . In equation (4-9) the response parameter $\beta S_x(\omega) \sqrt{k/m}$ is used and the same variations of the group $\beta S_1 / \sqrt{mk^3}$ may be used to illustrate the effects of changes in S_1 . The influence of the damping and the band width which arise from the groups $c/2\sqrt{km}$ and $\omega_c / \sqrt{k/m}$ should be investigated separately. Hence the spectral response relations may be plotted, for each given value of damping, in the manner shown in Figures (10,11)

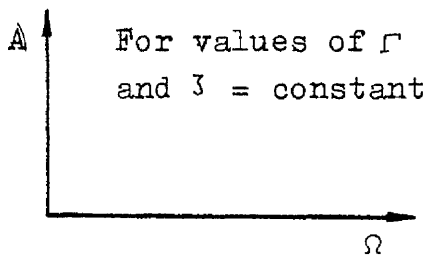


Figure 10

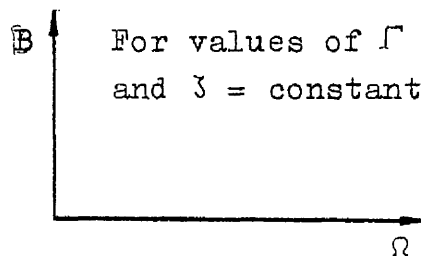


Figure 11

For any single value of $\beta S_1 / \sqrt{mk^3}$ i.e. for any single curve on Figure (11) one can integrate $\beta S_x(\omega) \sqrt{k/m}$ over the range $0 < \omega / \sqrt{k/m} < \infty$ to obtain

$$\beta \sigma_x^2 = \beta \int_0^\infty S_x(\omega) d\omega = \int_0^\infty \beta S_x(\Omega) \sqrt{k/m} d\Omega \quad (4-10)$$

where $\Omega = \omega/\sqrt{k/m}$.

The resulting values for $\beta\sigma_x^2$ can then be plotted against the corresponding values of $\beta S_1/\sqrt{mk^3}$, to obtain a separate curve for each value of damping. This implies that there is a fixed relationship connecting $\beta\sigma_x^2$, $\beta S_1/\sqrt{mk^3}$ and ζ , of the form

$$\beta\sigma_x^2 = \Xi_1[\beta S_1/\sqrt{mk^3}, \zeta] \quad (4-11)$$

$$\text{or} \quad \beta\sigma_x^2 = \Xi_2[\Gamma, \zeta]$$

Once the form of equation(4-11) has been established the magnitude of $\beta\sigma_x^2$ for any given combination of S_1, k, m, β and ζ is determined. In fact looking back on equation (2-10) derived from the Fokker - Planck equation

$$\begin{aligned} \langle x^2 \rangle &= \int_{-\infty}^{\infty} x^2 P(x) dx \\ \langle x^2 \rangle &= c \int_{-\infty}^{\infty} x^2 \exp \left(- \frac{\zeta \omega_n^3}{\pi S_1} (2x^2 + \beta x^4) \right) dx \end{aligned} \quad (4-12)$$

$$\text{but } S_1 = S_0/m^2 \text{ and } \frac{\zeta \omega_n^3 m^2}{\pi S_1} = \frac{\beta}{\beta} \frac{\sqrt{mk^3}}{\sqrt{mk^3}} = \beta \zeta / \pi \beta S_1 / \sqrt{mk^3} = \beta \zeta / \Gamma \pi$$

hence the non-dimensional form of equation (4-12) is

$$\beta \langle x^2 \rangle = c \int_{-\infty}^{\infty} \beta x^2 \exp \left(- \zeta / \Gamma \pi (2\beta x^2 + \beta^2 x^4) \right) dx \quad (4-13)$$

which shows a unique relationship of the form

$$\beta\sigma_x^2 = \Xi_2[\Gamma/\zeta] \quad (4-14)$$

The occurrence of the ratio of the two non-dimensional groups in the probability density function shows that for Gaussian (white noise) excitation the second moment of the response displacement can be described in terms of a single non-dimensional parameter namely the ratio Γ/ζ . Whether this holds true for the spectral response is yet to be investigated in chapter 5.

Finally, regarding the velocity and acceleration non-dimensional quantities related to the corresponding spectral values, these can be defined as follows.

$$A_v = k^2 S_{\ddot{x}} / S \omega_n^2 \quad A_a = k^2 S_{\ddot{x}} / S_1 \omega_n^4$$

$$B_v = \beta S_{\ddot{x}} / \omega \quad B_a = \beta S_{\ddot{x}} / \omega_n^3$$

where $\omega_n = \sqrt{k/m}$.

These quantities are expected to depend on the same parameters on which the corresponding displacement quantities depend as per equations (4-8), (4-9). However once the response displacement spectrum is obtained it is a simple matter to obtain the response velocity and acceleration spectra through the relation

$$S_{\dot{x}}(\omega) = S_{\ddot{x}}(\omega) \omega^2 = S_x(\omega) \omega^4$$

4.3 Discussion

The responses of the Duffing system are conveniently plotted by making use of the non-dimensional groupings outlined above. This is so whether excitations are at a discrete frequency or random. Further the groupings in the two cases do at first seem remarkably similar. These similarities however are only superficial and the groupings are in fact extremely different. Specifically the response relationships in the two cases are as follows.

$$k^2 x_o^2 / F_o^2 = \varphi_1 (\beta F_o^2 / k^2, \omega / \sqrt{k/m}) \quad (4-15)$$

for the discrete system

$$k^2 S_{xx}(\omega) / S_{xx} = \varphi_2 (\beta S_{xx} / \sqrt{mk^3}, \omega / \sqrt{k/m}) \quad (4-16)$$

for the random. Where in these equations the rest of the groups are assigned constant values. Comparisons can only be made if some relation is established between $\beta F_o^2 / k^2$ and $\beta S_{xx} / \sqrt{mk^3}$ and between $k^2 x_o^2 / F_o^2$ and $k^2 S_{xx}(\omega) / S_{xx}$. No such equivalence exists and the only common parameter in the two equations is the frequency. This eliminates any hope of obtaining enlightenment about the random responses from the better known results for sinusoidal excitation.

Regarding the system under band limited or high pass filtered excitation processes equations (4-8), (4-9) still apply. The influence and the meaning of the term however changes. This is further discussed in chapter 6.

Finally it should be made clear that the non-dimensional form of the response displacement in the time domain is $\sqrt{\beta} x(t)$.

CHAPTER 5

RESPONSE TO BROAD BAND EXCITATION

With reasonable confidence on the simulation procedure having been established, specific problems regarding the response of the Duffing system, were setup for investigation. The theoretical concept of ideal white noise excitation in general leads to considerable simplification of the mathematical analysis involved in theoretical response prediction methods. In order however for the analysis to change from an interesting exercise of higher mathematics to a practical response prediction method, this type of excitation should be compared to more realistic ones. The Fokker - Planck approach assumes stationarity of the response of the Duffing system under white noise excitation, and produces its joint probability density function under such excitation. The simulation procedure on the other hand can produce samples of the response to a broad band signal of given frequency cut-off. Thus a question arises, as to how wide the band width must be before the findings of the Fokker - Planck approach apply to the more realistic broad band excitation. The question of stationarity of the output is also very important not only as a check of comparability of the two methods but also as a property of the response of the system for a given excitation. These questions are the subject of Sections 5.1 and 5.2. The description of the displacement response spectrum, as calculated through the simulation procedure, is the subject of Section 5.3. In the next section an attempt is made to link the properties described in Section 5.3 to existing theory and to compare the simulation derived statistical properties with the corresponding ones obtained through the Fokker - Planck approach. Finally in Section 5.5 the spectral properties are used to provide a simple means of sketching an approximate shape for the response displacement spectrum of the system under broad band Gaussian random excitation.

5.1 Excitation Spectra. Broad Band Excitation as an Approximation to White Noise.

It should be restated here that the aim of this project is to investigate the response of the Duffing system under broad band excitation. The purpose of this section is simply to investigate the comparability of the Fokker - Planck approach to the simulation process.

In numerical simulation white noise can only be approximated by a 'suitably' broad band signal. In the case of a linear signal for example a broad band signal of frequency cut-off ω_c is suitable to simulate white noise excitation, if ω_c is such that

$$\int_{\omega_c}^{\infty} |H(\omega)|^2 S_1 d\omega \approx 0$$

where S_1 is the intensity of the white noise excitation and $H(\omega)$ is the transfer function of the linear system. In the case of a nonlinear system however the possibility of sub or superharmonic excitation or more complicated mixed frequency responses may be expected. This coupled with the absence of a transfer function for the Duffing system, require more careful justification for the use of broad band signals to simulate white noise excitation or vice versa.

Manning [24] has predicted, using the heuristic approach and analog computer simulations that the resonant frequency of the response spectra of the Duffing system under white noise excitation will shift to higher frequencies as the intensity of excitation is increased. The equivalent linearization technique seems to suggest this too. Thus the starting point of this investigation is to observe the effect on the response of the Duffing system under a broad band excitation of given intensity and different frequency cut offs.

Looking back in Section 4.2 a measure of excitation intensity and hence nonlinearity is given by the non-dimensional parameter $\Gamma = \beta S_1 \omega_n / k^1$. A series of programs were run to obtain the response of the system under broad band excitation for a fixed value of β and a range of cut-off frequencies $\Omega_c (= \omega_c / \omega_n)$.

The process was repeated for selected values of Γ and different values of damping ζ . The range of frequency cut offs in some early cases varied from $6\omega_c$ to $70\omega_c$. No significant changes were observed in the spectral values or the statistical estimations of the mean, variance, third and fourth moments of the response. Further the probabilistic information obtained through the simulation process agreed very well with the corresponding predictions of the Fokker Planck approach.

Examples are shown in Table 5.1. The numbers in brackets are the variance of the estimations over the forty realisation used in each case. It is seen here that as Ω_c increases the estimations become less consistent (numbers in brackets). This is due to the fact that the record length is shortened for increased Ω_c with constant number of points per record

Table 5.1

$\Gamma/\zeta \backslash \Omega_c$	6	10	20	∞	
10, $\zeta=0.2$	1.65(0.07)	1.67(0.04)	1.7(0.4)	1.65	$\beta\sigma_x^2$
	2.27(0.006)	2.25(0.025)	2.23(0.04)	2.28	Ku
160, $\zeta=0.01$	7.35(6.6)	7.37(6.3)	7.02(14.0)	7.30	$\beta\sigma_x^2$
	2.13(0.03)	2.05(0.04)	2.06(0.05)	2.20	Ku

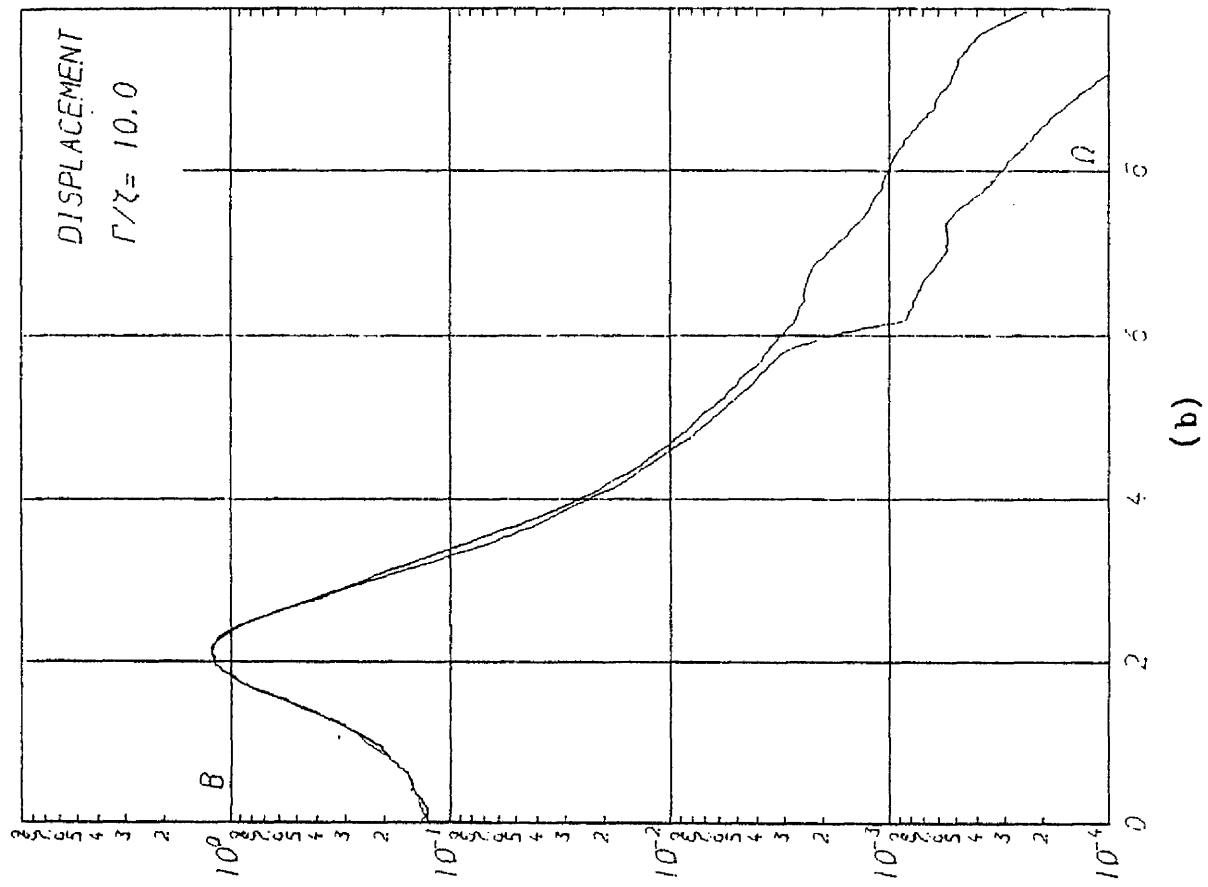
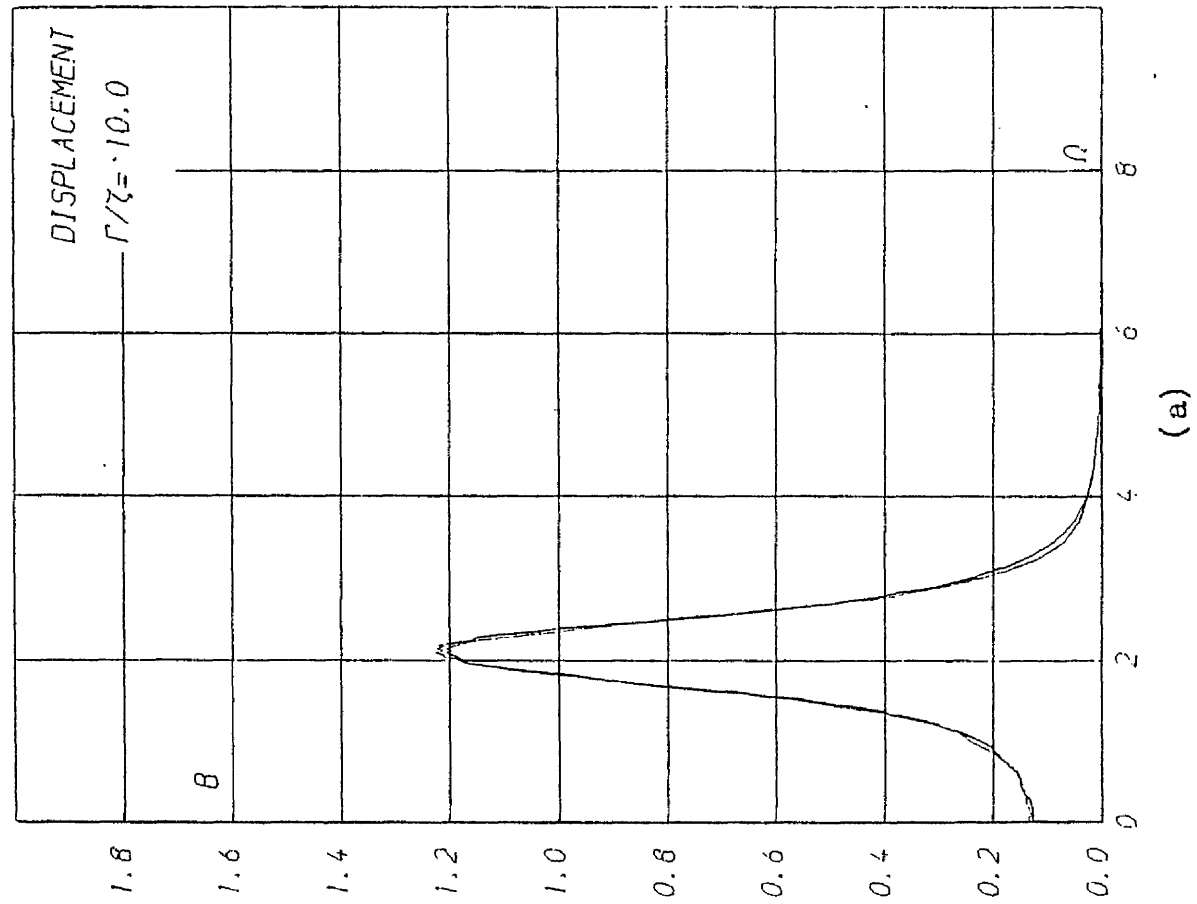
Harmonic response in the form third harmonic to the frequency was observed at a constant 3 orders of magnitude less than the resonant peak for the displacement spectra. Further it was observed that when ω_c moved below the range of frequencies where the third harmonic excitation occurred the change in the response was insignificant (to a varying degree for displacement, velocity and acceleration responses as was to be expected). This was further justified by the work done in the case of band limited excitation (Chapter 6), which proved that ω_c has to slice a major part off the range of response frequencies which are excited by a broad band signal of the same intensity, before any significant deviations are observed from 'normal' behaviour of the system. The term 'normal' is used here to describe the pattern for the response

of the system to broad band excitation as it is described in Section 5.3. Figures 12.a,b show the non-dimensional smoothed spectral response displacement and velocity of the Duffing system under a broad band excitation of the same intensity (Γ) and two different band widths.

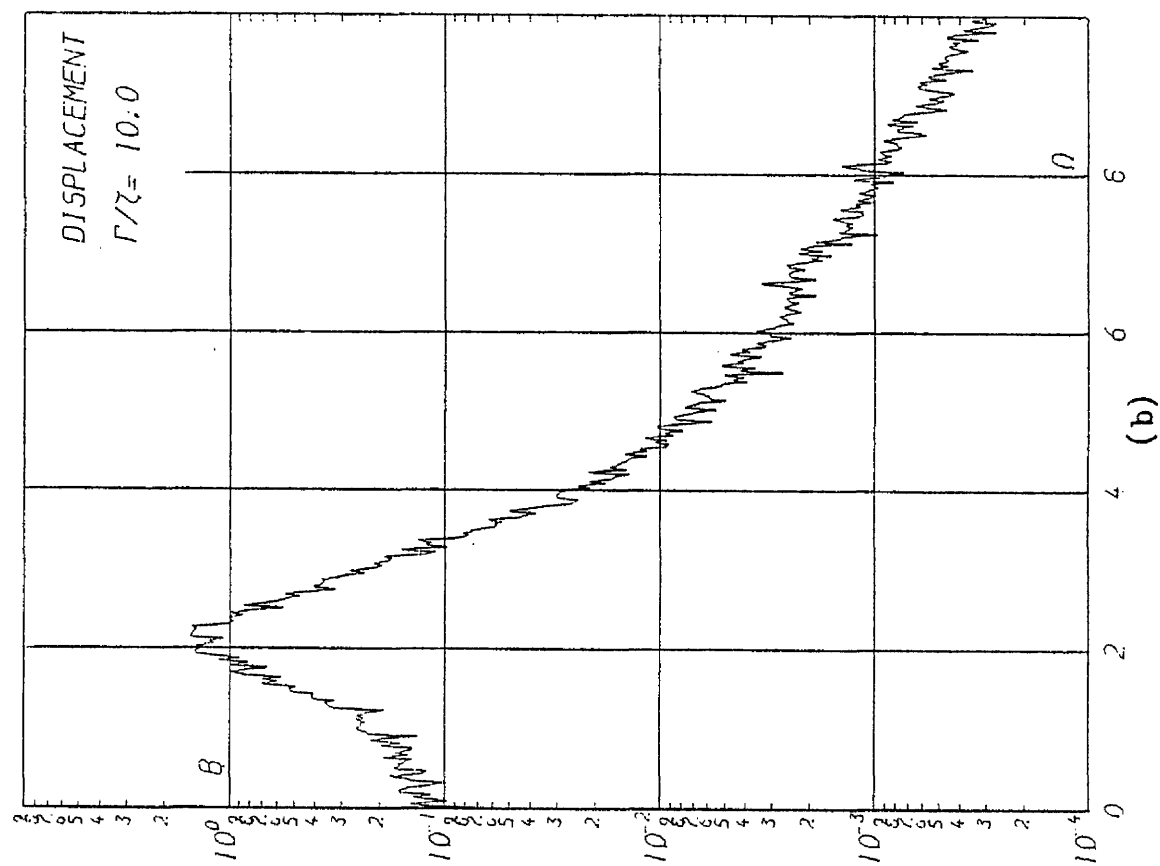
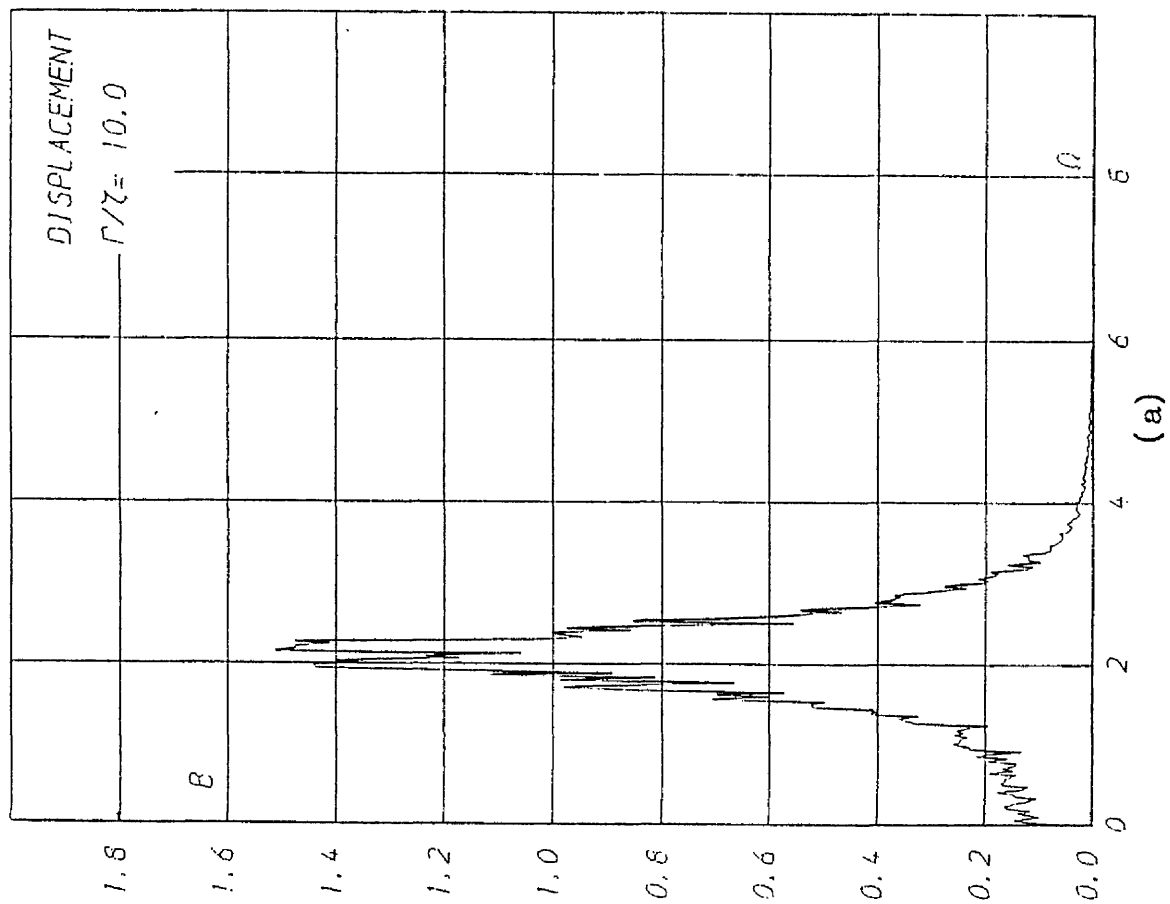
Hence it was established that there can be a 'limit frequency' ω_L such that given a broad band signal with cut off frequency $\omega_c \geq \omega_L$, the response of the Duffing oscillator to this broad band signal is to a good approximation the same as to a white noise signal of the same intensity. The non-dimensional form of the limit frequency will be $\Omega_L = \omega_L/\omega_n$ where ω_n is the natural frequency of the linear system, i.e. $\omega_n = \sqrt{k/m}$. Of course ω_L cannot be precisely defined (the same is also true with the linear system). However the following hypothesis provided a criterion for an evaluation of Ω_L for different intensities of input and damping ratios. It was assumed that any spectral value of the response displacement which is less than $1/100^{\text{th}}$ of the peak value of the smoothed spectrum is insignificant i.e. Ω_L is found where

$$S_{\ddot{x}}(\Omega_L) = S_{\ddot{x}}(\Omega_r)/100$$

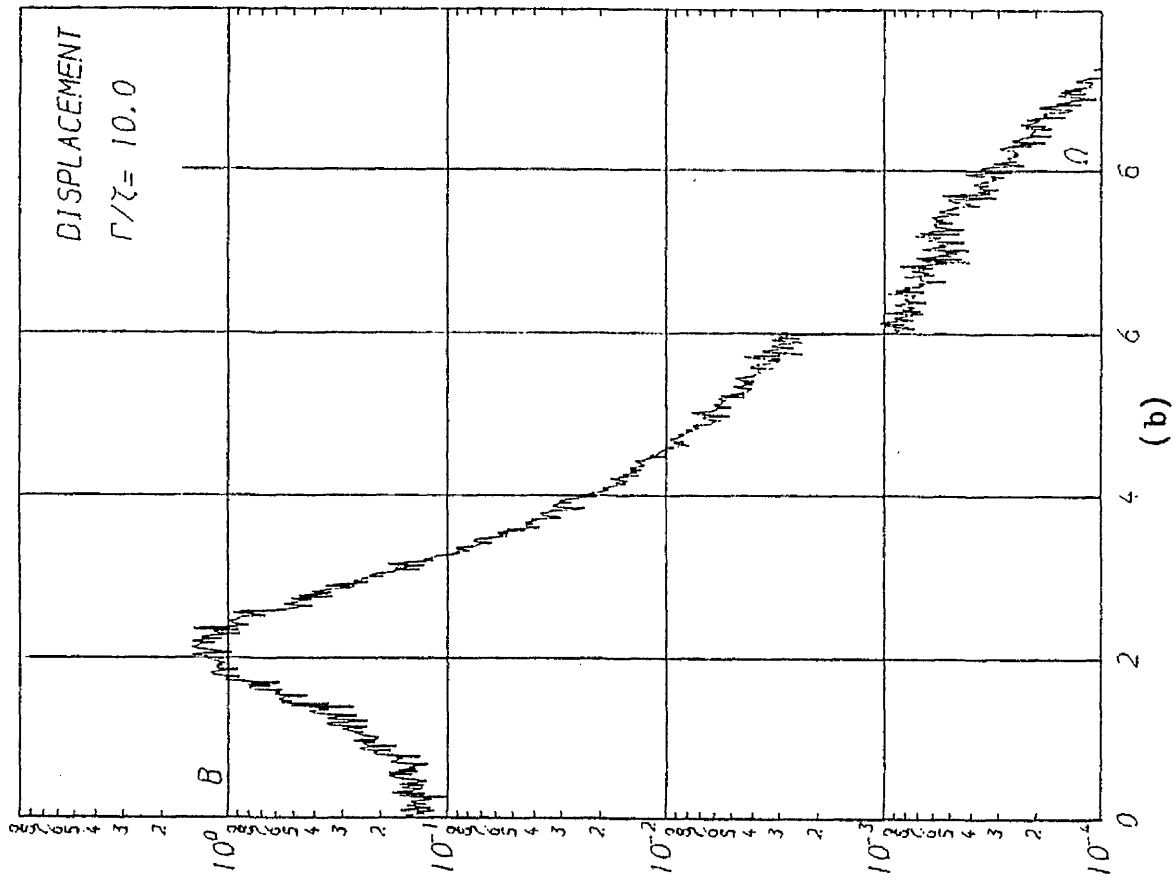
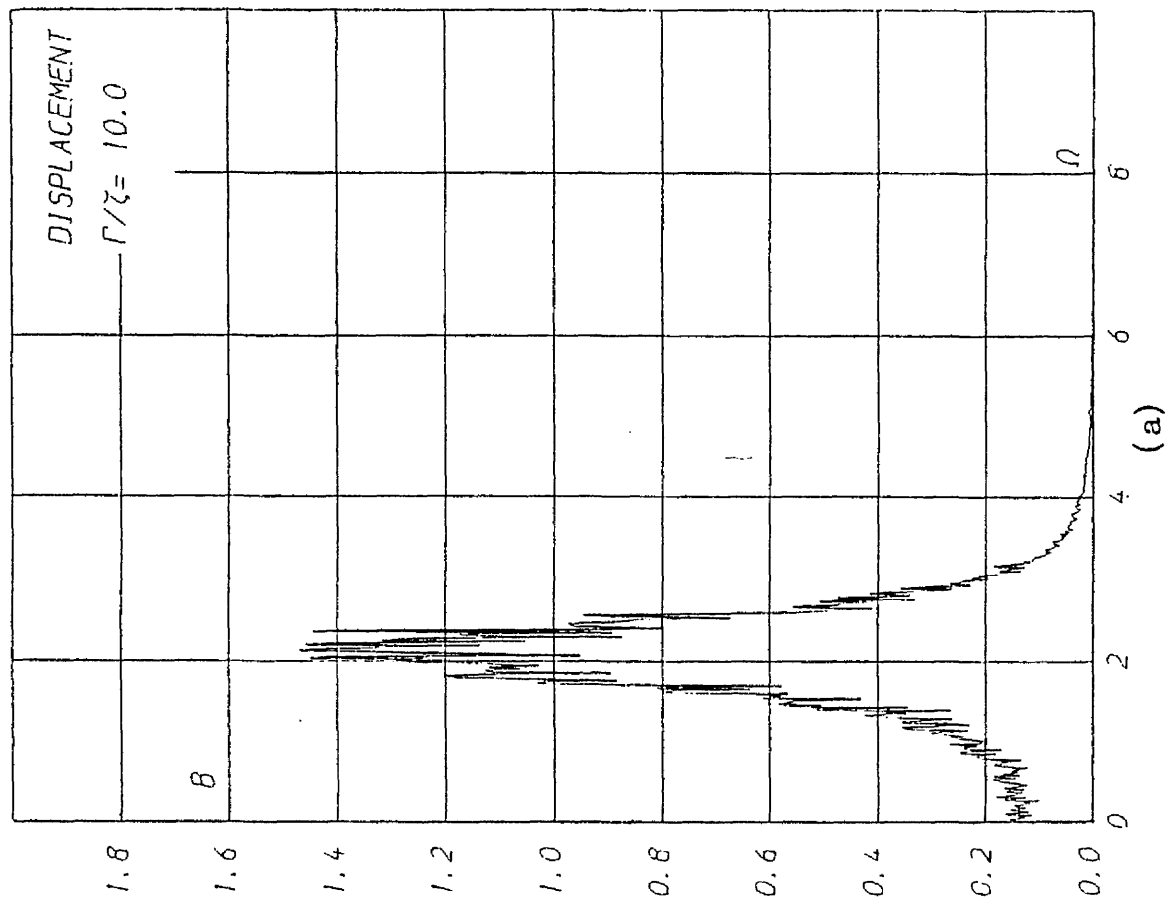
where Ω_r is the abscissa of the maximum value of the smoothed displacement spectrum. The response remains practically the same for values of ω_c much larger than the one defined above. As mentioned earlier third harmonic response was observed with a magnitude approximately $S_{\ddot{x}}(\Omega_r)/1000$, hence the broad band signal with frequency cut off $\omega_c = \omega_L$ will give a distorted picture of the third harmonic part of the response. However the advantage of having $\omega_c \approx \omega_L$ are greater frequency resolution and more reliable statistics through longer records. The disadvantage is increased computer time. This can be seen in Figures 13,14 where the unsmoothed form of the spectra of Figure 12 are shown. Figure 14 has a greater frequency resolution as a result of the reduced band width of the excitation and the constant number of points in each realisation. The corresponding computer time involved to produce the two responses is 7.16 and 8.84 seconds respectively. The cut off frequencies can be clearly seen in the logarithmic Figures 13b and 14b at $\Omega = 6, 10$. The slope at $\Omega = 6$ in



Figures 12a,b Smoothed displacement spectra for $\Omega_c = 6, 10$



Figures 13a,b Unsmoothed displacement spectra $\Omega_c = 10, \Delta f = 0.0147$



Figures 14a,b Unsmoothed displacement spectra $\Omega_c = 6$, $\Delta f = 0.0088$

Figure 12b is due to the smoothing process of the spectrum and is much sharper in reality as can be seen from Figure 14. In Figure 12b a small third harmonic response can also be observed. The above observations will be noticable through out the spectral response curves to be presented in this chapter. Not all the response spectra presented in the following sections were obtained for $\Omega_c = \Omega_u$. This is due to the fact that knowledge of the ω_u value can only be obtained from the simulation process itself.

In retrospect however one can state a rule of thumb regarding the range of cut off frequencies a broad band can have in order that the probabilistic information of the Fokker-Planck equations apply to the response. In Section 5.4 a simple relationship will be developed between the excitation parameter Γ , the damping coefficient ζ and the resonant frequency of the response displacement spectrum Ω_r . Using this relationship and the observations regarding the third harmonic response outlined in this section one can confidently expect the findings of the Fokker - Planck approach to be valid for a broad band excitation if $\Omega_c \geq 3\Omega_r$. Figure 15 shows a plot of Ω_u versus Γ/ζ for different values of ζ evaluated using the criterion $(S_{\ddot{x}}(\Omega_u) = S_{\ddot{x}}(\Omega_r)/100)$ outlined earlier.

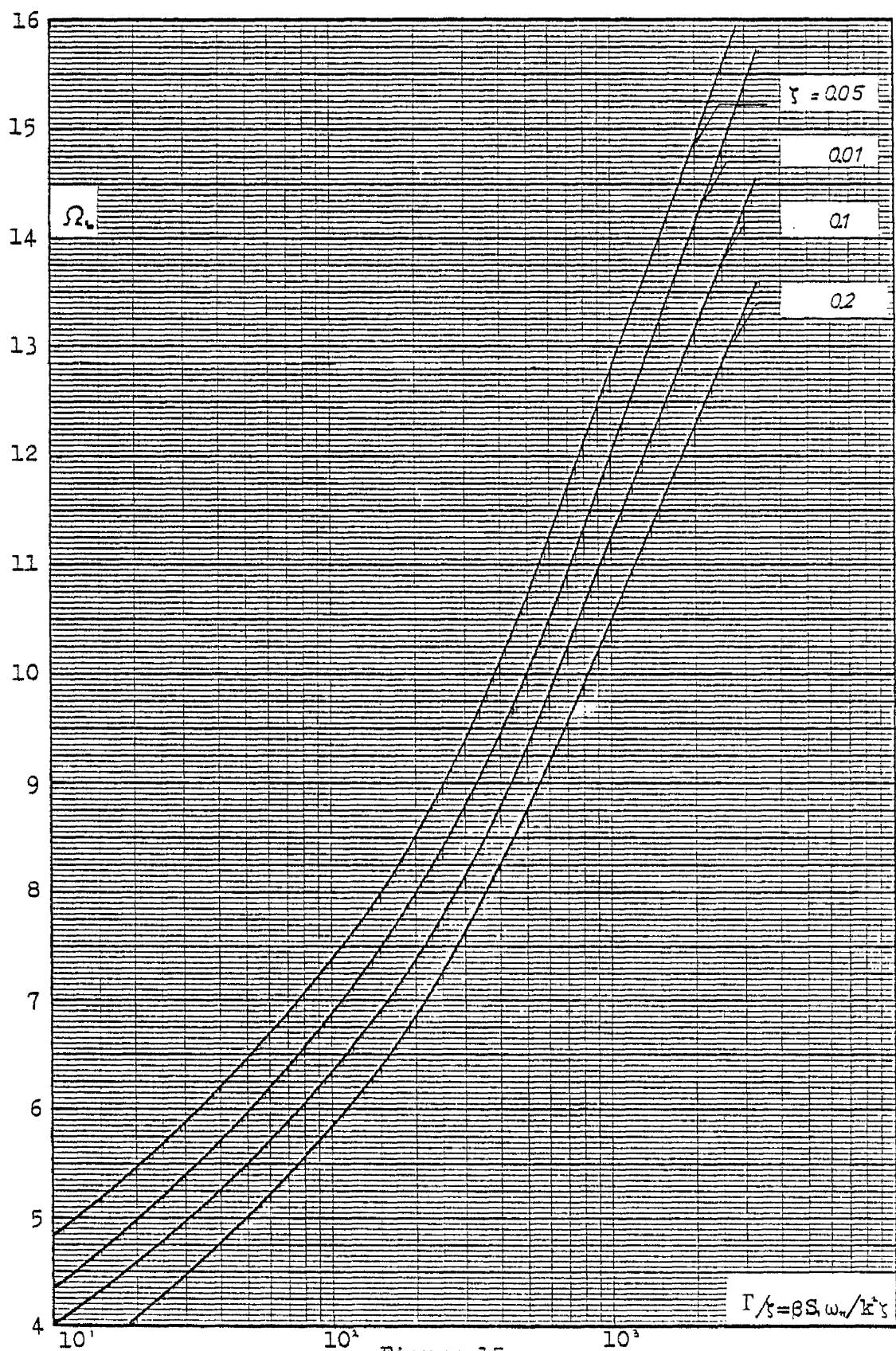


Figure 15
The Limit Frequency Ω_L

5.2 Stationarity of Response. The Autocorrelation Function

One of the criteria of stationarity of a signal is the invariance of the autocorrelation function with respect to time shift. Here the displacement and velocity responses for a given input were used to estimate their auto- and cross-correlation functions. As mentioned earlier (Chapter 3) forty realisations (4096 point each) of response displacement and velocity were provided through each program run for the given excitation and system characteristics. The above correlations were calculated for each set of data repeatedly, using the steady state part of the response and a different starting point (in time) everytime. All estimations agreed in shape well, the values of $R_{xx}(0), R_{\dot{x}\dot{x}}(0)$ were very close to the values of $\sigma_x^2, \sigma_{\dot{x}}^2$ calculated from the spectra and inversion of the spectrum provided (Figure 16a,b) correlations functions which were very similar to the ones obtained directly from the data. The small discrepancies were due to the different number of data points involved in the two approaches i.e. for the spectrum derived correlations the complete record was used (40 x 4096 points transient) whereas in the rest only part of the response was used. The test was repeated with more than one excitation signals of the same intensity with the estimations failing to disagree.

An other indication of stationarity was the values of variances calculated for the statistical properties of the response. As mentioned in Chapter 3 each response statistical value was calculated along each realisation and the resulting forty values were averaged to obtain the mean value. At the same time a variance was calculated for the particular quantity. Although based on forty values these variances showed a very small scatter of the statistical values over the forty realisations. Examples are shown in Table 5.2. It can also be seen from the table that the simulations involving higher damping tend to be more consistent

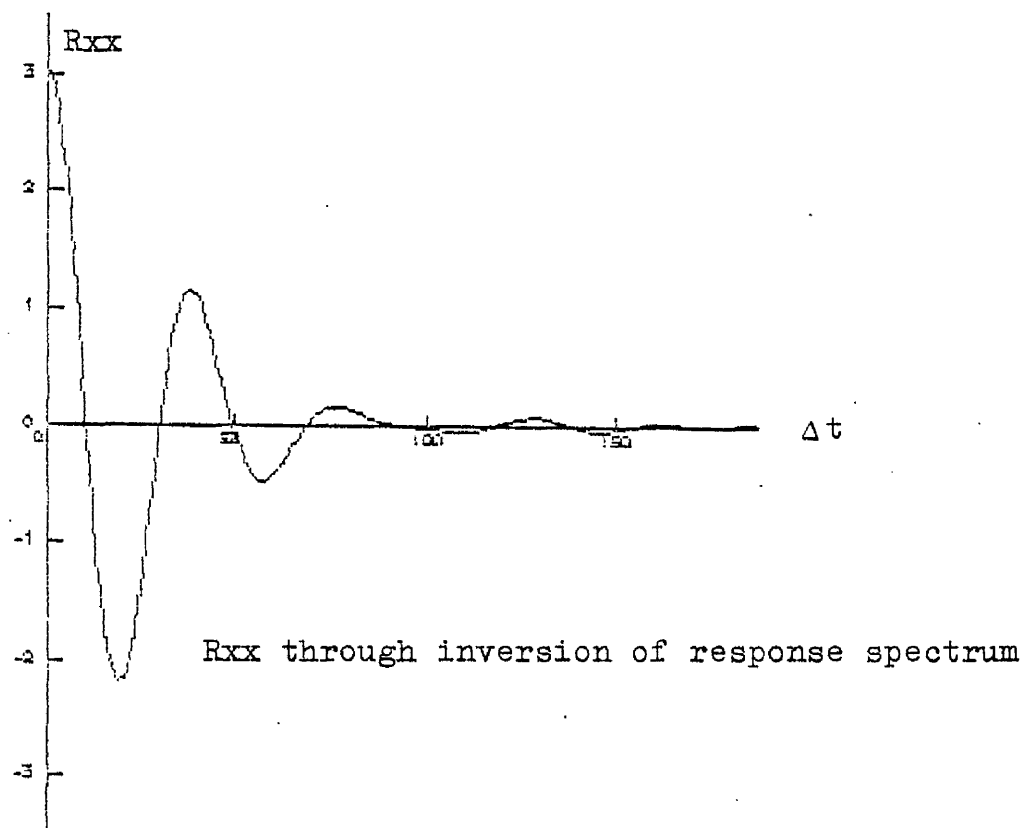
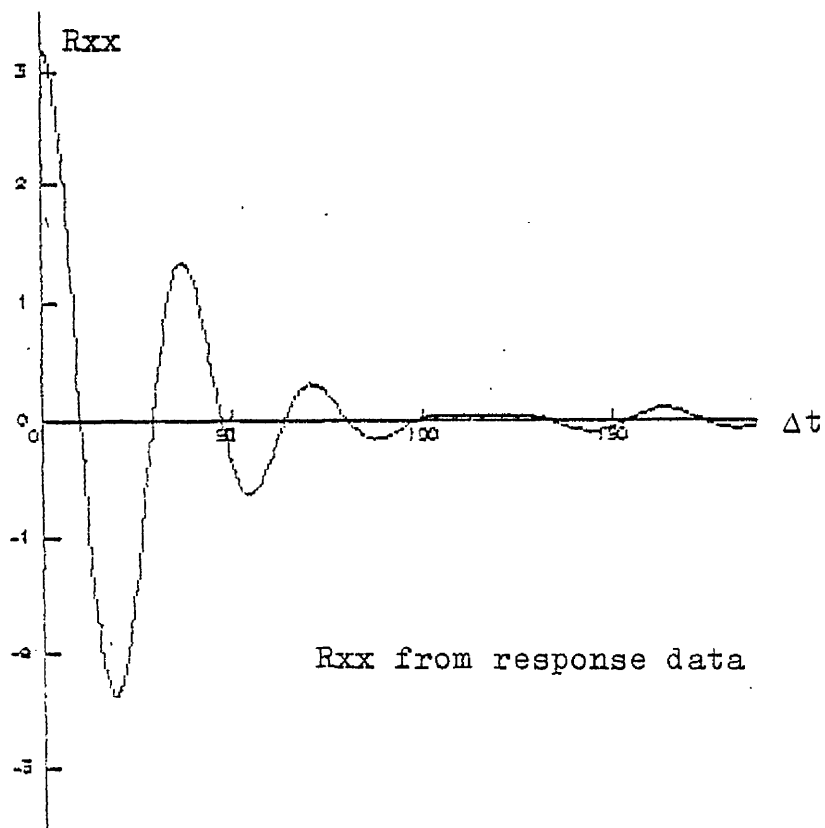


Figure 16a

$$\Delta t = 0.01475$$

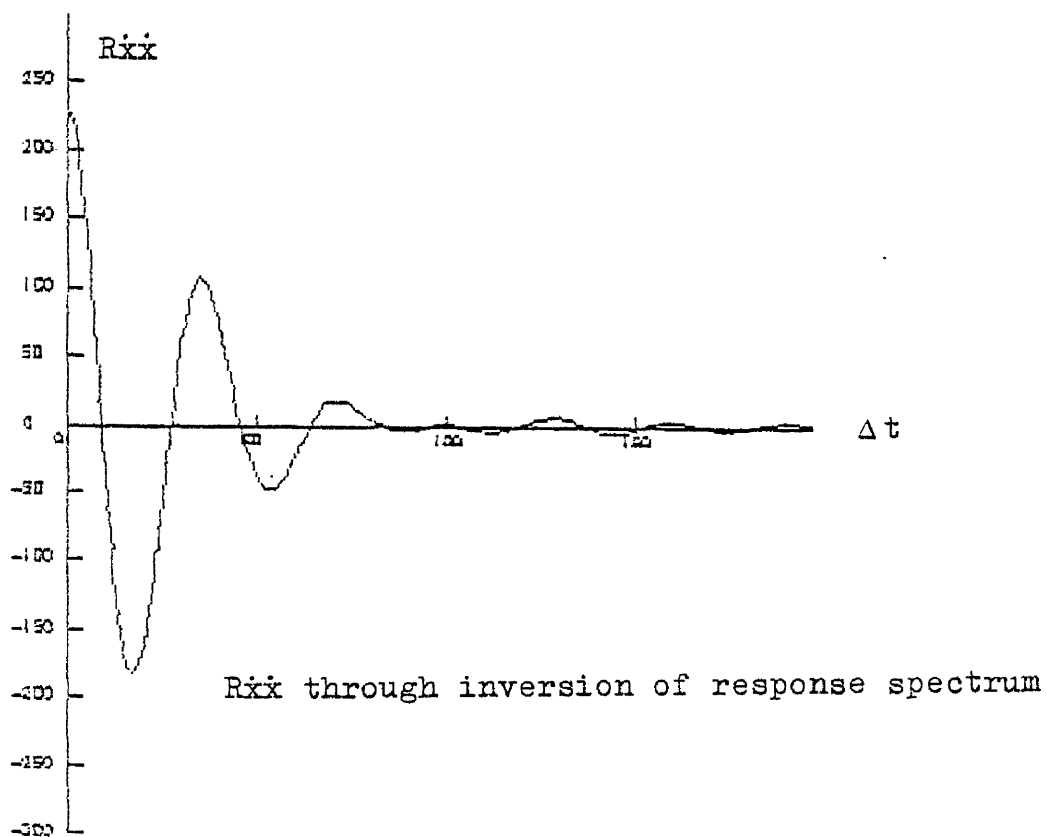
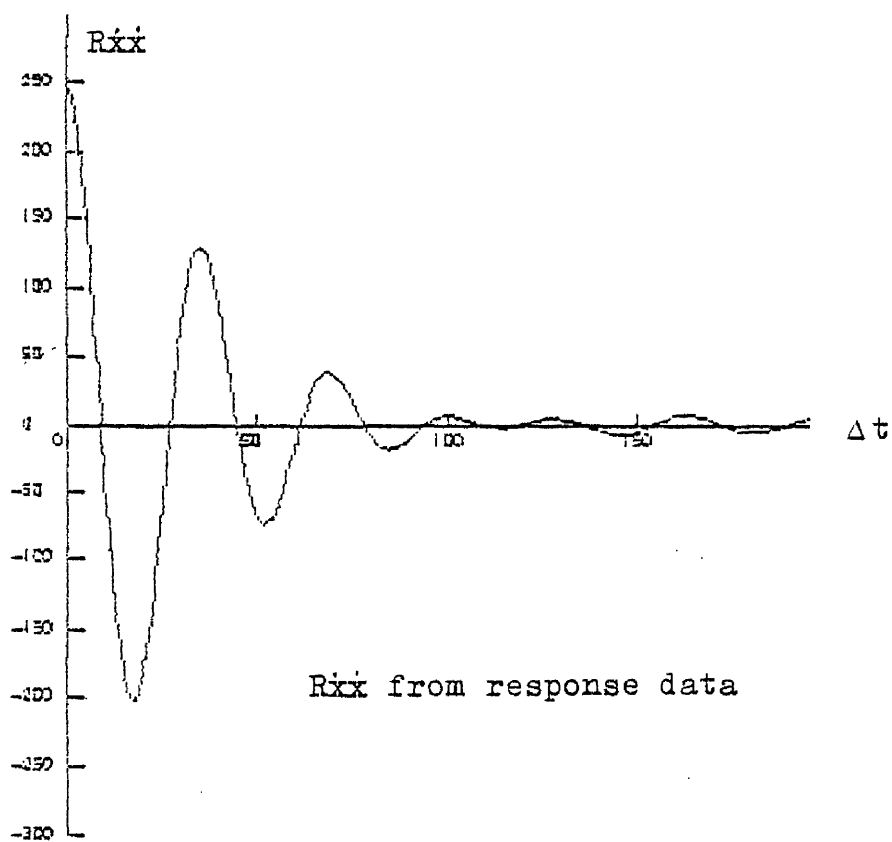


Figure 16b
 $\Delta t = 0.01475$

Table 5.2

Γ / ζ	3200		500		160		10	
ζ	0.20	0.01	0.20	0.01	0.20	0.01	0.20	0.01
$\beta\sigma_x^2$	33.74	32.88	13.24	12.82	7.39	7.02	1.66	1.52
$SD/\beta\sigma_x^2$	0.12	0.21	0.10	0.39	0.08	0.37	0.07	0.40
Ku	2.10	1.95	2.17	1.95	2.19	2.07	2.28	2.08
SD/Ku	0.05	0.12	0.06	0.11	0.05	0.12	0.04	0.12

Finally comparison of ensemble averaged statistical values, with the corresponding values obtained through averaging along each realisation, produced poor agreement. However this is a result of the different number of values involved in each calculation. Ensemble averaging involved forty one values whereas each realisation involves 4096 points less the transient part which is usually between 500–1500 points for the different excitation intensities and system parameters used in this investigation.

The shape of the autocorrelation function seems to behave as

$$\int_{-\infty}^{\infty} |\tau R(\tau)| d\tau < \infty$$

which is a condition under which the random quantity $S_T(\omega)$, the spectral estimation over a signal of duration T , will tend to the true spectral value as $T \rightarrow \infty$ [7.] The consistency of different spectral estimations give further support to the above argument. However the response being non Gaussian there is no directly available estimator for the confidence limits of the spectral values

5.3 Observations on the Response Spectra of the Duffing System Under Broad Band Random Excitation

The numerical simulation outlined in chapter three provided time records of response displacement and velocity. These were processed by a separate program, which derived the response spectra (using a Fast Fourier Transformation algorithm) and calculated the statistical values of mean square variance, kurtosis and skewness (Chapter 3, Appendix C.4).

A sample of the raw response spectra was shown in Figures 13a,b. The excitation spectrum is by definition perfectly smooth (Section 3.2) and the response spectra obtained for the linear case ($\beta = 0$) were equally smooth. However this was not the case with the nonlinear system Figures 13,14. The 'spiky' shape of the response spectra of the nonlinear system was smoothed using a frequency averaging technique (moving average) of twenty one adjacent spectral estimations (data tapering and other 'mild' smoothing techniques did not have noticable affect). This was necessary in order that the spectral shape was more clearly defined in figures where spectra were plotted against linear scales. The logarithmic scales suppressed the phenomenon as seen in Figure 14. The averaging process reduces the effective frequency resolution but this does not present a problem for a record which is already oversampled as far as the F.F.T. algorithm is concerned (Section 3.2). Perhaps it is worth noting that this phenomenon may be misinterpreted if the frequency resolution of the analysis is small (Δf large). In this case the spectrum appears to have more than one peak especially so if the band of response frequencies is broad (i.e. large value of Γ/ζ see later). However if a different input record is used to obtain the response spectra the multiple peaks usually change frequency and if the frequency resolution is increased the peaks split. Figures 13, 14 give an indication of this phenomenon which becomes much more pronounced as the width of the spectrum increases. The spiky spectrum is regarded as an inadequacy of the numerical procedure to calculate a smooth spectrum for a non Gaussian process for the number of samples used. A negligible

improvement was obtained through the doubling of the number of realisations. This seems to suggest that the number of realisations must be greatly increased before any worthwhile improvement is observed on the spectral smoothness.

On the basis of chapter 4 all results presented here are in non-dimensional form. At this point a reminder of the non dimensional quantities involved may not be out of place. For the system

$$m\ddot{x} + c\dot{x} + k(x + \beta x^3) = F(t)$$

Where $F(t)$ is a broad band random force of spectral intensity S_{\cdot} . The displacement related non-dimensional quantities Γ, B, A are defined as follows

$$\Gamma = \beta S_{\cdot} \omega_n / k^2, (\omega_n^2 = \frac{k}{m})$$

and may be thought of as an adjusted (for the particular system) excitation parameter. $B = \beta S_{\cdot} \omega_n$ is the nondimensional response displacement spectrum ($\beta S_{\cdot} / \omega_n$ for velocity and denoted by Bv). $A = B/\Gamma = k^2 S_{\cdot} / S_{\cdot}$ this does not define a transfer function but it is reminiscent of the transfer function of a linear system (for velocity $k^2 S_{\cdot} / S_{\cdot}, \omega_n^2 = Av$). As already discussed in Chapter 4 the statistical quantities may be obtained as a function of the ratio Γ/ζ whereas the dimensional analysis indicates that these parameters (Γ, ζ) should be separate when describing the response spectra. ($\zeta = c/2\sqrt{km}$). In Figure (17a-f) the response spectra for $\zeta = 0.05$ and different values of Γ are shown as suggested by the analysis. Subsequent figures show response spectra plotted for constant values of the ratio Γ/ζ . Although the presentation of response characteristics in terms of the separate parameters Γ and ζ may be more accurate in some sense there are indications that the use of the ratio particularly facilitates description of response under broad band excitation with the obvious advantage of reducing the number of independent system variables to one. Plotting non-dimensional response spectra (B) for constant values of the ratio Γ/ζ ensures that the spectral curves will contain the same area as discussed in Chapter 4. The B curves

Figures (18a-e), (19a-e) confirm this and show that the spectral shapes are extremely similar. In these figures, where the quantity B is plotted against the non-dimensional frequency $\Omega (= \omega/\omega_n)$ for constant values of Γ/ζ between 10 and 3200 and ζ values of 0.2, 0.1, 0.05, 0.01, the main body of the curves are almost overlapping, the resonant frequencies (Ω_r) coincide and the peak values $B(\Omega_r) = B_{\max}$ are at the same level. However the agreement is not so good at the tails of the curves. Since the area enclosed is by definition the same, the peak shapes must be slightly different in order that the area contained under the curves remain the same. In fact the value of $B(0)$ is higher as the value of ζ is increased (see Table 5.3) but changes very little for different values of Γ/ζ e.g. for $\zeta = 0.2$ $B(0) = 0.12$ for $\Gamma/\zeta = 10$ and $B(0) = 0.3$ for $\Gamma/\zeta = 3200$. At the same time $B(\Omega_r)$ changes from $B(\Omega_r) = 1.2$ for $\Gamma/\zeta = 10$ to $B(\Omega_r) = 6.2$ for $\Gamma/\zeta = 3200$ and the width of the peak at $1/2 B(\Omega_r)$ from 1.1Ω to 4.5Ω . This shows that by far the most important part of the response spectrum lies on either side of the resonant frequency where the spectral shapes for constant Γ/ζ ratio almost coincide. When the spectral quantity $A = B/\Gamma = k_x^2 S_x/S_1$ is plotted against the corresponding non-dimensional frequency for constant values of Γ/ζ yet another interesting observation can be made regarding the value of the quantity A at zero frequency. For each value of Γ/ζ there is a small range of values within which the values of $A(0)$ concentrate. Figures (20a-e). This is a consequence of the relative invariability of the $B(0)$ values wrt Γ and gives a more clear demonstration of the weak influence of the excitation level on the low frequency response of the system for this type of excitation. Assume for a moment that a set of non dimensional curves for a given value of Γ/ζ were derived through the simulation of a single system for different values of ζ (i.e. all system parameters constant except ζ). As Γ (which expresses the excitation level) varies proportionally to ζ , to maintain the ratio Γ/ζ constant, the $A(0)$ values concentrate near a single value. Now the $A(0)$ values are proportional to the ratio $B(0)/S_1$, but as already seen the value of $B(0)$ for some excitation level and constant ζ depends mainly on ζ . Hence the concentration of the $A(0)$

values show a nearly proportional dependence of the zero frequency response on the damping parameter ζ . The plots of A are reminiscent of the transfer function of a linear system for different values of damping and indeed the definition of $A = k^2 S_x / S_1$ would be the transfer function if the system were linear. However there is no such thing as a transfer function for the nonlinear system since the quantity bears no connection with any other form of excitation but the one that caused it (Broad band). The fact that $A(0)$ values concentrate in a particular range for a given value of Γ/ζ is a further property of the system. It demonstrates the effect of damping on the low frequency components of the response. One tends to think of the value $A = k^2 S_x / S_1$ at zero frequency as the static solution for a given excitation level divided by that excitation level. However this is far from being the case here. For a linear system the quantity $A(0) = B(0)/\Gamma$ would be the value of the transfer function at zero frequency and equal to unity.

From the above discussion the following conclusions may be drawn. The $B(0)$ values depend mainly on the value of ζ the damping coefficient and the $A(0)$ values mainly on the value of the ratio Γ/ζ . Although the static solution must contribute to the zero frequency response its contribution is negligible (expressed through the small variation of $B(0)$ values for constant ζ and the scatter of values of $A(0)$ for different damping ratios and constant Γ/ζ).

Observing the spectral plots the following general conclusions may be drawn. The resonant frequency (Ω_r), the width of the spectral peak (W), the value of $B(\Omega_r)$ and the area under the B curves, all increase as the ratio of Γ/ζ is increased. The opposite is true for the value of $A(0)$. These processes are smooth as can be seen from Figures (21-25), where these quantities are plotted against the ratio Γ/ζ . Further the spectral peaks appear symmetric about the resonant frequency.

Harmonic response is observed at three times the resonant frequency of the response spectrum. For the displacement

spectrum the third harmonic response is at a constant three orders of magnitude smaller than the response at resonance i.e. $B(3\Omega_r) \approx B(\Omega_r)/1000$. The third harmonic response is best observed in the velocity spectra Figures (27-29b). This type of response is further discussed in the next Chapter.

As mentioned earlier the properties of the system may be observed more accurately in terms of Γ and ζ instead of their ratio. However such a representation would be more suitable for a mathematical approach. For engineering applications, where more practical considerations are of importance, the representation of response properties in terms of the ratio Γ/ζ seems more advantageous. The advantages being a less complex description of response by use of one variable (Γ/ζ) instead of two (Γ and ζ) and the dependence of the statistical and spectral values of the same parameter (Γ/ζ). Further if the fact that the spectral values calculated through the simulation process are not exact (bias, numerical integration errors etc.), is taken into account, then the presentation of these values as functions of the ratio Γ/ζ simply does away with complicated and not so accurate information and at the same time preserves essential features of the response. For example Figure (24) assigns a single value of $B(\Omega_r)$ for each value of Γ/ζ say $B(\Omega_r) = 3.75$ at $\Gamma/\zeta = 500$. Whereas the spectral peak values in Figure (18d) scattered between $B(\Omega_r) = 3.6$ and 4. For forty realisations the error involved in the case of Gaussian data in the calculation of spectral values is $\approx 15\%$. Hence it seems pointless to quote the above values of $B(\Omega_r)$ separately as it would be the case if the results were presented in terms of Γ and ζ instead of their ratio. Finally the representation of results in terms of Γ/ζ does not exclude the possibility of producing the sets of curves which would present the results in terms of Γ and ζ as in Figure (26) (small adjustments would have to be made and the spectral response curves enclosed would be useful).

Table 5.3

Values of $B(\Omega_w)$

Γ/ζ \ ζ	0.20	0.10	0.05	0.01
10	1.19	1.35	1.45	1.28
40	2.05	1.98	2.00	2.12
160	2.85	2.96	3.03	2.92
500	3.62	3.87	3.73	3.97
3200	6.25	6.06	6.30	7.40

Values of $B(0)$

Γ/ζ \ ζ	0.20	0.10	0.05	0.01
10	0.12	0.06	0.04	0.01
40	0.20	0.10	0.06	0.01
160	0.22	0.14	0.06	0.01
500	0.21	0.15	0.09	0.02
3200	0.32	0.19	0.09	0.03

Values of $A(0)$

Γ/ζ \ ζ	0.20	0.10	0.05	0.01
10	0.06	0.06	0.08	0.10
40	0.025	0.025	0.028	0.03
160	0.007	0.009	0.008	0.009
500	0.0021	0.003	0.0035	0.004
3200	0.0005	0.0005	0.0006	0.001

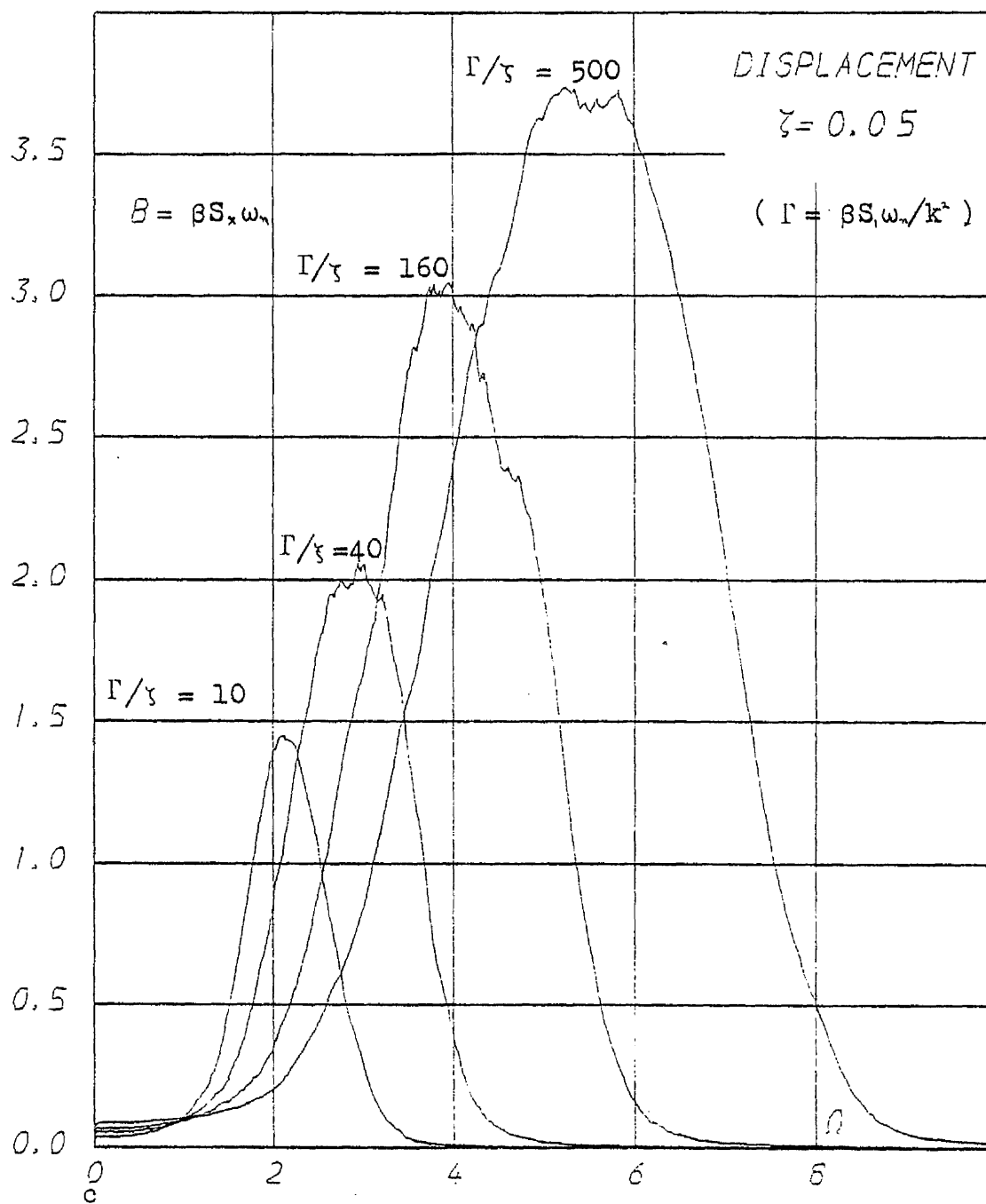


Figure 17a

Figures 17a-17f illustrate response spectra for constant $\zeta = 0.05$

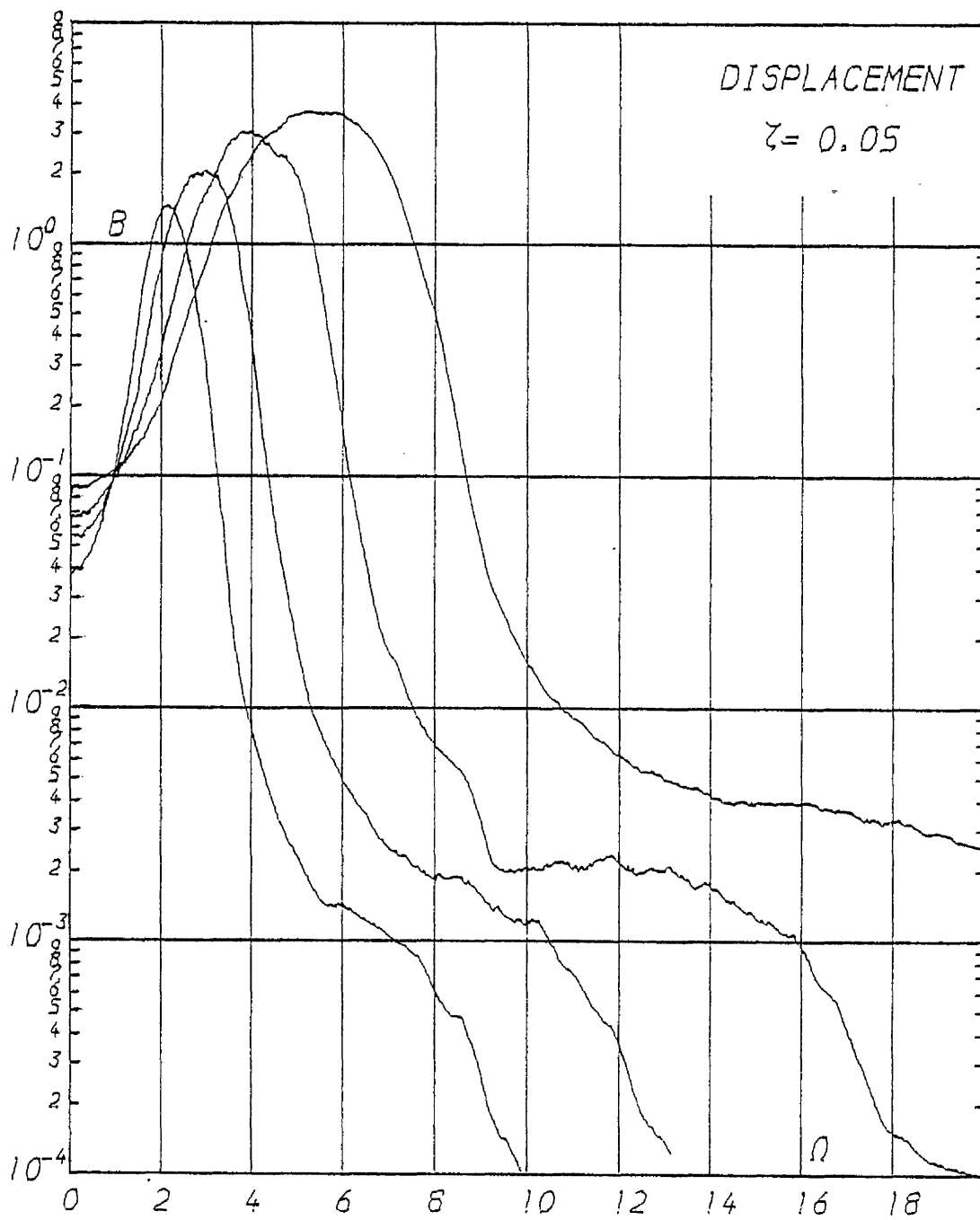


Figure 17b

See also Figure 17a

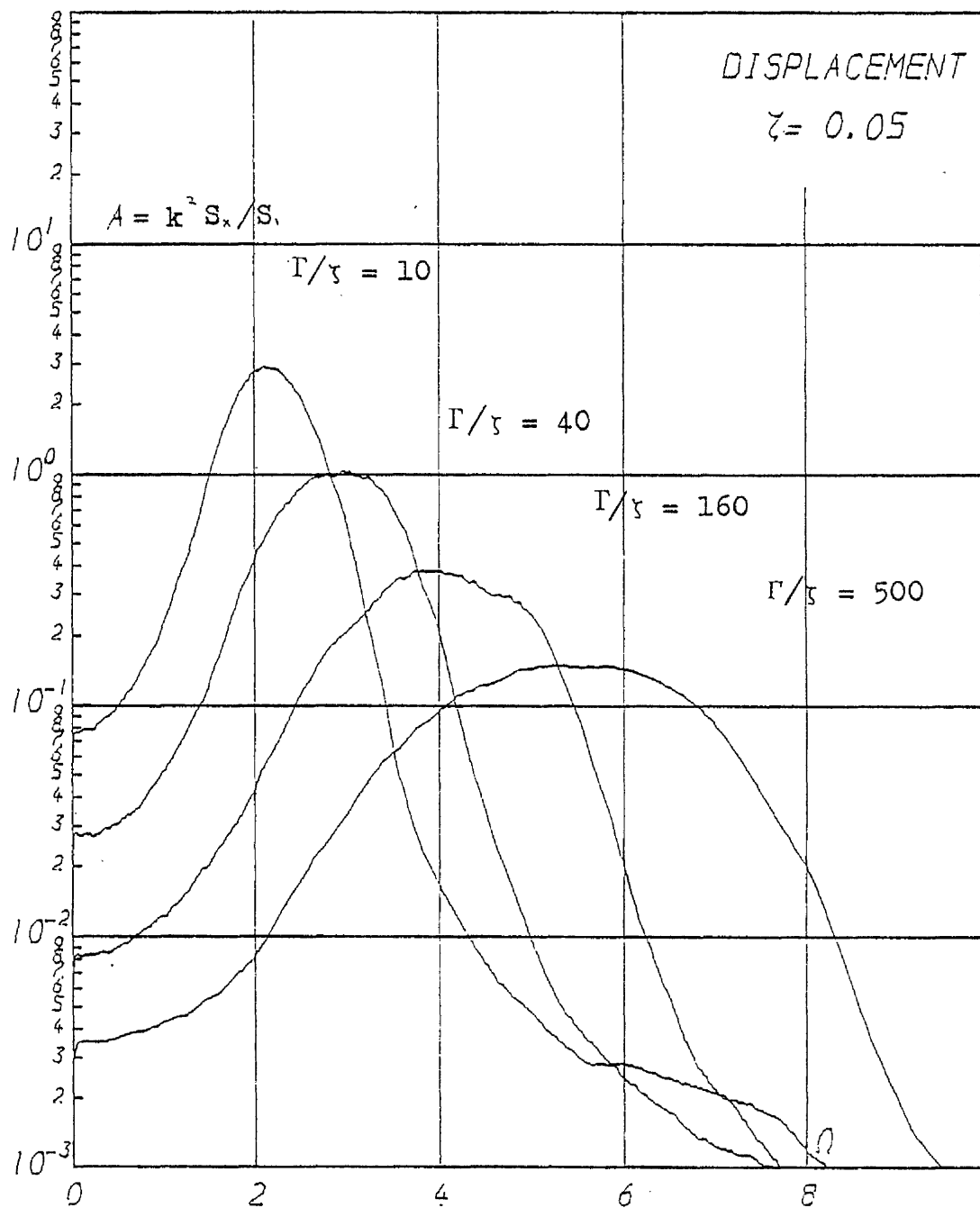


Figure 17c

See also Figure 17a

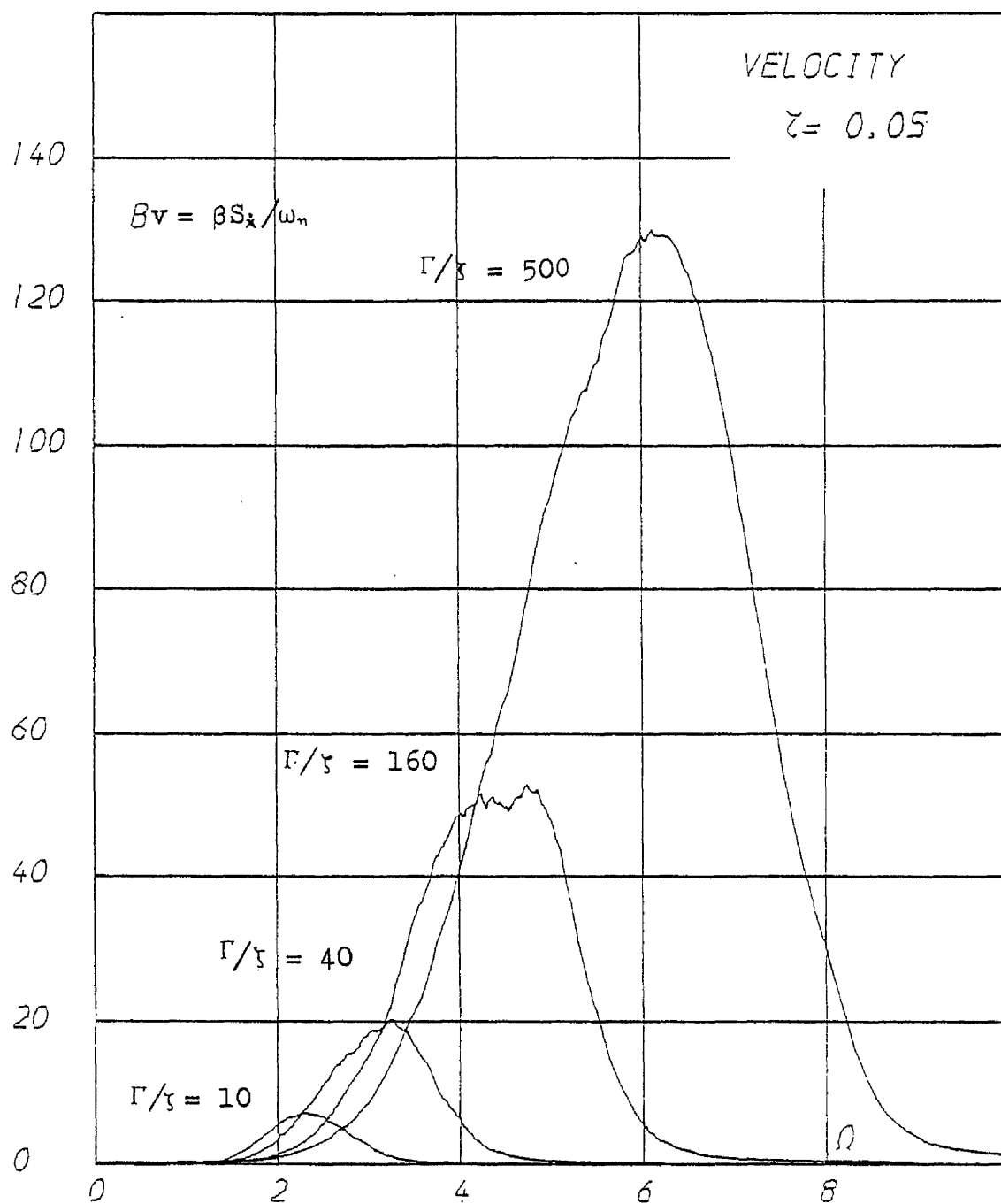


Figure 17d

See also Figure 17a

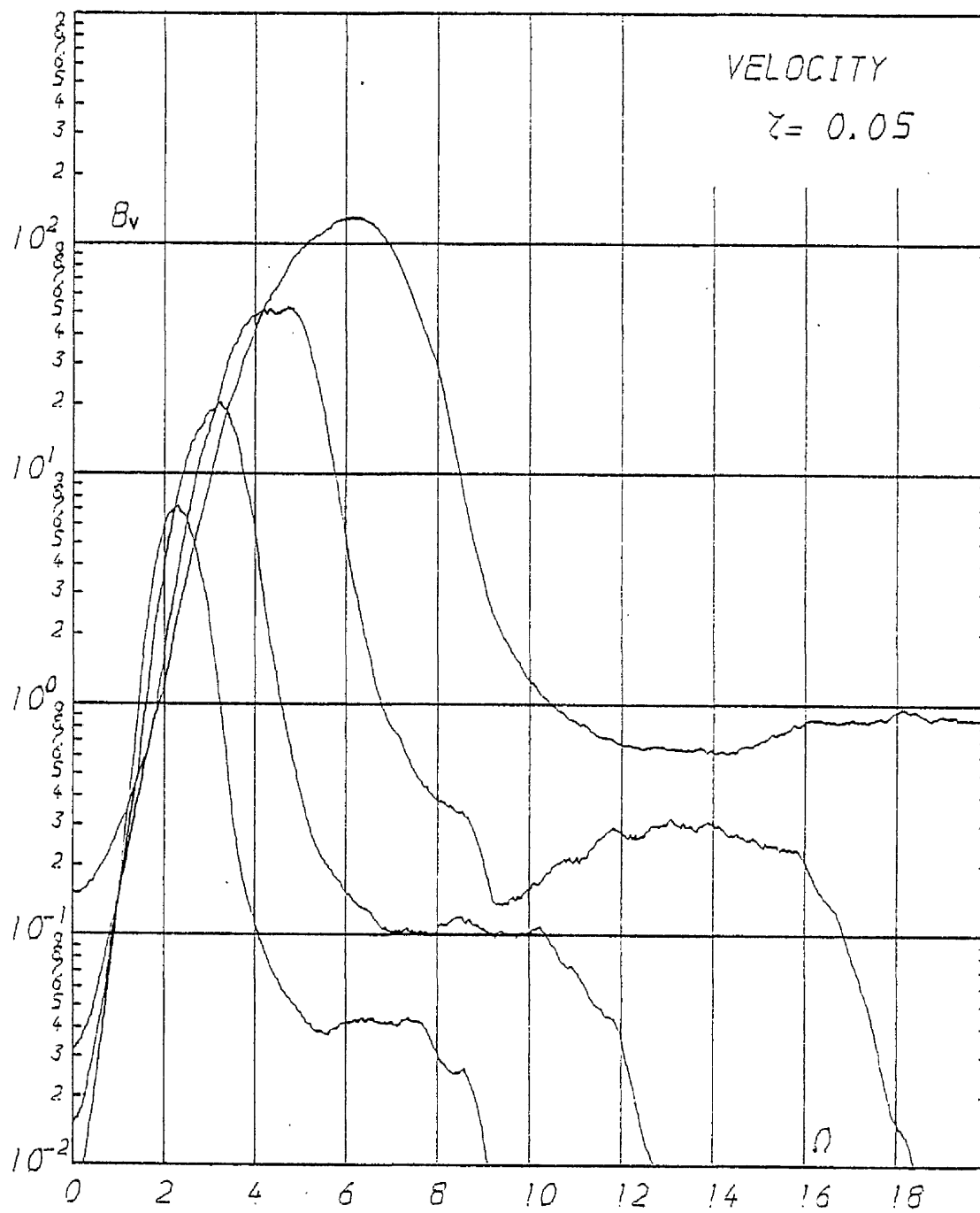


Figure 17e

See also Figure 17a

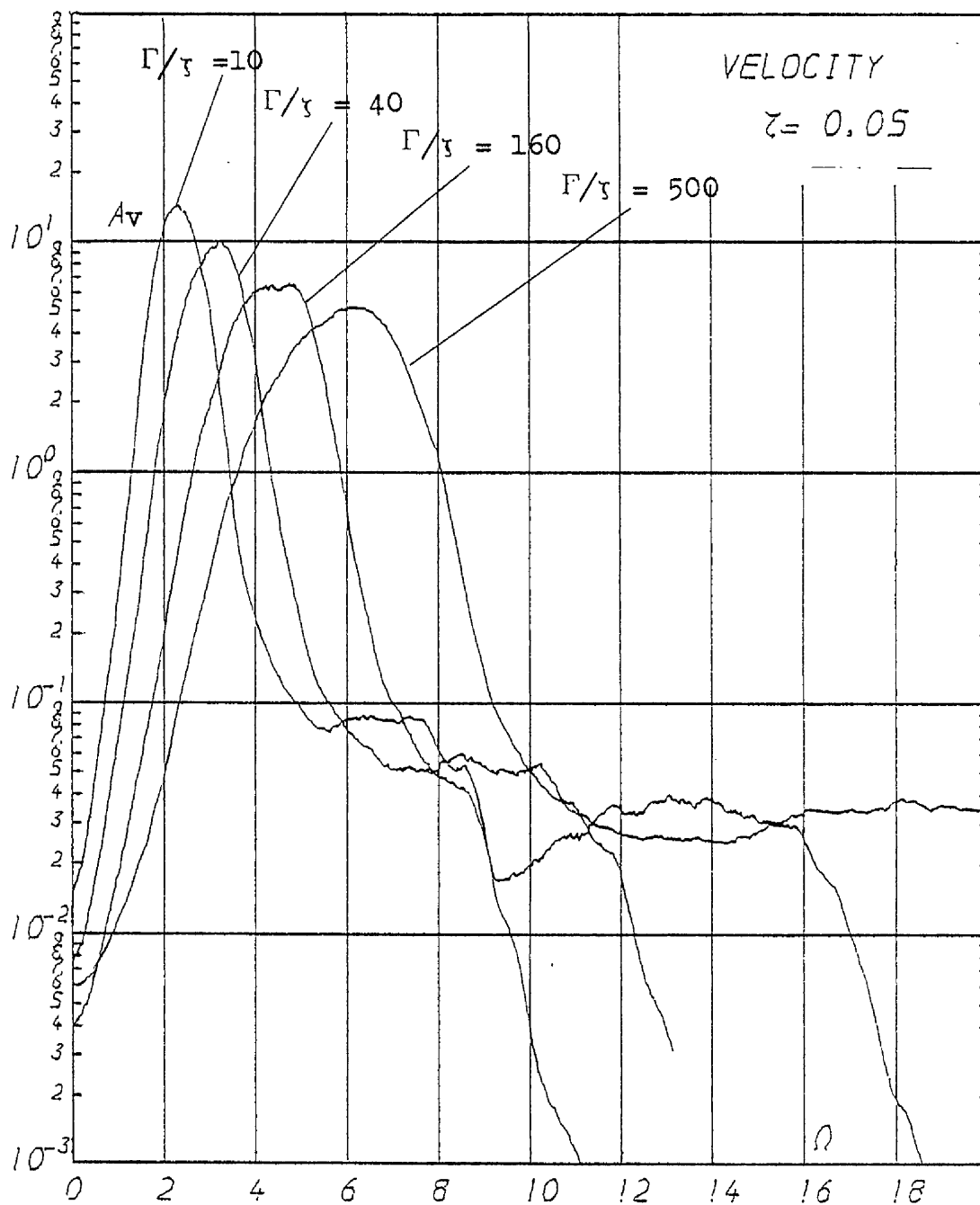


Figure 17f

See also Figure 17a

$$(A_v = k^2 S_*/(S, \omega_n^2))$$

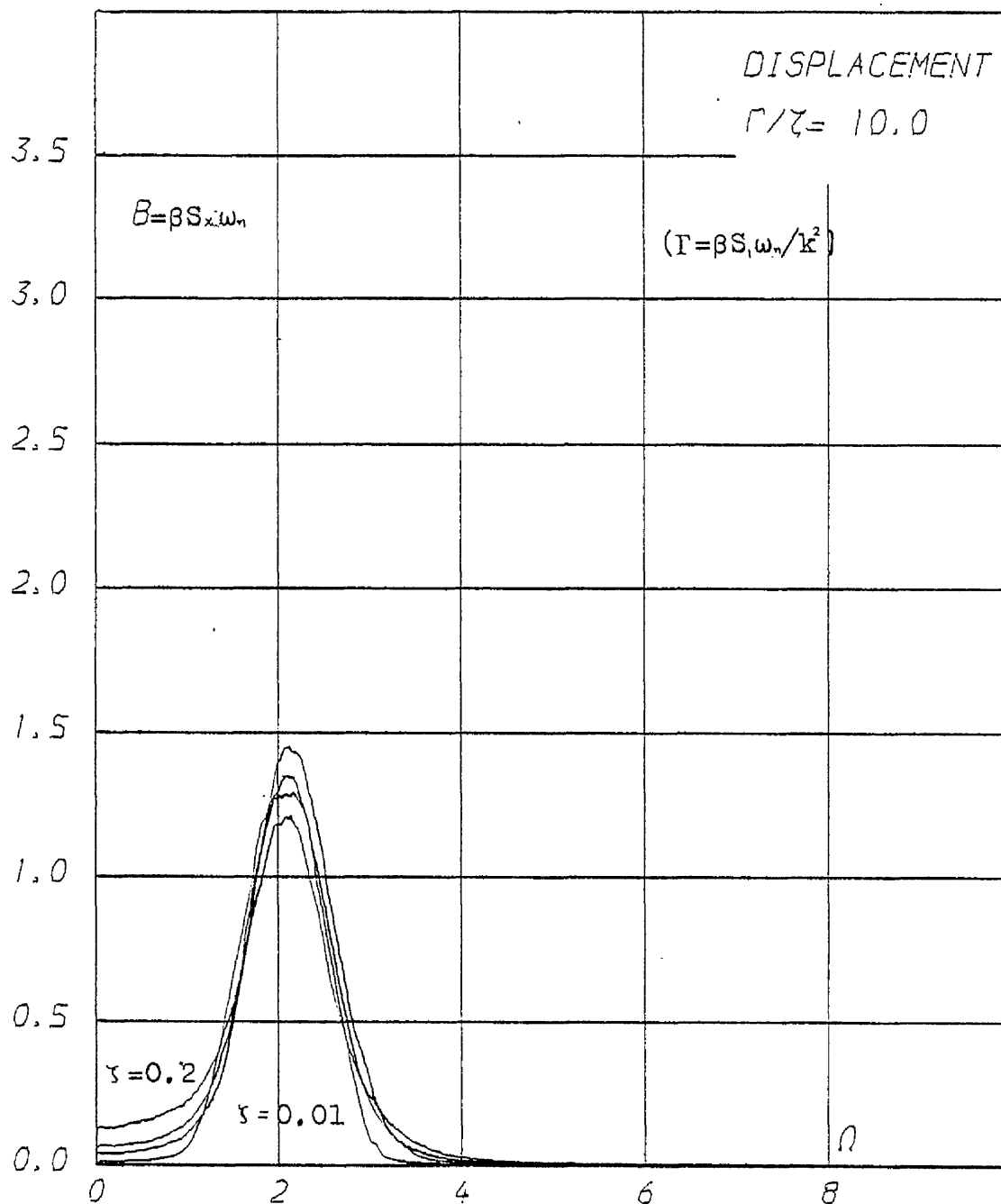


Figure 18a

Figures 18a-20e illustrate response spectra of Γ/γ values with $\gamma = 0.2, 0.1, 0.05, 0.01$

For B spectra the value of Γ for the particular curve is judged by the magnitude of the $B(0)$ value of that curve. The order from top to bottom is $\gamma = 0.2, 0.1, 0.05, 0.01$. As shown above.

For A spectra see Figures 20a-20e.

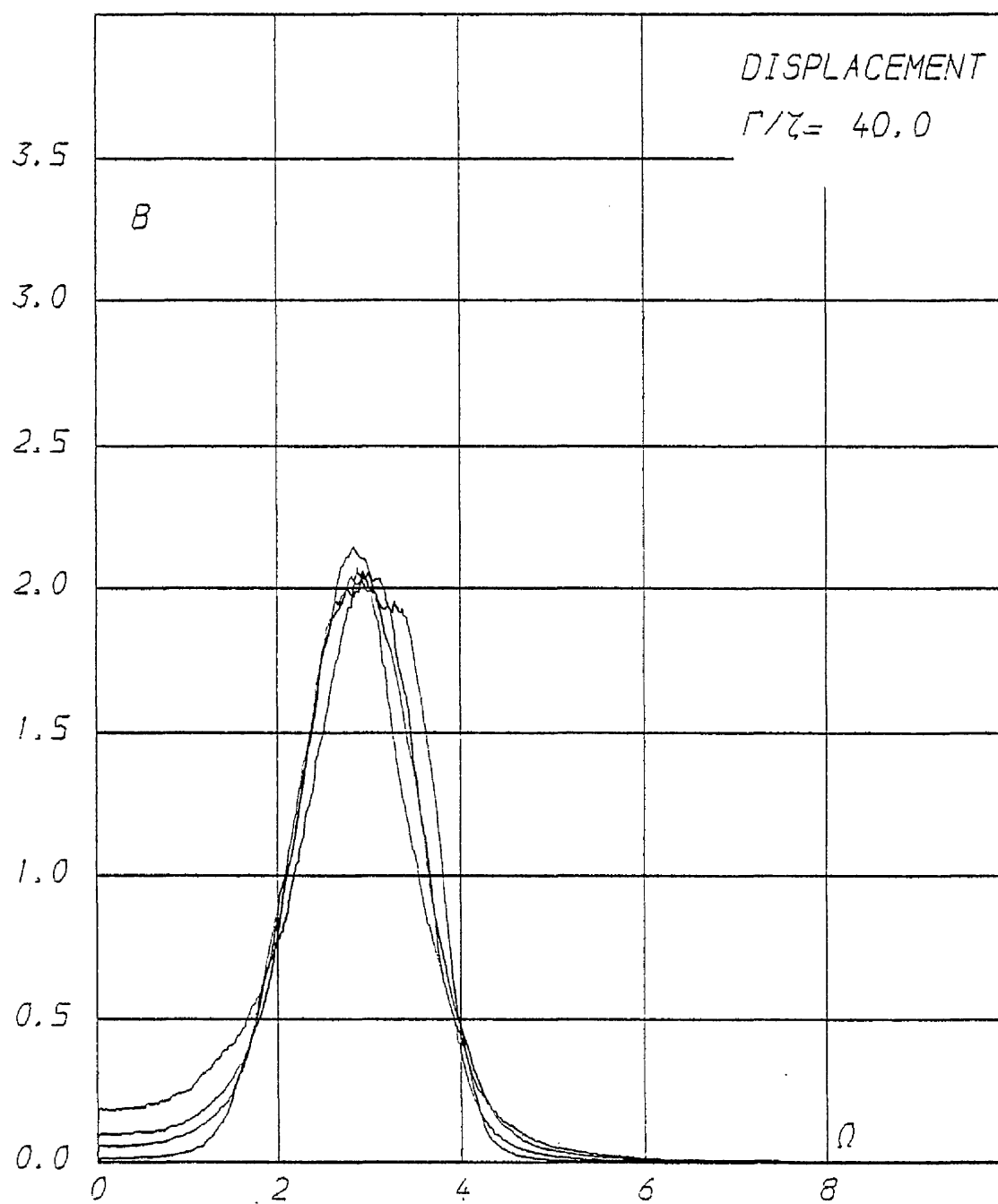


Figure 18b

See also Figure 18a

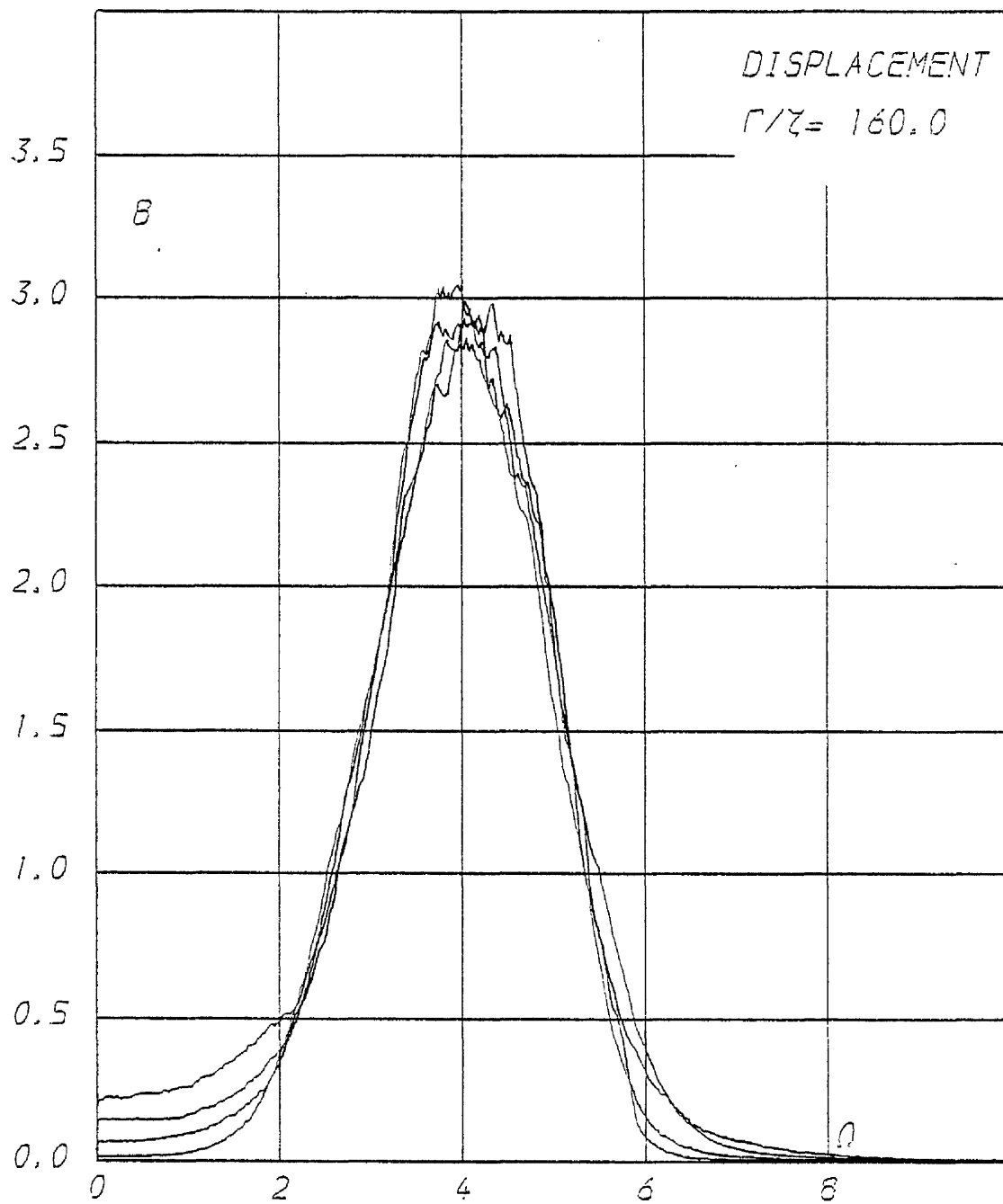


Figure 18c

See also Figure 18a

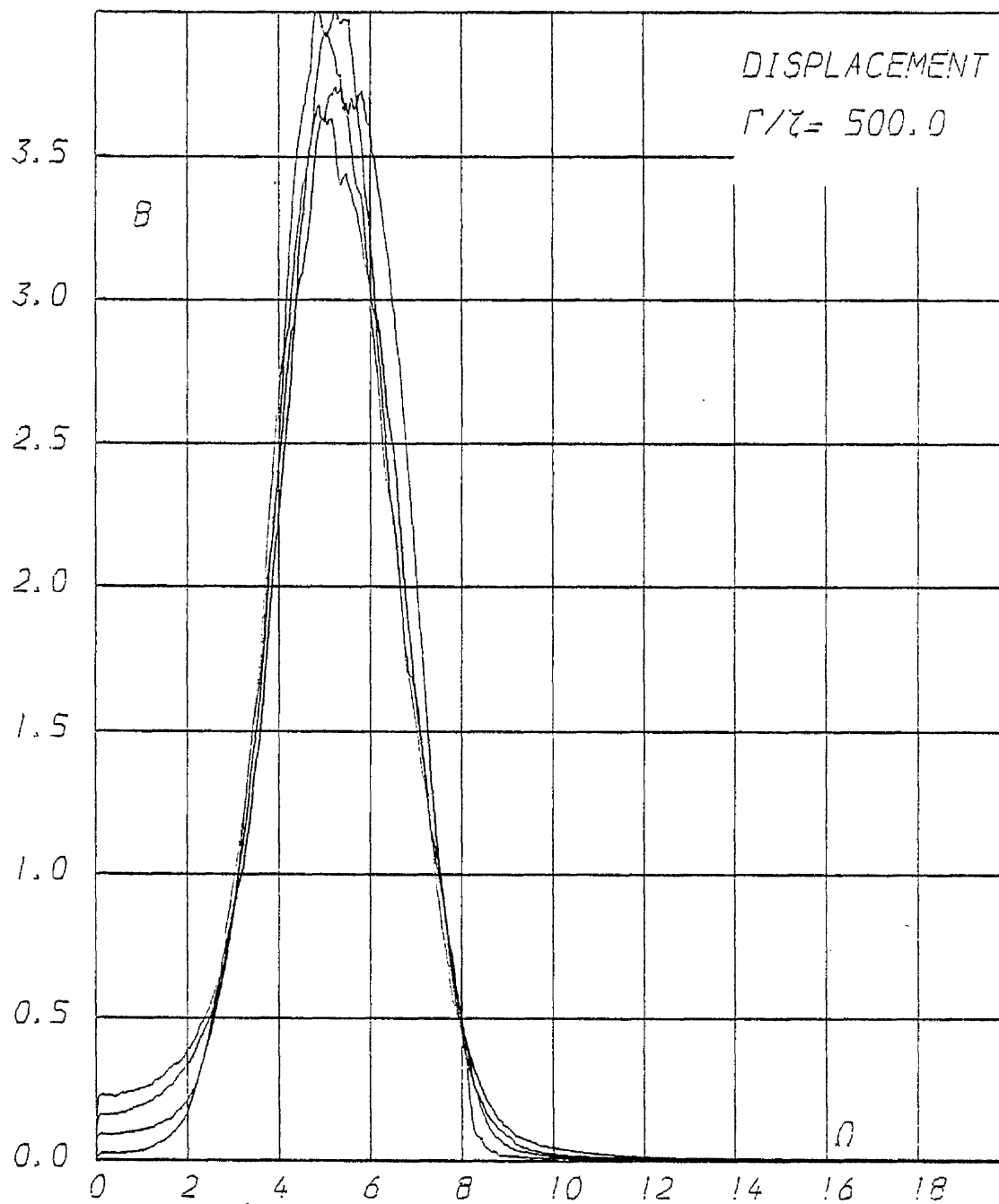


Figure 18d

See also Figure 18a

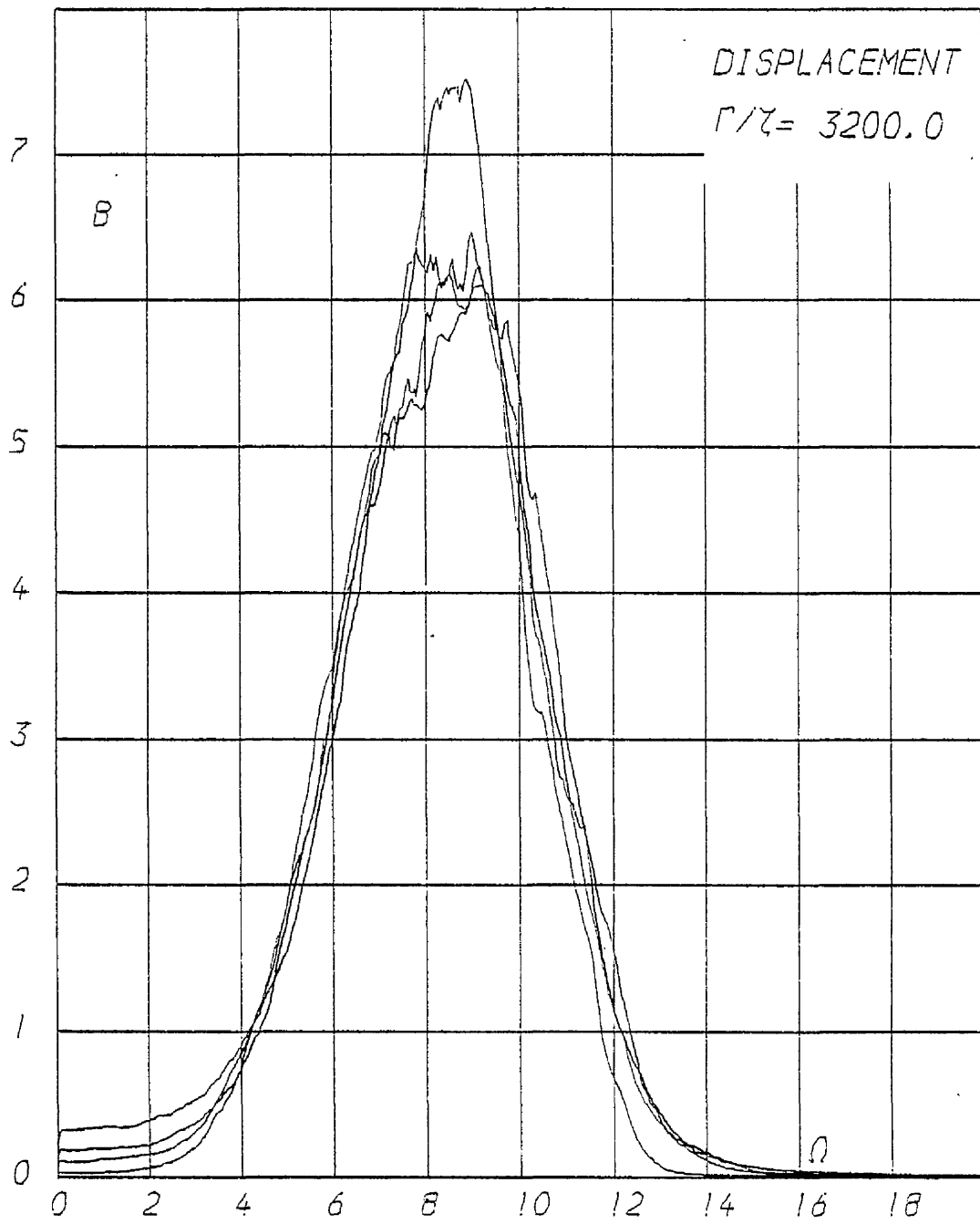


Figure 18e

See also Figure 18a

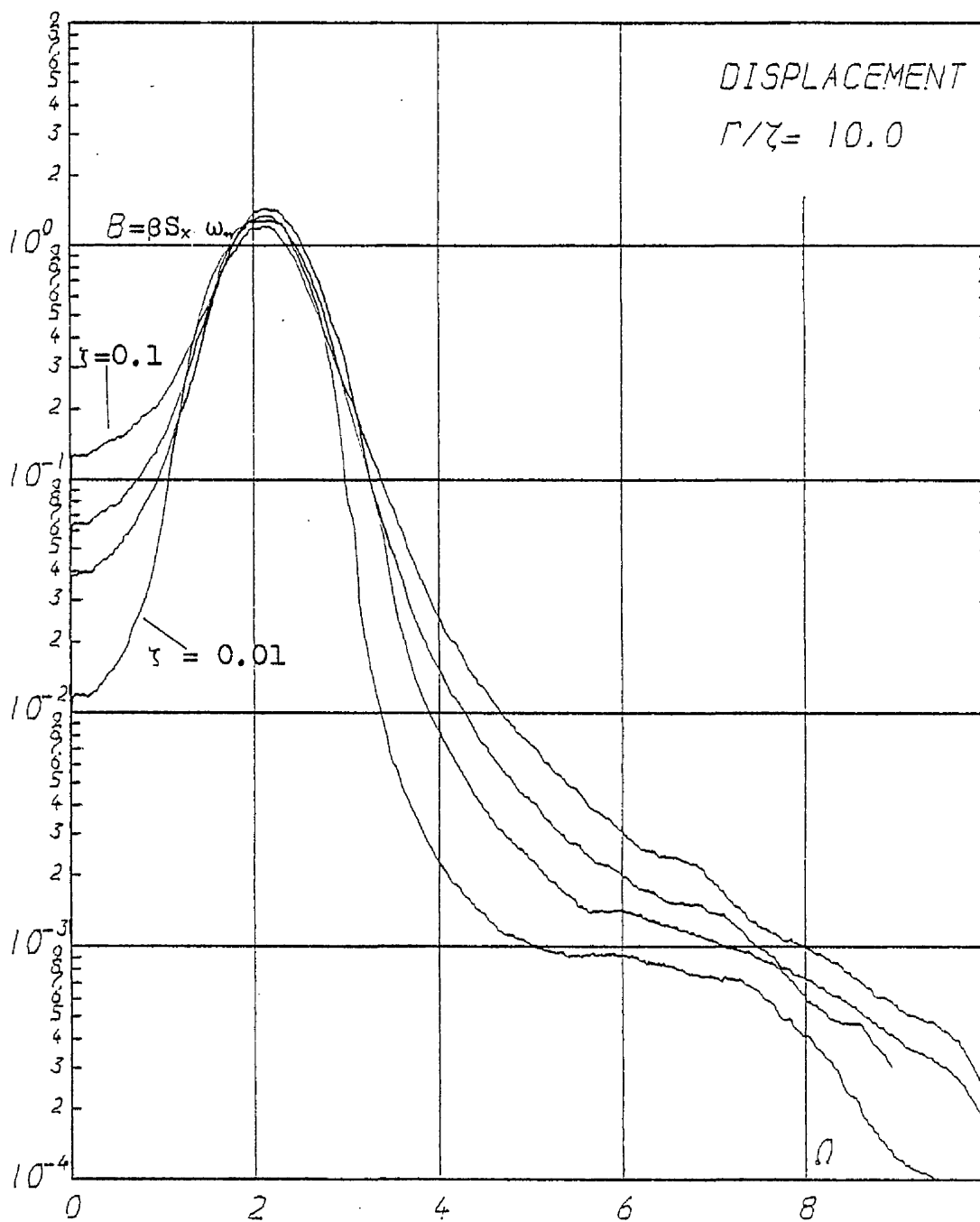


Figure 19a

Figures 19a-19e as Figures
18a-18e logarithmic scales

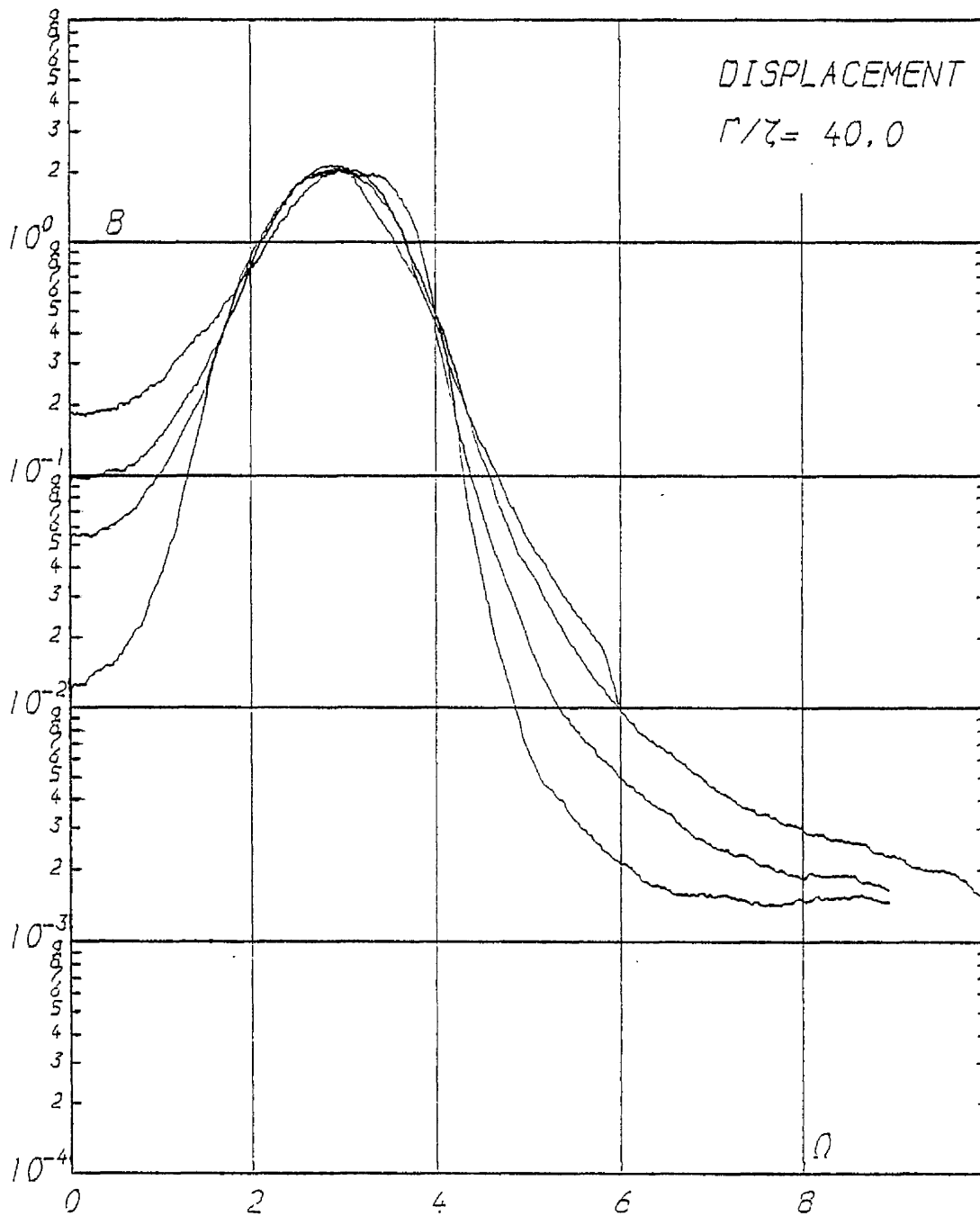


Figure 19b

See also Figure 19a

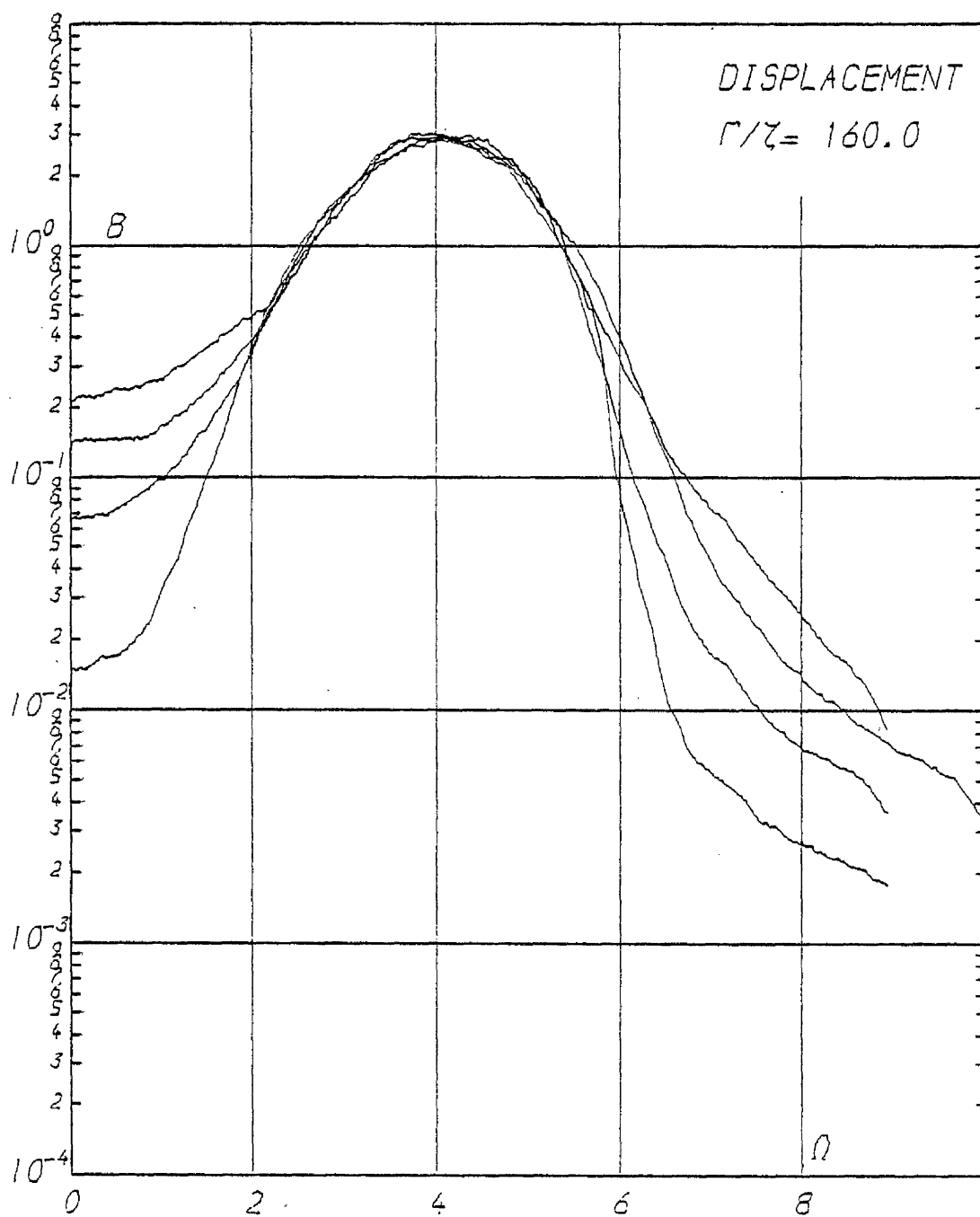


Figure 19c

See also Figure 19a

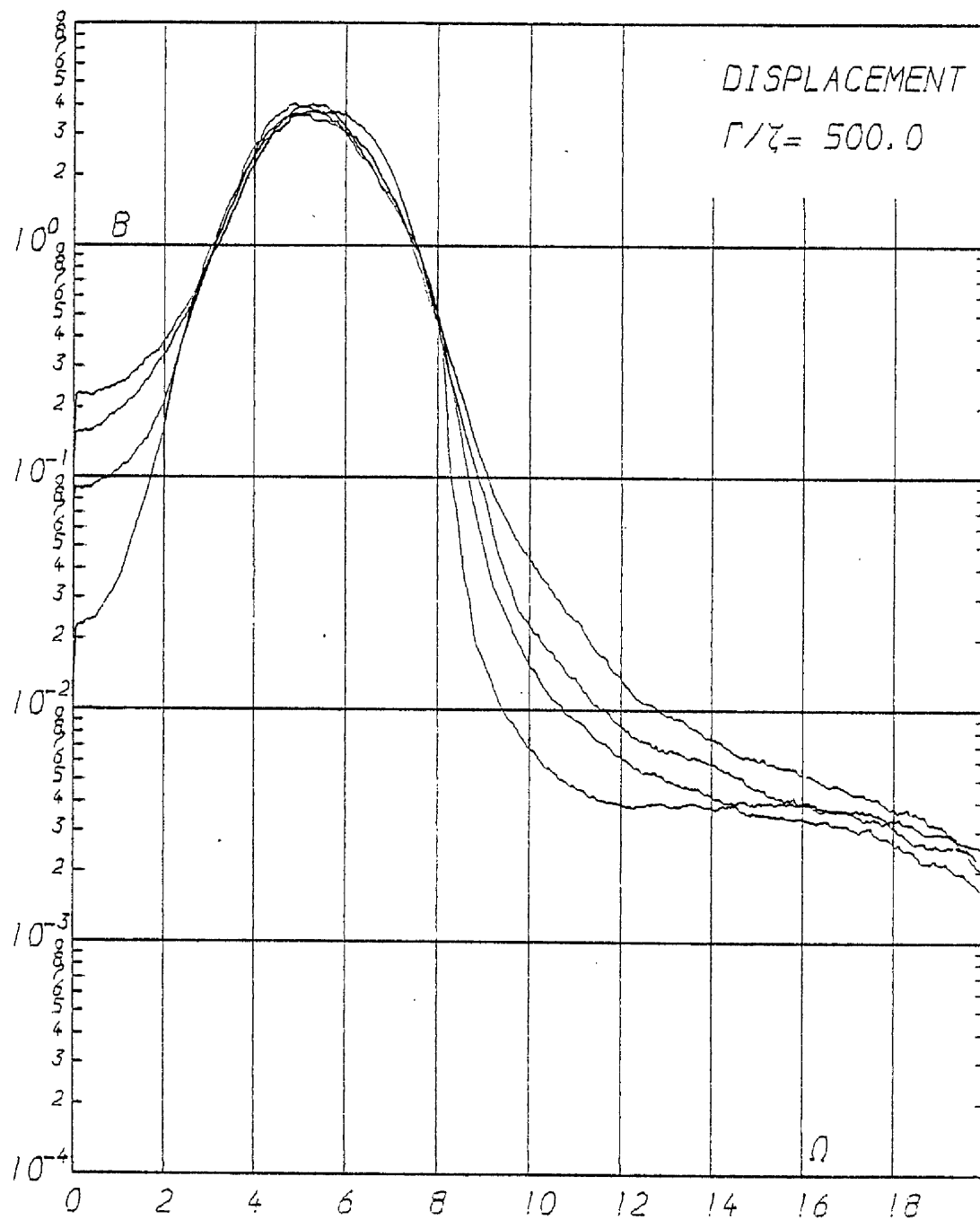


Figure 19d

See also Figure 19a

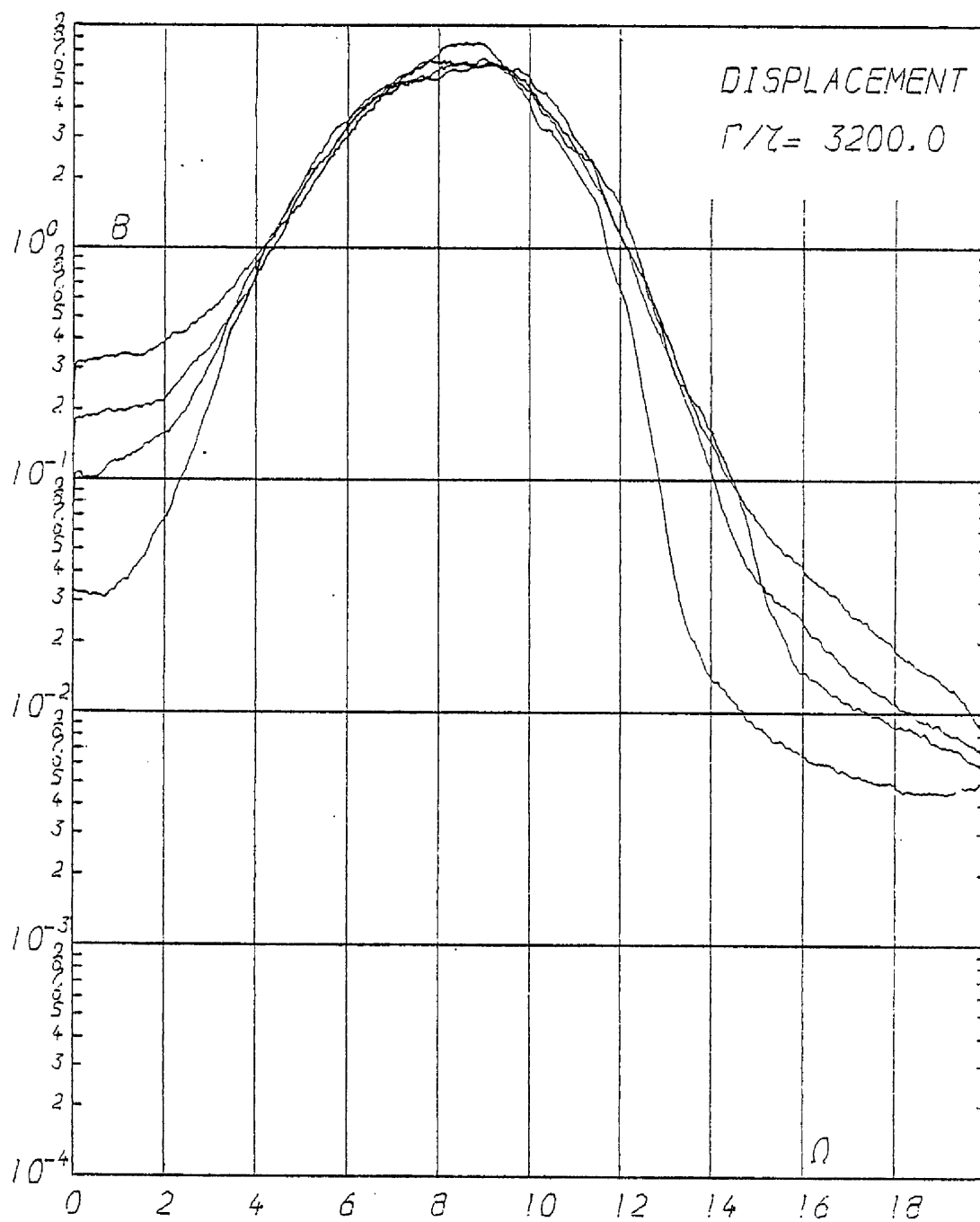


Figure 19e

See also Figure 19a

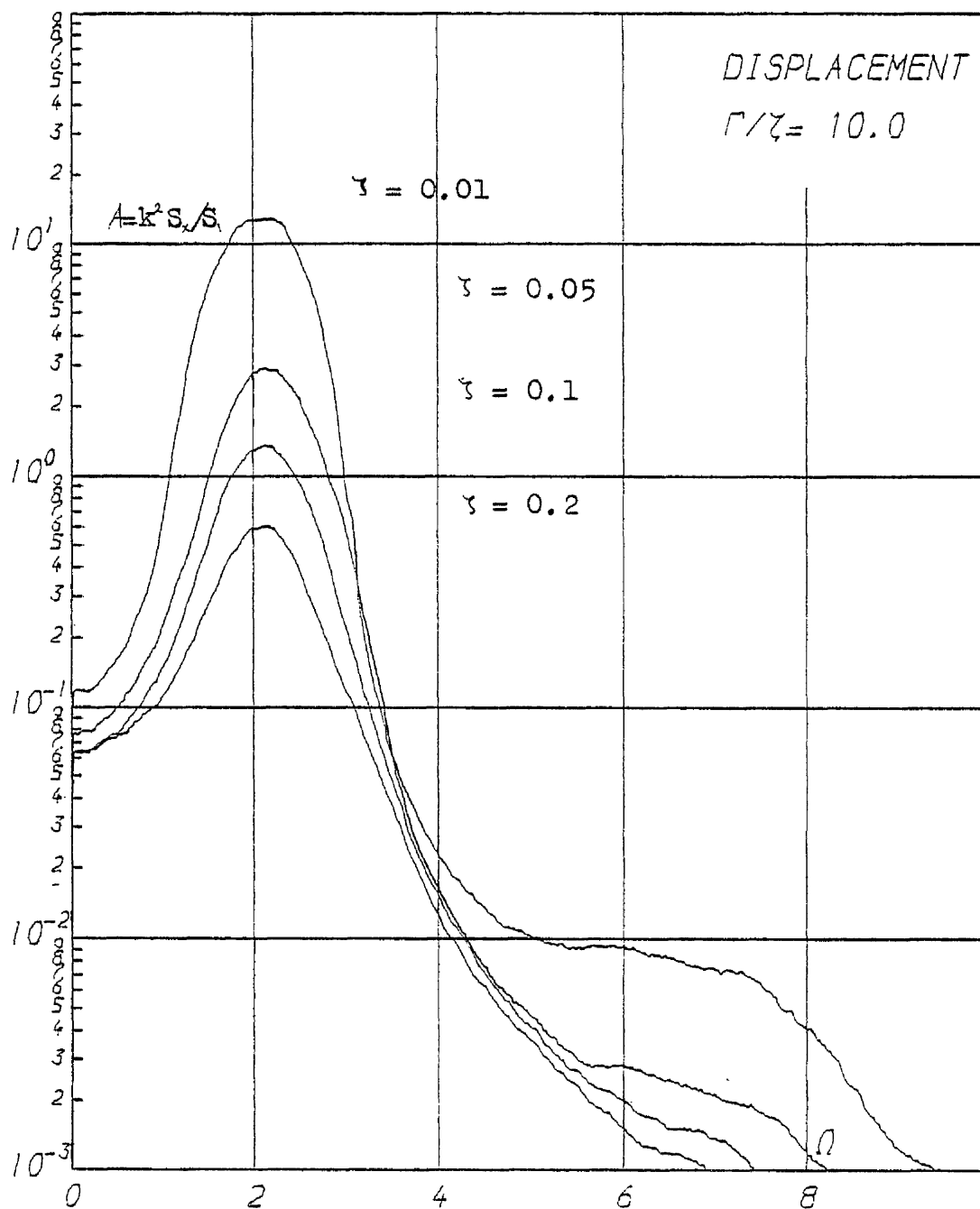


Figure 20a

For A spectra the value of ζ for the particular curve is judged by the magnitude of the $A(\Omega_r)$ value of that curve in the order shown above.

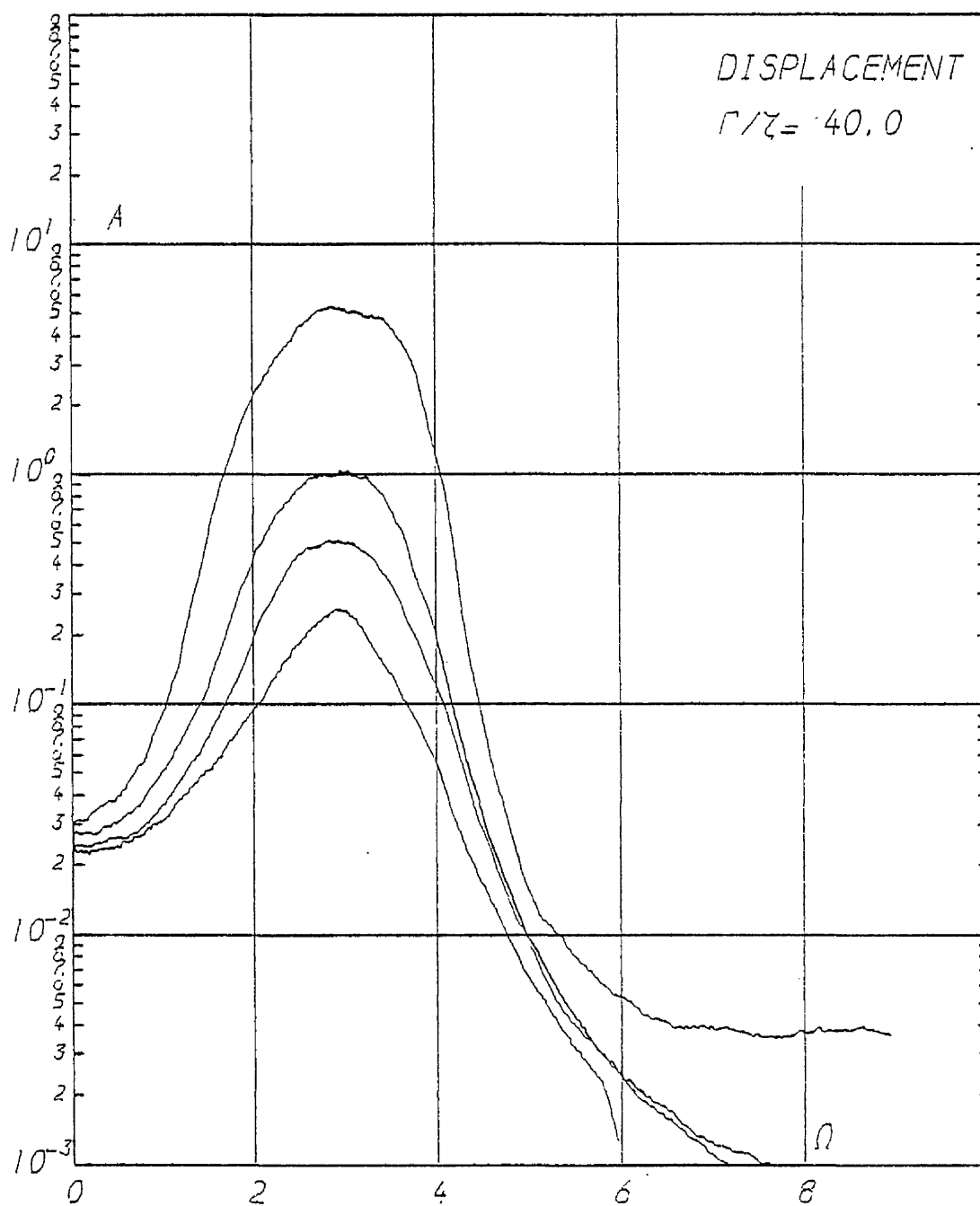


Figure 20b

See also Figure 20a

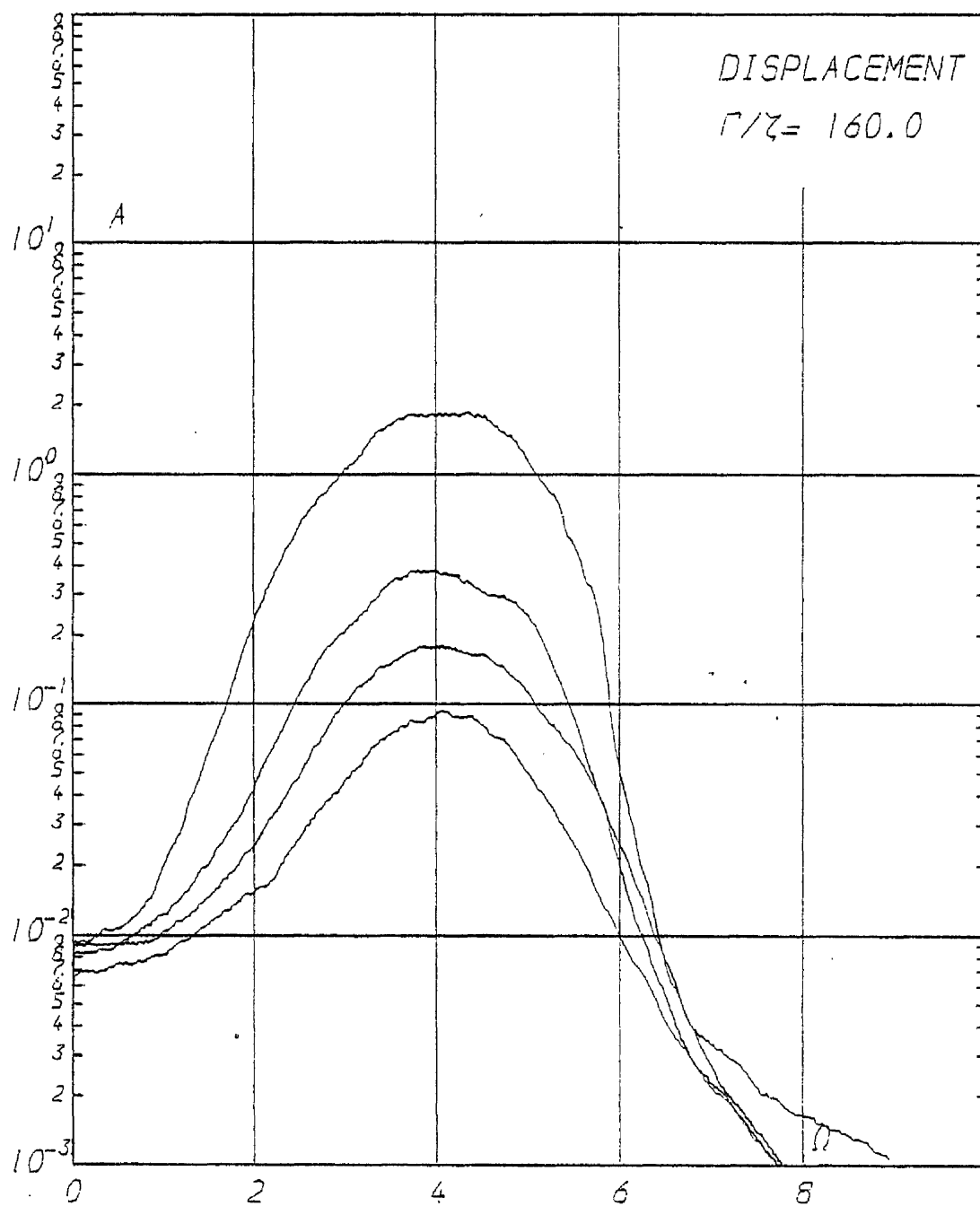


Figure 20c

See also Figure 20a

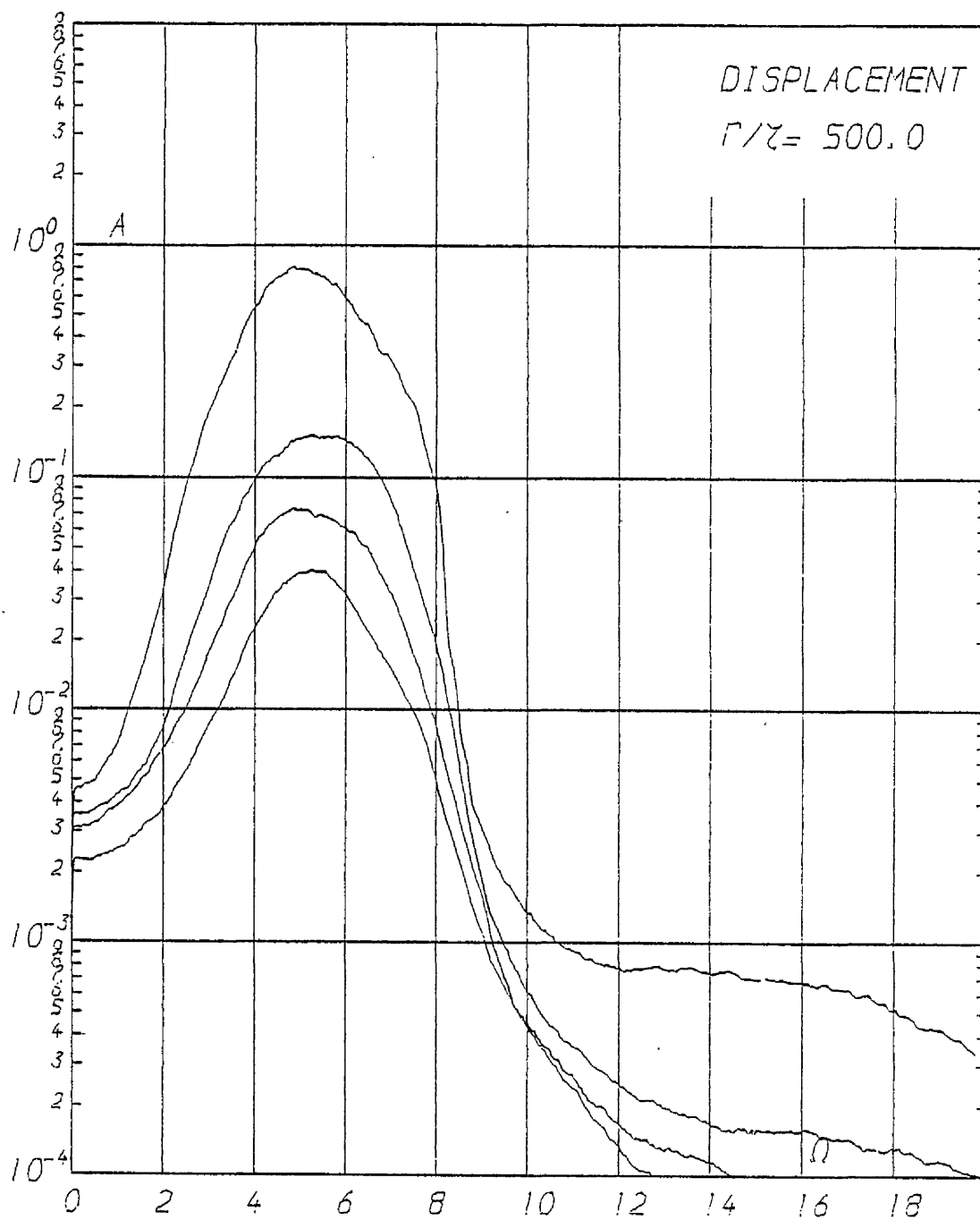


Figure 20d

See also Figure 20a

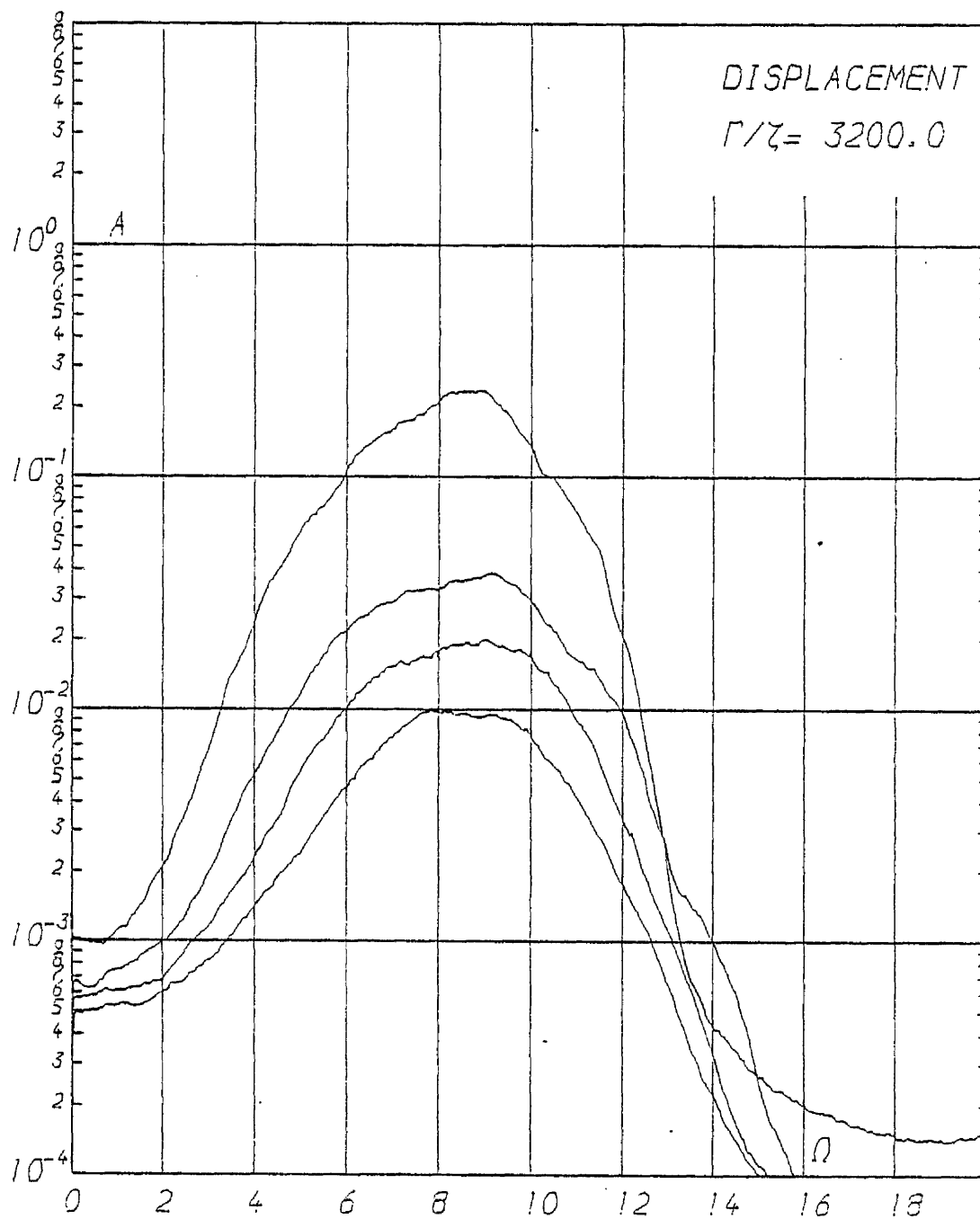


Figure 20e

See also Figure 20a

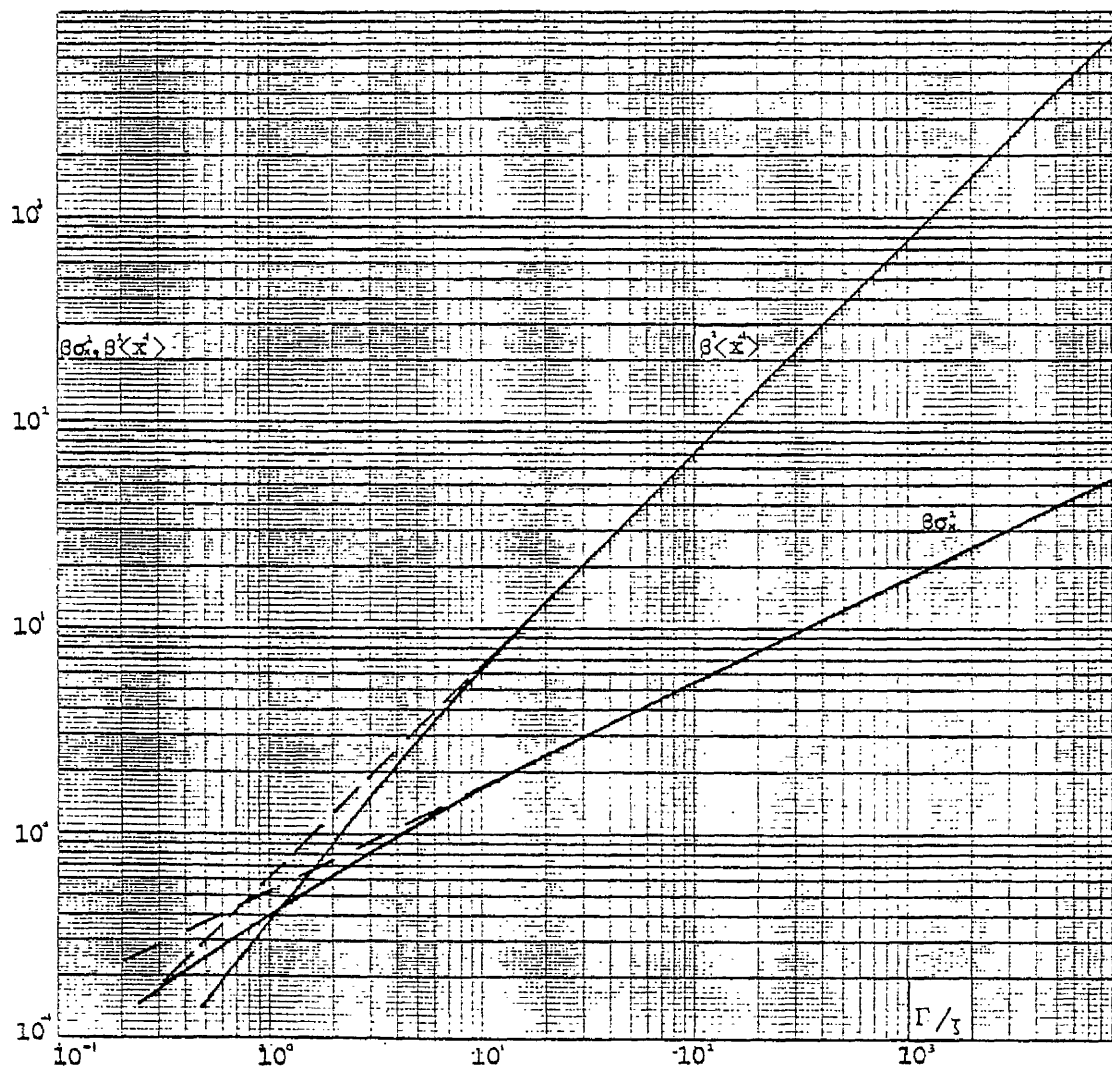


Figure 21

Second and fourth moments of response displacement
versus Γ/γ values ($\Gamma = \beta S_1 \omega_n / k^1$)

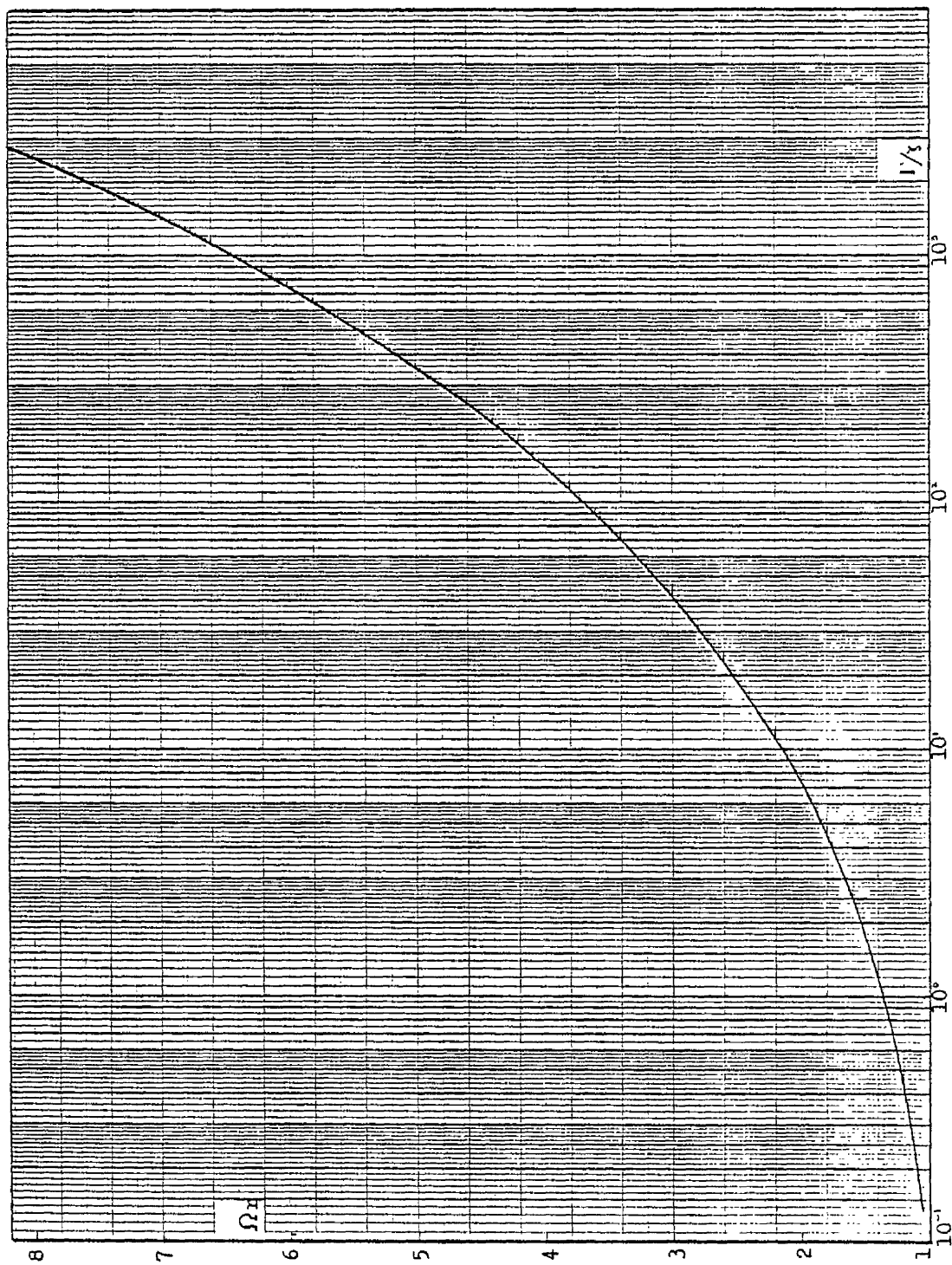


Figure 22
Response displacement resonant frequency Ω_r versus Γ/γ

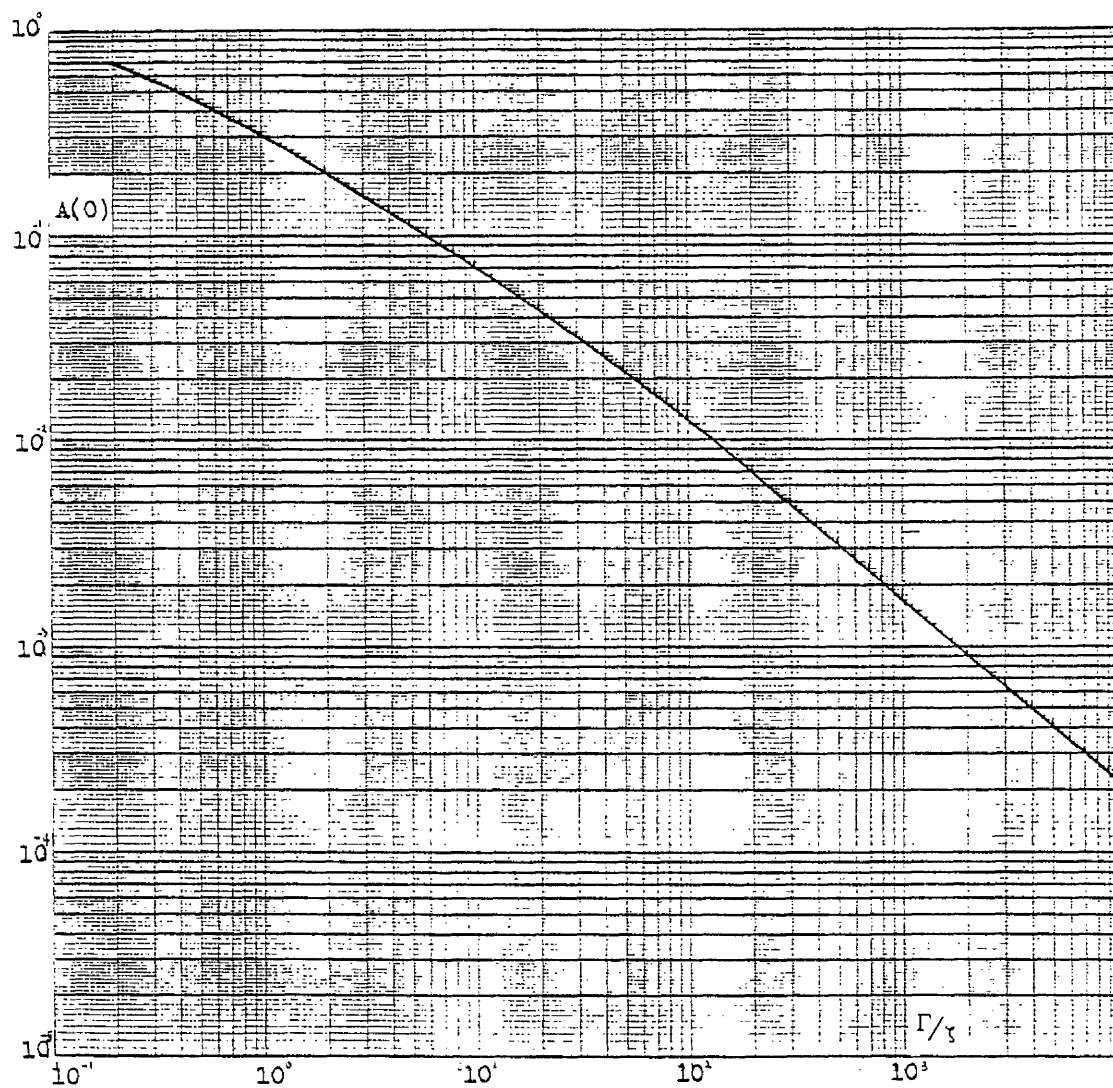


Figure 23

Value of the non-dimensional quantity $A(= k^2 S_x/S_1)$ at near zero frequency versus Γ/λ .

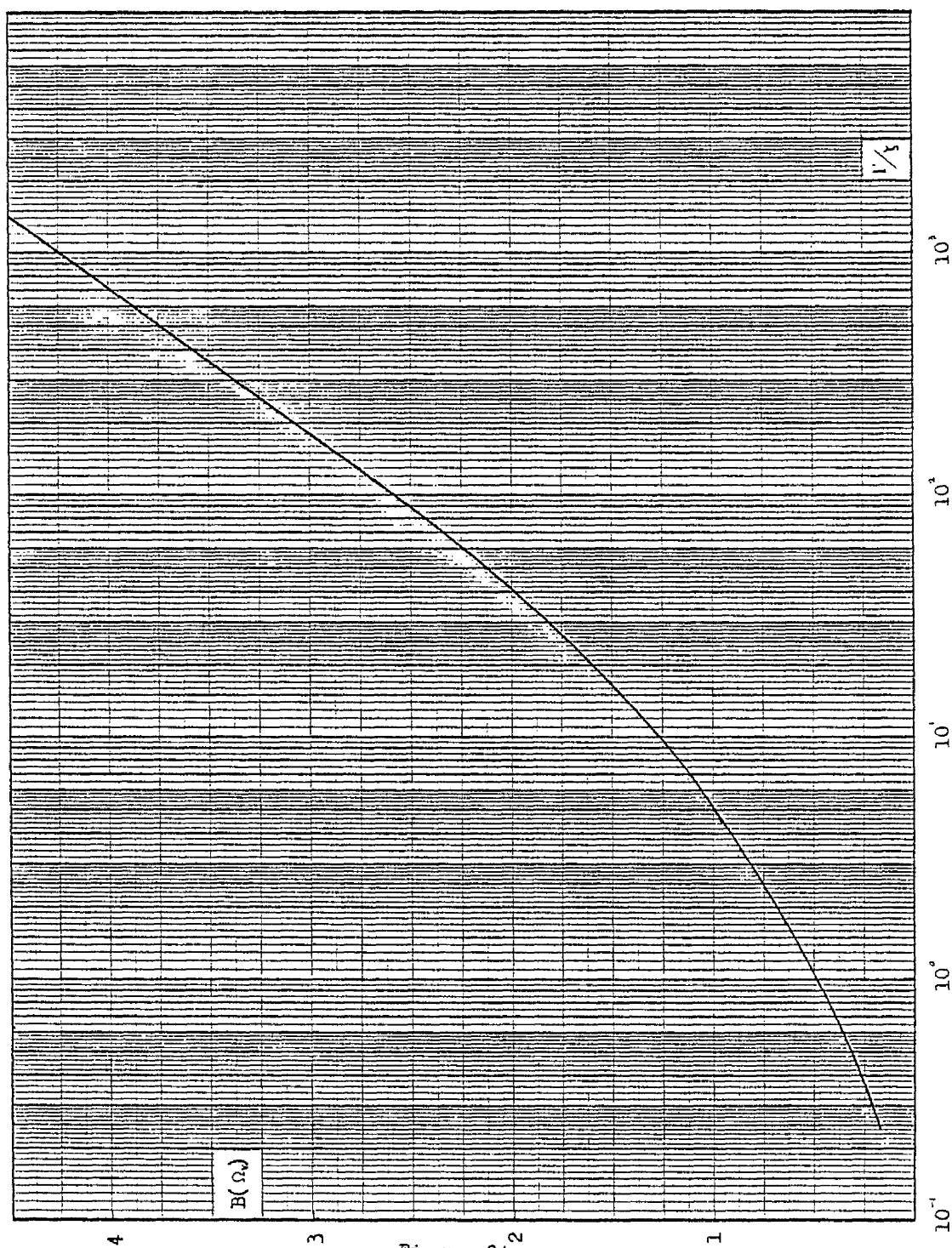


Figure 24
Maximum value of $B(= \beta S_x \omega_n)$ versus Γ/γ

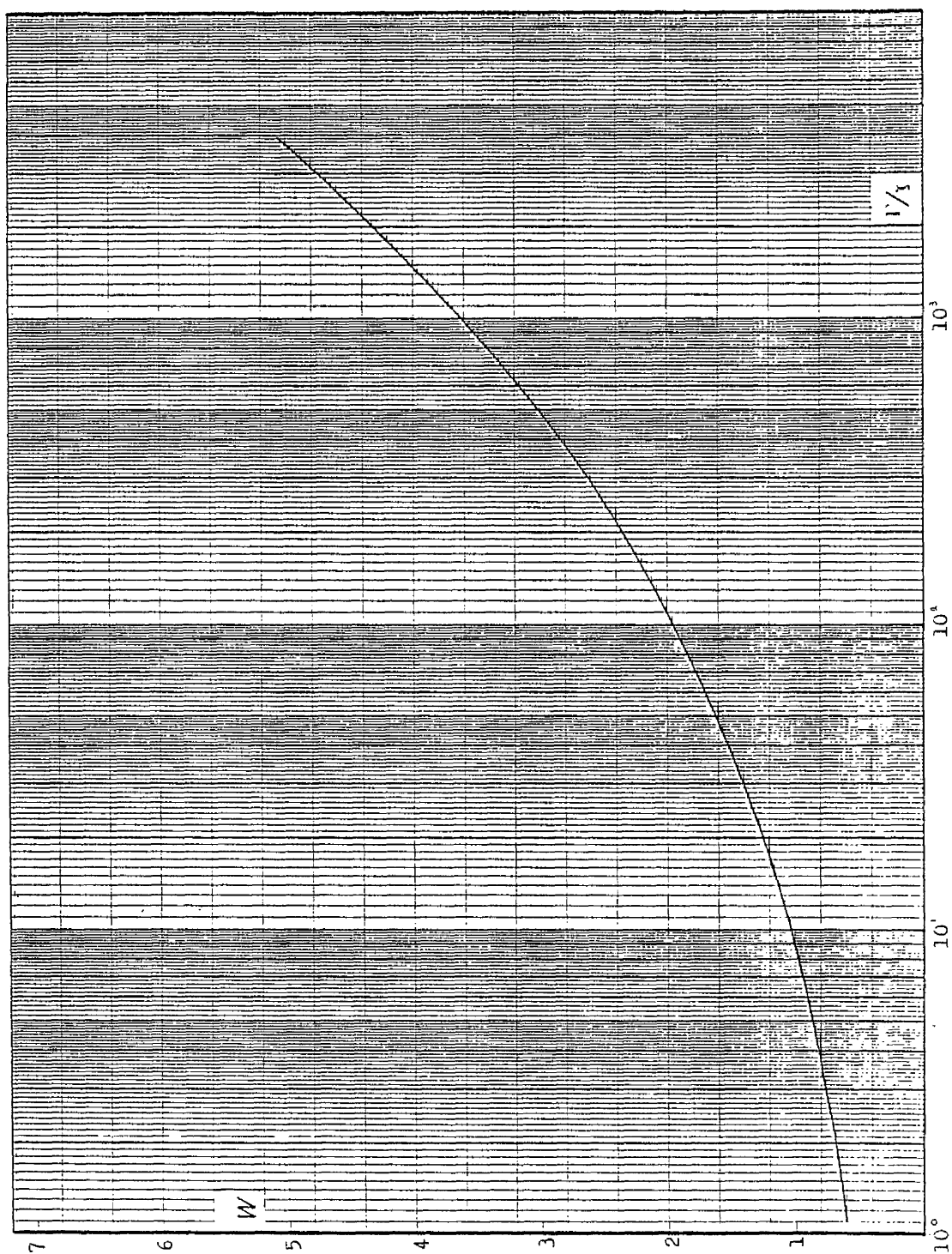


Figure 25
Width of B curves at $B(\Omega_r)/2$ versus I'/I

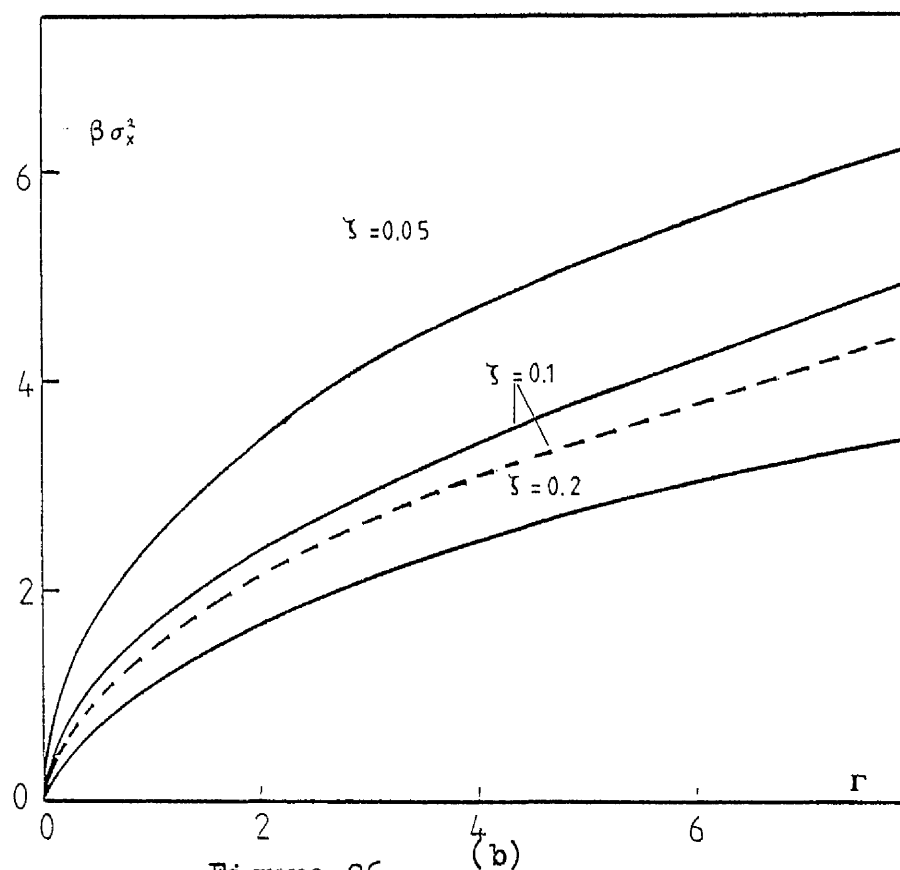
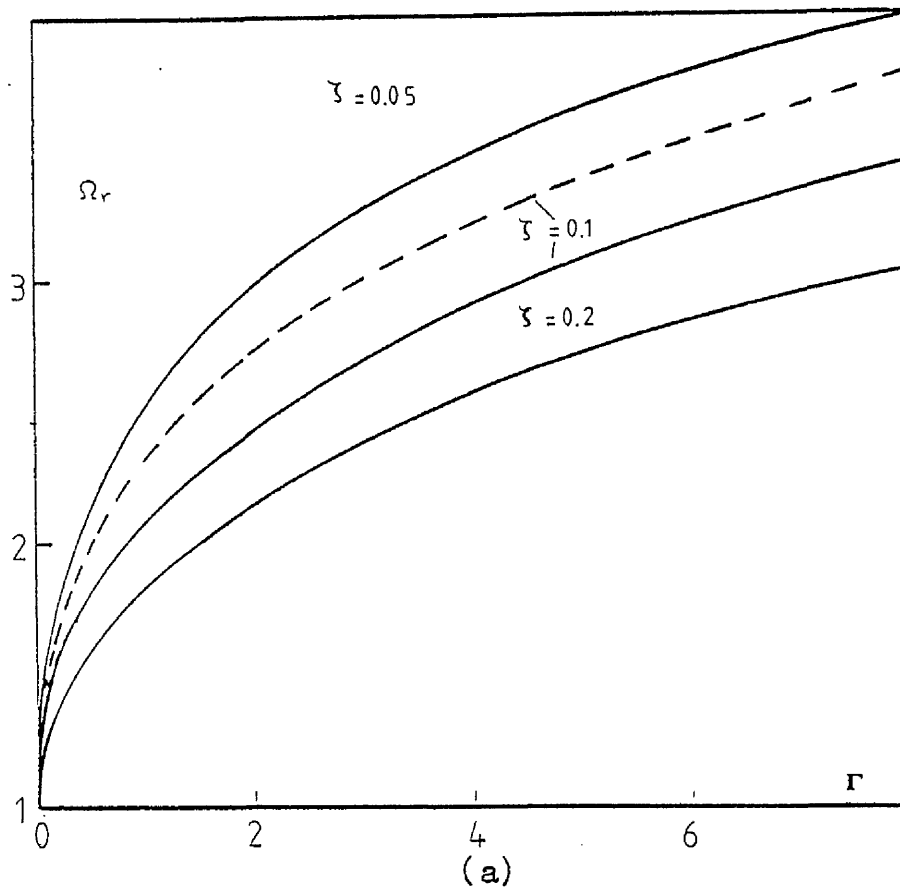


Figure 26

Figure(a) Resonant frequency of response displacement versus Γ for different values of γ .

Figure(b) Response mean square displacement $-\beta \sigma_x^2-$ r for different values of γ . (curves in broken line show results of conventional equivalent linearisation technique.

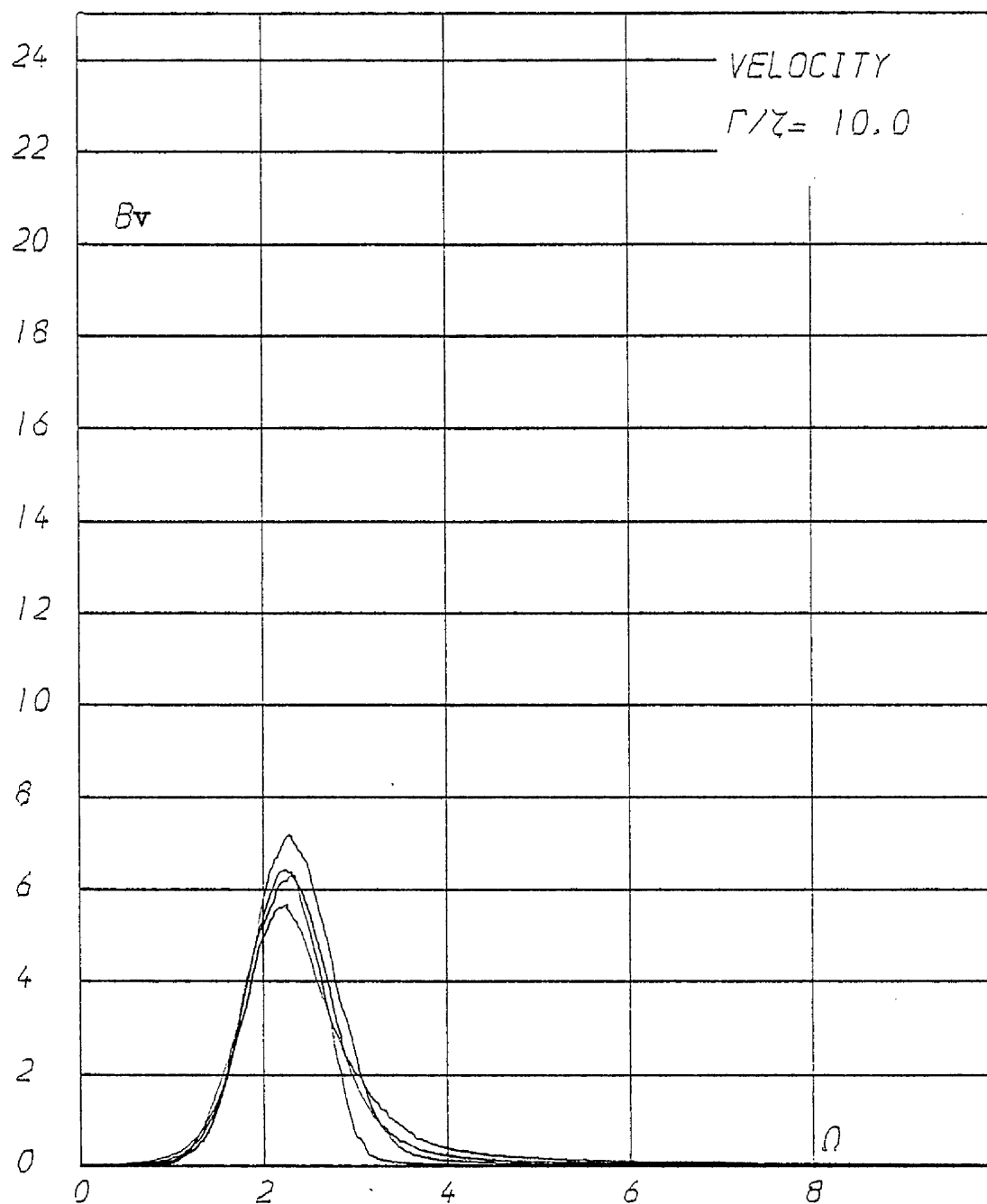


Figure 27a

Figures 27a-29c

Selected non-dimensional response velocity spectra
for γ from 0.01 to 0.2
($Bv = \beta S_{\dot{x}}/\omega_{\eta}$, $Av = k^2 S_{\ddot{x}}/(S_1 \omega_{\eta}^2)$)

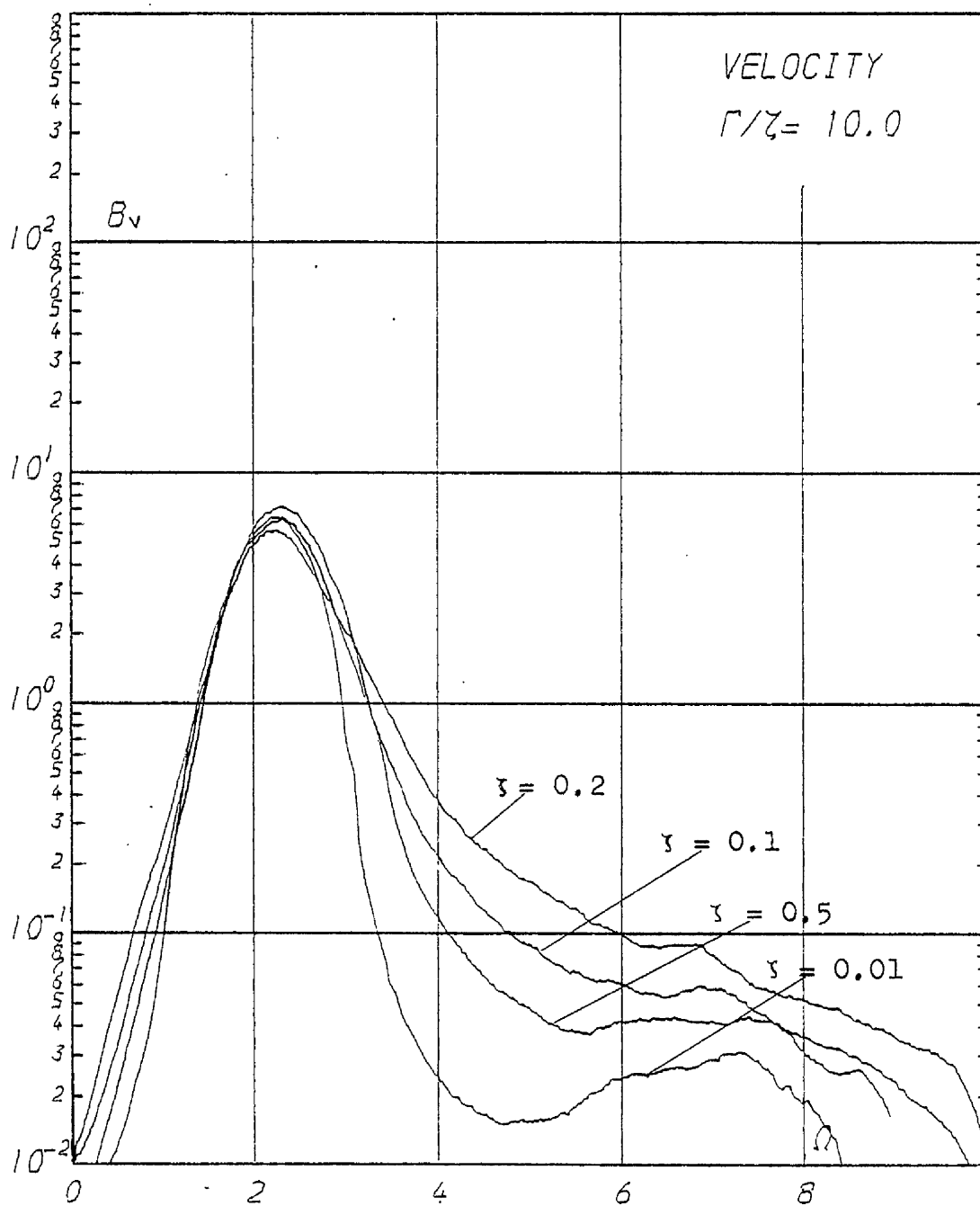


Figure 27b

See also Figure 27a

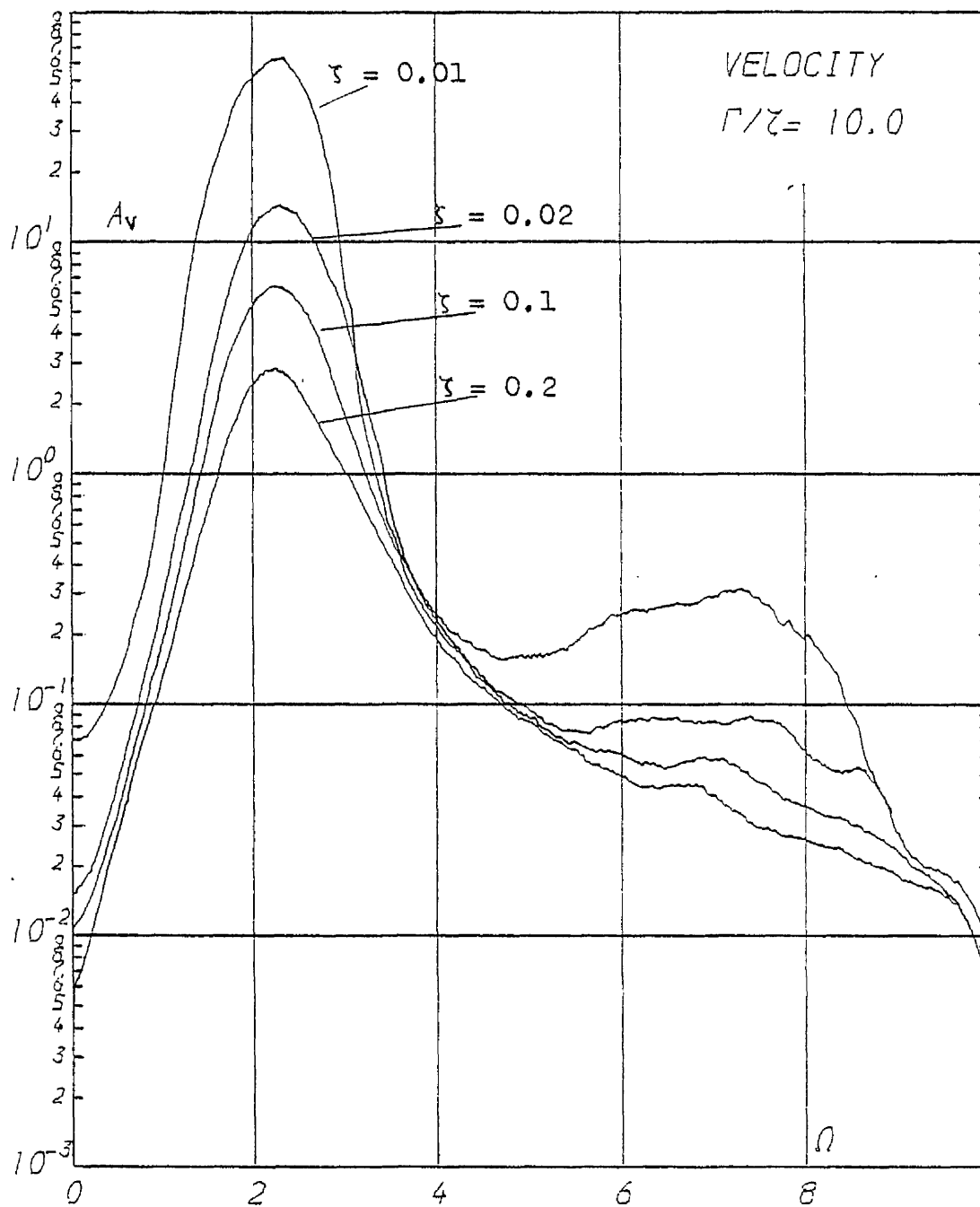


Figure 27c

See also Figure 27a

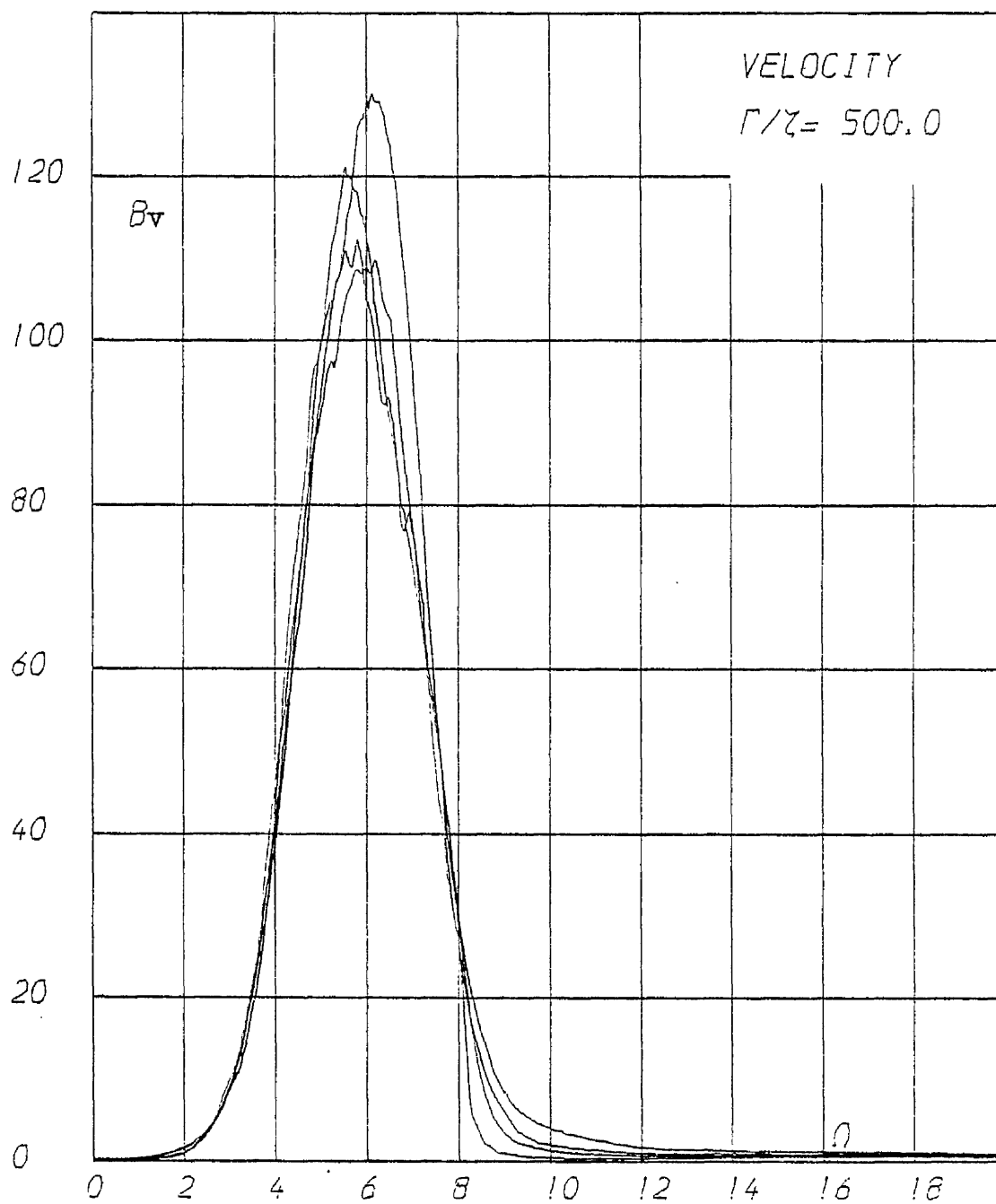


Figure 28a

See also Figures 27a-c

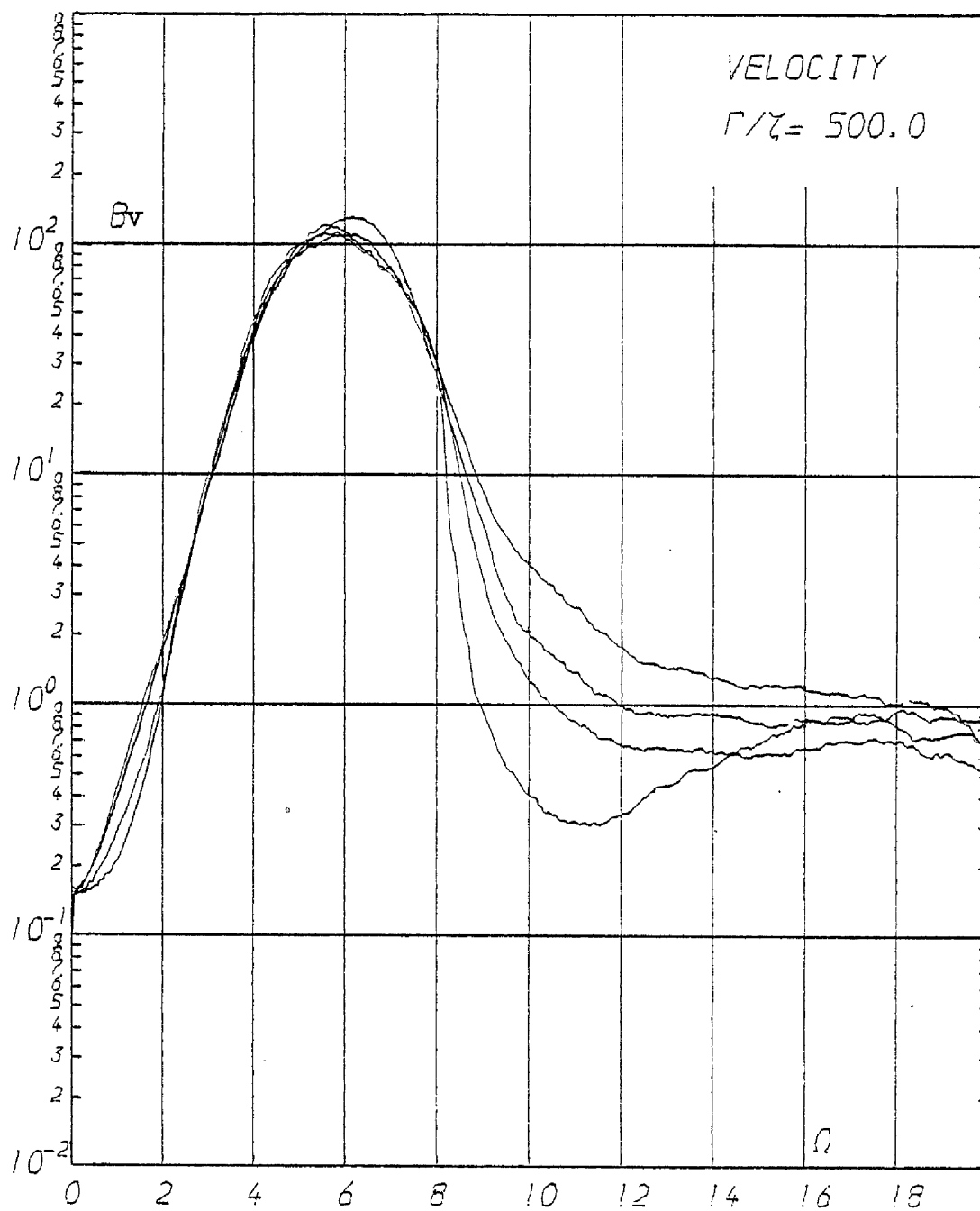


Figure 28b

See also Figures 27a-c

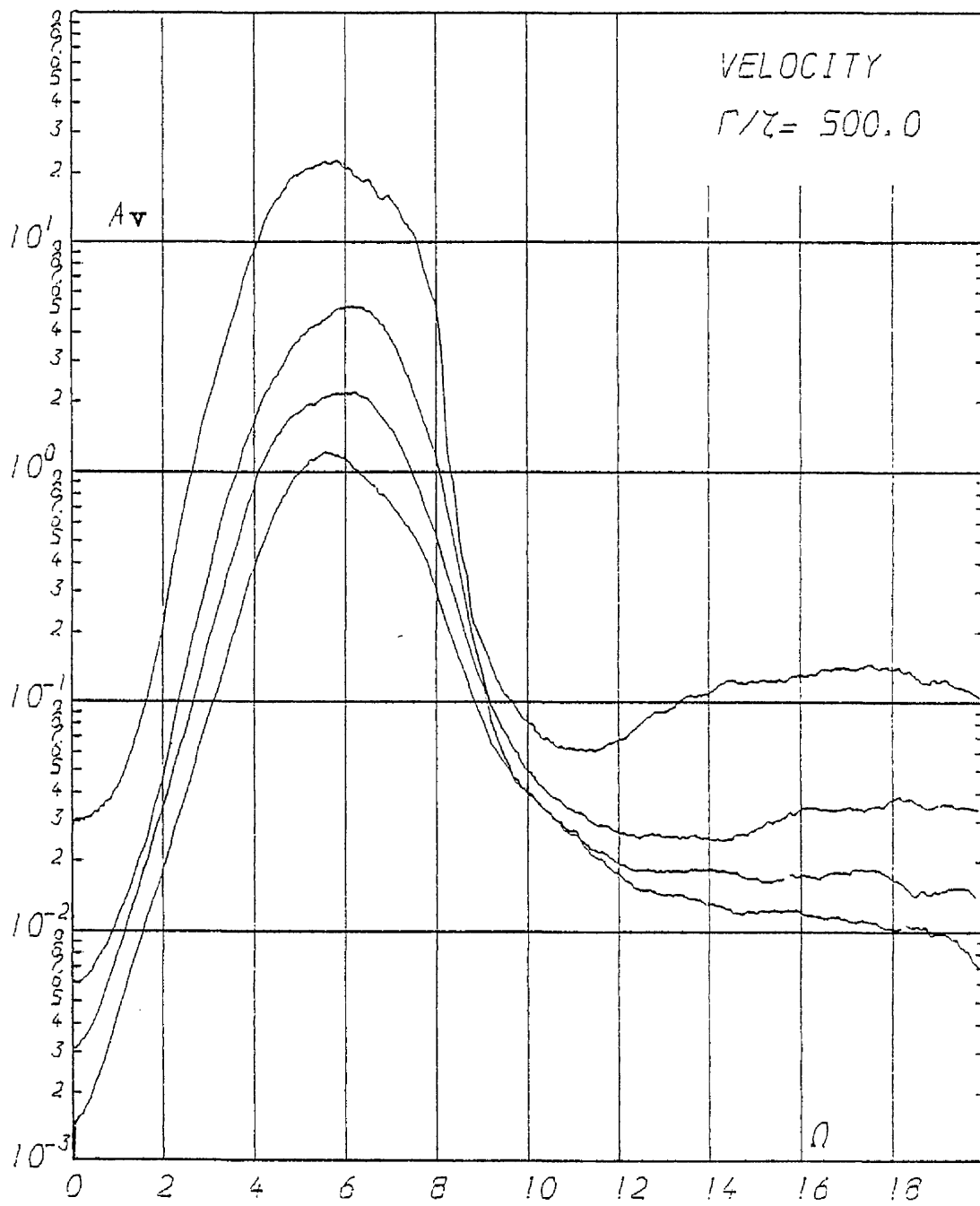


Figure 28c

See also Figures 27a-c

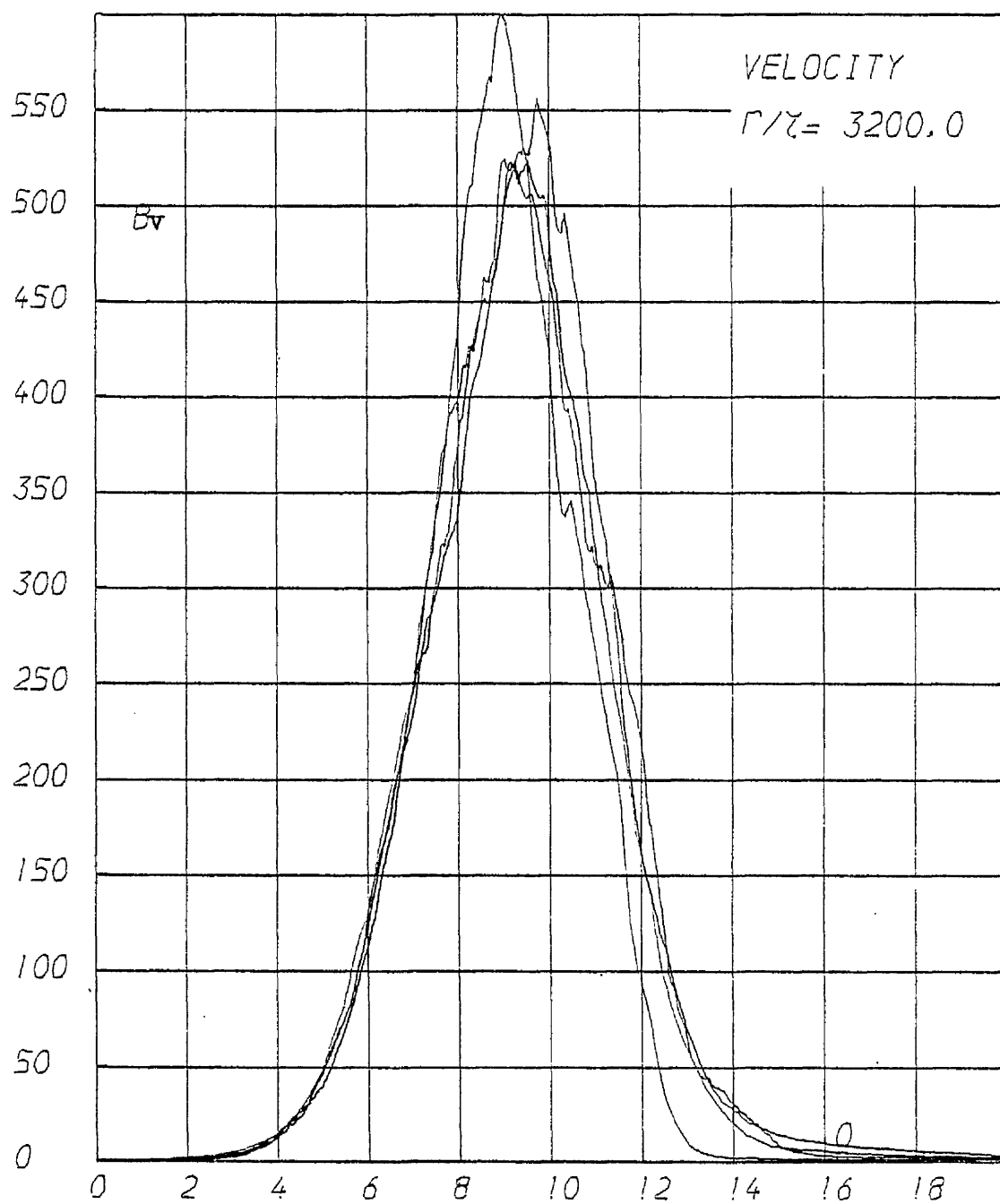


Figure 29a

See also Figures 27a-c

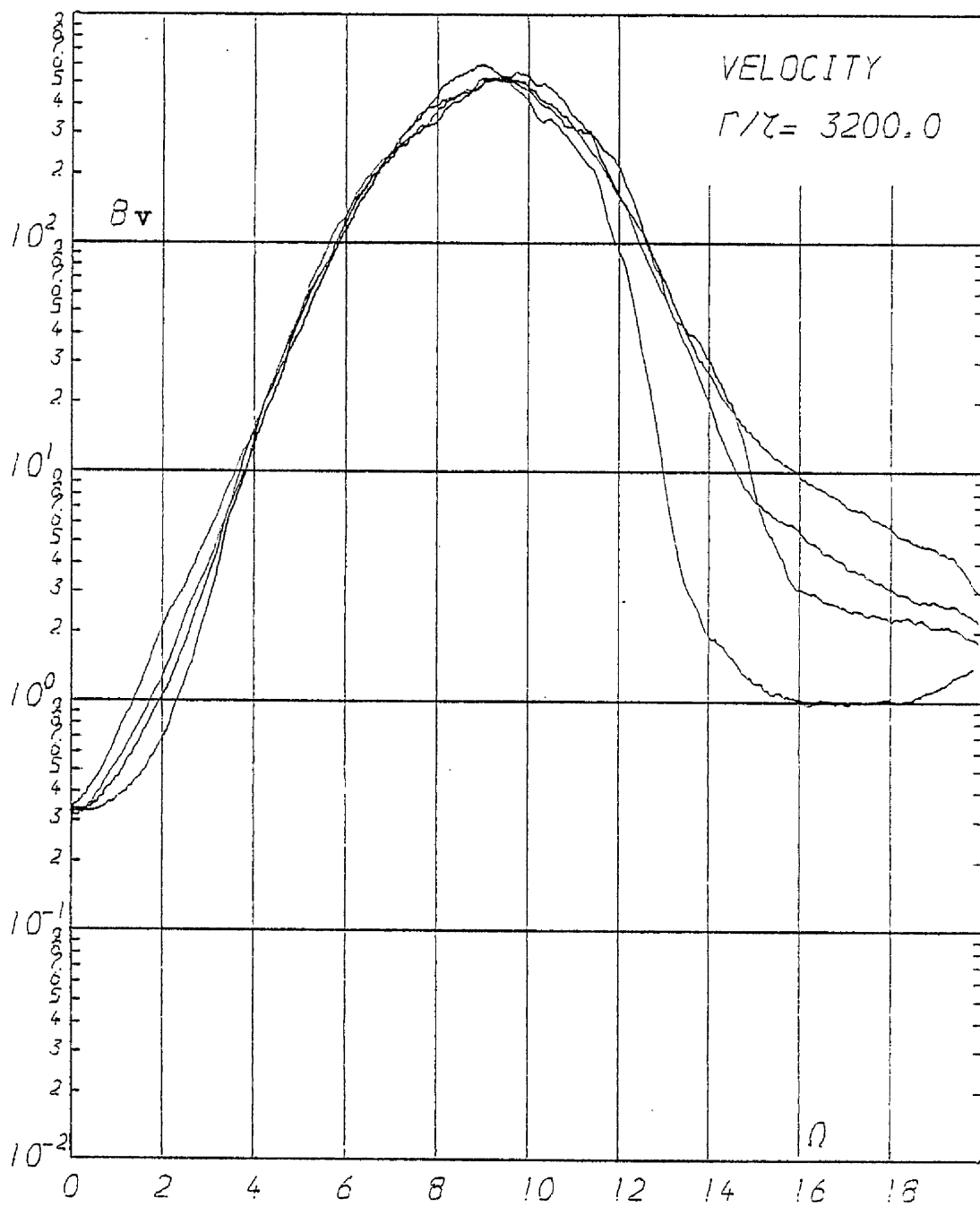


Figure 29b

See also Figures 27a-c

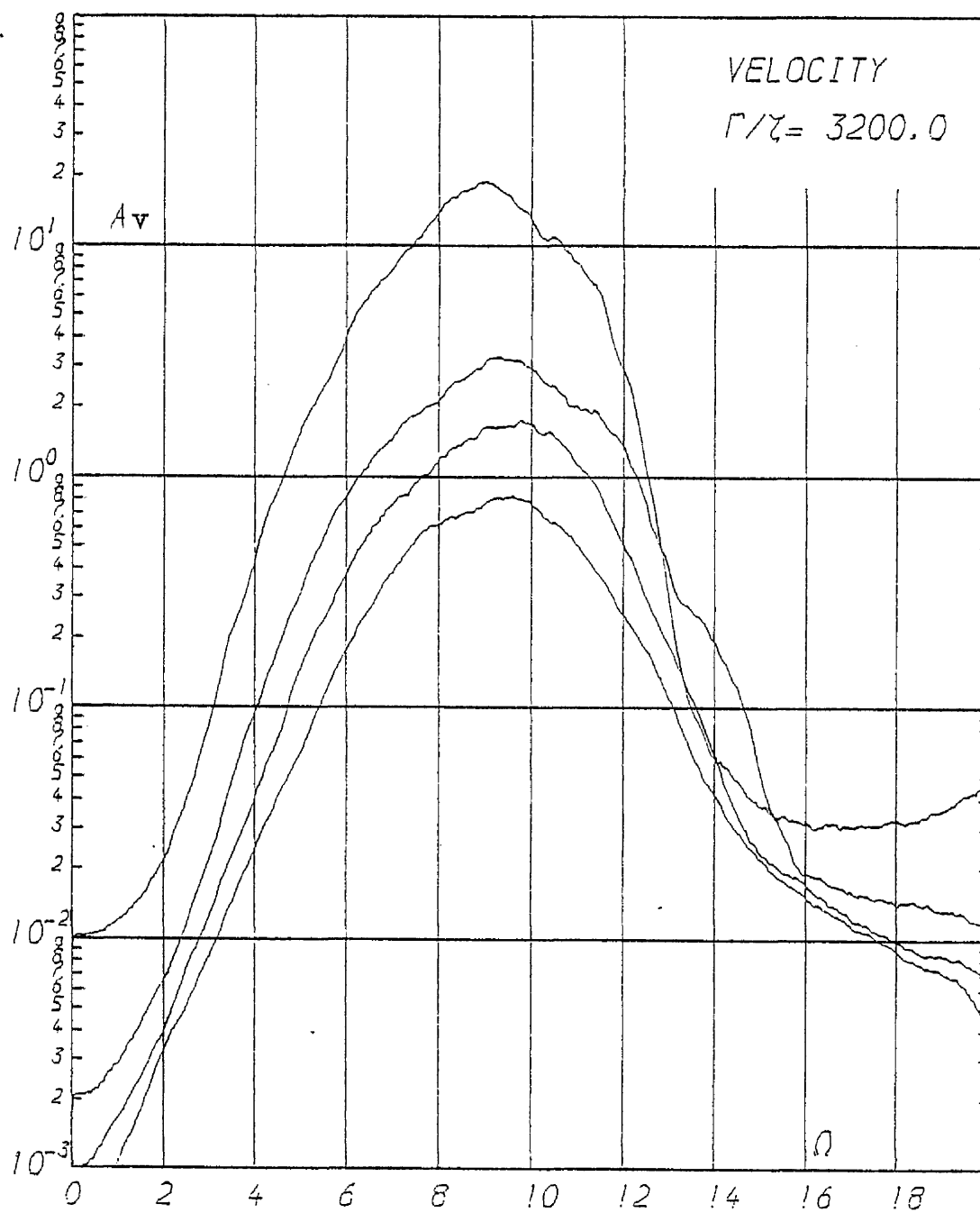


Figure 29c

See also Figures 27a-c

5.4 Connection with Existing Theory

In this section an attempt will be made to express some of the response properties in simple mathematical relations by investigating their connection with existing theory.

It has been established in Section 5.2 that the response of the Duffing system under a 'suitable' broad band random process approximates, to a good degree the response of the system under white noise excitation. This makes possible the use of the exact expression for the joint probability density function of the response displacement and velocity, (which is derived through the solution of the appropriate Fokker - Planck equation. Section 2.1) to calculate the response statistics. The probability density function for the non-dimensional response displacement may be expressed in terms of the ratio Γ/γ (Section 4.2)

$$P(x\sqrt{\beta}) = c \exp \left\{ -\gamma/\Gamma [\beta x^2 + \frac{1}{2}\beta^3 x^4] \right\} \quad (5-1)$$

where c is the normalising constant governed by

$$\int_{-\infty}^{\infty} P(x\sqrt{\beta}) dx = 1/\sqrt{\beta}$$

The odd moments of displacement are zero since equation(5-1) is an even function. The non zero moments are best calculated through numerical integration since the x^4 term in equation (5-1) diminishes the importance of the tails of the function. R.H.Lyon [17] has developed exact expressions for the moments of response displacement involving parabolic cylinder function. However it is possible to derive a simple expression for the displacement variance using the equivalent linearization technique. As already mentioned (Section 2.3) Wolaver [12] has proved that the equivalent linear system will have the same response displacement variance as the Duffing system, provided that the natural frequency of the equivalent linear system is calculated using the exact response probability density function of the nonlinear system. Thus for the system

$$\ddot{x} + 2\gamma\omega_n \dot{x} + \omega_n^2(1+\beta x^2)x = F(t)/m \quad (5-2)$$

the equivalent linear system

$$\ddot{x}_e + 2\gamma_e\omega_e \dot{x}_e + \omega_e^2 x_e = F(t)/m \quad (5-3)$$

where $\gamma_e\omega_e = \gamma\omega_n$

$$\omega_e^2 = \omega_n^2(1+\beta E(x^4)/E(x^2))$$

Will have the same variance provided the ratio $E(x^4)/E(x^2)$ is calculated using the equation (5-1). The statistical value of Kurtosis (Ku) evaluated by the simulation process also provides an estimation of this ratio

$$Ku = \left(\sum_{i=1}^M (x_i - \hat{x})^4 \right) / M\sigma_x^4 \quad (5-4)$$

where M is the number of points involved in the calculation and \hat{x} the mean value of these points. Since

$$\hat{x} \simeq 0 \text{ therefore } E(x^2) = \sigma_x^2$$

$$\sum_{i=1}^M x_i^4 / M = Ku \sigma_x^4 \simeq E(x^4)$$

$$\text{therefore } Ku \simeq E(x^4)/E(x^2)^2$$

$$\text{therefore } KuE(x^2) \simeq E(x^4)/E(x^2) \quad (5-5)$$

Hence the equivalent linear frequency becomes

$$\omega_e^2 = \omega_n^2(1+\beta Ku\sigma_x^2) \quad (5-6)$$

and equation (5-3) becomes

$$\ddot{x}_e + 2\gamma\omega_n \dot{x}_e + \omega_n^2(1+\beta Ku\sigma_x^2)x = F(t)/m \quad (5-7)$$

$$\begin{aligned} \sigma_{x_e}^2 &= S_1 \pi / 4 \gamma_e \omega_e^3 m^2 \\ &= S_1 \pi / 4 \gamma \omega_n \omega_e^2 m^2 \\ &= S_1 \pi / 4 \gamma \omega_n^3 (1+\beta Ku\sigma_x^2) m^2 = \sigma_x^2 \end{aligned} \quad (5-8)$$

where S_1 is the intensity of the excitation spectrum.

Rearranging equation (5-8)

$$(\sigma_x^2)^2 \beta Ku 4 \gamma \omega_n^3 + \sigma_x^2 4 \gamma \omega_n^3 = S_1 \pi / m^2 \quad (5-9)$$

multiplying both sides with $m^2 \beta \omega_n / k^2 \gamma$

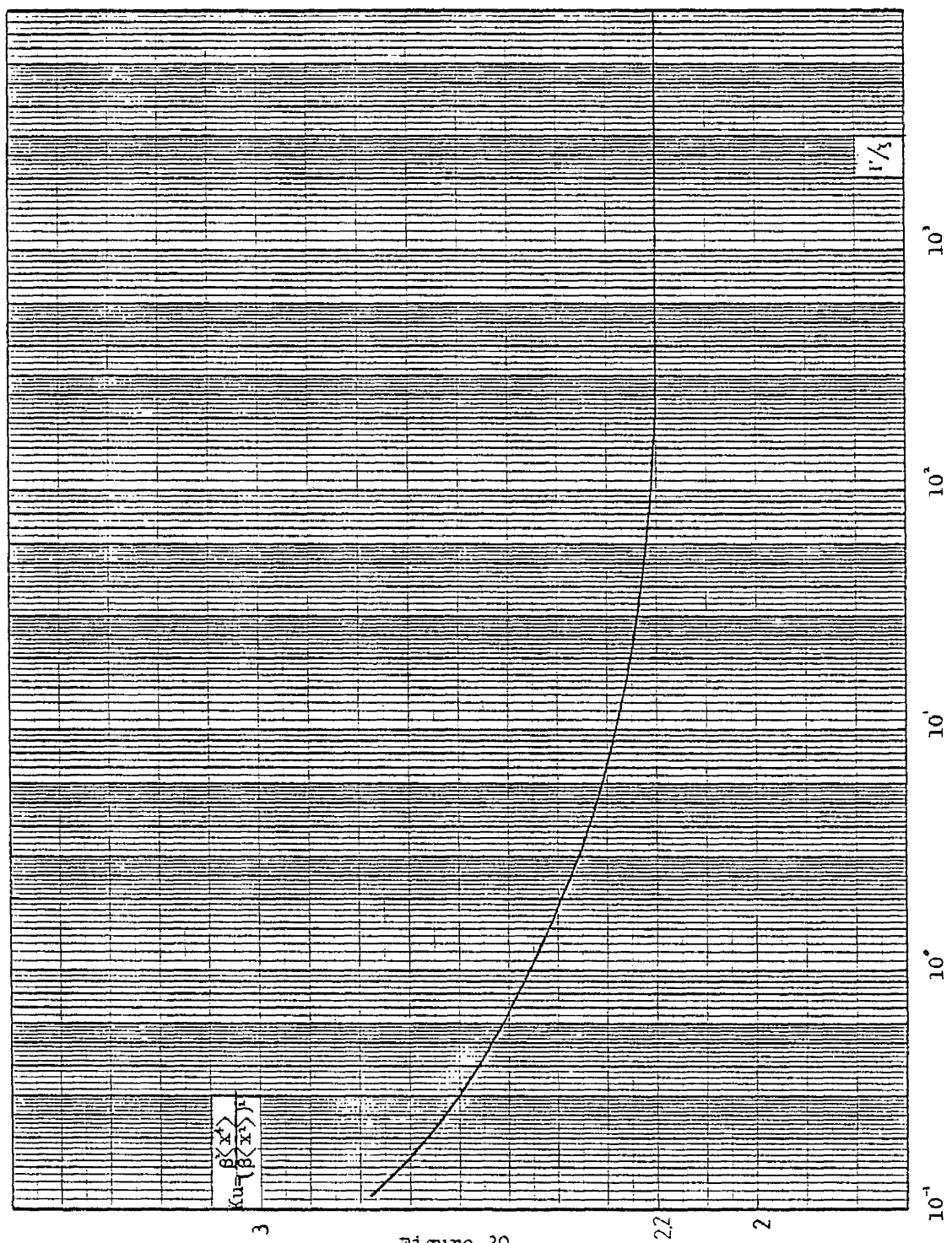


Figure 30
Kurtosis Ku versus Γ/Γ_1 through Fokker - Planck equation

$$(\beta\sigma_x^2)^2 4Ku/\pi + \beta\sigma_x^2 4/\pi = \beta S_1 \omega_n/k^2 \zeta = \Gamma/\zeta \quad (5-10)$$

or

$$\beta\sigma_x^2 = (-1 + \sqrt{1 + Ku\pi\Gamma/\zeta}) / 2Ku \quad (5-11)$$

Provided the correct value of Ku is used in the above equation, it should provide the exact value of $\beta\sigma_x^2$ for the response displacement for a given value of Γ/ζ . Kurtosis is a function of Γ/ζ as indeed all statistical values of the system that can be derived from equation (5-1).

$$Ku = \beta^2 E(\dot{x}^4) / (\beta E(\dot{x}))^2 = E(\dot{x}^4) / (E(\dot{x}))^2$$

Figure 30 shows the asymptotic behaviour of Kurtosis versus Γ/ζ . The values were calculated numerically from the exact expression for the probability density function of displacement. It can be seen that as $\Gamma/\zeta \rightarrow \infty$, $Ku \rightarrow 2.2$ and as $\Gamma/\zeta \rightarrow 0$, $Ku \rightarrow 3$ (linear case, Gaussian distribution). This behaviour justifies possible use of equation (5-10) as an empirical relation with a suitable constant value for Ku. Table (5.4) displays the values of Ku calculated by the simulation process and the exact probability function. Also displays the values of $\beta\sigma_x^2$ calculated by the simulation process, the exact probability function, and equation (5-10) with Ku as evaluated by the simulation process. The corresponding fourth moments are also displayed. The entries in that table are all non-dimensional. Further the entries with suffix eqc are calculated with a constant value of $Ku = 2.3$.

Figure (31) shows the displacement response spectrum of the nonlinear system for $\Gamma/\zeta = 500$ and the corresponding spectrum of the equivalent linear systems for $Ku = 2.2$

($Ku = 3$ is the value used in the equivalent linearization technique when the exact probability density function is ignored as in Section 2.2). Although the spectral shapes are different their resonant frequencies seem to be the same. Looking back at equation (5-6)

$$\omega_i^2 = \omega_n^2 (1 + \beta Ku \sigma_x^2)$$

for $\Omega = \omega_i / \omega_n$

Table 5.4

r / ζ	1	2	3	4	5	6	7	8	9	10
	$\beta\sigma_s^2$	$\beta\sigma_{FP}^2$	$\beta\sigma_{Eq}^2$	$\beta\sigma_{Eqc}^2$	Ku_s	Ku_{FP}	$\beta^2\langle x^4 \rangle_s$	$\beta^2\langle x^4 \rangle_{FP}$	$\beta^2\langle x^4 \rangle_{Eq}$	$\beta^2\langle x^4 \rangle_{Eqc}$
0.5	0.25	0.25	0.24	0.25	2.52	2.57	0.16	0.15	0.15	0.14
1.0	0.39	0.40	0.40	0.41	2.46	2.45	0.39	0.39	0.39	0.38
2.0	0.63	0.63	0.63	0.64	2.38	2.40	0.94	0.95	0.94	0.93
5.0	1.10	1.10	1.11	1.11	2.30	2.32	2.78	2.82	2.82	2.82
10.0	1.65	1.65	1.65	1.64	2.27	2.29	6.18	6.20	6.19	6.19
20.0	2.49	2.42	2.44	2.40	2.22	2.25	13.80	13.38	13.22	13.25
40.0	3.54	3.53	3.60	3.48	2.15	2.23	26.18	28.00	27.71	27.85
80.0	5.10	5.10	5.13	5.01	2.19	2.22	57.19	57.78	57.77	57.73
160.0	7.26	7.31	7.45	7.18	2.13	2.20	109.80	118.35	118.22	118.44
500.0	13.08	13.14	13.44	12.85	2.10	2.20	359.28	379.85	379.33	379.78
3200.0	33.30	33.57	34.60	32.84	2.07	2.20	2295.40	2479.70	2978.12	2980.47

Columns 1,5,7 Simulation Values.

" 2,6,8 From $P(x)$ through Fokker-Planck equation.

" 3,9 From equivalent lin. technique using column 5.

" 4,10 From equivalent lin. technique and $Ku = 2.3$

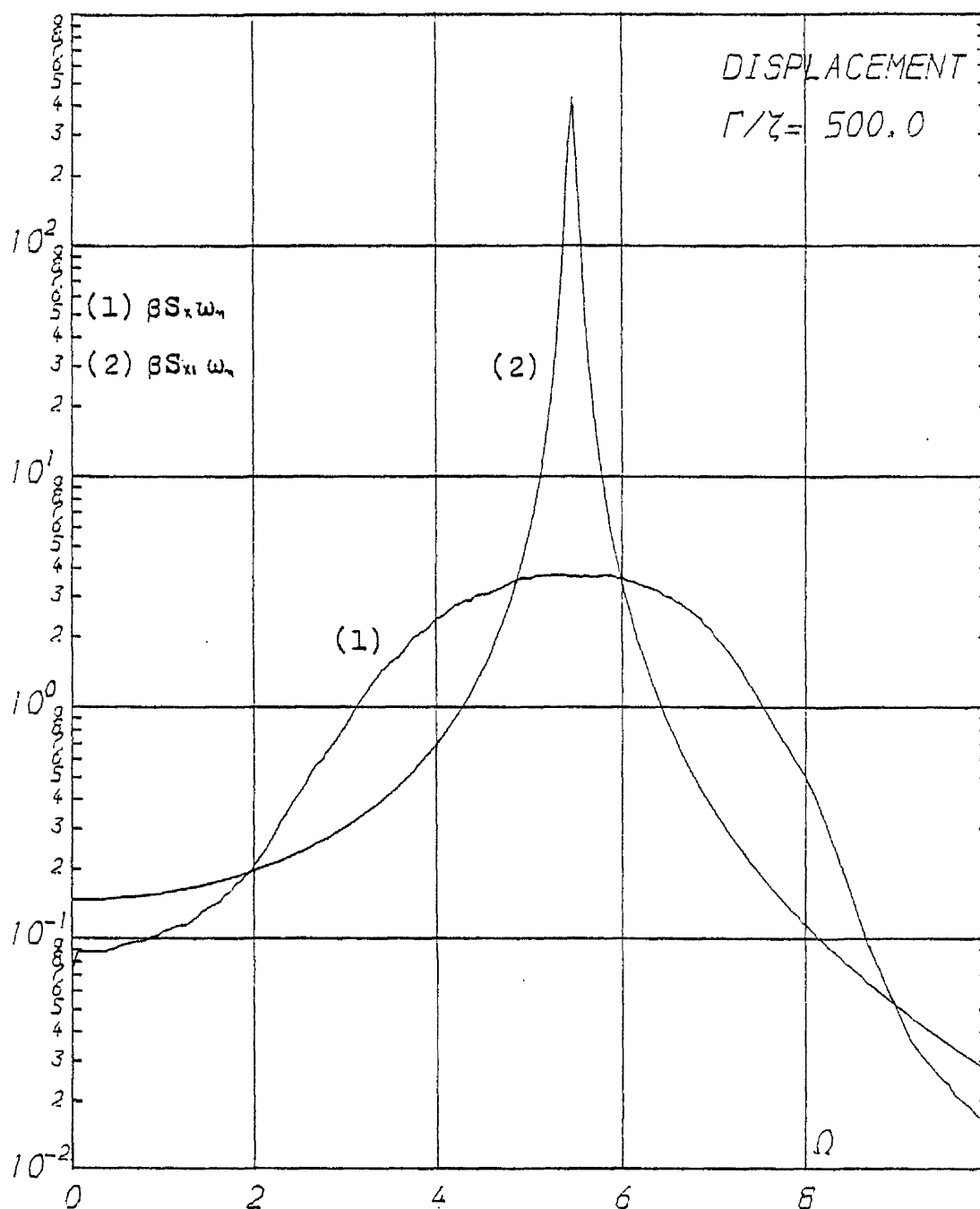


Figure 31

Comparison of response displacement spectra

(1) Duffing system $\zeta = 0.05, \Gamma/\zeta = 500$

(2) Corresponding Equivalent linear system

$$(S_{x1} = |H_e(\omega)|^2 S_{\zeta})$$

$$\Omega^2 = 1 + \beta K u \sigma_x^2 \quad (5-12)$$

if equation (5-10) is solved for $\beta\sigma$ (positive root only) and substituted above, the following relation may be obtained

$$(\Omega^4 - \Omega^2) 4/(Ku\pi) = \Gamma/\zeta \quad (5-13)$$

or

$$\Omega^2 = (1 + \sqrt{1 + Ku\pi\Gamma/\zeta})/2 \quad (5-14)$$

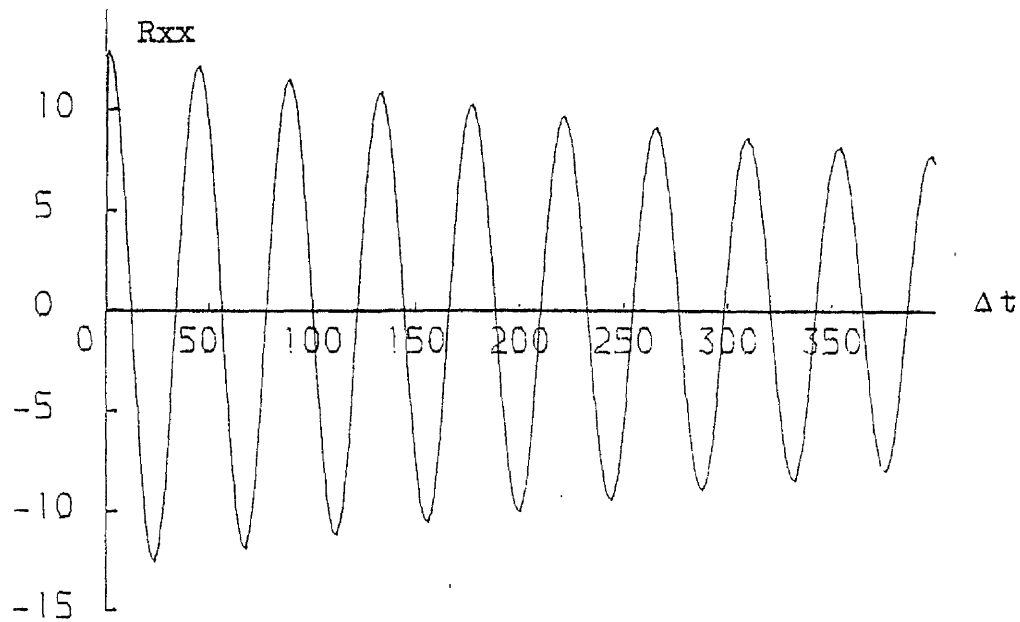
The above equation provides a simple relationship between the natural frequency of the equivalent linear system and the ratio Γ/ζ . Table 5.5 displays the computed values of resonant frequency of the displacement response spectra of the nonlinear system and the resonant frequencies of the equivalent linear systems for different values of Γ/ζ . Thus the combination of three fundamentally different methods has produced two useful formulae, equation (5-10) which describes a parabolic relationship between the nondimensional response displacement variance $\beta\sigma_x^2$ (or area under B curves) and Γ/ζ , and equation (5-12) which describes a similar valid relationship between the natural frequency of the equivalent linear system and Γ/ζ . From this last relationship the resonant frequency of the response displacement spectrum may be predicted since the resonant frequency of the two systems (i.e. linear and nonlinear) seems to be the same over a large range of Γ/ζ values.

Table 5.5

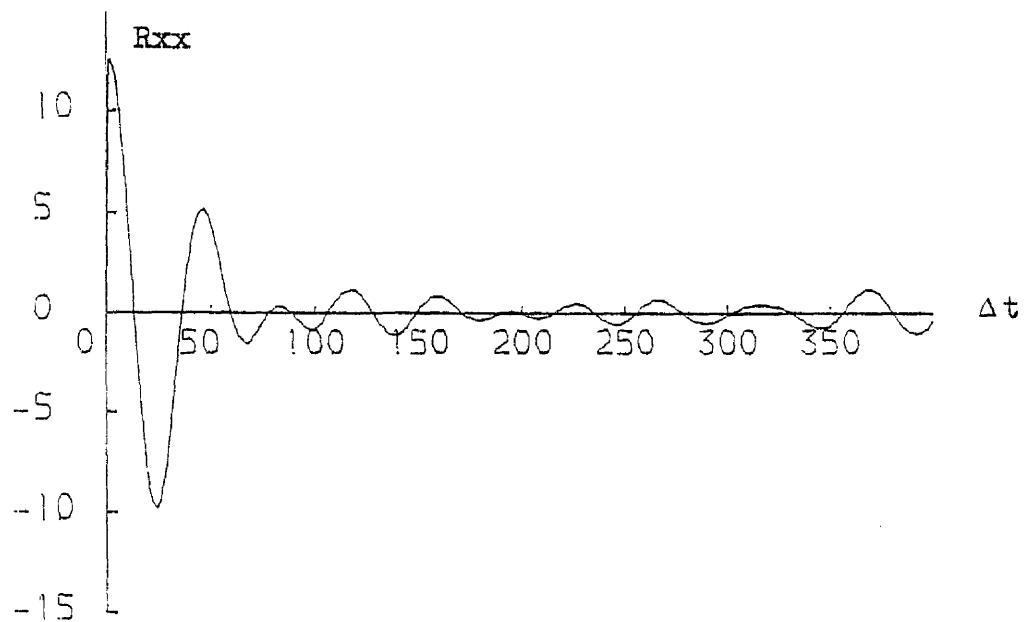
Γ/ζ	10	40	160	500	3200
Ω_r	2.11	3.01	4.07	5.28	8.60
Ω_{req}	2.18	2.95	4.10	5.40	8.52
Ω_{reqc}	2.16	2.97	4.14	5.46	8.65
Ω_{req3}	2.32	3.19	4.46	5.90	9.35

As mentioned before the property of the equivalent linear system that was utilised to obtain equation (5-10) was proved

mathematically by Wolaver [12]. Wolaver has also proved that the MacLaurin series expansion of the approximate auto correlation function $R_{xx}(\tau)$ of the stationary displacement obtained from the equivalent linear system agrees with the exact autocorrelation function up to the τ^3 term. However the significance of this can only be appreciated when the autocorrelation functions of the nonlinear system and its corresponding equivalent linear system are compared as in Figure 32. It is seen there that the frequency of oscillation of the two functions are almost identical for the first cycle at least. This of course determines the resonant frequency of the response. The difference in width of response spectral peaks is also obvious from Figure 32. The corresponding spectra are shown in Figure 31.



(a) Equivalent linear system $\Delta t = 0.01665$



(b) Duffing system $\Delta t = 0.01665$

Figure 32

Response displacement autocorrelation function
for $\gamma = 0.05$, $\Gamma/\gamma = 500$, $\omega_n = \pi/2$

5.5 Graphical Representation

In this section the properties of the response displacement spectrum summarised in Figures 21-25 are utilised to provide a simple graphical method of sketching the response displacement spectrum in its non-dimensional form as $B = \beta S_x(\Omega) \omega_n$ for a given value of Γ/ζ . The method may be split in two stages. Given a particular value of Γ/ζ , in the first stage an isosceles triangle of area equal to $\beta \sigma_x^2 (=f(\Gamma/\zeta))$ is designed to represent the spectral response (Figure 33) with its apex at Ω_r and its height approximately equal to $B(\Omega_r)$. The triangular shape gives a rough idea of the systems spectral response, that may be adequate for some practical applications. A more detailed sketch may be developed from this basic figure, if the data provided by Figures 23,24,25 are used to clip the peak, obtain the value of $B(0) = A(0) \Gamma$ and modify the width at $\frac{1}{2}B(\Omega_r)$ heights.

As it can be seen from Figure 33, the idea of approximating the response spectrum by a isosceles triangle is suggested by the symmetry of the spectra about Ω_r and the similar slope of the peak sides. Once it was decided that the essential features of the approximate shape would be

- its area = $\beta \sigma_x^2$ (from equation (5-10)) and
- its apex positioned at Ω_r (from equation (5-12)), a slope had to be found that would best fit the spectral shape.

Thus if the height of the triangle is denoted by h and its base by $2a$ then

$$\beta \sigma_x^2 = ha \quad (5-15)$$

$$\tan \theta = h/a$$

where θ is the base angle.

$$\text{therefore} \quad a = \sqrt{\beta \sigma_x^2 \sqrt{1/\tan \theta}} \quad (5-16)$$

$$h = \sqrt{\beta \sigma_x^2 \tan \theta}$$

By trial and error the value of $\tan \theta = 1.428$ was judged to give best overall results. Hence in order to draw the triangular figure one would have to evaluate (assuming $K_u = 2.2$) for a given value of Γ/ζ

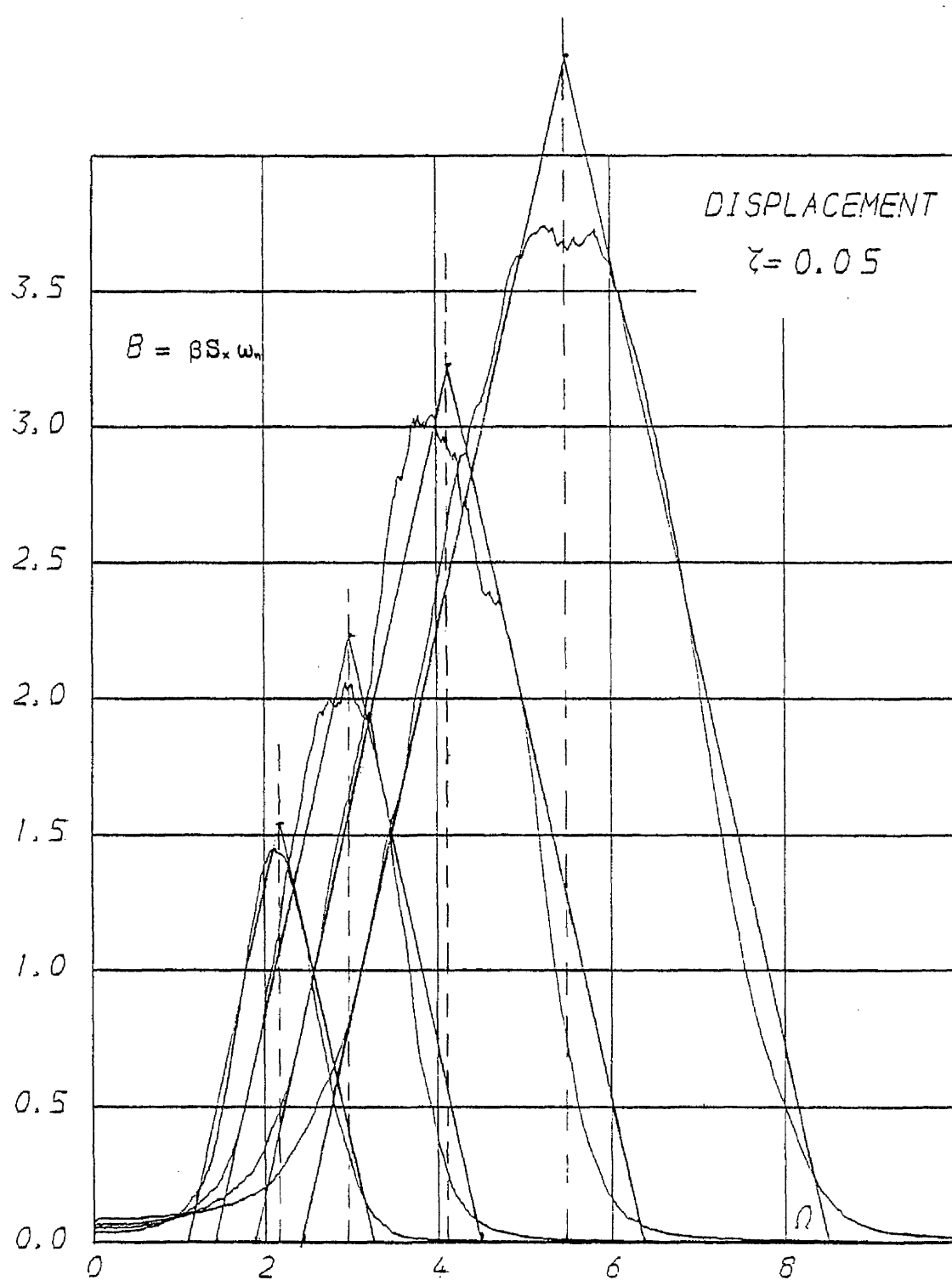


Figure 33

Graphical representation method of
non-dimensional response displacement
spectra

$$a) \quad \Omega_c = \left[(1 + \sqrt{1 + 2.2\pi\Gamma/\zeta})/2 \right]^{1/2}$$

to position the figure (or more accurately $\Omega_r = \Omega_c \sqrt{1 - \zeta_c^2}$)

$$b) \quad \beta\sigma_x^2 = (-1 + \sqrt{1 + 2.2\pi\Gamma/\zeta})/4.4$$

$$c) \quad h = 1.195 \sqrt{\beta\sigma_x}$$

$$a = 0.83 \sqrt{\beta\sigma_x}$$

Then simply draw the isosceles triangle with its apex positioned along a line at Ω_r , height h , and base $2a$. This is demonstrated in Figure 33 and over estimates the computed values of $B(\Omega_r)$ by 6.5, 10.7, 6.8, 14.7% for $\Gamma/\zeta = 10, 40, 160, 500$ respectively. For a Gaussian signal (this is not such) the confidence limits for forty averages suggest an error $\pm 15.8\%$.

An improvement on this figure may be brought about by reading the appropriate computed value of $B(\Omega_r)$ from Figure 24 and the value of $A(0)$ from Figure 23 to find $B(0) = A(0)\Gamma$ and adjusting the shape free hand. This last improvement becomes more important as ζ increases since $B(0) \rightarrow 0$ as $\zeta \rightarrow 0$. In Figure 33 it seems there is very little correction to be made for the width of the curve at the height of $\frac{1}{2}B(\Omega_r)$. However Figure 25 can always be used to double check the width of the refined sketch at frequencies where $B(\Omega) = \frac{1}{2}B(\Omega_r)$. The response spectra of acceleration and velocity may be obtained from the displacement spectrum through

$$Bv(\Omega) = \beta S_{\ddot{x}}(\Omega)/\omega_n = \beta S_{\dot{x}}(\Omega)\omega_n \Omega^2 = B(\Omega)\Omega^2$$

$$Ba(\Omega) = \beta S_{\ddot{x}}(\Omega)/\omega_n^3 = \beta S_{\dot{x}}(\Omega)\omega_n \Omega^4 = B(\Omega)\Omega^4$$

and $Av(\Omega) = Bv(\Omega)/\Gamma$, $Aa = Ba(\Omega)/\Gamma$ (see also section 4.2). Note the non-dimensional form of the areas under particular spectra

$$\frac{\beta \sigma_x^2}{\omega_n^2} = \int_0^\infty \beta \Omega^2 S_x(\Omega) \omega_n d\Omega$$

$$\frac{\beta \sigma_{\dot{x}}^2}{\omega_n^4} = \int_0^\infty \beta \Omega^4 S_x(\Omega) \omega_n d\Omega$$

Examples of acceleration spectra shown in Figure 34 and velocity spectra in Figures 27-28b.

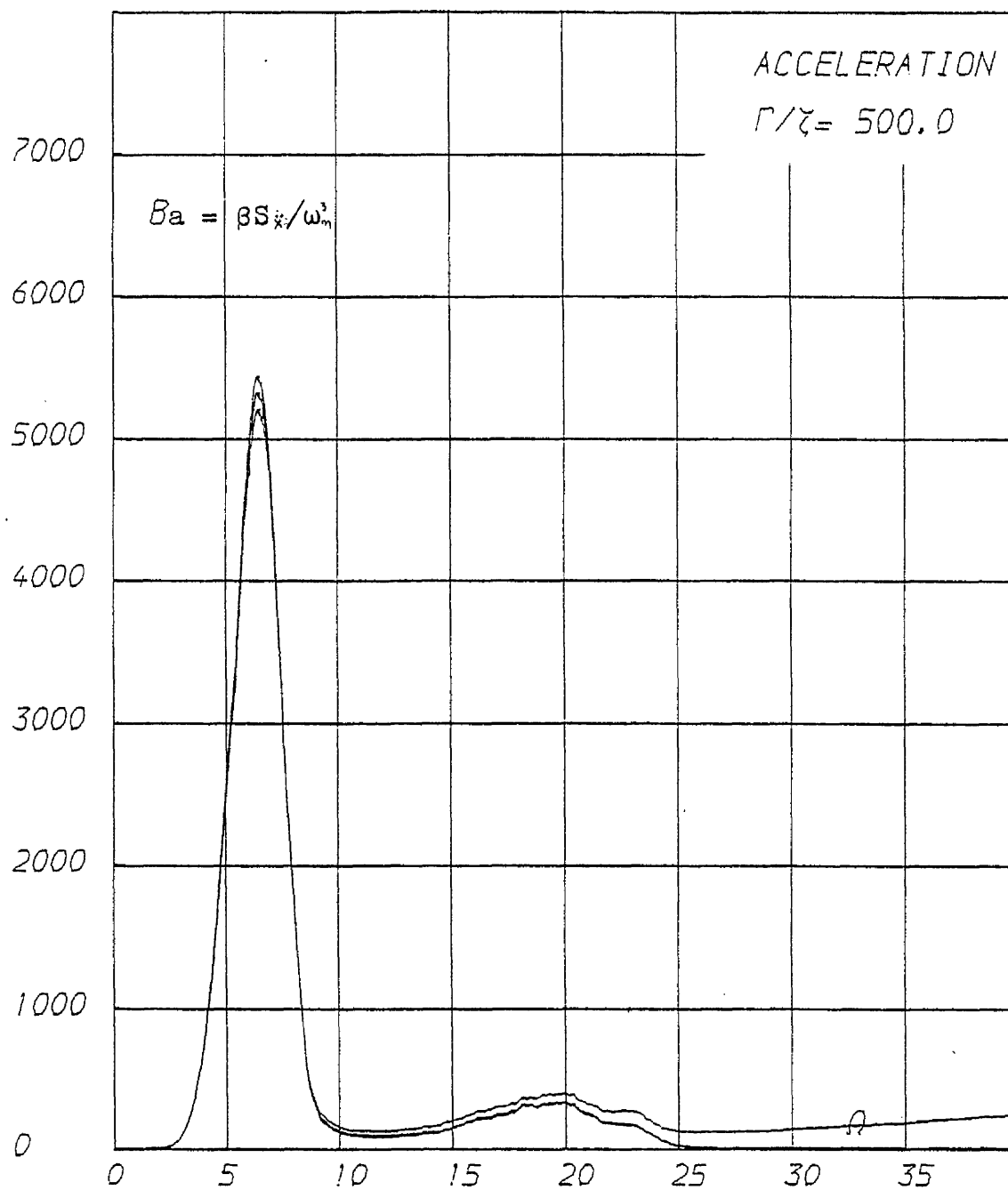


Figure 34

Non-dimensional response acceleration spectrum

See also Figure 5

CHAPTER 6

EFFECTS OF DIFFERENT FORMS OF EXCITATION SPECTRA

This chapter may be thought of as a first attempt in investigating the response of the Duffing system under band limited and high pass filtered random excitations. It is also hoped that this work will provide more insight to the behaviour of the system under broad band excitation and prepare the ground for future research regarding these types of excitation. An attempt will be made to answer mainly two questions. First, whether it is possible to describe the response spectra for the Duffing system under the aforementioned excitations using the ratio Γ/ζ instead of the separate parameters Γ and ζ and second, whether the equivalent linearization technique, either in its conventional or improved form, is applicable for this type of excitation for the large nonlinearities investigated. Finally, in Section (6.3) an argument is put forward in favour of a possible property of the system that could provide a link between the radically different behaviours of the system under the different forms of excitation spectra considered.

6.1 Response Spectra Under Band Limited Process

Looking back in Section (4.2) it can be seen that the formulations derived through dimensional analysis for the system under broad band excitation, are still valid for the system under band limited random excitation. This is due to the fact that the definition of the excitation spectrum remains practically the same. Hence the response spectra may be expressed in the form

$$k^2 S_x(\omega)/S_1 = \Phi_1[\beta S_1/\sqrt{mk^3}, c/2\sqrt{km}, \omega_c/\sqrt{k/m}, \omega/\sqrt{k/m}] \quad (6-1)$$

or

$$A = \Phi_1[\Gamma, \zeta, \Omega_c, \Omega]$$

and

$$\beta S(\omega)\sqrt{k/m} = \Psi_1[\beta S_1/\sqrt{mk^3}, c/2\sqrt{km}, \omega_c/\sqrt{k/m}, \omega/\sqrt{k/m}] \quad (6-2)$$

or

$$B = \Psi_1[\Gamma, \zeta, \Omega_c, \Omega]$$

Naturally functions Φ_1, Ψ_1 are in general different from the corresponding functions Φ, Ψ of equations (4-8), (4-9), used to describe the response under broad band. Another noticeable difference in the formulation of the problem is the importance of the Ω_c term (the cut off frequency). The influence of this term on the response of the system under broad band excitation has been proved unimportant. Here however the value of the cut off frequency (Ω_c) is expected to have a decisive influence on the response of the system. Again the area under a single B curve represents a nondimensional mean square response displacement of the system.

$$\beta \sigma_x^2 = \int_0^\infty \beta S_x(\Omega)\sqrt{k/m} d\Omega \quad (6-3)$$

where $\Omega = \omega/\sqrt{k/m}$.

It is seen here that the number of parameters necessary to describe the system response has increased by one (Ω_c). However in the broad band case the number of parameters were further reduced by describing the system in terms of the ratio Γ/ζ instead of the separate parameters Γ and ζ as suggested by equations (4-8), (4-9). Hence it is important

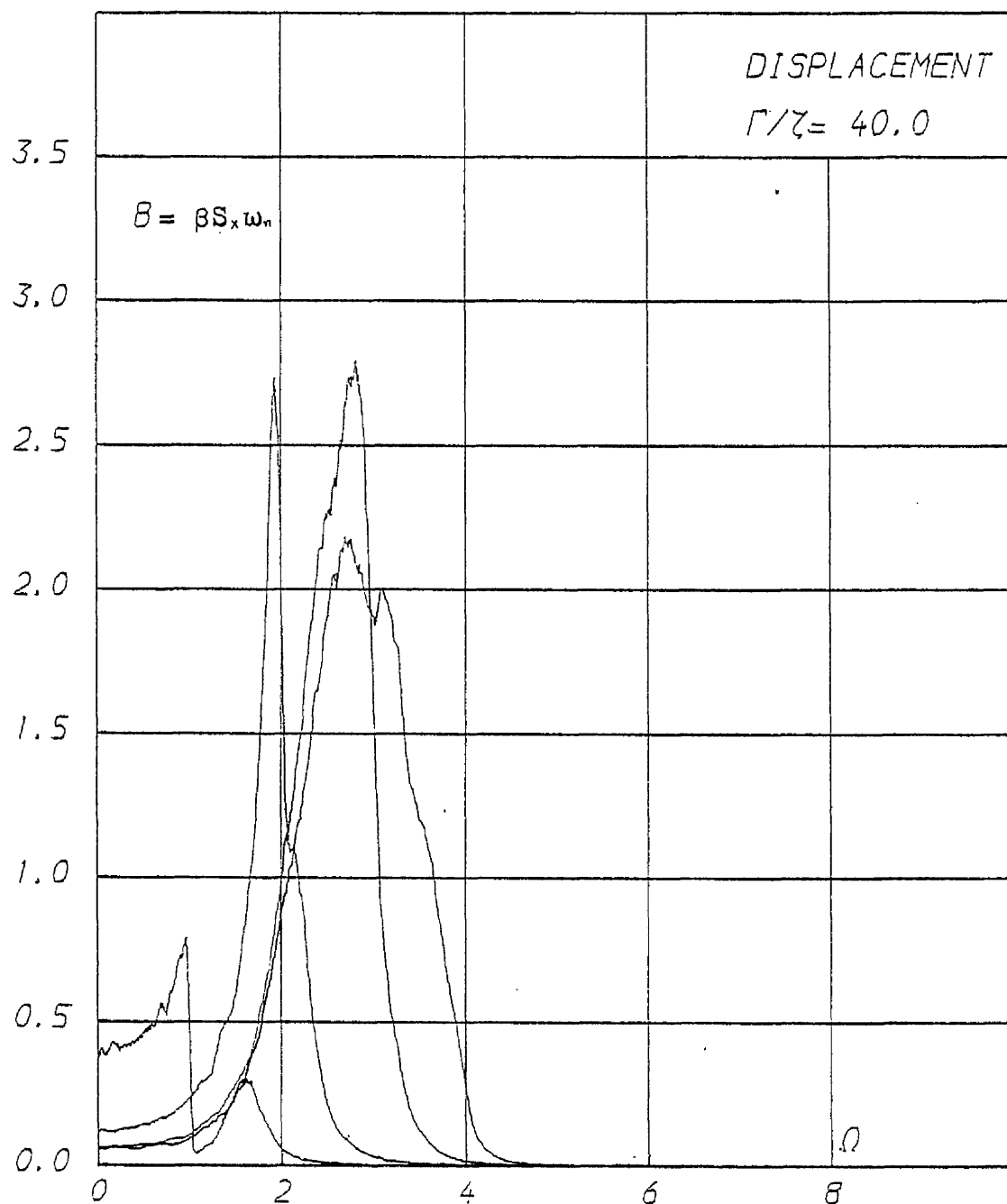


Figure 35a

$$\gamma = 0.05$$

Figures 35a-36b Response displacement
 spectra with excitation spectrum
 Cut off frequencies $\Omega_c = 4, 3, 2, 1$ ($\Gamma = \beta S_x \omega_n / k^1$)

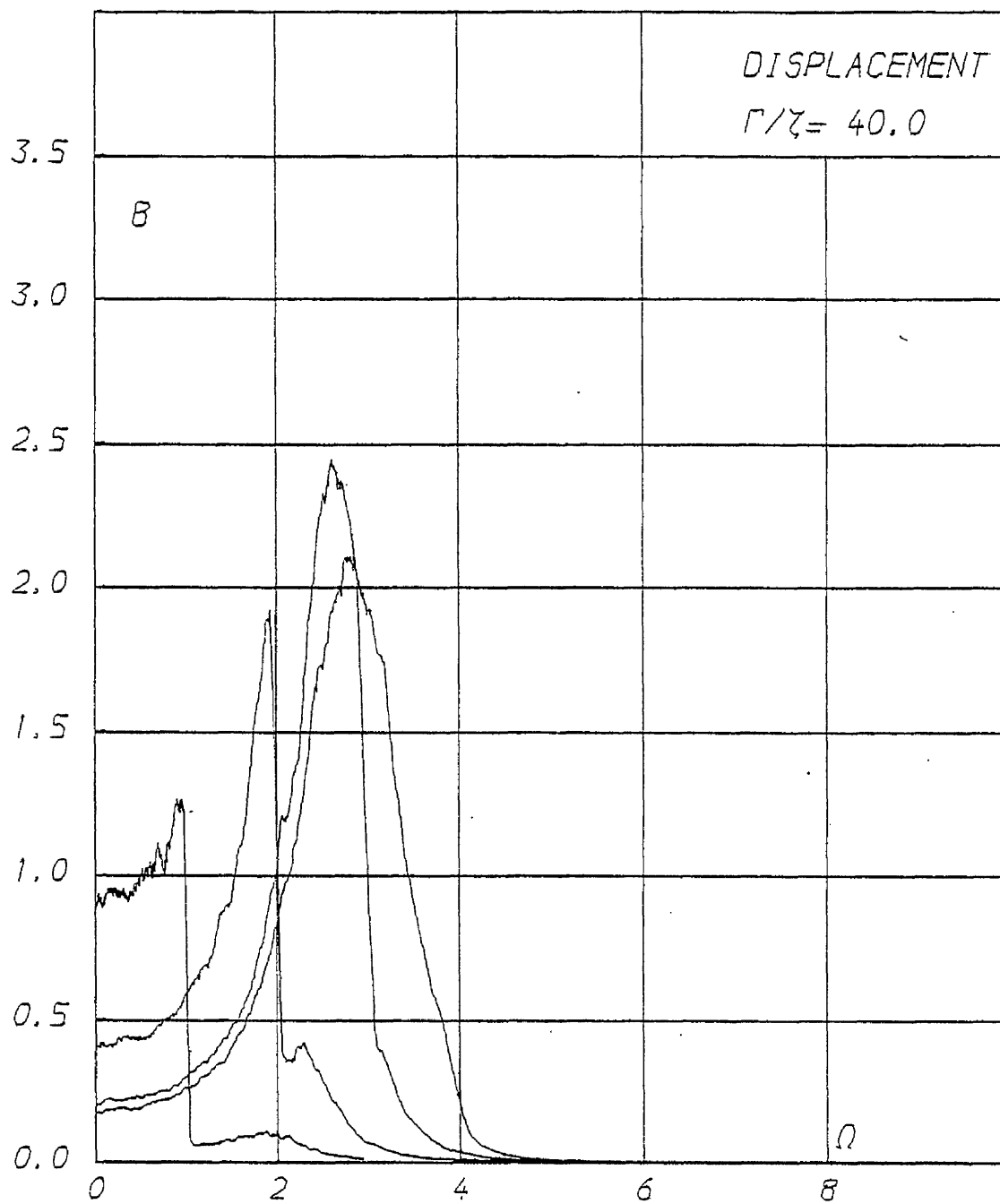


Figure 35b

$$\zeta = 0.2$$

See also Figure 35a

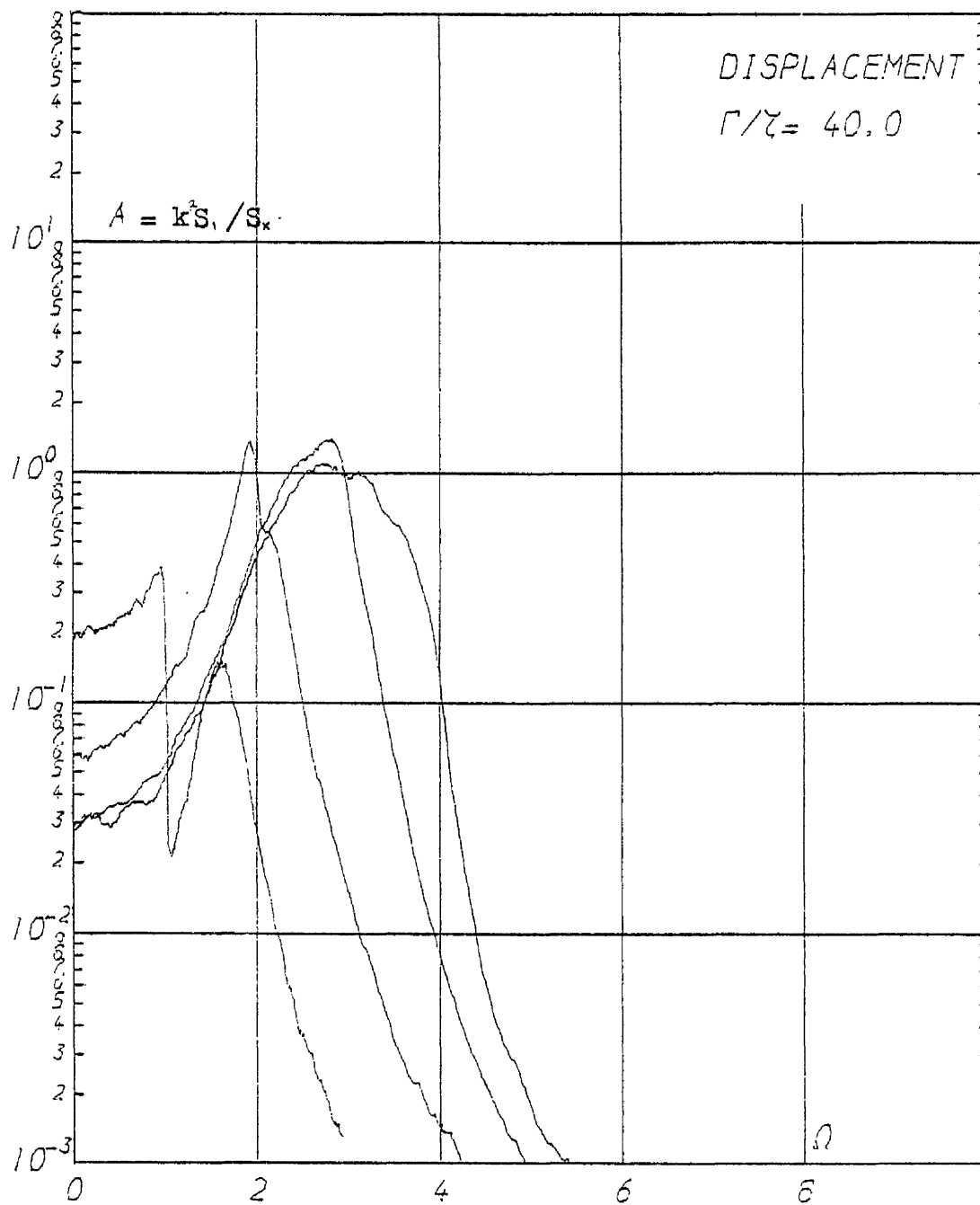


Figure 36a

$$\zeta = 0.05$$

See also Figure 35a

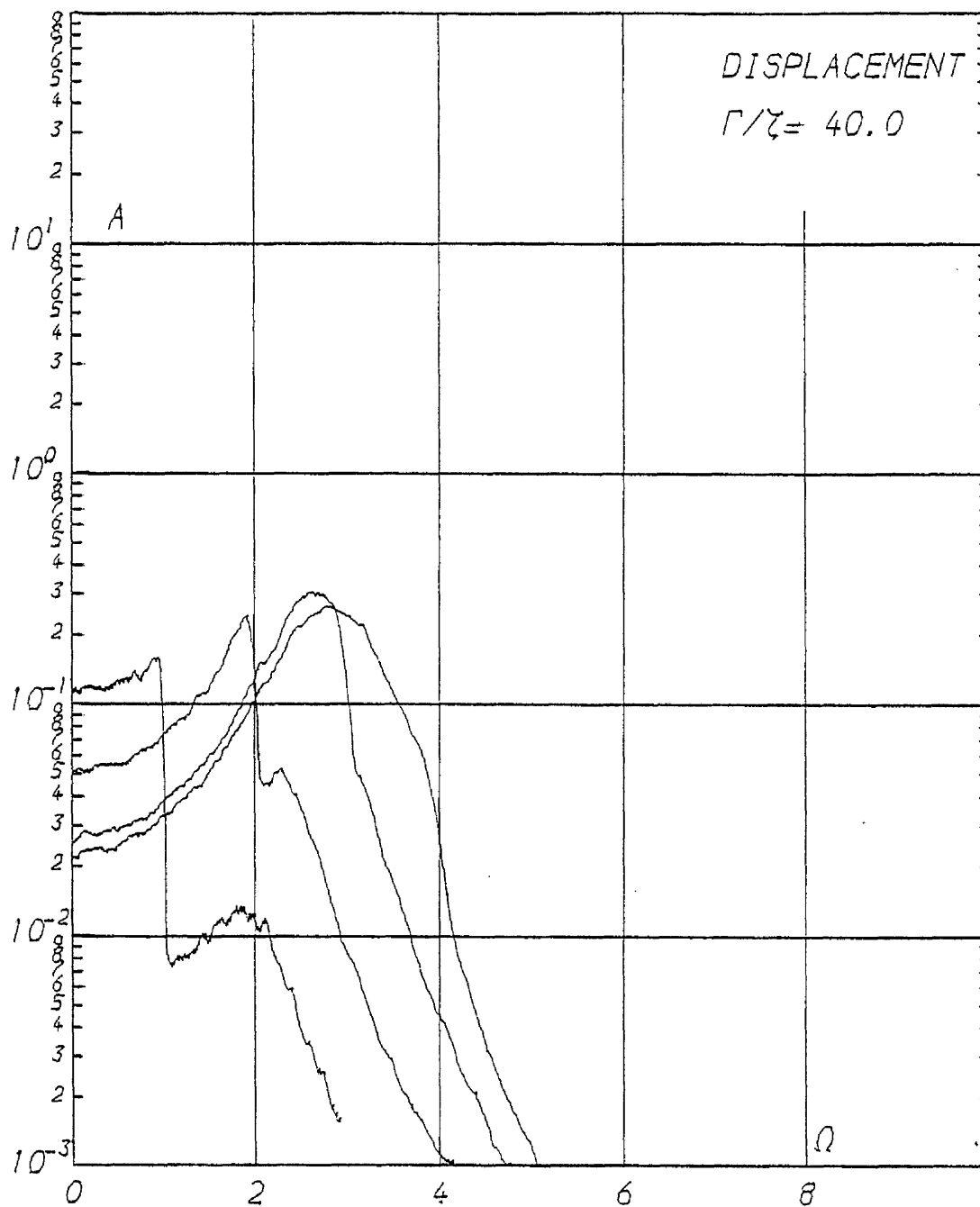


Figure 36b

See also Figure 36a

$$\zeta = 0.2$$

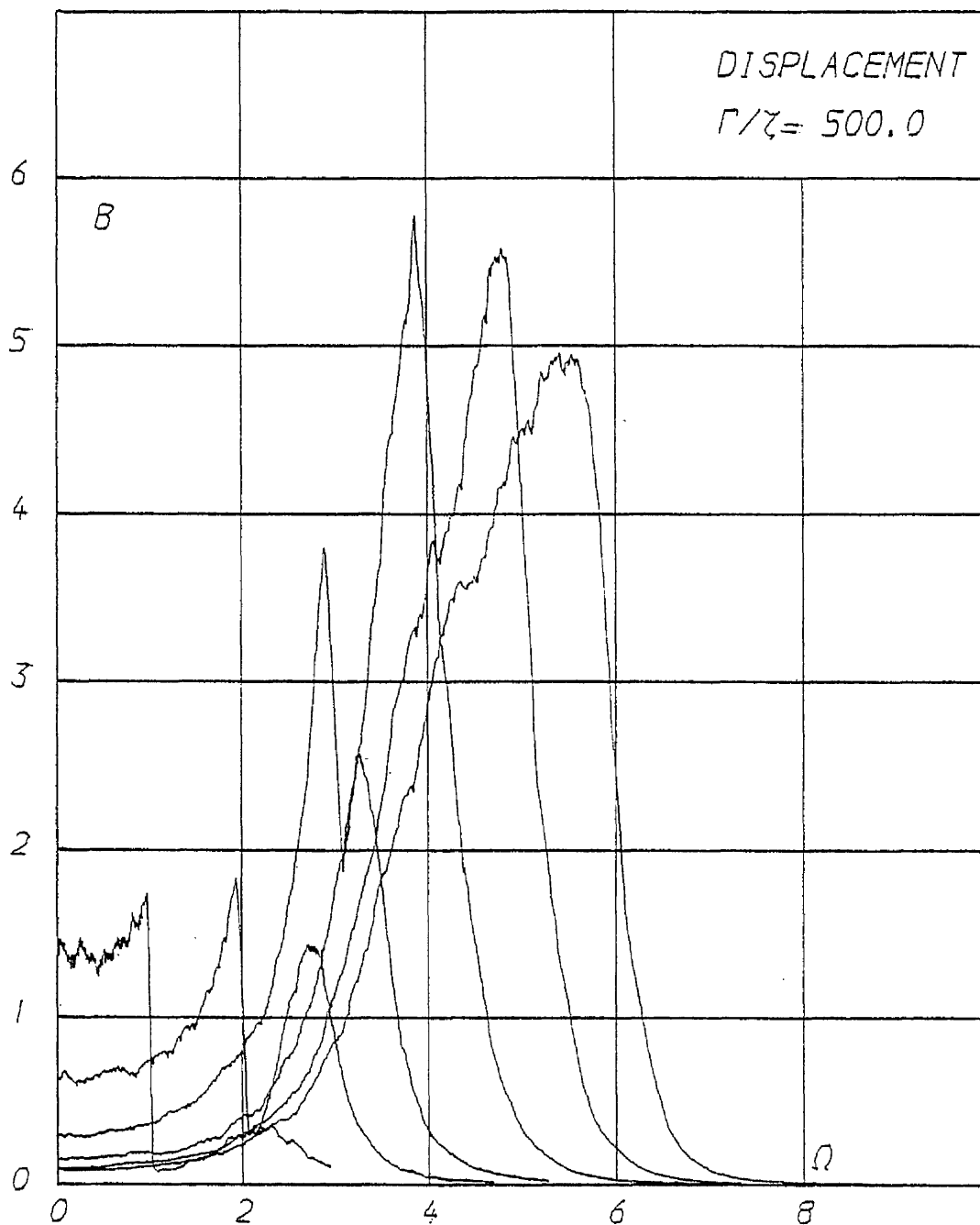


Figure 37a

$\zeta = 0.05$

Figures 37a-38b Response displacement
spectra with excitation

Cut off frequencies at $\Omega_c = 6, 5, 4, 3, 2, 1$ (for $\zeta = 0.05$)
and cut off frequencies at $\Omega_c = 6, 5, 4, 3$ (for $\zeta = 0.2$)

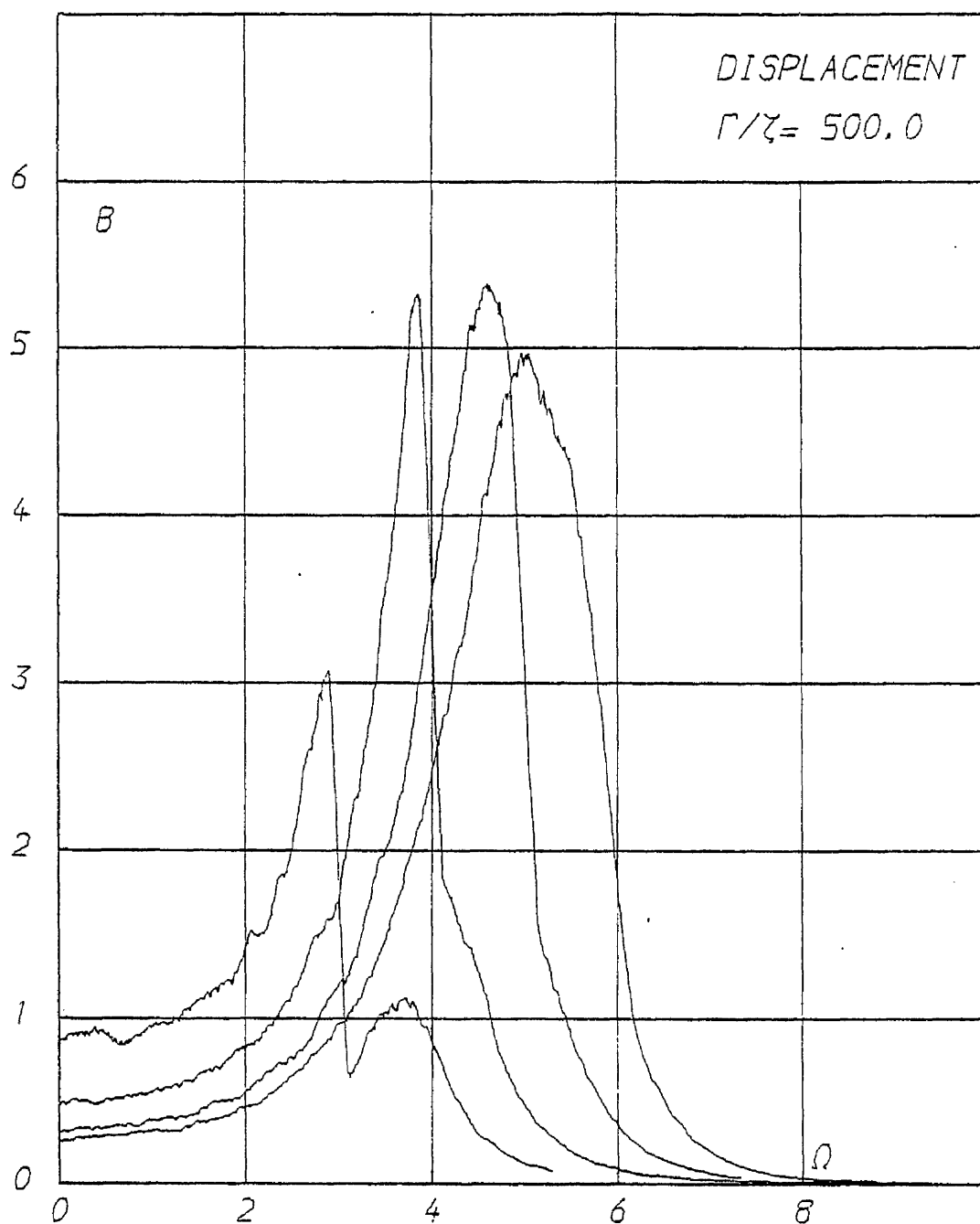


Figure 37b

See also Figure 37a

$$\zeta = 0.2$$

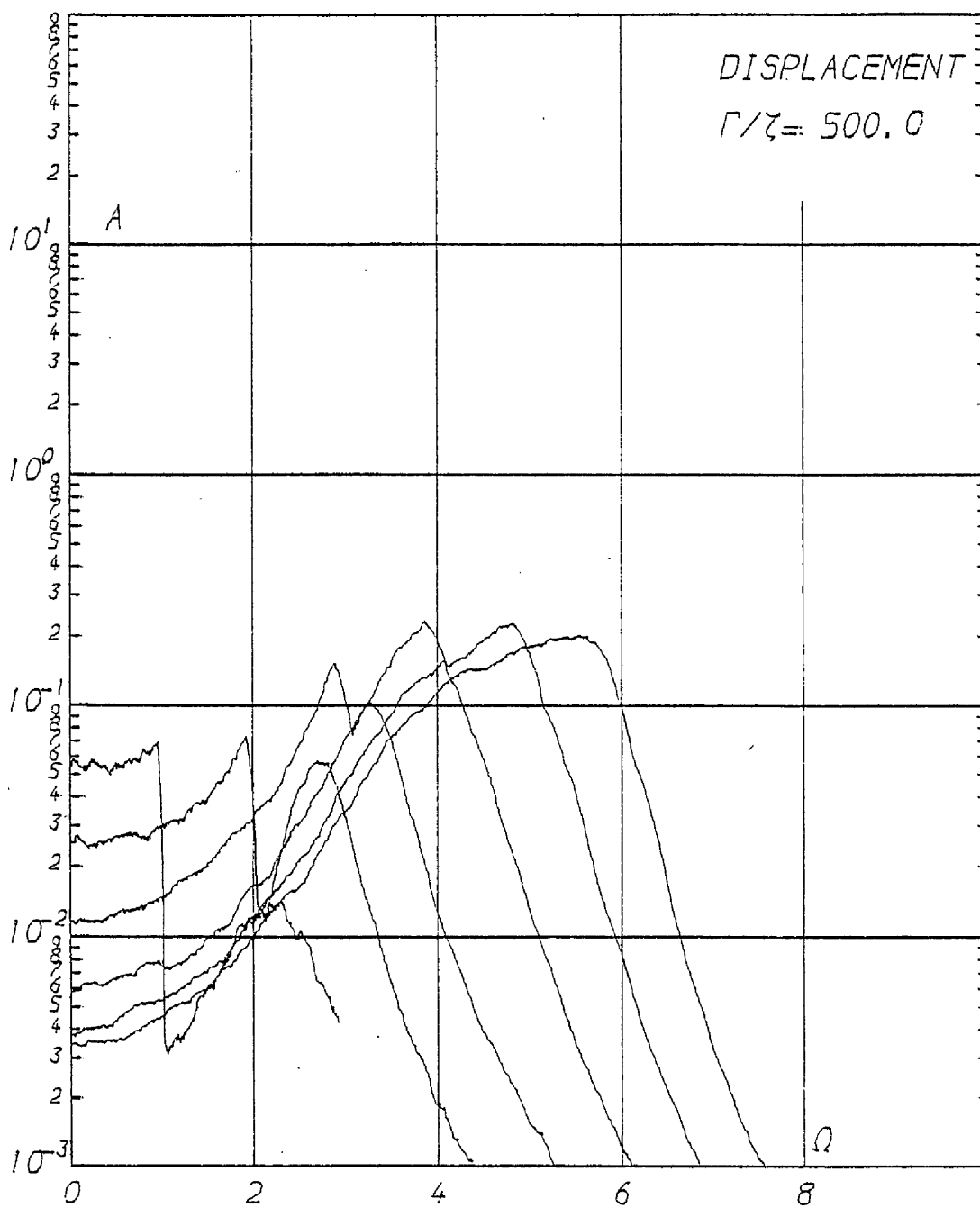


Figure 38a

See also Figure 37a

$$\gamma = 0.05$$

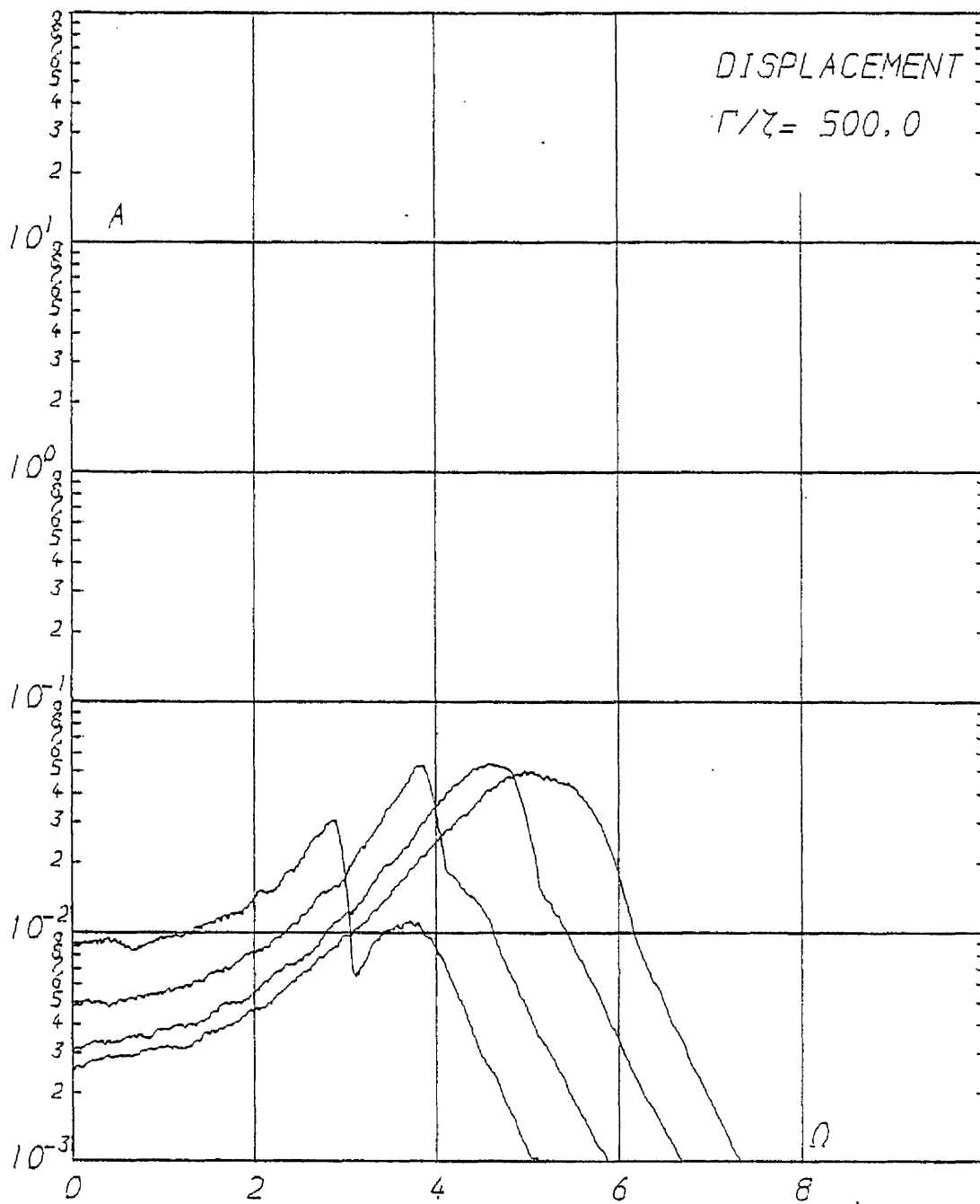


Figure 38b

See also Figure 37a

$$\zeta = 0.2$$

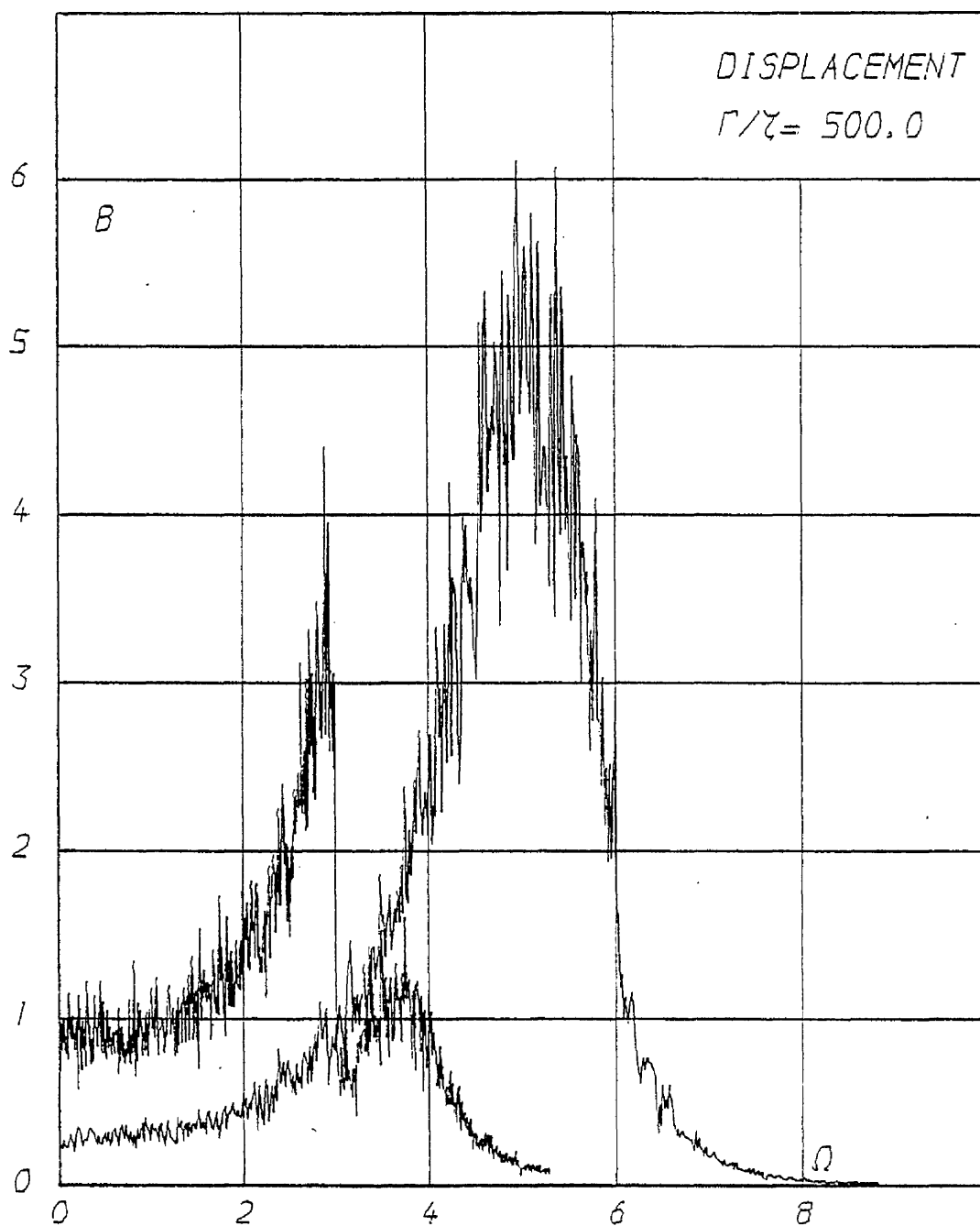


Figure 39

Sample of response spectra before
 frequency averaging ($\gamma = 0.2$)

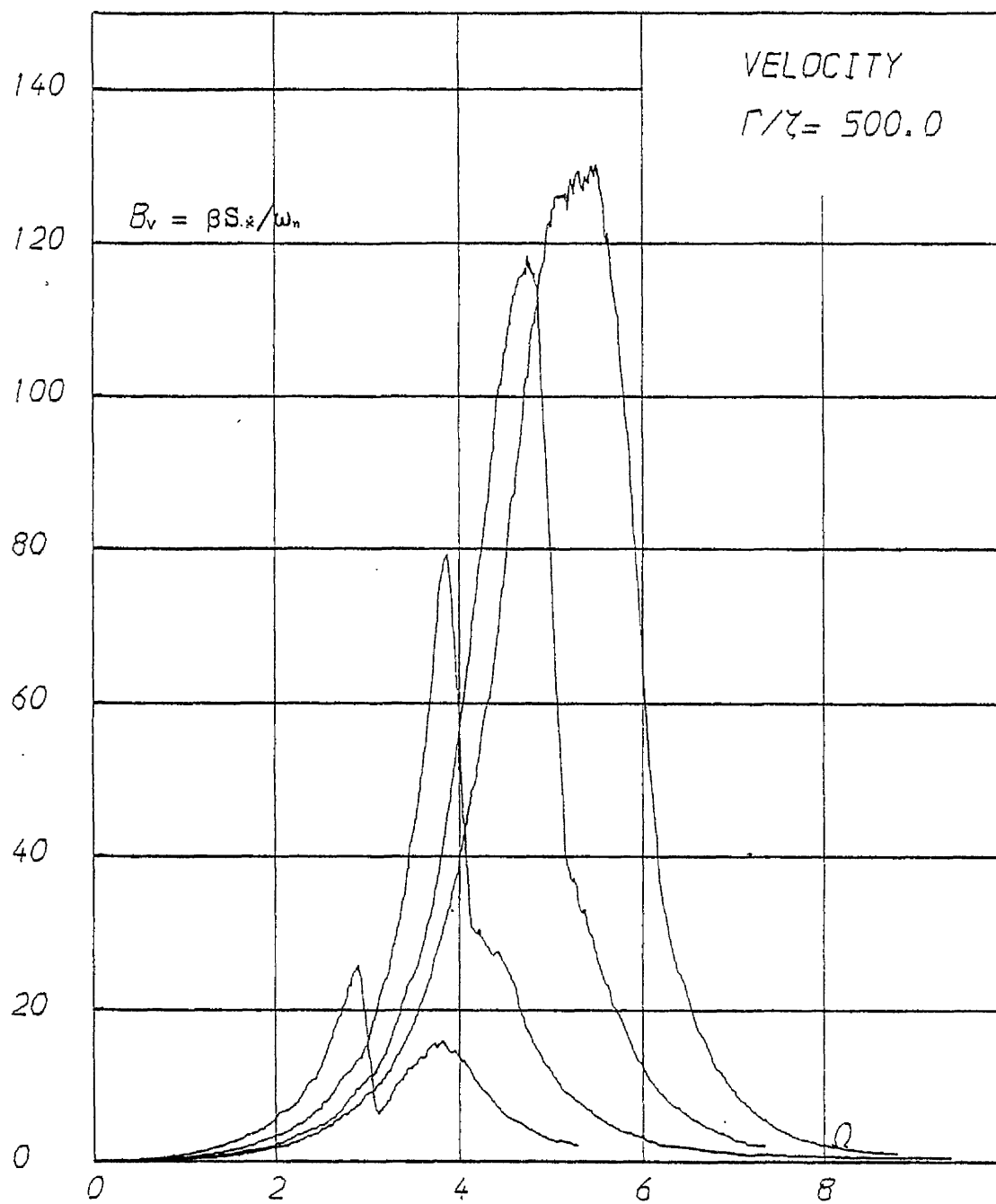


Figure 40

Example of velocity response spectra
 ($\zeta = 0.2$) corresponding to Figure (37b)

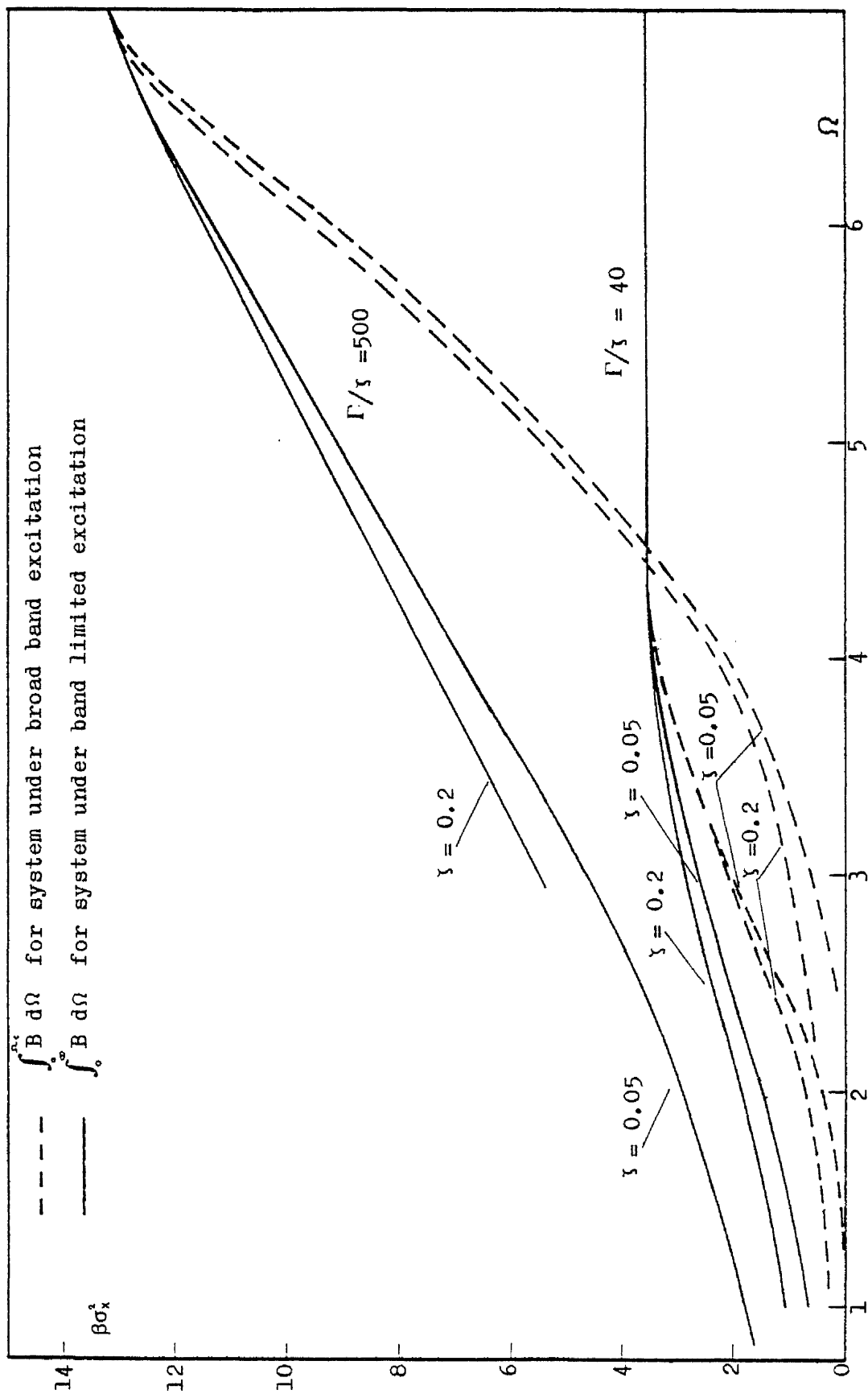


Figure 41

Area under non-dimensional response displacement spectrum
for the Duffing system under band limited excitation

to investigate if this simplification can apply for this case too.

Figures 35 to 40 show the response spectra for values of $\Gamma/\zeta = 40$ and 500 for different cut off frequencies and for two damping ratios $\zeta = 0.05, 0.20$. Figure 41 shows the area under the spectrum as the band limit is reduced and also shows the area under the response spectrum to the corresponding broad band signal (same intensity) up to the cut off frequency of the band limited process. As mentioned earlier the parameters describing the system have increased by one, namely the frequency cut off of the band limited process. This may be defined simply as $\Omega_c = \omega_c / \omega_n$. But a more complicated definition involving the broad band resonant frequency and the peak width (hence indirectly Γ/ζ) may be more meaningful say $\Omega_c = \Omega_r \pm aW$ where $a \in \mathbb{R}$ and W the width of the resonant peak as defined in Chapter 5. The work done in this section did not indulge in establishing such precise relationships, but attempts provide a first look into this subject which may be found beneficial to further research into the subject. It may be said that the general pattern established in the previous chapter on the behaviour of the response spectra to a broad band excitation is in general retained less so however as Ω_c is reduced below Ω_r (the resonant frequency for the broad band excitation). As far as the main body of the spectrum is concerned, the shape of the response spectra for $\Omega_r < \Omega_c < \Omega_L$ (Ω_L is the limit frequency (see Section 5.2)) could have been produced (to a good approximation) by a simple truncation, at Ω_c , of the broad band response spectra. Further for a given pair of values of Γ/ζ and Ω_c , the corresponding response spectra have the same B maximum, $A(0)$, W and $\beta\sigma_x^2$ values which are different from the corresponding ones of the broad band case (i.e. same Γ/ζ but $\Omega_c \geq \Omega_L$). Hence if $\Omega_r < \Omega_c < \Omega_L$ the response spectra for this case may be described for each value of Ω_c , in the manner the response spectra for the broad band case were described i.e. in terms of figures similar to Figures (21-25) which may be thought of as derived for $\Omega_c \geq \Omega_L$. However further reductions of Ω_c i.e. $\Omega_c < \Omega_r$,

seems to suggest that Γ/γ cannot any longer adequately describe the response spectra and that Γ and γ should be treated as separate parameters.

At this point it may seem strange for the usefulness of the Γ/γ parameter to diminish. This parameter has served the purpose of a general system parameter, combining both excitation and damping values. As discussed earlier this strange combination, although it may serve the purpose of describing the spectral quantities A,B with a varying degree of success depending on the type of excitation and the individual values of Γ and γ , it is more suitable for describing statistical quantities. A possible future mathematical solution of the problem, will probably find the combination unsuitable for the purpose of describing spectral quantities and split it in its components Γ and γ . For the present taking into account the limitations of the numerical techniques to describe spectral values (Bias , length of records, numerical integration accuracy, etc.) it seems a very attractive proposition especially for engineering purposes. The motivation behind the use of the ratio Γ/γ as a simple parameter describing the response under broad band excitation, was its appearance in the non-dimensional form of the probability density of the response displacement derived through the solution of the appropriate Fokker - Planck equation (Chapter 4). This solution is not available however for band limited excitation. The statistical quantities calculated by the numerical simulation technique suggest a different arrangement for the joint probability function, although the question of statistical independence of velocity and displacement was not attacked the values of Kurtosis for velocity suggest that its probability distribution is no longer Gaussian and depends on Ω_c . In fact by observing the Kurtosis values in Table 6.1, it is seen that as Ω_c is reduced from the broad band value (Ω_b), the value of K_u for the response velocity drops gradually from 3 (Gaussian) to some minimum value (≈ 2.3). This seems to happen as Ω_c is in the range of frequencies near the resonant frequency of the system under broad band

excitation (Ω_c). As Ω_c is further reduced, the Kurtosis value gradually increases towards the Gaussian value 3. The Kurtosis values of the displacement remained roughly at the same level as for the broad band input, however this is not conclusive since the error involved in the evaluation of this quantity depends on the fourth moment and may require much longer records in order that small changes are confidently detected.

Table 6.1

Computed Values of Kurtosis

		$\Gamma/\zeta = 40$				$\Gamma/\zeta = 500$			
ζ Ω_c		Displacement		Velocity		Displacement		Velocity	
		0.05	0.20	0.05	0.20	0.05	0.20	0.05	0.20
Ω_c		2.15	2.23	2.64	2.90	2.14	2.17	2.63	2.79
6		—	—	—	—	2.05	2.11	2.33	2.40
5		—	—	—	—	2.03	2.08	2.22	2.30
4		2.18	2.19	2.67	2.63	2.02	2.10	2.15	2.30
3		2.09	2.15	2.31	2.38	2.11	2.09	2.30	2.46
2		2.13	2.13	2.27	2.39	2.11	—	2.50	—
1		2.11	2.15	2.81	2.70	2.00	—	2.80	—

The mean response values for displacement and velocity were zero as expected. There were no tests carried out on the stationarity of the response, although the consistent spectral estimations suggest stationarity.

An interesting observation can be made on the response spectral shape when the cut off frequency is reduced below the resonant frequency of the broad band case. In Figure 35a for example it is seen that there are two peaks in the response spectrum for $\Omega_c = 1$ one that coincides with the frequency cut off of the input and the second appears at a slightly higher frequency ($\Omega \approx 1.75$). This is a phenomenon that may be linked with the behaviour of the system response at low frequencies in the case of the broad band excitation

(the effect of damping at these frequencies) and the response under high pass filtered excitation. An attempt to link these phenomena will follow the observations on the response of the system under a high pass filtered process.

The applicability of the equivalent linearization technique was also investigated. The analysis presented in Section 2.2 is, up to equation (2-26), in principle valid for any type of random excitation. Hence for the system

$$\ddot{x} + 2\zeta\omega_n \dot{x} + \omega_n^2(x + \beta x^3) = F(t) \quad (6-4)$$

the equivalent linear system

$$\ddot{x}_1 + 2\zeta_e \omega_e \dot{x}_1 + \omega_e^2 x_1 = F(t) \quad (6-5)$$

where

$$\zeta_e \omega_e = \zeta \omega_n \quad \text{and} \quad \omega_e^2 = \omega_n^2 \left(1 + \beta \frac{E(x^4)}{E(x^2)}\right) \quad (6-6)$$

is expected to give the best approximation to the response of the nonlinear system in the mean square sense. This was proved true when $F(t)$ is broad band provided the ratio $E(x^4)/E(x^2)$ is given the exact value (Section 5.4). In the case of band limited excitation an approximate evaluation of this ratio was possible through the simulation technique. Hence

$$\omega_e^2 = \omega_n^2 (1 + \beta K u \sigma_x^2) \quad (6-7)$$

where Ku is the value of Kurtosis and σ_x^2 the variance of the response displacement as calculated by the numerical simulation. The variance of the equivalent linear system may be calculated through

$$\sigma_{x_1}^2 = \int_0^{\omega_e} S_1 |H_e(\omega)|^2 d\omega$$

therefore

$$\sigma_{x_1}^2 = \int_0^{\Omega_e} \omega_e S_1 |H_e(\Omega)|^2 d\Omega \quad (6-8)$$

where S_1 is the intensity of the band limited random process and $H_e(\omega)$ the transfer function of the equivalent linear system. The integral may be evaluated as per

$$\sigma_y^2 = \int_{\Omega_1}^{\Omega_2} \omega_o S \left| H(\Omega) \right|^2 d\Omega$$

$$\sigma_y^2 = [I(\Omega_2, \gamma) - I(\Omega_1, \gamma)] \pi S / 4 \omega_o^2$$

where $\Omega = \omega/\omega_o$ and

$$I(\Omega, \gamma) = (1/\pi) \tan^{-1} [2\gamma\Omega^2 / (1-\Omega^2)] + \quad (6-9)$$

$$+(\gamma/2\pi\sqrt{1-\gamma^2}) \ln [(1+\Omega^2+2\Omega\sqrt{1-\gamma^2}) / (1+\Omega^2-2\Omega\sqrt{1-\gamma^2})]$$

Hence the results of the equivalent linearization technique can be compared with those of the simulation, by comparing the value of $\sigma_{x_1}^2$ from equation (6-8) with the value of σ_x^2 for the nonlinear system obtained from equation (6-3) numerically. Table (6.2) displays the corresponding values of $\beta\sigma_{x_1}^2$ and $\beta\sigma_x^2$. The values of $\beta\sigma_{x_1}^2$ were obtained by evaluating equation (6-7) using the value of Ku quoted in the simulation results for the particular case.

Also displayed in Table 6.2 are the values of $\beta\sigma_{x_c}^2, \beta\sigma_{x_1}^2$. The value $\beta\sigma_{x_c}^2$ was calculated through the equivalent linearization method by making use of the value $\beta\sigma_x^2$ (obtained through simulation) and a constant value of Kurtosis $Ku = 2.2$ (the asymptotic value of Kurtosis for broad band excitation). The $\beta\sigma_{x_1}^2$ value was calculated using the conventional equivalent linearization technique i.e. the equivalent linear frequency was calculated using the value of $\beta\sigma_{x_1}^2$ obtained from the linearized system equation ($\beta = 0$) for the given excitation using equation (6-9) and $Ku = 3$. The values of $\beta\sigma_x^2$ are also shown in Figure 4.1. It can be seen that the equivalent linearization technique under its present form produces poor results especially for large Γ/γ values and especially when Ω_c is in the vicinity of Ω_r . In particular the conventional equivalent linearization technique is proved totally unsuitable for the system under band limited excitation.

Table 6.2

	$\zeta = 0.20$				$\zeta = 0.05$			
	$\beta\sigma_x^2$	$\beta\sigma_{x_1}^2$	$\beta\sigma_{x_c}^2$	$\beta\sigma_{x_3}^2$	$\beta\sigma_x^2$	$\beta\sigma_{x_1}^2$	$\beta\sigma_{x_c}^2$	$\beta\sigma_{x_3}^2$
Ω_c	$\Gamma/\zeta = 40$							
∞	3.47	3.54	3.56	3.07	3.49	3.70	3.56	3.07
4	3.31	3.71	3.70	0.004	3.35	3.76	3.74	0.001
3	2.85	3.94	3.76	0.003	2.77	4.50	4.28	0.0007
2	1.85	1.91	1.72	0.002	1.55	1.59	1.23	0.0046
1	1.14	1.07	0.80	0.002	0.66	0.49	0.47	0.0007
	$\Gamma/\zeta = 500$							
∞	13.24	13.22	13.14	11.28	13.43	13.31	13.14	11.28
6	11.33	15.15	14.47	0.0004	11.39	15.94	14.89	0.0001
5	9.58	16.72	15.18	0.0003	9.22	19.53	17.86	0.00001
4	7.45	10.28	7.36	0.0002	6.90	23.52	9.34	0.00005
3	5.54	4.58	3.85	0.0002	4.47	3.15	2.39	0.00007

For broad band the exact value of $\beta\sigma_x^2$ from the Fokker-Planck approach is 3.53, 13.14 for $\Gamma/\zeta = 40, 1500$ respectively.

6.2 Response Spectra Under High Pass Filtered Process

Figures 43a. to 44b. show the response displacement and velocity spectra of the Duffing system under high pass filtered process, for a Γ/γ value of 500 and damping ratio $\gamma = 0.2, 0.05$ at different cut off frequencies. The number of parameters describing the system are the same as for the band limited case. Although there are two cut off frequencies for the input spectrum (Figure 42) only the lower one is of significance to the system, since the upper frequency is positioned such that it is above the limit frequency for the broad band case (Section 5.1). The upper cut off

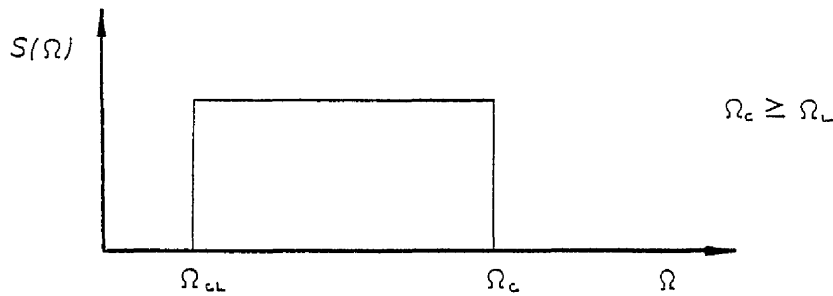


Figure 42

frequency would become important if it were lower than the limit frequency and in that case the input would probably be described as narrow band. Again the non-dimensional definition of the low cut off frequency used here is $\Omega_{cl} = \omega_{cl}/\omega_n$ but a more useful definition may be in terms of the resonant frequency that would be possible for the system under broad band excitation of the same intensity and the width of the corresponding peak, as described for the band limited case. Hence the relationships predicted through the dimensional analysis in Section (4.2) are still valid

$$k S_x(\omega)/S_i = \Phi_1 \left[\beta S_i / \sqrt{mk^3}, c/2\sqrt{km}, \omega_{cl} / \sqrt{k/m}, \omega / \sqrt{k/m} \right]$$

$$\text{or} \quad (6-10)$$

$$A = \Phi_1 \left[\Gamma, \gamma, \Omega_{cl}, \Omega \right]$$

and

$$\beta S_x(\omega) k/m = \Psi_1 \left[\beta S_i / \sqrt{mk^3}, c/2\sqrt{km}, \omega_{cl} / \sqrt{k/m}, \omega / \sqrt{k/m} \right]$$

$$\text{or} \quad (6-11)$$

$$B = \Psi_1 \left[\Gamma, \gamma, \Omega_{cl}, \Omega \right]$$

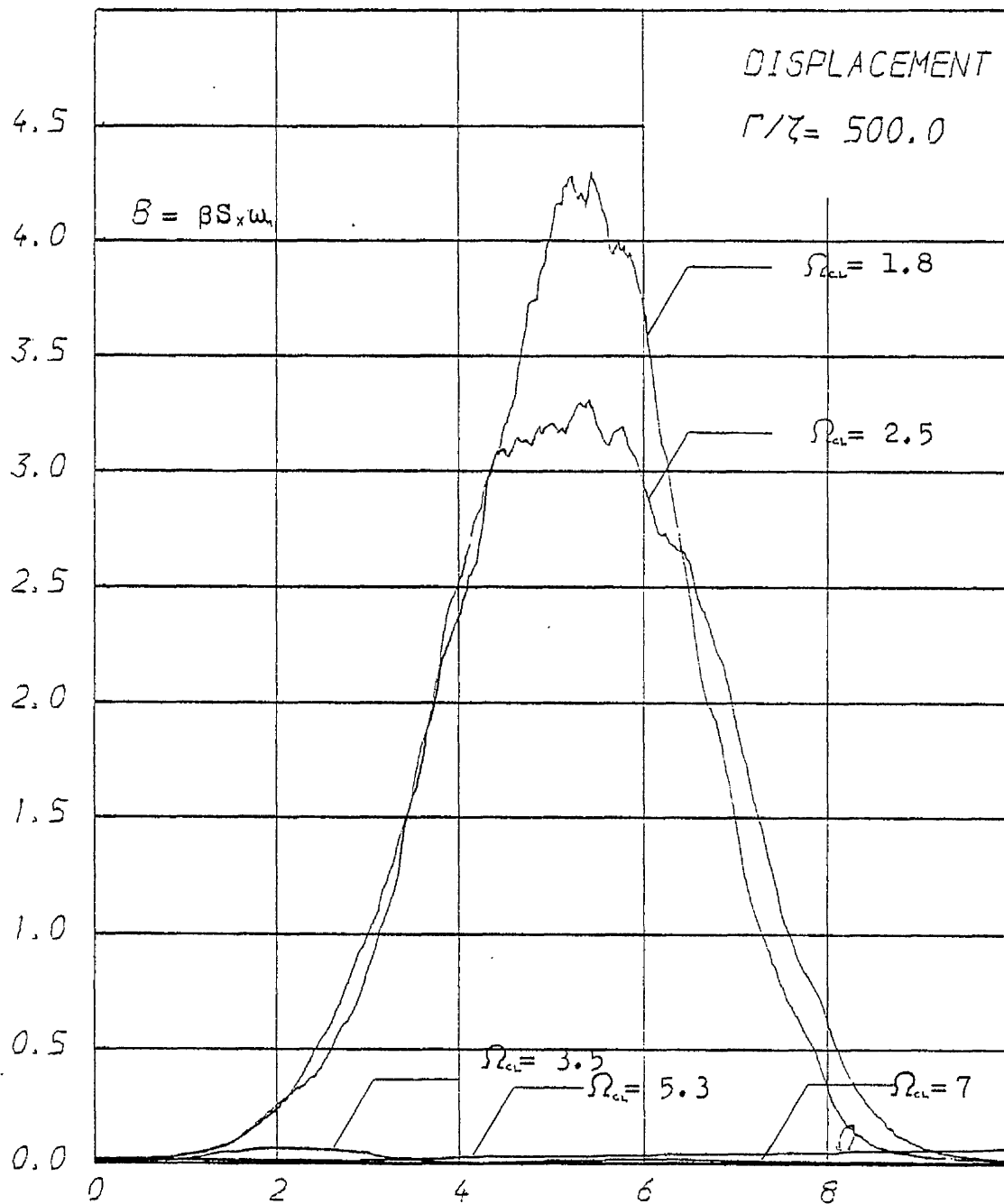


Figure 43a

($\gamma = 0.05$)

Figures 43a-44b Response displacement spectra under high pass filtered process for various low cut off frequencies (Ω_{cl})

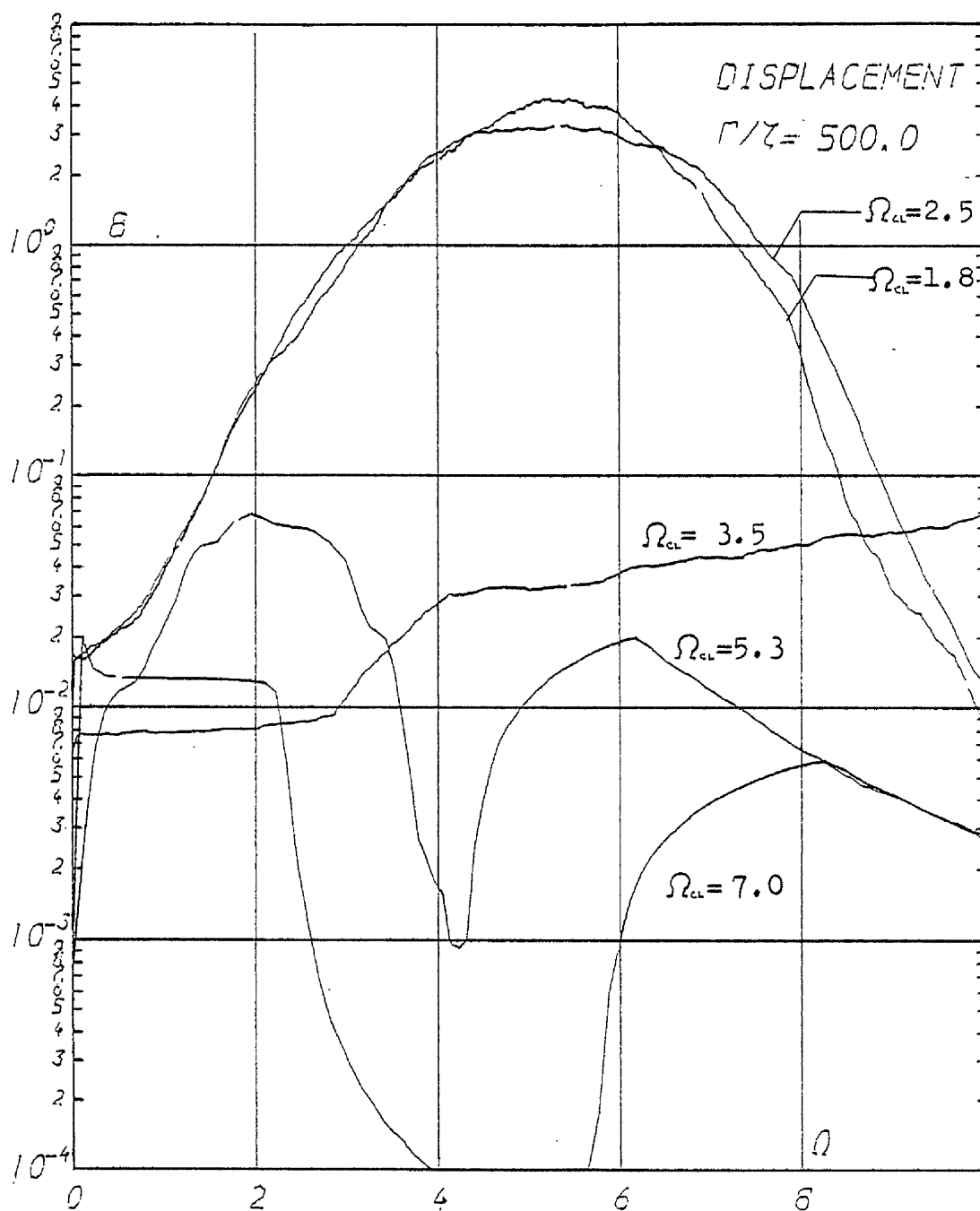


Figure 43b
 logarithmic plot of Figure 43a

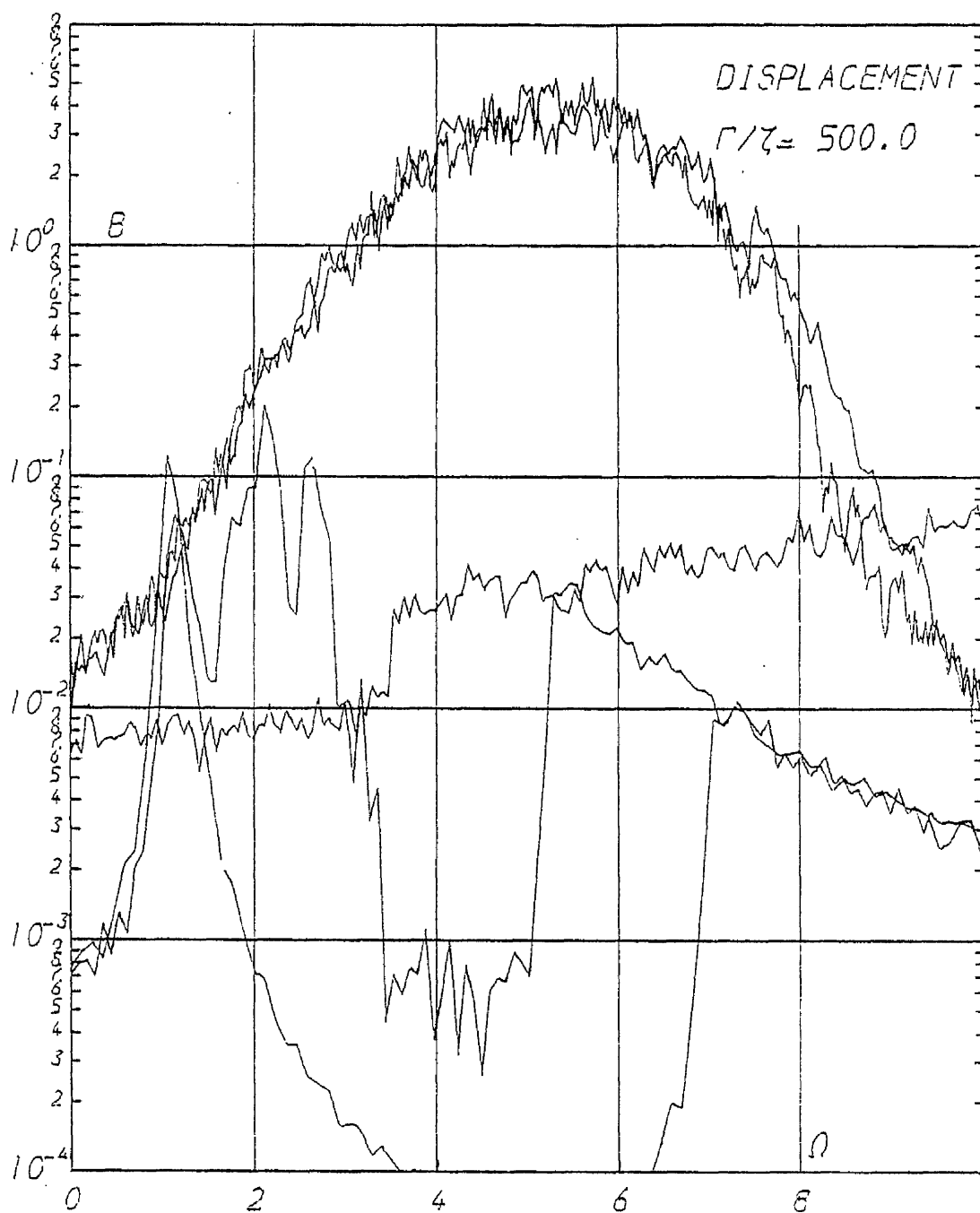


Figure 43C

As Figure 43b before frequency averaging ($\gamma = 0.05$)

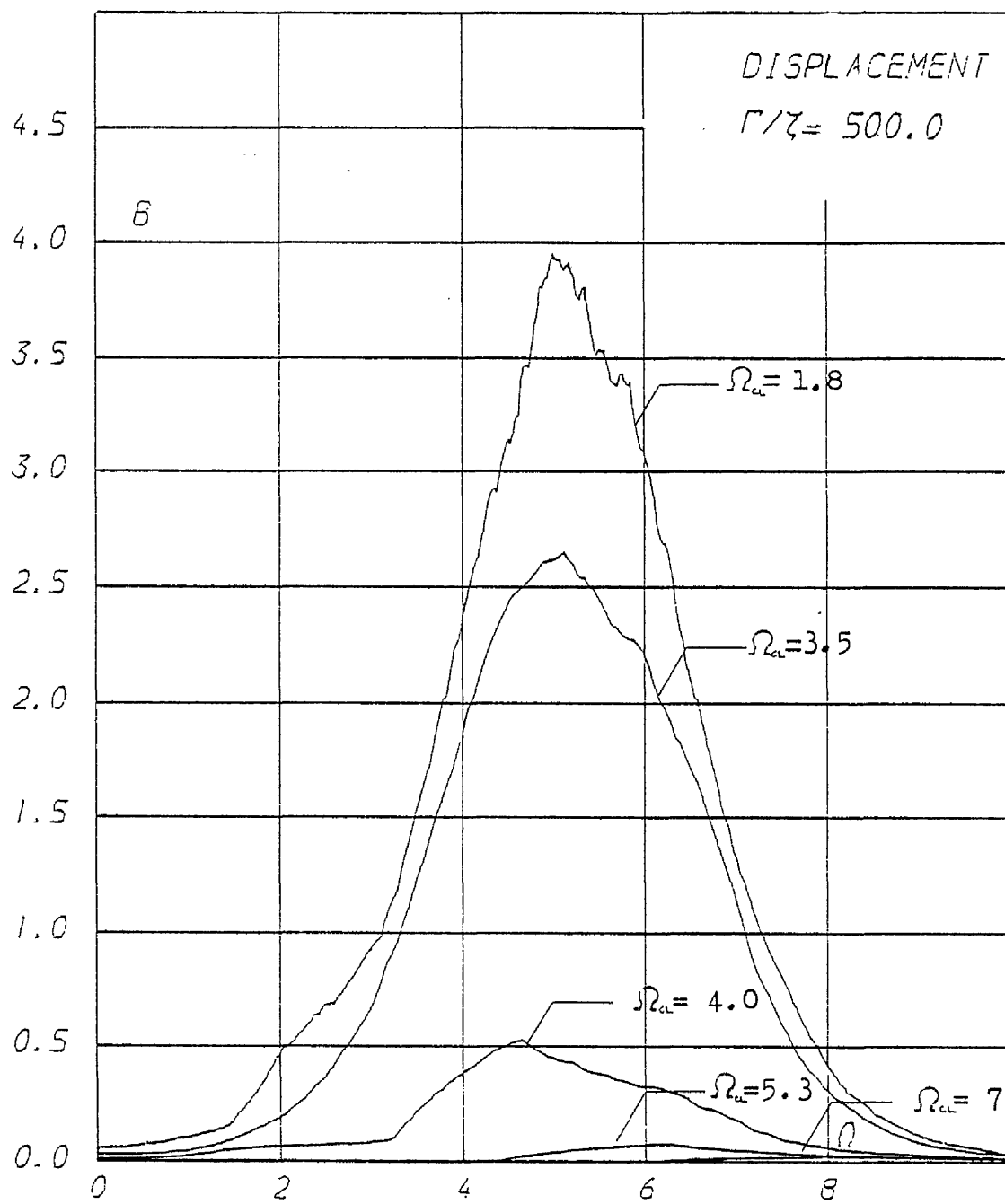


Figure 44a

($\gamma = 0.2$)

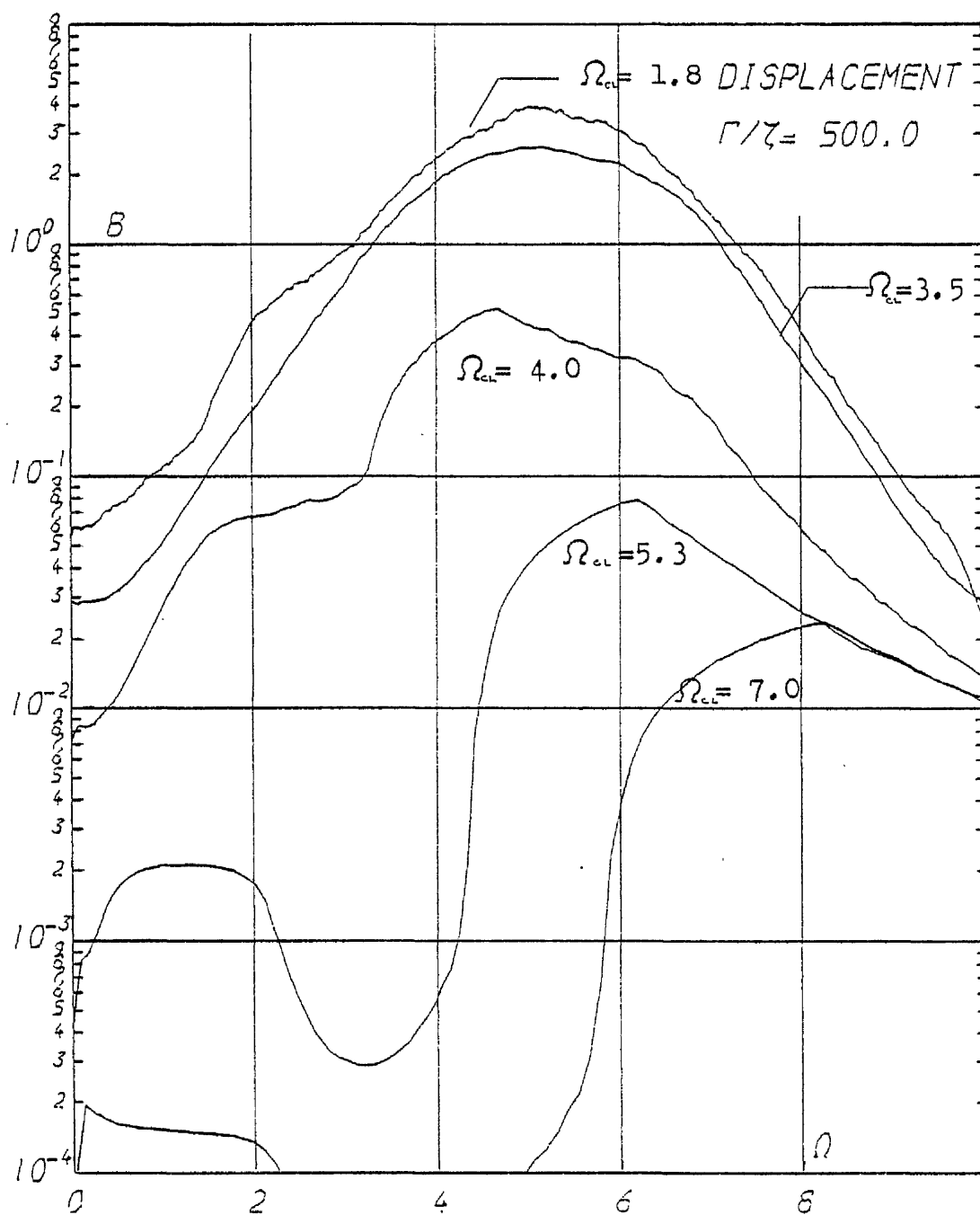


Figure 44b

($\gamma = 0.2$)

logarithmic plot of Figure 44a

Observing the response spectra and statistics it is seen that as the low cut off frequency Ω_{cl} is increased gradually from zero (broad band case) the response remains practically unaffected, and almost identical to the response under broad band excitation. At some value of Ω_{cl} above $\Omega = 1$ and well below Ω_r there is a drop of the response spectra to nearly noise level. This transition depends on the damping of the system and occurs more abruptly and at a lower frequency as damping is reduced. Thus it is seen that the ratio Γ/γ is not a suitable parameter for the description of the response of the system under this type of excitation except when $\Omega_{cl} < 1$. The critical frequency ($\Omega_{cl,cr}$) where this transition occurs is a function of both Γ and γ treated as independent parameters i.e.

$$\Omega_{cl,cr} = \Xi [\Gamma, \gamma] \quad (6-12)$$

The equivalent linearization technique can be applied for this type of excitation as well. Equation (6-9) can be used to evaluate

$$\beta \sigma_{x_e}^2 = \int_{\Omega_{cl}}^{\Omega_c} \omega_e S_1 \left| H_2(\Omega) \right|^2 d\Omega \quad (6-13)$$

where $\omega_e^2 = \omega_n^2 (1 + Ku \beta \sigma_{x_e}^2)$, $\gamma_e = \gamma \omega_n / \omega_e$ etc. and with the values of Ku and $\sigma_{x_e}^2$ as calculated through the simulation. Table 6.3 shows the value of $\beta \sigma_{x_e}^2$ as computed through the simulation, the values of $\beta \sigma_{x_e}^2$ as described above, the value of $\beta \sigma_{x_e}^2$ calculated as $\beta \sigma_{x_e}^2$ only with $Ku = 2.2$ and the values of $\beta \sigma_{x_e}^2$ calculated through the conventional equivalent linearization technique. For values of $\Omega_{cl} > \Omega_{cl,cr}$ (practically no response) all three values obtained through the equivalent linearization technique agree well with the simulation values.

Table 6.3
 $\Gamma/\zeta = 500$

Ω_{cl}	$\zeta = 0.2$				$\zeta = 0.05$			
	$\beta\sigma_x^2$	$\beta\sigma_{x1}^2$	$\beta\sigma_{xc}^2$	$\beta\sigma_{xs}^2$	$\beta\sigma_x^2$	$\beta\sigma_{x1}^2$	$\beta\sigma_{xc}^2$	$\beta\sigma_{xs}^2$
7.00	0.099	0.097	0.097	0.097	0.057	0.024	0.024	0.024
5.30	0.249	0.242	0.240	0.242	0.19	0.060	0.059	0.063
4.00	1.66	0.99	0.775	0.643	—	—	—	—
3.50	9.22	13.26	1.443	1.105	2.84	0.436	0.524	0.22
2.50	—	—	—	—	12.57	13.61	13.61	1.136
1.80	12.62	13.08	13.42	13.54	12.98	13.58	13.23	46.80
0.00	13.24	13.22	13.14	11.28	13.43	13.31	13.14	11.28

However when Ω_{cl} is in the vicinity of Ω_{clcr} this agreement is no longer there. $\beta\sigma_{x1}^2$ seems to be a more reliable estimate in this range while the value obtained through the conventional equivalent linearization technique ($\beta\sigma_{xs}^2$) is in total disagreement with the simulation results.

6.3 Discussion

All three types of excitation considered up to now, may be thought of as special cases of a more general type of excitation of the form shown in Figure 44 .

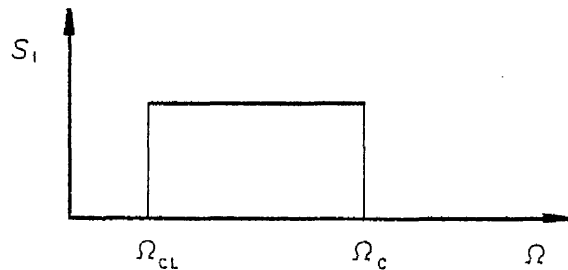
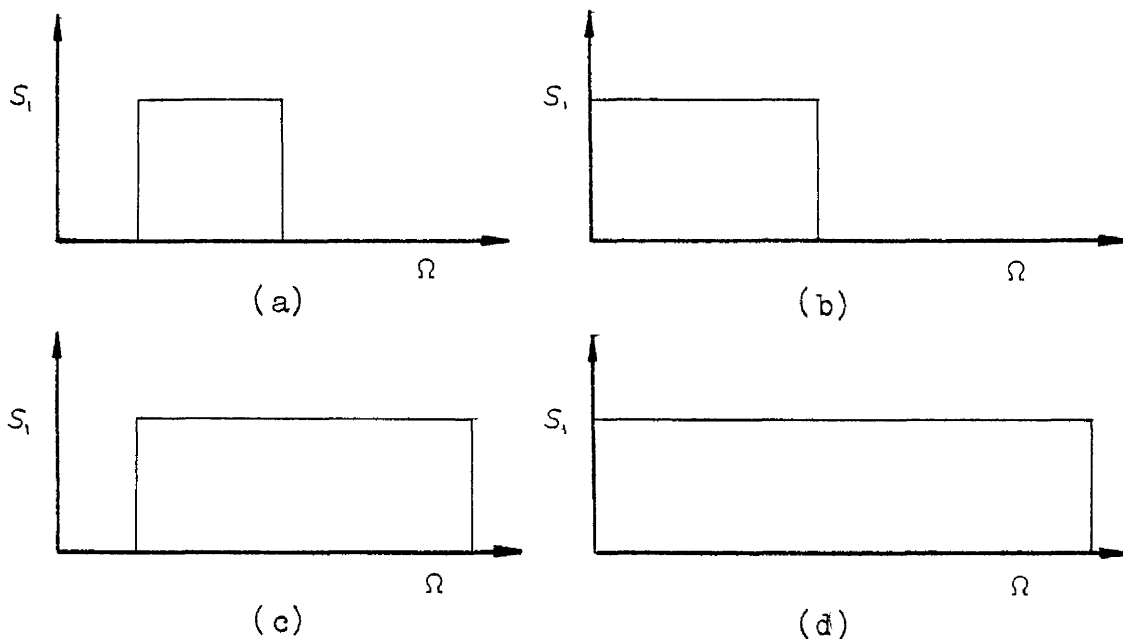


Figure 44

Where for broad band excitation $\Omega_{cl} = 0$, $\Omega_c > \Omega_r$
 for band limited excitation $\Omega_{cl} = 0$, $\Omega_c < \Omega_r$
 and for high pass filtered process $\Omega_r > \Omega_{cl} > 0$ and $\Omega_c > \Omega_r$
 where Ω_r is the resonant frequency of the response displacement spectrum under broad band excitation. Although the response spectra of the system under these excitations exhibit radically different behaviour for certain values of Ω_{cl} and Ω_c the responses are almost indistinguishable. The following is an attempt to throw some light on this phenomenon .

The range of frequency cut offs beyond which the level of response drops to noise level, for the system under high pass filtered process, seems to overlap with the range of frequencies at which the response under band limited excitation develops the second peak. These frequency ranges cannot be defined clearly with the present amount of data. However the simulation for $\Gamma/\zeta = 500$, $\zeta = 0.2$ suggest that the response under high pass filtered process drops to noise level roughly above 4Ω whereas under band limited excitation the double peaked spectrum occurs for cut off frequencies below 3Ω . The two ranges overlap by 1Ω . Clearly the coincidence of the two phenomena in this narrow range deserves further investigation. It may suggest that the most significant part of the excitation whether broad band or band limited or high pass filtered is the one enclosed by this narrow band. At this stage one could think of the third harmonic excitation. The phenomenon is a result of

excitation frequencies near the resonant frequency of the system and not of excitation of the same frequency. Naturally these are not the only harmonics which result from the excitation of the system but they are the most readily observable ones. It could be that the excitation within the overlapping frequency ranges stated above is responsible for the bulk of the response. In other words, most of the response observed is a combination of response over that small frequency range. It can be seen from the response spectra under band limited and high pass filtered processes that such a narrow band can be defined by assigning as its upper frequency the highest frequency used in the band limited experiments and as its lowest the lowest one used for the high pass filtered process experiments. For such an excitation the response will probably be very close to the responses obtained under the corresponding band limited and high pass filtered process which are themselves comparable with the response under broad band excitation. Figure 44a shows the four possible types of excitation that could result the same response for a given system.



(a) Narrow Band (b) Band Limited
(c) High Pass Filtered (d) Broad Band

Figure (44a)

The question therefore is how narrow band can this excitation become before its response is radically different.

On the question of the suitability of the equivalent linearization technique in predicting the mean square response displacement of the Duffing system under the two types of excitation considered in this chapter the following conclusions may be drawn. The conventional equivalent linearization technique is totally misleading in its predictions (value $\beta\sigma_x^2$ in Tables 6.2 and 6.3) for both cases. In the band limited case the equivalent linearization method with $\beta\sigma_x^2$ from simulation and $K_u = 2.2$ provided the best approximation to the simulation results. Further the predictions of this version of the equivalent linearization techniques are very misleading over a range of frequency cut offs in the vicinity of Ω_r (the resonant frequency of the system under broad band excitation).

For the high pass filtered process the method with both $\beta\sigma_x^2$ and K_u as computed through the simulation provided the best approximation to the simulation values. Further for very low values of $\Gamma/\zeta (< 1)$ it is expected that all three types of equivalent linearization methods will provide better agreement with simulation due to the fact that the resonant frequency (Ω_r) of the nonlinear system under broad band excitation will be close to the natural frequency and the shapes of the two spectra, (Duffing and equivalent linear systems) will be very similar.

The prime objective of this study has been to obtain the response spectra of the Duffing system excited by a Gaussian broad band random process, through the use of numerical simulations and to identify behavioural patterns of these spectra. The task was greatly simplified by the use of dimensional analysis which indicated a useful way of reducing the number of parameters. In fact the dimensional analysis applied to this mechanical systems reduces the number of independent variables by three. In Chapter 4 it was shown that the description of the non-dimensional spectra is possible in terms of two basic parameters namely Γ and γ . However when the actual spectra were produced it was possible to describe most of their properties as a function of one variable only, the ratio Γ/γ . The appearance of this ratio in the expression for the probability density function for the stationary system response, derived through the solution of the appropriate Fokker - Planck equation, makes it particularly suitable for describing such statistical quantities that can be obtained from this function. The resonant frequency is also a function of the ratio Γ/γ as has been proved by the simulations and confirmed to some extent by the equivalent linearization technique in Section 5.4. Thus it is possible to express two important properties of the response spectrum as functions of the ratio Γ/γ ; namely the area under the spectrum and the resonant frequency. Strictly speaking the spectral shapes are not a function of Γ/γ , as it is proved mainly from the near zero frequency response, and can only be accurately described in terms of the separate variables Γ and γ . However the similarity of the spectral shapes for constant Γ/γ and the inherent inaccuracies of the simulations, makes it possible to describe the resulting spectral shapes in terms of the ratio Γ/γ within the confidence limits of the numerical simulation. A result of this is the graphical method described in Section 5.5 for sketching the response spectrum for the Duffing system under broad band excitation for a given value of Γ/γ .

In ensuing the aims of this study it was possible to make secondary observations which are worth noting at this point.

Most important of these is perhaps the light shed on the term 'weak' nonlinearity used in connection with the approximate techniques. Non-dimensionalizing the expression for the mean square response of the system derived by the perturbation technique (Equation 1-8) and the heuristic approach the following expression is obtained*

$$\beta \langle x^2 \rangle = \frac{\pi}{4} \frac{\Gamma}{\gamma} (1 - 3 \frac{\pi}{4} \frac{\Gamma}{\gamma}) \quad (7-1)$$

To avoid negative values here Γ/γ must be < 0.42 and the equation is expected to break down much earlier. In fact for $\Gamma/\gamma = 0.1$ $\beta \langle x^2 \rangle = 0.06$ which under estimates the true answer by ≈ 10 . For this value of $\Gamma/\gamma = 0.1$, $\Omega_r = 1.085$ i.e. a minor shift from the natural frequency. Also the peak value of the linear system i.e. with $\beta = 0$

$$S_x(\omega_r) = S_1/4\omega_n^4 m \quad \text{for light damping} \quad (7-2)$$

$$\text{since } S_1 = \Gamma k^2 / \beta \omega_n \therefore \beta S_x(\omega_r) \omega_n = \Gamma / 4\gamma \quad (7-3)$$

for $\Gamma/\gamma = 0.1$ $B(\omega_r) = \beta S_x(\omega_r) \omega_n = 0.025$ which compares with the extrapolated value shown in Figure 24. These values indicate a nonlinearity that could be safely ignored for most applications, since the system is practically linear. It was mentioned in the introduction that a number of simulations (mainly analog) have been performed by various researchers for the purpose of verifying results obtained by different approximate methods. Unfortunately the simulations were performed for systems with weak nonlinearities. For example the highest value of Γ/γ used by A.B. Budgor and co-workers [28] to prove the accuracy of 'Krainchman's' method was $\Gamma/\gamma = 0.1$ and J.E. Manning [24]. (New heuristic approach) $\Gamma/\gamma = 1.2$. It is at least ambitious to expect observations based on results for such low values to hold true when the real nonlinear behaviour of the system manifests itself.

* In Equation (1-8) $\sigma_x^2 = \frac{\pi S}{4\gamma \omega_n^4 m}$ i.e. response for $\beta = 0$ but $\beta \neq 0$ and $\beta \sigma_x^2 = \frac{\Gamma}{\gamma} \frac{\pi}{4}$

Still on the topic of 'degree' of nonlinearity, it may be stated that in general, it is only through dimensional analysis and certain theoretical considerations that one can define a measure of the amount of nonlinearity inherent in a system's response. In particular for the Duffing system the amount of nonlinearity is by definition the term βx^3 for sinusoidal excitation and $\beta \sigma_x^2$ for random. However these terms imply previous knowledge of the response and it is perhaps more convenient to think of the system becoming more nonlinear as its γ , (sinusoidal) or Γ , (random) values increase. The advantage being that these quantities (γ, Γ) involve only system and excitation parameters.

Of the approximate techniques the equivalent linearization technique deserves a further mention here. As already seen in (Section 2.2) there are two ways one can evaluate the expectations (equation (2-25)) required for calculating the natural frequency (ω_e) and damping coefficient (γ_e) of the equivalent linear system; either by use of the linearized equation (conventional equivalent linear technique) or by use of the exact probability density function of the nonlinear response. Both approaches for the Duffing system under broad band excitation, (or indeed white noise) lead to equations (7-4) and (7-5)

$$(\beta \sigma_x^2)^2 \frac{4Ku}{\pi} + \beta \sigma_x^2 \frac{4}{\pi} = \Gamma/\gamma \quad (7-4)$$

$$(\Omega^4 - \Omega^2) \frac{4}{(Ku\pi)} = \Gamma/\gamma \quad (7-5)$$

The two approaches differ only in terms of the value of Ku used. For the conventional equivalent linearization technique (Section 2.2) Ku is constant and equal to 3, since it uses the linear system to evaluate equation (2-25). In the other case Ku is determined by the exact probability density of the nonlinear response, and varies in the range 3 to 2.2. For $Ku = 3$ equation (7-4) systematically under estimates the value of $\beta \sigma_x^2$, whereas equation (7-5) over estimates Ω_r the resonant frequency of the spectrum. When the true value of Ku is used equation (7-4) gives the correct value of $\beta \sigma_x^2$ for a given value of Γ/γ . This however is not original

information since to calculate Ku , $\beta\sigma_x^2$ has to be found beforehand using the probability density function. The one and only original contribution of the equivalent linearization technique to our problem is equation (7-5). This equation provides the resonant frequency of the response displacement spectrum of the Duffing system in terms of the excitation parameter Γ . Although it was known [12] (Appendix B.1) that the autocorrelations of the two systems (equivalent linear and Duffing) were similar in some respects, it was possible to observe the coincidence of their resonant frequencies only through the numerical simulations. The differences in other respects between the spectra of the two systems for $\Gamma/\gamma = 500$ was shown in Figure 31. However for small values of Γ/γ (≤ 0.1) the spectrum of the equivalent linear system is remarkably similar to the nonlinear one as A.B.Budgor and co workers [28] have shown with their own simulations. This supports the notion that for 'weak' non linearity the Duffing system behaves like a linear system with a slight shift of resonant frequency as far as its response spectrum is concerned.

In Chapter 5 it was shown that the properties of the response of the Duffing system under mathematical white noise (derived through the solution of the appropriate Fokker - Planck equation) also apply to the response of the system under Gaussian broad band random excitation. It seems however that this is not always the case. I.W.Wedig has produced the response spectra of the trilinear system

$$m \ddot{x} + 2cx + g(x) = F(t) \quad (7-6)$$

$$g(x) = k[(1+\gamma)x - \gamma x_0]$$

with $\gamma = 0$ for $|x| < x_0$ and $x_0 = -x$ for $x \leq -x_0$.

under mathematical white noise. Figure 45 is reproduced from reference [33] the symbol σ_n^2 in this figure stands for the mean square response of the linearized system (i.e. $\gamma = 0$) under white noise force excitation of intensity S_n . i.e. $\sigma_n^2 = \pi S_n / (4 \omega_n^3 m^2)$. Qualitatively the behaviour shown in Figure 45 may be explained as follows. The response spectrum has two resonant frequencies $\omega_1 = \sqrt{k/m}$ and $\omega_2 = \sqrt{k(1+\gamma)/m}$. The amount of response at each frequency is

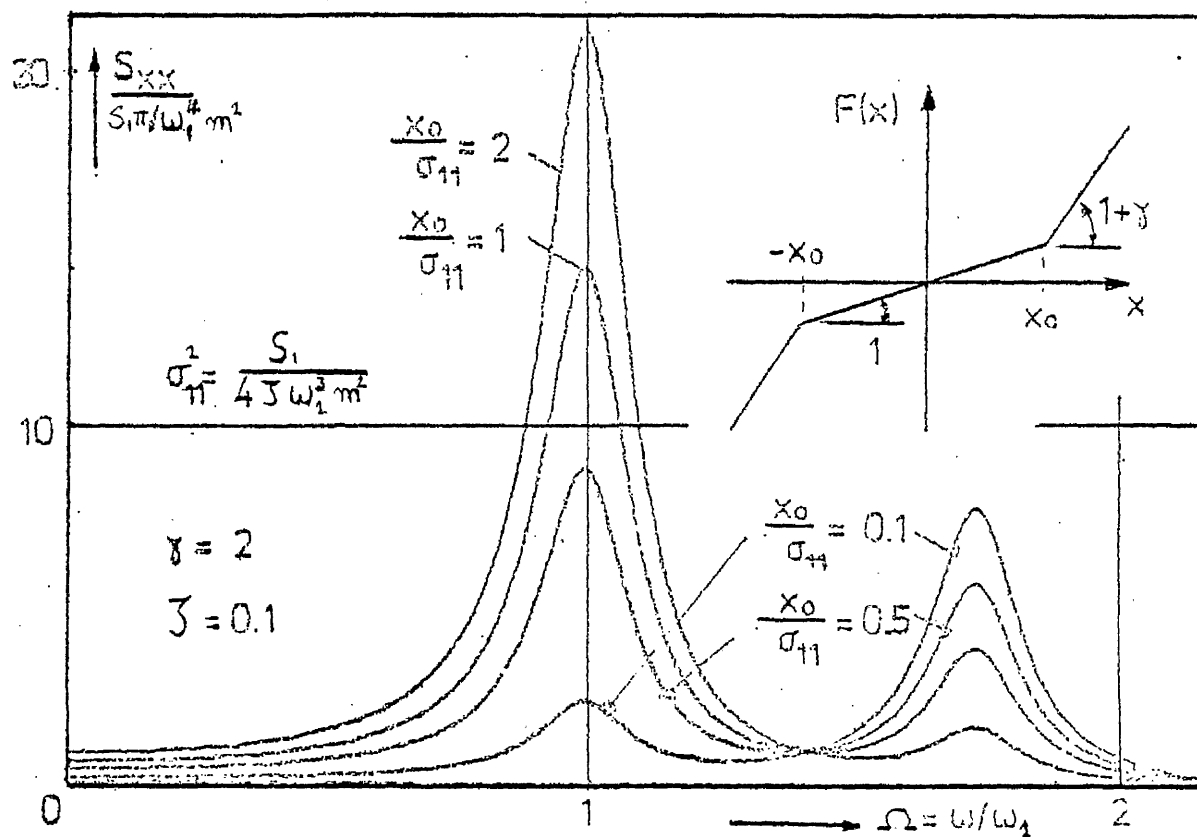


Figure 45

Response Spectra of the piece wise linear system, equation (7-6) under white noise excitation (reproduced from Ref. [33])

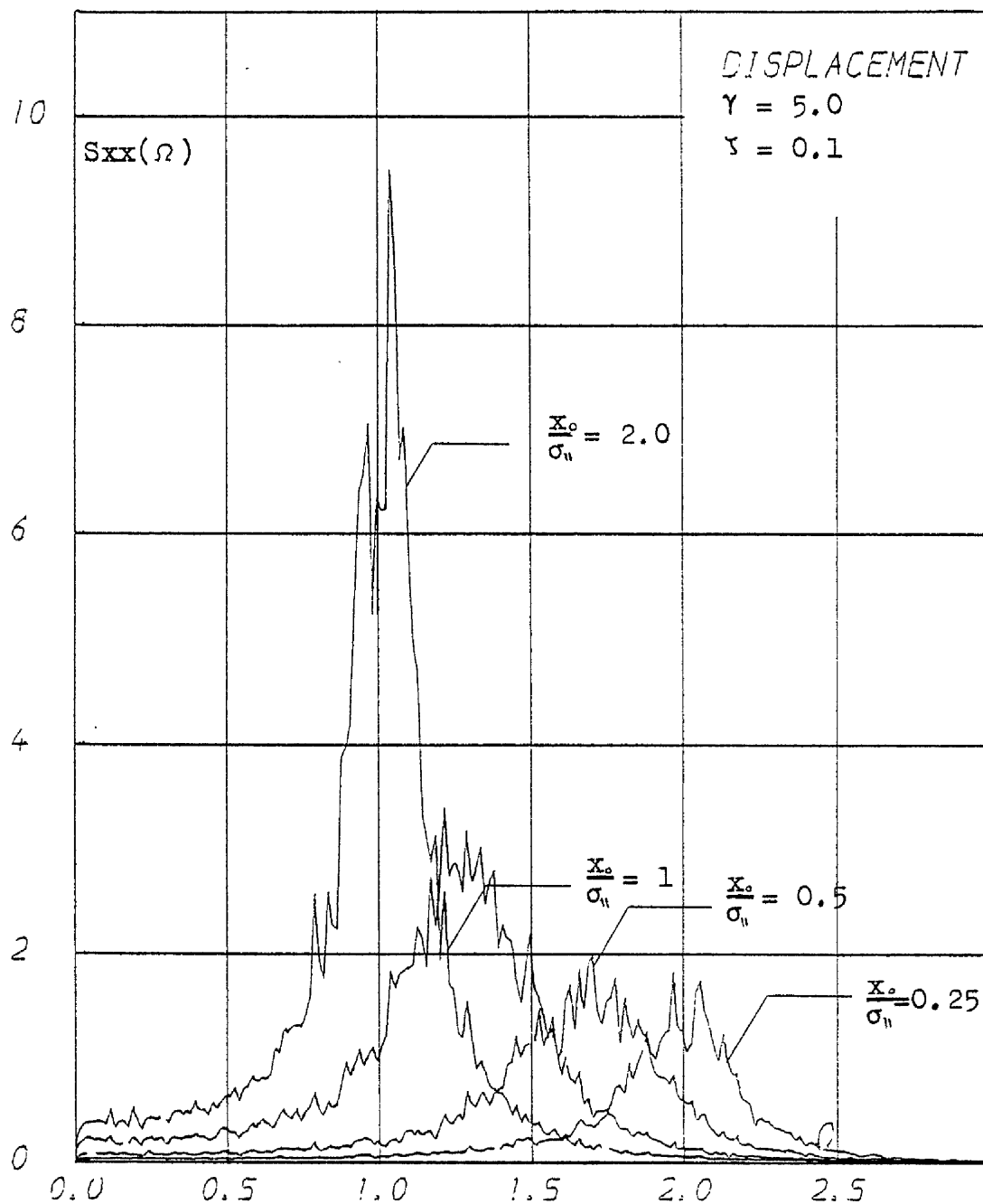


Figure 46a

Figure 46a Response displacement spectra of the piece wise linear system, equation (7-6), under broad band excitation (simulation results)

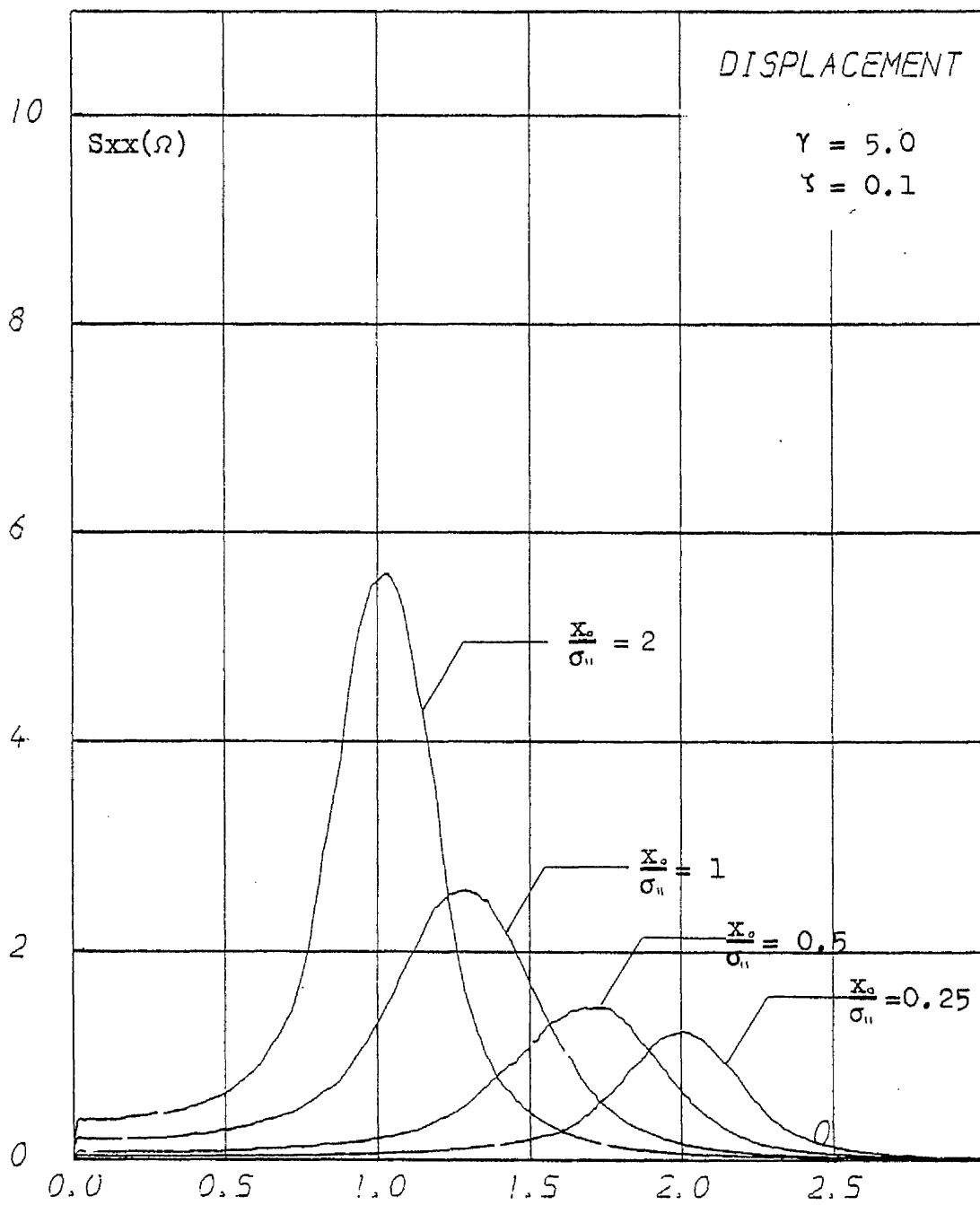


Figure 46b

As for Figure 46a after
frequency averaging

determined by the quantity x_0/σ_n . For low values of σ_n most of the excitation results in displacements $x < |x_0|$ hence most of the response has resonant frequency ω_1 . As σ_n increases most values of $F(t)$ produce response which is outside the $-x_0$ to x_0 range, hence most of the response has resonant frequency ω_2 . The existence of such closed form solution was considered a good test case for the simulation programs. However as it can be seen from Figure 46 the simulated response displacement spectra for this system under broad band excitation are radically different from Figure 45. The fact that the system parameters for the two figures are different is irrelevant. What is important is that the simulation spectra do not have two peaks at ω_1 and ω_2 but as the ratio x_0/σ_n is reduced there is a gradual shift in a single resonant frequency in the range ω_1 to ω_2 . This discrepancy between the responses under mathematical white noise and broad band was also confirmed by Professor I.W.Wedig in a private communication to Professor J.D.Robson and is also discussed in a second paper by I.W.Wedig [34]. Further if the piecewise linear stiffness of equation (7-6) is thought of as an approximation for part of the Duffing cubic stiffness or vice versa then the general behaviour of the spectra of Figure 46 agrees with the response spectra shown in Chapter 5, better than those for white noise excitation in Figure 45.

In general it may be stated that in investigating the response of nonlinear systems, there is always the danger on the part of the researcher in thinking with a linear background. The inapplicability of the linear intuition and theory was well demonstrated for the response of the Duffing system under the three different types of excitation considered in this work. I.W.Wedig's example is a further warning possible unsuitability of mathematical white noise excitation to describe realistic excitations for nonlinear systems.

In this project the response power spectra of the Duffing system under broad band excitation were described in relative detail. However the description of the response in general

is far from complete. The response being non - Gaussian needs to be described in terms of higher order spectra as well. In this respect the simulation process used here may be found useful, although the number of realisations per estimation will probably have to be increased. Certain aspects of the response under band limited, and high pass filtered processes were briefly investigated posing more questions than producing answers. Future research in this direction will probably reveal much more interesting behaviour in terms of probability distributions and 'jumps' of the type seen in Section 6.2. The variety of geometrically shaped excitation spectra to be used is enormous, but perhaps more interesting would be the case where the response of a linear system under broad band excitation was used as excitation for the nonlinear system or the simpler case of the Duffing system under narrow band excitation. This problem was treated by R.H.Lyon and M.Heckl [32] in terms of the equivalent linearization technique. R.H.Lyon has also proved that multi-valued behaviour (jump) cannot exist when the excitation is broad band. A broad band signal may be thought of as a random sequence of impulses, each impulse imparting a certain amount of Kinetic energy to the mass regardless of its state of motion. In this way, the power of the signal is not affected by the state of motion but depends on the impulse statistics. This forces the dissipation to be constant and equal to the power input (when the system reaches its steady state) and consequently, its mean square velocity which is proportional to the dissipation is determined.

Clearly from the above, what is needed for the occurrence of jumps is an excitation which can exchange energy with the system over a cycle or so in order that more than one 'equilibrium' level may be attained consistent with the equations of motion. It is well known that sinusoidal excitation satisfies this requirement [35], but the argument also suggests that a random source which correlates with itself and hence with its response over a few cycles of motion can produce the same effect. As it was seen in Chapter 3 the present numerical simulation can cope

with jump phenomena for deterministic excitation, however it should be used with caution for random analysis and the response spectra for such an excitation will probably present problems of interpretation.

An investigation of the softening Duffing system ($\beta < 0$) would also be very interesting.

The equivalent linearization technique is applicable for negative β . Figure 47 shows a plot of $\beta\sigma_x^2$ versus Γ/γ for negative values of β using the equivalent linearization technique according to

$$\beta\sigma_x^2 = (-1 \pm \sqrt{1 + Ku\pi\Gamma/\gamma})/2Ku \quad (7-7)$$

for a constant value of $Ku = 3$.

Although the present simulation technique is in principle capable of dealing with a negative β the problem of singularities in the solution should be closely observed, since the numerical integration techniques cannot function in a range where singularities occur. It is worth noting that according to equation (7-7) there are two possible values for $\beta\sigma_x^2$ for given Γ/γ (for positive β there are also two values for $\beta\sigma_x^2$ but one is negative hence inadmissible), and that the value of Γ/γ cannot exceed -0.1061 without $\beta\sigma_x^2$ becoming a complex number.

The simulation programs are listed in Appendix C4. It can be seen from a closer study of these lists, that the only major change needed to deal with different forms of non linearity will have to be made in subroutine FCN of the numerical integration program which defines the set of differential equations describing the system of interest. This naturally widens the choice of possible future investigations enormously. Further it may be confidently stated that any simulation work with nonlinear systems will have a lot to benefit from previous dimensional analysis of the problem, which will facilitate the planning of simulation experiments and the description of the outcome

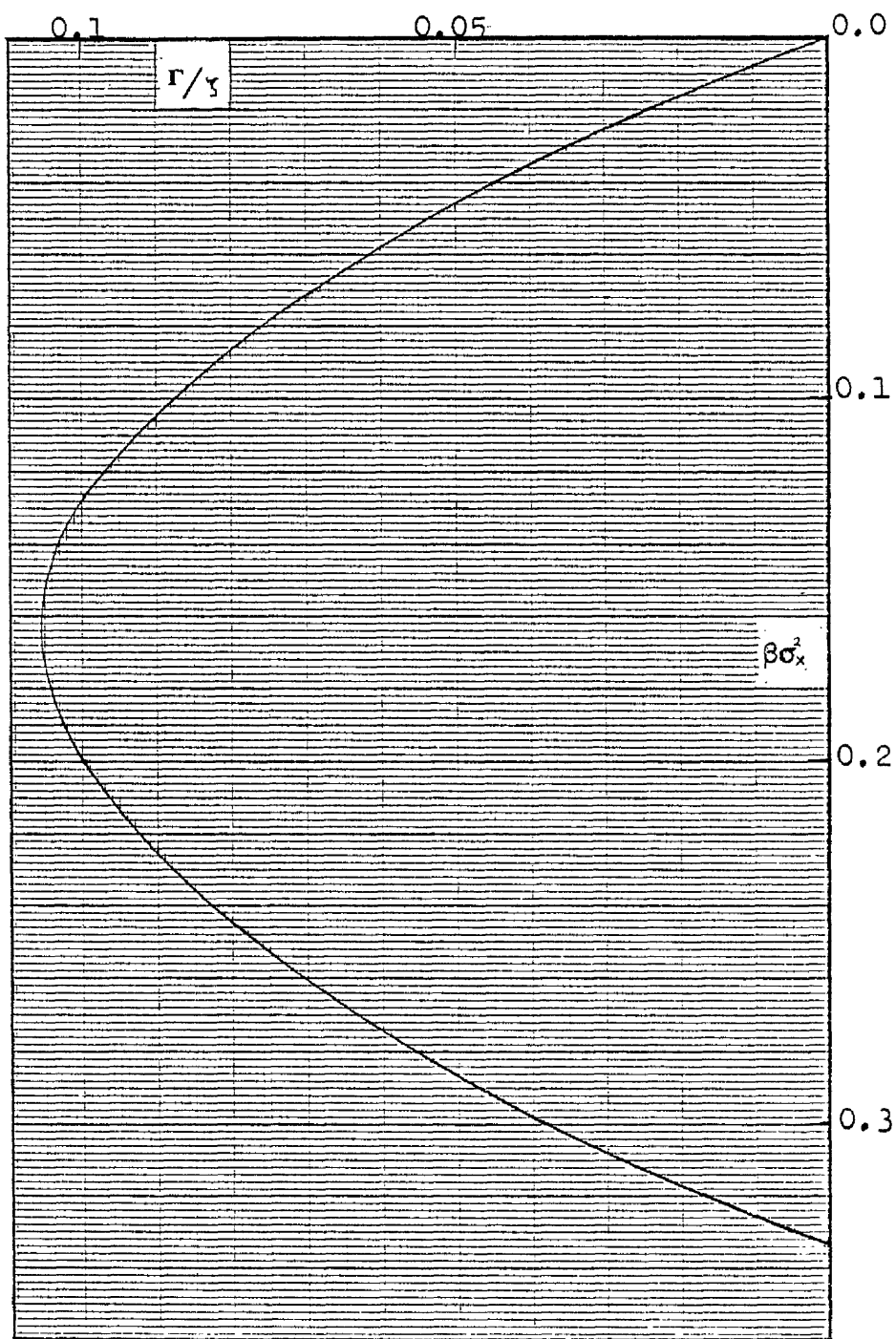


Figure 47

Prediction of the non-dimensional response displacement variance of the softening Duffing system (-ve β) under broad band excitation, through the equivalent linearization method

REFERENCES

1. S.O.Rice —'Mathematical Analysis of Random Noise'
 Selected Papers on Noise and Stochastic
 Processes. Dover Public. INC. N.Y. 1353.
2. R.K.Otnes —'Applied Time Series Analysis' Vol.2.
L.Enochson J.Wirey and Sons 1978.
3. J.Bendat —'Random Data : Analysis and Measurement
A.Piersol Procedures'.
 Wiley — Interscience 1971.
4. R.M.Bracewell —'The Fourier transformation and its
 Application'.
 McGraw Hill Book Company 1965.
5. S.H.Crandall —'Random Vibration in Mechanical Systems'.
W.D.Mark Academic Press N.Y. 1963.
6. S.H.Crandall —'Random Vibration', Vol.2 M.I.T. Press
 1963 Pages 85 — 100.
7. A.Papoulis —'Probability Random Variables and
 Stochastic Processes'.
 McGraw Hill Kogakusha,Ltd., 1965.
8. T.T.Soong —'Random Differential Equations in
 Science and Engineering'. Academic
 Press 1973.
9. R.H.Lyon —'Empirical Evidence for Nonlinearity
 and Direction for Future Work'.
 J.A.S.A. 35(1963) 1712—1781.
10. T.K.Caughey —'Derivation and Application of the
 Fokker-Planck Equation to Describe
 Nonlinear Systems Subjected to White
 Random Excitation'.
 J.A.S.A. 35(1963) 1683—1695.

11. T.K.Caugey - 'Analysis of a Nonlinear System With
J.K.Dienes White Noise Input'.
J.App. Physics 32(1961) 2476-

12. L.E.Wolaver - 'Second Order Properties of Nonlinear
Systems Driven by Random Noise'.USAF
Aerospace Research Lab. ARL-65-61,
Wright - Patterson Air Force Base,
Ohio, April, 1965.

13. R.H.Lyon - 'On the Vibration Statistics of a
Randomly Excited Hard Spring Oscillator'.
J.A.S.A. 32(1960) 716 - 719.

14. R.H.Lyon - 'On the Vibration Statistics of a
Randomly Excited Hard Spring
Oscillator',II.
J.A.S.A. 33(1961) 1395 - 1403.

15. S.T.Ariaratnam - 'Random Vibrations of Nonlinear
Suspensions'.
J.Mech.Eng.Science 2 No.3 (1960).

16. S.H.Crandall - 'Zero Crossings, Peaks and Other
Statistical Measures of Random
Responses'.
J.A.S.A. 35(11) 1693 - 1699.

17. N.Krylov - 'Introduction to Nonlinear Mechanics :
N.Bogoliubov Asymptotic and Approximate Methods'.
(Ann.Math.Studies No.11)
Princeton Univ. Press (1947).

18. R.C.Booton,Jr. - 'Nonlinear Control Systems with Random
Inputs'. I.E.E.E.Trans.Circuit Theory,
CT-1 :9-18 (1954).

19. T.K.Caugey - 'Equivalent Linearisation Techniques'.
J.A.S.A. 35(1963) 1706-1711.

20. S.H.Crandall —'Random Vibration of Systems with
Nonlinear Restoring Forces'.
Proc.Inter.Symp. Nonlinear Vibrations
Kiev, Sept, 1961, 1:306—314 (1963).

21. P.D.Spanos —'Stochastic Linearization in
Structural Dynamics'.
App.Mech. Reviews 34(1981).

22. S.H.Crandall —'Perturbation Techniques for Random
Vibration of Nonlinear Systems'.
J.A.S.A. 35(1963) 1700—1705.

23. S.H.Crandall —'The Spectrum of Random Vibration of a
Nonlinear Oscillator'. Presented at
the 11th Intern. Congress of
Apt.Mech. Munich 1964.

24. J.E.Manning —'Response Spectra for Nonlinear
Oscillators'.
J.Eng. Industry (1975) 1223—1226.

25. R.H.Kraichman —'Dynamics of Nonlinear Stochastic
Systems'.
J.Math.Phys.2,124 — 148 (1961).

26. R.H.Kraichman —'Irreversible Statistical Mechanics
of Incompressible Hydromagnetic
Turbulence'.
Phys.Rev. 103, 1407—1422 (1958).

27. J.B.Morton —'Consolidated Expansions for Estimating
S.Corrsin the Response of Randomly Driven
Nonlinear Oscillator'.
J.Stat.Phys.2: 153 (1970).

28. A.B.Budgor —'Studies in Nonlinear Stochastic
K.Lindenberg Processes.II. The Duffing Oscillator
K.E.Shuler Revisited'.
J.Stat.Phys. 5 : 375 (1976).

29. W.J.Duncan —'Physical Similarity and
 Dimensional Analysis'.
 Edward Arnold and Co.London(1953).
30. C.M.Focken —'Dimensional Methods and their
 Applications'.
 Edward Arnold and Co.London(1953).
31. A.V.Kanellopoulos —'Physical Similarity and
 Dimensional Analysis'.
 (In Greek) 1958.
32. R.H.Lyon —'Response of Hard-Spring Oscillator
M.Heckl to Narrow-Band Excitation'.
 J.A.S.A. 33(1964) 1404-1411.
33. W.Wedig —'The Integration of Nonlinear
 Stochastic Systems with
 Applications to the Damage and
 Ambiguity Identification'.
 2 A.M.M. (1981) Vol, 1-2.
34. W.Wedig —'Modal and Damage Analysis by
 Elastic Structures Frequency
 Separation by Nonlinear Filter'.
 ISCME-Conference, June,1982
 Washington D.C.
35. J.J.Stoker —'Nonlinear Vibrations'.
 Interscience Publishers Inc.
 N.Y. (1950) Chapter IV.

APPENDIX A

A.1. The Duffing System Under Sinusoidal Excitation

This section will give a brief review of the properties of the Duffing system under sinusoidal excitation and serve as a reminder of the nonlinearities of the system, which had to be taken into account when setting up the numerical simulation. This type of excitation was used as a check of the reliability of the simulation process in the first stages of this work.

Let us consider therefore a Duffing system having the equation of motion

$$m \ddot{x} + c\dot{x} + k(1+\beta x^2)x = F_0 \cos(\omega t + \phi) \quad (\text{A.1-1})$$

where $\omega_n = \sqrt{k/m}$

by considering only the fundamental component of the response as a suitable approximation it is easy to show that the amplitude response x_0 , must satisfy (see also Section A.2).

$$\left[\left(1 + \frac{3}{4}\beta x_0^2 - \Omega^2 \right)^2 + (2\zeta\Omega)^2 \right] x_0^2 = \bar{F}_0^2 \quad (\text{A.1-2})$$

where $\Omega = \omega/\omega_n$

$$\bar{F}_0 = F_0 / m\omega_n^2 \quad \text{and} \quad \zeta = \frac{c}{2\sqrt{km}}$$

For fixed excitation amplitude and light damping the response curves generally have the form sketched in Figure (A.1-1) which depicts the steady-state peak response amplitude as a function of the frequency of excitation. The curved resonant peak of Figure (A.1-1) lies at the heart of one of the more important nonlinear phenomena, the jump. In the shaded region the theoretical response is triple-valued but the locus between points two and five is unstable. When the frequency of excitation is very slowly increased from zero, the steady response amplitude follows the curve of Figure (A.1-1) from one to two. If the excitation frequency is increased further, there is an irregular transient motion, after which a steady state is achieved with amplitudes on the branch of the curve from three to four. Now when the excitation frequency is slowly decreased, there is no peculiarity in the response from point four until the point five is reached. Here if the

excitation frequency is further decreased, there is again an irregular transient followed by a return to the steady state along the branch of the curve from six to one. In Chapter (4) the non-dimensional form of the Duffing system was outlined and it can be seen in Figures (7 and 8) that the characteristic shape of the Figure (A.1-1) is still there.

While testing the simulation process, using sinusoidal excitation, it was possible to establish a general pattern for the behaviour of the settling time of the system when excited from rest. The term settling time implies the time interval after which the system settles into a steady oscillation, and should be discriminated from the term 'transient' which applies to linear systems only because of its properties. It is beyond the scope of this work to establish detailed account of this behaviour. It was only necessary to obtain a rough idea of the amount of data that should be excluded from the realisations when calculating the response spectra of the system under random excitation. It was observed that the duration of the settling time decreased with increased damping ratio as expected, the effect of changes in the non linearity parameter β or the level of excitation F_0 was relatively insignificant (all other parameters remaining constant). Figure (A.1-2) shows the effect of different damping values on the non-dimensional quantity $a = kx^3/F_0^2$. The following are some of the best known properties of the Duffing system.

- a) The free vibrations of the system are:-
 - 1) Symmetrical periodic oscillations but not sinusoidal.
 - 2) Period and oscillations depend on the amplitude of the response.
 - 3) The free vibration frequencies form a locus on an amplitude - ω - frequency graph called the free vibration backbone.
- b) The steady state response of the system to a periodic force excitation
 - 1) is generally periodic with same period as the excitation.

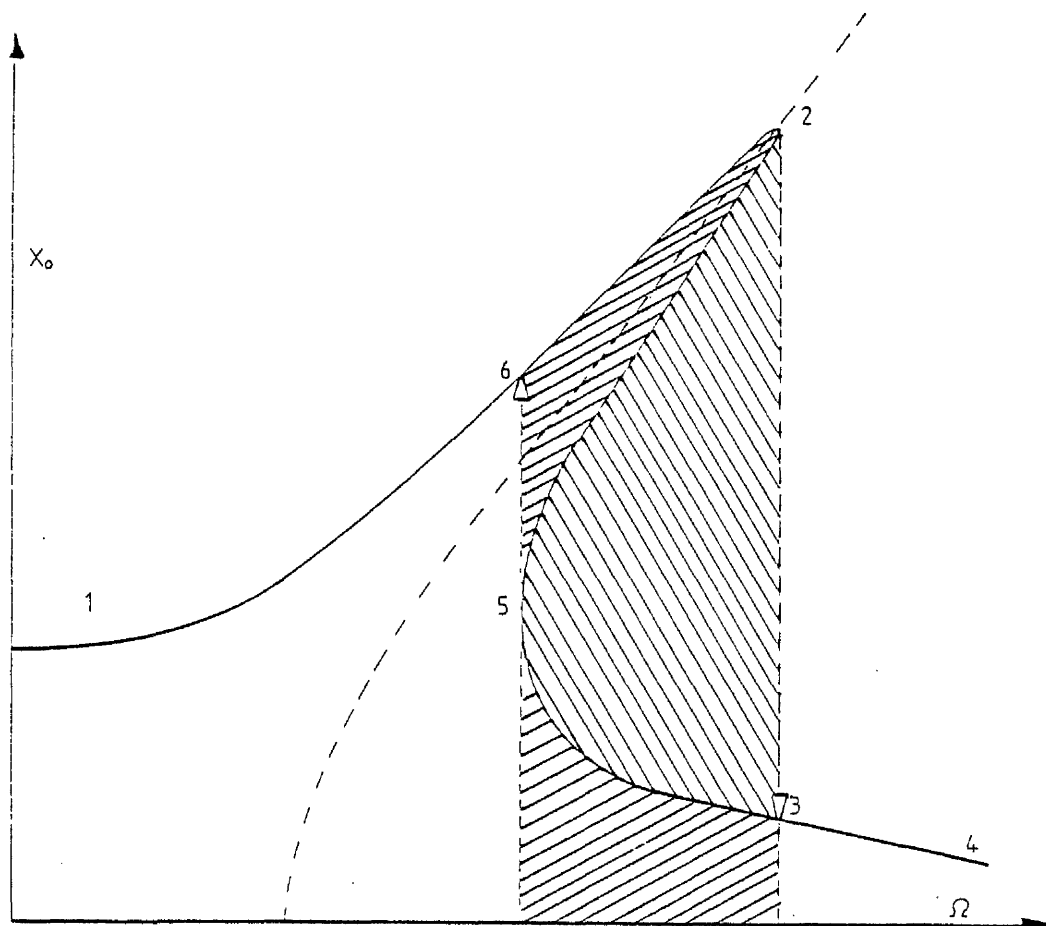


Figure A.1-1 Response displacement amplitude as a function of non-dimensional frequency for the Duffing system under sinusoidal excitation.

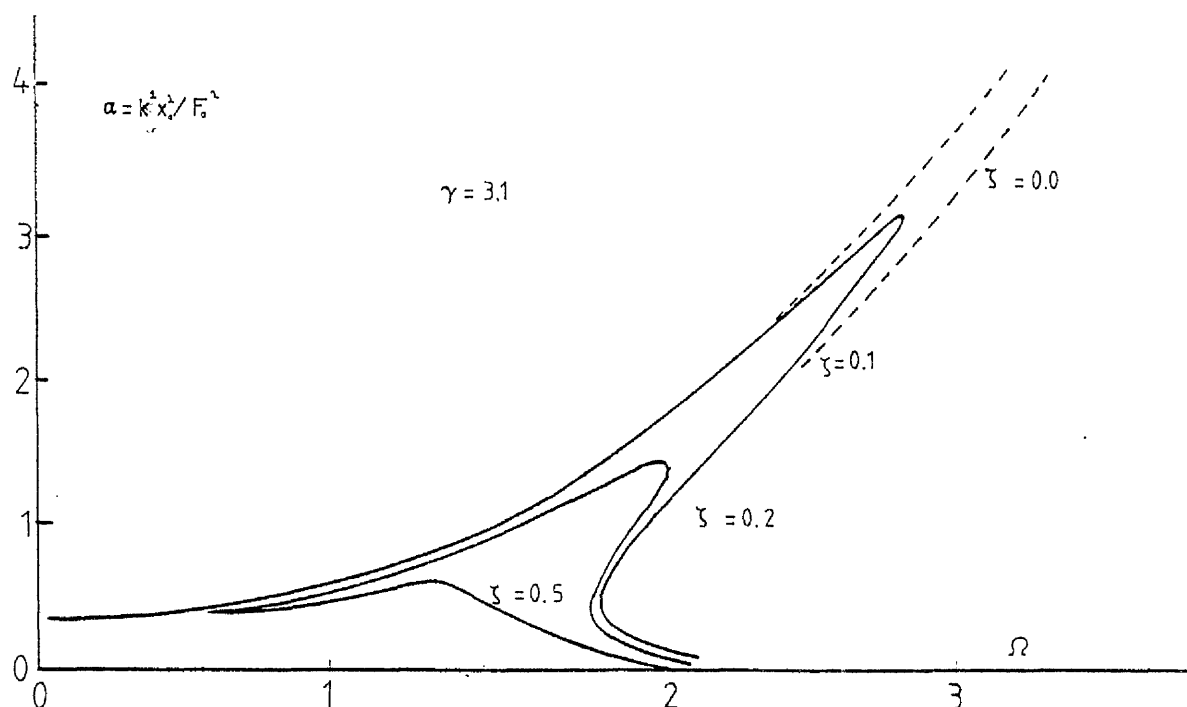


Figure A.1-2 Non-dimensional response displacement amplitude as a function of frequency for the Duffing system under sinusoidal excitation and different damping ratios.

- 2) The wave shape of the response oscillation is in general different from that of the excitation and also from the free vibration. Moreover the response wave shape changes with the level of excitation and with the nonlinear term.
- 3) Particularly when the excitation is sinusoidal of slowly varying frequency it is possible to observe the jump phenomenon.

A.2. Approximate Solution Involving Third Harmonics for the Duffing System Under Sinusoidal Excitation.

The possibility of improving the approximate solution given by equation (A.1-2) was also investigated by incorporating the third harmonic in the solution. This section contains details of the harmonic balance method to obtain expressions which will provide a response which is a mixture of the fundamental and third harmonic.

Consider again equation (A.1-1). If the solution

$$x = x_1 \cos \omega t + x_3 \cos 3\omega t + y_3 \sin 3\omega t \quad (\text{A.2-1})$$

is assumed. Then

$$\left. \begin{aligned} x^3 &= x_1^3 \cos^3 \omega t + x_3^3 \cos^3 3\omega t + y_3^3 \sin^3 3\omega t \\ &+ 3x_1^2 x_3 \cos^2 \omega t \cos 3\omega t + 3x_1^2 y_3 \cos^2 \omega t \sin 3\omega t \\ &+ 3x_3^2 x_1 \cos^2 3\omega t \cos \omega t + 3x_3^2 y_3 \cos^2 3\omega t \sin 3\omega t \\ &+ 3y_3^2 x_1 \sin^2 3\omega t \cos \omega t + 3y_3^2 x_3 \sin^2 3\omega t \cos 3\omega t \\ &+ 6x_1 x_3 y_3 \cos \omega t \cos 3\omega t \sin 3\omega t \end{aligned} \right\} \text{A.2-2)}$$

Substituting (A.2-2) in (A.1-1)

$$\left. \begin{aligned} &-m\omega^2 x_1 \cos \omega t - 9m\omega^2 x_3 \cos 3\omega t - 9m\omega^2 y_3 \sin 3\omega t \\ &-c\omega x_1 \sin \omega t - 3c\omega x_3 \sin 3\omega t + 3c\omega y_3 \cos 3\omega t \\ &+ k x_1 \cos \omega t + k x_3 \cos 3\omega t + k y_3 \sin 3\omega t \\ &+ k x^3 - F_0 \cos \omega t \cos \varphi + F_0 \sin \omega t \sin \varphi = 0 \end{aligned} \right\} (\text{A.2-3})$$

We can obtain suitable coefficients for $\cos \omega t$, $\cos 3\omega t$ in (A.2-1) by requiring that the coefficients of $\cos \omega t$, $\sin \omega t$, $\cos 3\omega t$, $\sin 3\omega t$ in (A.2-3) should vanish.

With $\lambda = \frac{x_3}{x_1}$, $\mu = \frac{y_3}{x_1}$, this requirement leads to equation (A.2-4)

$$\left. \begin{aligned} x_1 \left\{ -m\omega^2 + k + \frac{3}{4} k \beta x_1^2 \left\{ 1 + \lambda + 2\lambda^2 + 2\lambda^3 \right\} \right\} &= F_0 \cos \varphi \\ x_1 \left\{ -c\omega + 3k \beta x_1^2 \mu \right\} &= -F_0 \sin \varphi \\ -9m\omega^2 \lambda + 3c\omega \mu + k \lambda + \frac{1}{4} k \beta x_1^2 \left\{ 1 + 3\lambda^3 + 6\lambda + 3\mu^2 \lambda \right\} &= 0 \\ -9m\omega^2 \mu - 3c\omega \lambda + k \mu + \frac{3}{4} k \beta x_1^2 \left\{ \mu^3 + 2\mu + 2\mu^2 \lambda \right\} &= 0 \end{aligned} \right\} (\text{A.2-4})$$

These expressions equations(A.2-4), can be reduced to equation (A.1-2) under the assumption that the third harmonic components in the solution are much smaller than the fundamental i.e. $\lambda, \mu \ll 1$, so that all products of λ, μ vanish and equations(A.2-4) become

$$x_1 [-m\omega^2 + k + \frac{3}{4}k\beta x_1^2] = F_0 \cos\varphi$$

$$x_1 (-c\omega) = -F_0 \sin\varphi$$

$$\text{therefore } x_1^2 [(-m\omega^2 + k + \frac{3}{4}k\beta x_1^2) + (c\omega)^2] = F_0^2$$

(A.2-5) or (A.1-2)

The set of equations (A.2-4) were solved numerically. The solution showed that the ratio of third harmonic to fundamental in the response did not exceed 0.15 for the highest nonlinearity examined ($\gamma = \beta F_0^2 / k^2 = 3.11$ see also Section 4.1 for the significance of γ). It should be noted that although the solution in this appendix is expected to provide more accurate values for the response, it is still an approximation to the exact answer since it ignores the rest of the harmonics.

Table A2 shows the response predictions for the two approaches for $\gamma = 3.11$, $\zeta = 0.1$. The values for the fundamental are also plotted in Figure (A.2-1) in their non dimensional form i.e. $\alpha = kx_1^2 / F_0^2$ versus $\Omega = \omega / \sqrt{km}$.

Table A.2 $\gamma = 3.11$ $\chi = 0.1$

x_1	0.90	1.10	1.30	1.50	1.80	2.00	2.65	2.80
Ω^*_u	1.88	1.86	1.89	1.94	2.07	2.18	2.60	2.68
Ω_u	1.88	1.86	1.89	1.95	2.09	2.20	2.61	2.70
Ω^*_L	—	0.55	0.96	1.24	1.58	1.78	2.41	2.58
Ω_L	—	0.72	1.01	1.28	1.62	1.83	2.46	2.60
$\mu 10^{-3}$	0.30	0.40	0.60	0.70	0.90	1.00	1.10	1.10
$\mu 10^{-3}$	—	35.80	7.60	3.90	2.50	2.00	1.40	1.30
λ_u	0.68	1.06	1.47	1.87	2.41	2.73	3.50	3.64
λ_L	—	15.50	7.20	5.36	4.52	4.31	4.06	4.02

* Values corresponding to equation (A.2-5)

— Equation (A.2-5)

... Equation (A.2-4) i.e. involving third harmonics

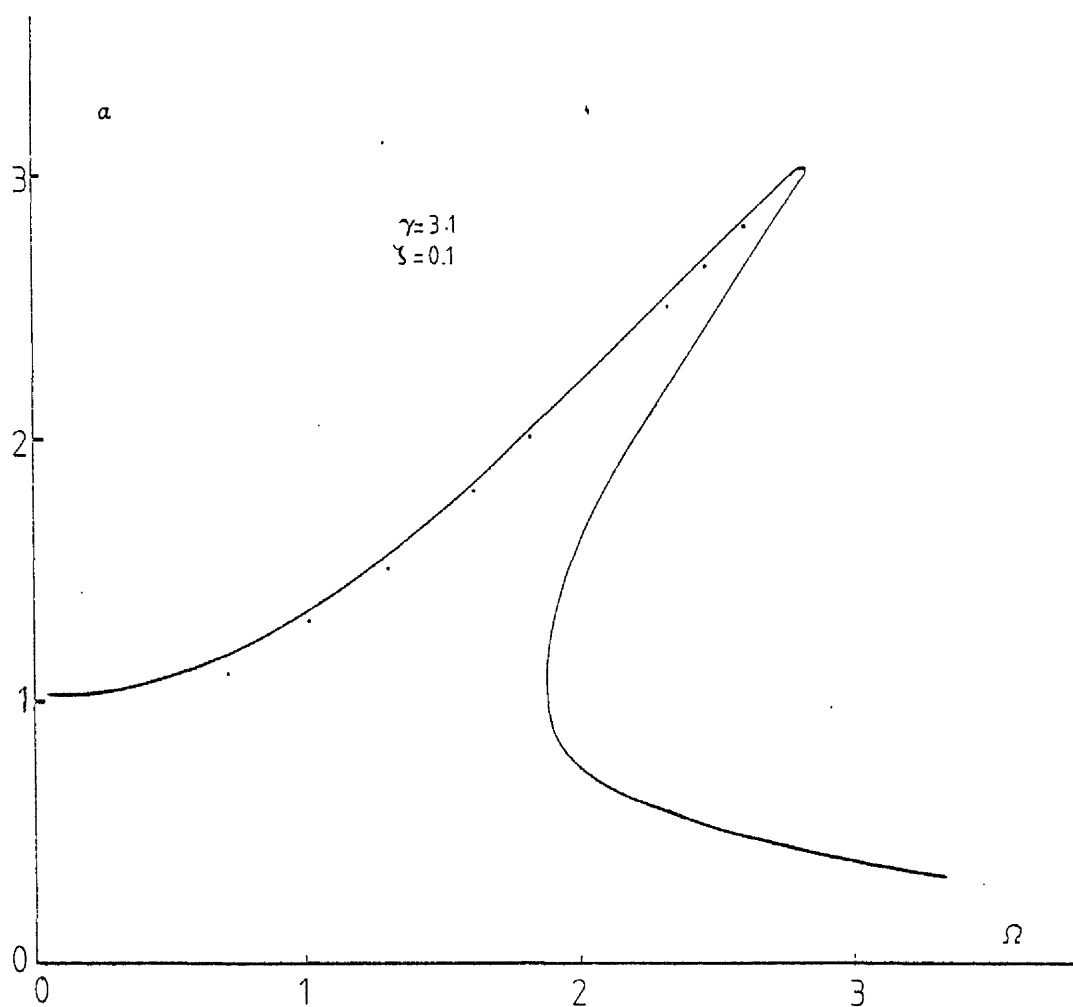


Figure A.2-1

A.3. The Duffing System Under Modulated Sinusoidal Excitation

Consider the response to be expected from the Duffing system equation (A.1-1) due to an excitation of the form

$$F(t) = F_0 \sin(\omega_e t) \cos(\omega t + \phi) \quad (A.3-1)$$

where $\omega_e \ll \omega$

instead of the excitation $F(t) = F_0 \cos(\omega t + \phi)$ used earlier equation (A.1-1). Hence the Duffing system is now excited under a sinusoid of slowly varying amplitude. It will be understood that this form of amplitude variation is quite arbitrarily chosen: the $\sin \omega_e t$ function is simply a convenient function providing a fluctuating envelope and so giving some slight resemblance to a part of a narrow band random excitation. Consider again equation (A.1-2). The behaviour indicated by this equation is usually portrayed by response curves of the form of Figure (A.3-1) but it will be more convenient here to plot response for constant values ω , and this is done by Figure (A.3-2) for $\beta = 1$, $\gamma = 0.1$ as typical values. Provided that the ratio ω_e/ω is small enough one can use Figure (A.3-2) to determine the amplitude of response x_0 arising from any amplitude of excitation of the given fixed frequency. This provides the envelope x_α of the response which corresponds to the excitation envelope $F_0 \sin \omega_e t$, and typical x_α, t curves as plotted in Figure (A.3-3). The effects of the jump phenomena can be seen clearly in Figure (A.3-3). For small enough excitations they have no effect as the F_0, x_0 relationship involves one branch of Figure (A.3-2), but greater excitation amplitudes involve the alternative branch so that much greater amplitudes then arise and response amplitudes only return to lower values when the form of Figure (A.3-2) permits it. The important point here is that in general the response of the system to a particular excitation is affected by both upper and lower values of Figure (A.3-2) during different points of its history. Only in special cases will a single branch predominate over an extended interval of time.

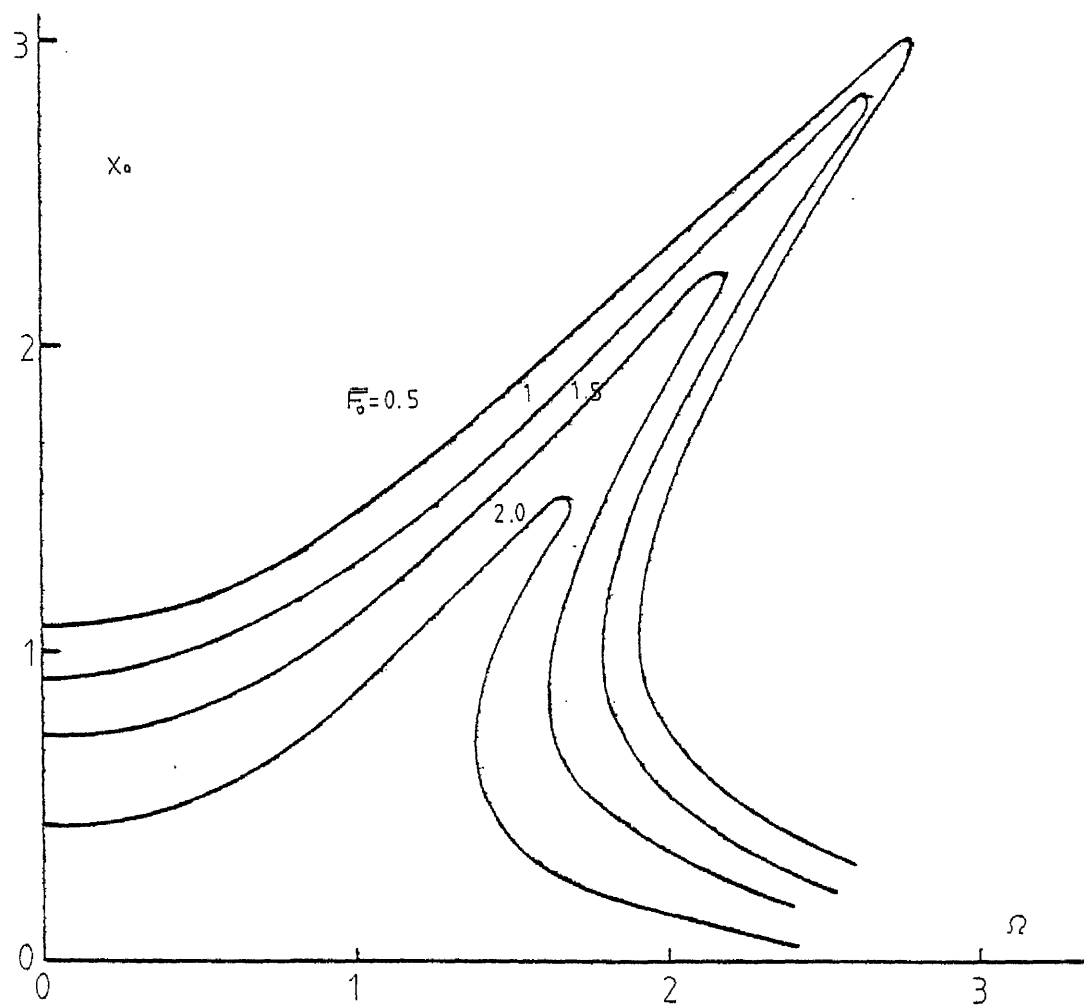


Figure A.3-1 Response displacement amplitude as a function of non-dimensional frequency for the Duffing system under sinusoidal excitation.

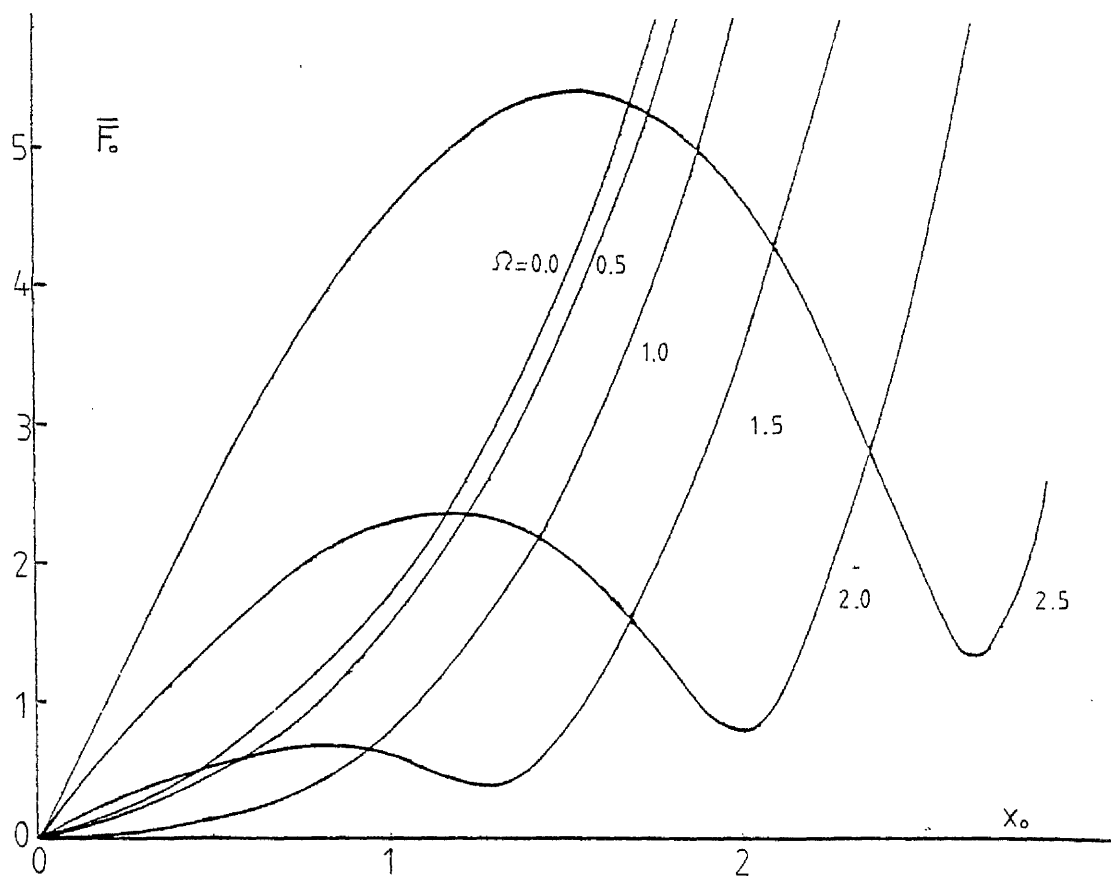


Figure A.3-2

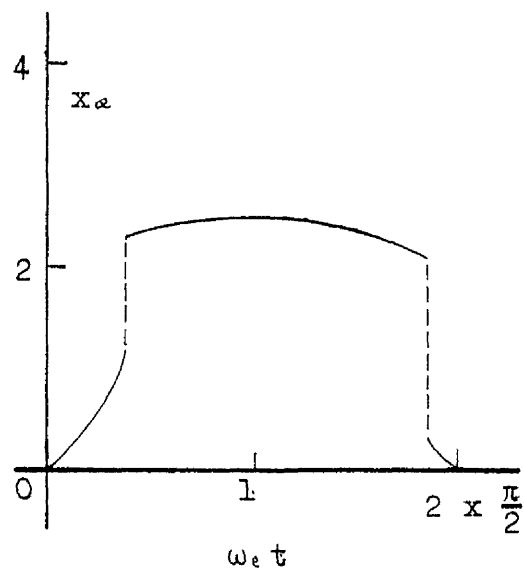
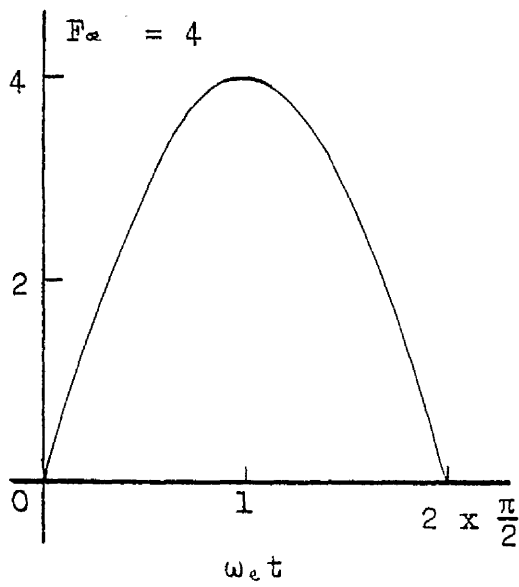
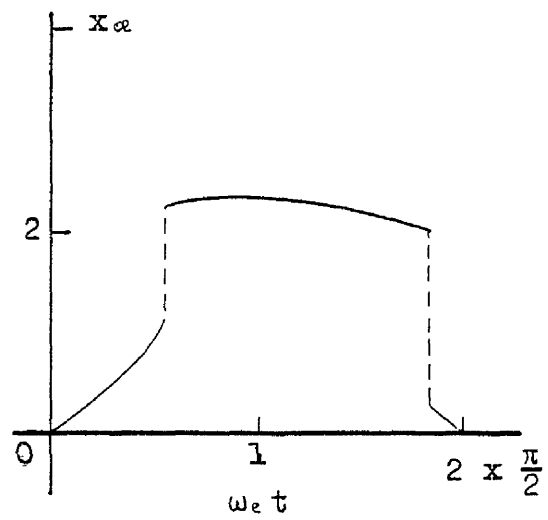
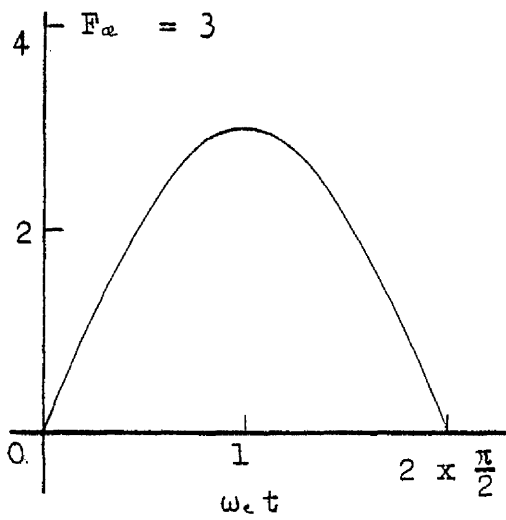
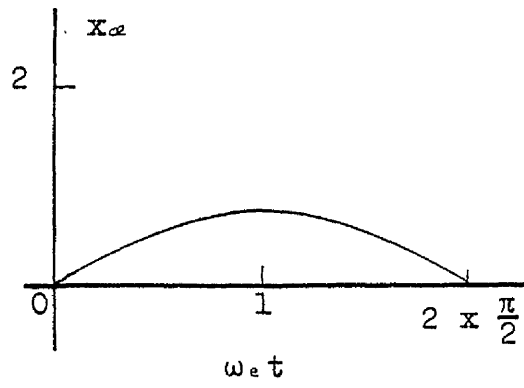
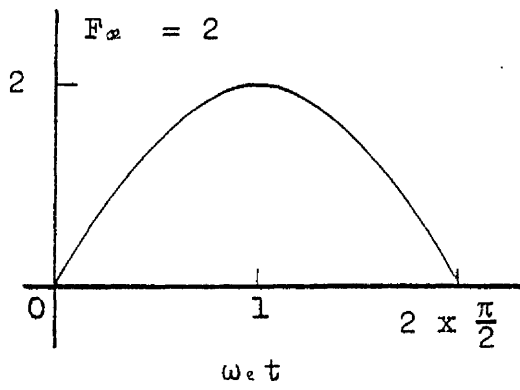


Figure A3-3

APPENDIX B

B.1. Notes on the Equivalent Linearization Technique

Consider the nonlinear system

$$\ddot{x} + b\dot{x} + g(x) = F(t) \quad (\text{B.1-1})$$

Where $F(t)$ is white noise Gaussian process. The solution of the corresponding Fokker - Planck equation (Section 2.1) results in the following stationary probability distribution.

$$P_s(x, \dot{x}) = c \exp\left\{-\frac{b\dot{x}^2}{S_0} - G(x)\right\} \quad (\text{B.1-3})$$

where

$$G(x) = \frac{2b}{S_0} \int_0^x g(\eta) d\eta \quad (\text{B.1-3})$$

and S_0 the intensity of the white noise excitation. Then

$$R_{xx}(\tau) = -\frac{\partial^2 R_{xx}(\tau)}{\partial \tau^2} = -\int_{-\infty}^{\infty} \int_{-\infty}^{\infty} [2c\dot{x} + g(x)] P_s(x, \dot{x}) P_{\tau}(x, \dot{x}, t) dx d\dot{x} \quad t \geq 0$$

where $P_{\tau}(x, \dot{x}, t)$ = the transitional probability distribution and $P_{\tau}(x, \dot{x}, 0) = \delta(x - x_0, \dot{x} - \dot{x}_0)$

$$\frac{\partial^2 R_{xx}(\tau)}{\partial \tau^2} = -\int_{-\infty}^{\infty} \int_{-\infty}^{\infty} xg(x) P_s(x, \dot{x}) dx d\dot{x} = -R_{\dot{x}\dot{x}}(0) \quad (\text{B.1-4})$$

since $P_s(x, \dot{x})$ is odd symmetric in \dot{x}

but

$$R_{\dot{x}\dot{x}}(0) = -\int_{-\infty}^{\infty} \int_{-\infty}^{\infty} \dot{x}^2 P_s(x, \dot{x}) dx d\dot{x} = \frac{S_0}{2b} \quad (\text{B.1-5})$$

for the nonlinear system. Also equation (B.1-4)

$$R_{\dot{x}\dot{x}}(0) = E(xg(x))$$

but $\omega_e^2 = \frac{E(xg(x))}{E(x^2)}$ (see Section 2.2 (equation 2-22)) (B.1-6)

therefore

$$\omega_e^2 = \frac{S_0}{2b E(x^2)}$$

For the equivalent linear system (equation (2-18)) Section 2.2)

$$\ddot{x}_e + b\dot{x}_e + \omega_e^2 x_e = F(t) \quad (\text{B.1-7})$$

$$E(\dot{x}_1^2) = \frac{S_0}{2b\omega_c^2} = \frac{S_0 2b E(\dot{x})}{2b S_0} = E(\dot{x}^2) \quad (\text{B.1-8})$$

Which proves that the equivalent linear system have the same mean square response displacement as the nonlinear system. The same is also true for the response velocity of the two systems.

The MacLaurin series expansion of the autocorrelation function is

$$R_{xx}(\tau) = R(0^+) + R'(0^+) \tau + \frac{1}{2!} R''(0^+) \tau^2 + \frac{1}{3!} R'''(0^+) \tau^3 + \dots \quad \tau \geq 0$$

It was proved above that the first term is the same for both the nonlinear system and the equivalent linear. Further for the equivalent linear system.

$$R'(0^+) = 0, \quad R''(0^+) = -\omega_c^2 R(0), \quad R'''(0^+) = b \omega_c^2 R(0)$$

for the nonlinear system

$$R'(0^+) = \int_{-\infty}^{\infty} \int_{-\infty}^{\infty} \dot{x} \dot{x} P_s(x, \dot{x}) dx d\dot{x} = 0$$

$$\frac{R''(0^+)}{R(0)} = -\frac{1}{\sigma_x^2} \int_{-\infty}^{\infty} \int_{-\infty}^{\infty} x g(x) P_s(x, \dot{x}) dx d\dot{x} = -\omega_c^2$$

from equation (B.1-4) and (B.1-6)

$$\text{and} \quad \frac{R'''(0^+)}{R(0)} = \frac{b}{\sigma_x^2} \int_{-\infty}^{\infty} \int_{-\infty}^{\infty} x g(x) P_s(x, \dot{x}) dx d\dot{x} = b \omega_c^2$$

where

$$R'''(\tau) = b \int_{-\infty}^{\infty} \int_{-\infty}^{\infty} \left[b\dot{x} + g(x) - \frac{\dot{x}}{b} \frac{\partial g(x)}{\partial x} \right] P_s(x, \dot{x}) P_{\tau}(x, \dot{x}, t) dx d\dot{x}$$

but $\tau = 0$, P_s is odd symmetric in \dot{x} and $P_{\tau}(x, \dot{x}, 0) = x$

$$\text{therefore} \quad R'''(0) = b \int_{-\infty}^{\infty} \int_{-\infty}^{\infty} x g(x) P_s(x, \dot{x}) dx d\dot{x}$$

$$\text{therefore} \quad R'''(0) = -b R''(0)$$

Hence the MacLaurin series expansion of the autocorrelation of the two systems is identical for the first four terms.

B.2. Perturbation Analysis

The perturbation approach is well developed in the study of deterministic nonlinear problems when the nonlinearity is considered small. For nonlinear random differential equations, the same technique can be applied under certain restrictions.

Consider again the single degree of freedom nonlinear system whose response $x(t)$ is related to an excitation $F(t)$ by the differential equation

$$\ddot{x} + b\dot{x} + \omega_n^2(x + \epsilon g(x)) = F(t) \quad (B.2-1)$$

where $(x + \epsilon g(x))$ is the nonlinear restoring function. The total restoring force has been separated into a linear contribution plus a nonlinear part. The shape of the nonlinearity is described by the function $g(x)$ and the relative magnitude is indicated by the parameter ϵ . When $\epsilon = 0$, the oscillator is linear. The perturbation method is based on a series expansion in powers of ϵ and is only expected to be valid for motions in which the nonlinear part of the restoring force remains small in comparison with the linear part. The precise sense of the word small is seldom specified in most applications of the perturbation method. The basic step in the perturbation method is to assume that the solution to equation (B.2-1) permits an expansion in powers of ϵ

$$x = x_0(t) + \epsilon x_1(t) + \epsilon^2 x_2(t) + \dots \quad (B.2-2)$$

This expansion is assumed to satisfy equation (B.2-1) identically in ϵ . We therefore insert equation (B.2-2) into equation (B.2-1) and collect terms having the same power of ϵ .

$$\begin{aligned} [\ddot{x}_0 + b\dot{x}_0 + \omega_n^2 x_0 - F(t)] + \epsilon [\ddot{x}_1 + b\dot{x}_1 + \omega_n^2 x_1 + \omega_n^2 g(x_0)] + \\ + \epsilon^2 [\ddot{x}_2 + b\dot{x}_2 + \omega_n^2 x_2 + \omega_n^2 x_1 g(x_0)] + \dots = 0 \end{aligned} \quad (B.2-3)$$

If equation (B.2-3) is to be satisfied identically in ϵ , each square bracket must separate by vanish. This provides a chain of linear problems which $x_{r+1}(t)$ may be considered as a linear response to an excitation that is nonlinear function of the previously determined $x_r(t)$. The function $x_0(t)$ that

makes the first bracket in equation (B.2-3) vanish can be represented by the convolution integral

$$x_0(t) = \int_0^{\infty} f(t-\tau) h(\tau) d\tau \quad (\text{B.2-4})$$

where $h(\tau)$ is the response function to a unit impulse

$$h(\tau) = (\omega_n^2 - b^2/4)^{-1/2} \exp \left\{ -b\tau/2 \right\} \sin (\omega_n^2 - b^2/4)^{1/2} \tau \quad (\text{B.2-5})$$

In the same way, the function $x_1(t)$, which causes the second bracket in equation (B.2-3) to vanish, can be represented as

$$x_1(t) = -\omega_n^2 \int_0^{\infty} g[x(t-\tau)] h(\tau) d\tau \quad (\text{B.2-6})$$

and thus the entire chain of functions $x_v(t)$ needed for equation (B.2-2) can be obtained, at least in principle. In practice, the integrations required for $v \geq 2$ usually become intractable and the approximation $(x_0 + \epsilon x_1)$ is used.

For the case under study the perturbation technique has very little to offer and which is worth comparing with the results of the numerical technique since in practice it restricts its finding for very small departures from the linear range. Further the order ϵ^2 solution [24] leads to a very important conclusion; namely that the nonlinearity parameter, ϵ must be small compared to the damping loss factor b in order for the perturbation solution to be accurate or

$$\epsilon \frac{E(x_0^2)}{b} \ll 1$$

B.3. The Heuristic Approach

The underlying idea of this approach (named thus by Crandall [23]), is that provided the system damping is light, the stationary nonlinear response can be viewed as a sequence of free undamped vibration 'cycles' in which there is a slow random fluctuation of amplitude and phase. This concept provides a useful viewpoint for describing the statistical response of linear systems to Gaussian excitation. When extended to nonlinear systems the same picture can be used and more over correct quantitative results can be obtained for small nonlinearities, provided the deterministic variation of period with amplitude in free vibrations is accounted for. It should be noted that the procedure is devoid of mathematical rigor. Furthermore it is not especially advantageous from the stand point of simplicity of calculation and the range of nonlinearities with which it is capable of dealing is the same as that of the perturbation technique. In fact the expressions derived for the mean square response and autocorrelation function are identical.

For the nonlinear system

$$\ddot{x} + b\dot{x} + \omega_n^2(x + \epsilon g(x)) = F(t) \quad (B.3-1)$$

where $g(x) = \sum_{\eta=1}^{\infty} g_{\eta} x^{\eta}$ and $\epsilon > 0$, the stationary response to white Gaussian noise is such that at a fixed time the velocity function remains a Gaussian random variable with variance σ_v^2 , while the distribution of $x(t)$ becomes a non Gaussian random variable with unknown variance σ_x^2 . The peak velocity V retains its Rayleigh distribution while the distribution of peak displacement X becomes non Rayleigh. Because of the invariance with respect to ϵ of the distribution of V one can employ V as the fundamental measure of cycle amplitude. The expressions that can be derived thus are as follows [23]. For the expected frequency response

$$E(\omega_r) = \omega_n \left[1 + \frac{\epsilon}{\sigma_v^2} \sum_{\eta=1}^{\infty} \frac{g_{\eta}}{\sqrt{\pi}} \left(\frac{\sqrt{2} \sigma_v}{\eta+1} \right)^{\eta+1} \Gamma\left(\frac{\eta+2}{2}\right) \right]$$

where $\sigma_v^2 = \frac{\pi S}{b \omega_n}$ and S is the excitation intensity. For the mean square response

$$E(x^2) = \sigma_v^2 - \epsilon A$$

where

$$A = \sum_{\eta=0}^{\infty} \frac{g_{\eta}}{\sqrt{\pi}} (\sqrt{2} \sigma_0)^{\eta+1} \Gamma\left(\frac{\eta+2}{2}\right)$$

Indeed for the Duffing equation

$$E(x^2) = \sigma_0^2 - 3\epsilon\sigma_0^4$$

a result identical to perturbation and valid only for $\epsilon\sigma_0^4 \ll 1$.
For the autocorrelation function

$$R_{xx}(\tau) = \sigma_0^2 [\rho_0(\tau) - \epsilon A [\rho_0(\tau) + \rho_1(\tau)]]$$

where

$$\rho_0(\tau) = e^{-1/2b\tau} \left(\cos p\tau + \frac{b}{2p} \sin p\tau \right)$$

$$\rho_1(\tau) = \frac{\omega_n^2}{2p^2} e^{-1/2b\tau} \left[\left(p\tau + \frac{b}{2p} \right) \sin p\tau - \frac{1}{2} b\tau \cos p\tau \right]$$

$$p^2 = \omega_n^2 - b^2/4$$

Manning [24] has introduced some refinements in the above method by using the exact expressions for the envelope probability distribution for the free oscillations of displacement instead of velocity and obtained the spectrum of the response to white noise by decomposing each cycle of non linear vibration (or what is assumed to be the response) into its Fourier components. However the limitations of the approach remained the same. i.e. light damping, small non linearity.

APPENDIX C

C.1. Theory of Numerical Integration Methods

It must firstly be stated that the theory of Numerical Integration Methods is very complex. While the fundamental ideas behind the integration techniques are simple, their practical application is indeed very complicated. This is especially true of such factors as error estimation, predictor correctors, and similar parameters. Considerable research has been carried out to develop these techniques and several computer 'packages' are currently available. The specific details of the theory on which these packages are based need not concern the vibration analyst. It will be sufficient to have a general grasp of the principles involved so that prudent choice of the user-specified variables in such packages may be made.

To this end a brief description of the theory will be given here and will be of a sufficiently general nature to be applicable to a wide range of integration packages.

As stated above, it is required to solve a set of differential equations. These equations are generally of the second order, but to avoid needless complication a single equation of the first order will serve to illustrate the techniques for the time being. Consider the initial value problem

$$y' = f(x,y), y(x_0) = y_0 \quad (C.1-1)$$

The first step is to find the value y_1 which is the solution of the differential equation for $x = x_0 + h$, where h is some fixed value known as the step length (size). Recall Taylor's series to estimate y_1 ,

$$y(x+h) = y(x) + hy'(x) + \frac{h^2}{2!} y''(x) + \dots \quad (C.1-2)$$

writing $y' = f(x,y) = f:-$

$$y(x+h) = y(x) + hf + \frac{h^2}{2!} f' + \frac{h^3}{3!} f'' + \dots \quad (C.1-3)$$

where f, f', f'' are evaluated at $(x, y(x))$.

If h is small, terms in $h^2, h^3 \dots$ etc. may be neglected giving the approximation:-

$$y(x+h) = y(x) + hf \quad (C.1-4)$$

The computation may now proceed:-

$$y(x_0+h) = y_1 = y_0 + hf(x_0, y_0) \quad (C.1-5)$$

$$y(x_0+2h) = y_2 = y_1 + hf(x+h, y_1) \quad \text{etc.}$$

$$y(x_0+nh) = y_n = y_{n-1} + hf(x_0+(n-1)h, y_{n-1})$$

Figure (C.1-1) illustrates this technique graphically. In an attempt to follow the curve from the point (x_0, y_0) a distance h , in the x direction is moved at gradient $f(x_0, y_0)$. This defines the new point (x_0+h, y_1) . A further distance h is moved with gradient $f(x_0+h, y_1)$ to the point (x_0+2h, y_2) . This process is repeated throughout the range of integration. It can be seen that as the integration proceeds the estimated points gradually move away from the curve. For convenience, the step length is kept constant but this not need be the case. This very simple process is the Euler method it is a first order method since only terms up to the first power of h are considered in the Taylor's series. The omission of orders of h greater than or equal to 2, causes a truncation error of order h . Further error is introduced since the estimation of $y(x_n)$ is based upon the value $y(x_{n-1})$ which is itself an estimate. As illustrated graphically these errors can mount up as the integration proceeds.

However a much improved solution can be obtained by a simple modification. This is the adaptation of a correction procedure. Refer to Figure (C.1-2). As in the previous method the point y_1 is calculated. The derivative at this point is determined i.e. $f(x_0+h, y_1)$. The average of the derivatives at y_0 and y_1 is found and a new approximation $y_1^{(2)}$ is obtained i.e.

$$y_1^{(2)} = y_0 + \frac{h}{2}(f(x_0, y_0) + f(x_0+h, y_1)) \quad (C.1-6)$$

Further approximations y_1 can be made by using the current value y_1 i.e.

$$y_1^{(3)} = y_0 + \frac{h}{2}(f(x_0, y_0) + f(x_0+h, y_1^{(2)})) \quad (C.1-7)$$

After sufficient corrections have been made, the final value of y_1 can be used as a starting point to obtain the point y_2 . Similarly, corrective procedures can now be applied to y_1 . This process is repeated over the entire interval of integration. This is known as the Euler-trapezoidal method. It provides a simple example of a predictor corrector formula. The predictor-corrector methods employed in the integration packages are based upon the same principle but information on several previous values are used to obtain an increase in accuracy.

The Euler method would not be used in practice, in view of its simplicity and resultant inaccuracy. More refined versions based on the same principles are however, currently in use. The other class of methods in widespread use is the Runge - Kutta type. Many versions of this type exist but are all based on estimates of the derivative, not only at the ends of the interval h , but also at intermediate points. A further feature of these methods is that the calculation uses only the values at the initial point and previous estimates are neither used nor stored. A typical example of a Runge-Kutta method will be outlined to indicate the method of computation. The example is a fourth order version. The step size will be assumed constant but, again need not be so - in a variable step version the length of the step would be determined in accordance with some error criterion. Use of this method requires four quantities to be calculated at each integration interval namely:-

$$\left. \begin{aligned} a_n &= h f(x_n, y_n) \\ b_n &= h f(x_n + \frac{h}{2}, y + \frac{a_n}{2}) \\ c_n &= h f(x_n + \frac{h}{2}, y_n + \frac{b_n}{2}) \\ d_n &= h f(x_n + h, y_n + c_n) \end{aligned} \right\} \quad (C.1-8)$$

The value y_{n+1} is given by

$$y_{n+1} = y_n + \frac{1}{6}(a_n + 2b_n + 2c_n + d_n)$$

Since $y' = f(x, y) = \Delta y/h$ it can be seen that a_n, b_n, c_n, d_n are estimates of the increments in y at the left hand, twice

at the centre, and at the right hand of the integration interval. In calculating y_{n+1} , the previous estimates a_n , b_n , c_n , d_n , are available and a weighted-average value of these increments in y provide the estimate of the value y_{n+1} . Most dynamic systems can be represented by sets of second order differential equations of the form

$$y'' = f(x, y, y') \quad (C.1-9)$$

The derivative of Taylor's series is required

$$y'(x+h) = y'(x) + hy''(x) + \frac{h^2}{2!} y''(x) \dots$$

The Runge - Kutta method when applied to second order equations requires computation of the following variables at each step

$$a_n = \frac{h}{2} f(x_n, y_n, y'_n)$$

noting that y_n , y'_n are evaluated up to the term in h^4 in the relevant Taylor expansion.

$$b_n = \frac{h}{2} f(x_n + \frac{h}{2}, y_n + a_n, y'_n + a_n)$$

where $a_n = \frac{h}{2} (y'_n + \frac{a_n}{2})$

$$c_n = \frac{h}{2} f(x_n + \frac{h}{2}, y_n + a_n, y'_n + b_n)$$

$$d_n = \frac{h}{2} f(x_n + h, y_n + \beta_n, y'_n + 2c_n)$$

where $\beta_n = h(y'_n + c_n)$.

The new value y_{n+1} is now given by

$$y_{n+1} = y_n + h(y'_n + R_n)$$

where

$$R_n = \frac{1}{3} (a_n + b_n + c_n)$$

and

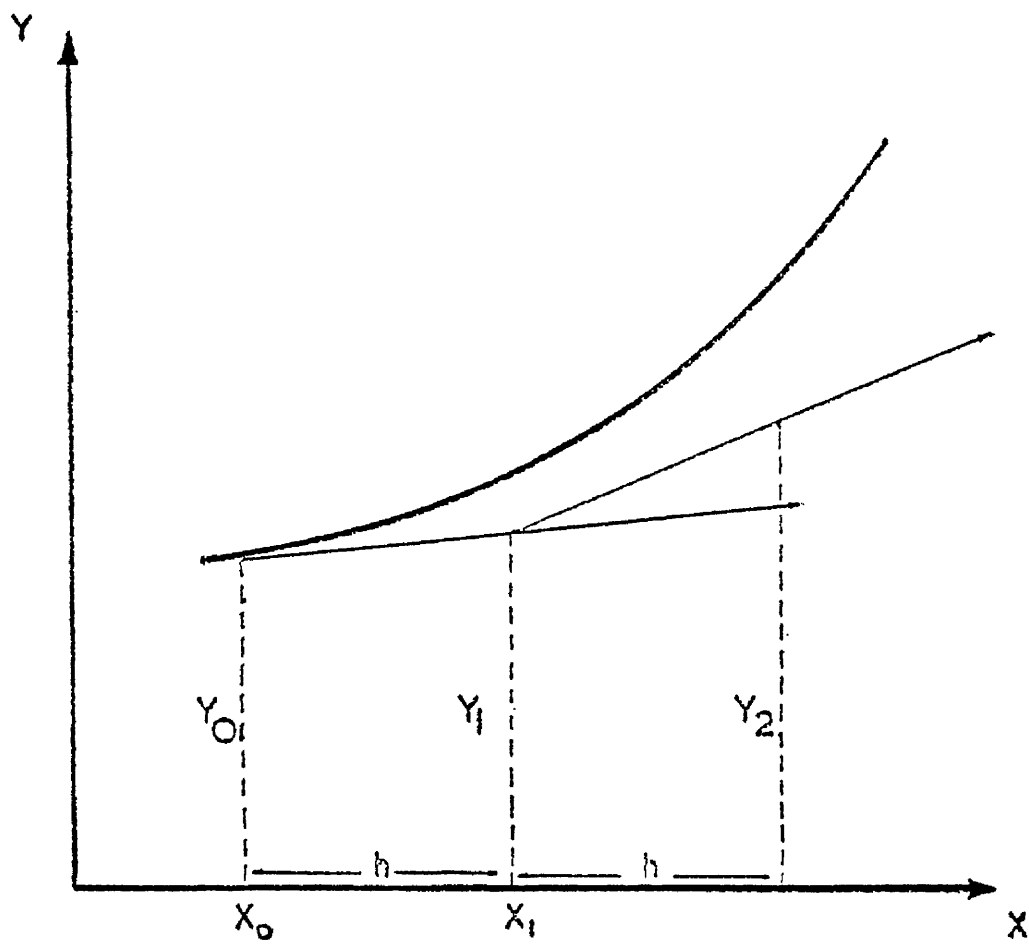
$$y'_{n+1} = y'_n + R_n^*$$

where

$$R_n^* = \frac{1}{3} (a_n + 2b_n + 2c_n + d_n)$$

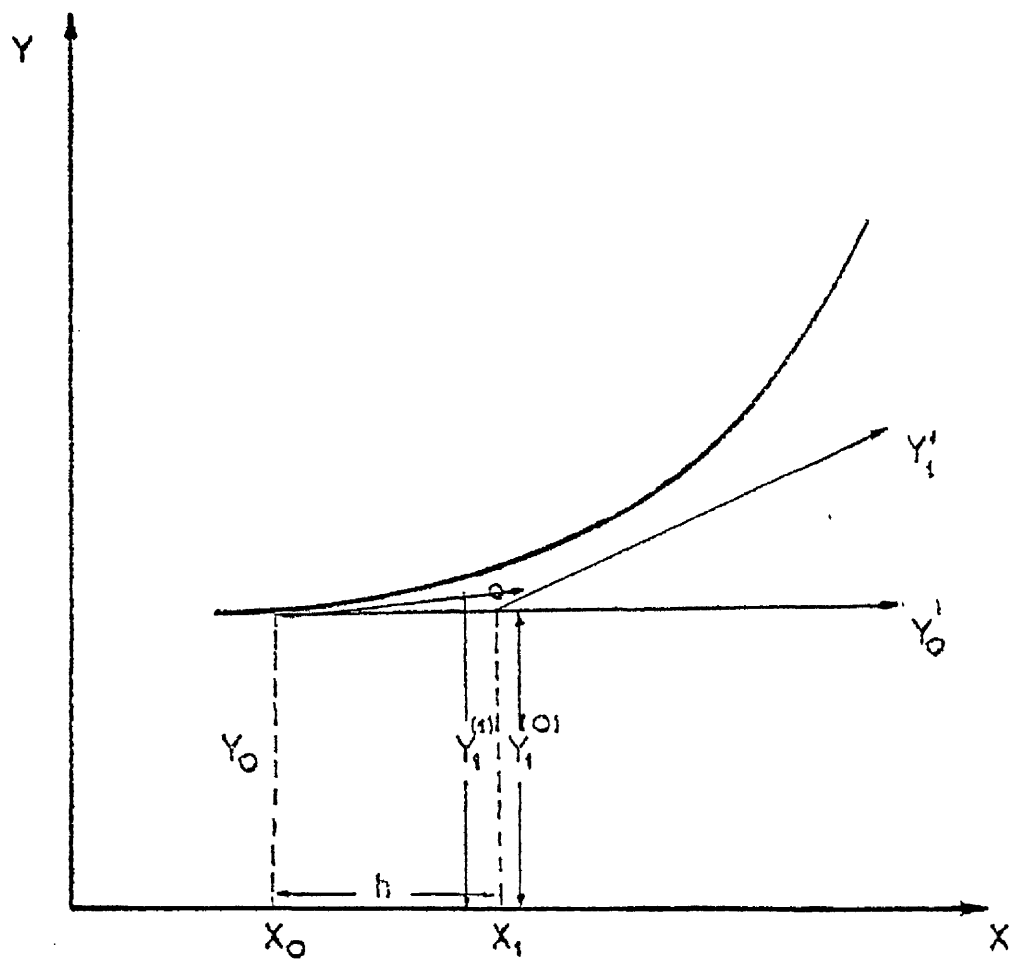
The next step in the routine will require y'_{n+1} . Repetition of the above sequence is performed throughout the interval of integration. In the methods described above, the step length h has been assumed constant. The facility of a variable step length is offered by many routines and will be mentioned here. The operation of these methods is as follows. A value of h is chosen within the program — usually as some fraction of a user-specified parameter and the first step executed. The value of the step length is reduced and the step re-executed. If the difference between two computed values satisfies the error criterion, the solution is accepted. If it is outwith the specified error, h is further reduced until the error criterion is satisfied. The specified error may be a relative or an absolute error and in many packages is specified either by the user or by default. Integration routines vary considerably in the type of error criterion adapted. It must be emphasised that while the simplest integration method will certainly give only approximate solutions, very sophisticated routines need not give highly accurate estimates. It is a fact that in striving for a high degree of accuracy, problems of stability can arise: i.e. the errors become greatly magnified as the computational sequence progresses until the routine breaks down. It is practically impossible to state with any certainty, that a particular routine will give good results with a particular type of problem, without prior testing. Clearly great care must be taken when using numerical integration methods — this cannot be stressed too highly — since the margin between a very good estimation and a very poor one can be slight.

The above outline of the theory of integration methods is, of necessity, brief. However, it should be sufficient for most applications when considered in conjunction with the information provided in package user-manual.



EULER'S METHOD

Figure C1-2



IMPROVED EULER METHOD

Figure C1-3

C.2. Excitation

a) Stationarity of the Signal

The excitation is defined by *

$$\begin{aligned} X(t) &= \sum_{n=1}^K c_n \cos(\omega_n t - \varphi_n) \\ &= \sum_{n=1}^K c_n (\cos \varphi_n \cos(\omega_n t) + \sin \varphi_n \sin(\omega_n t)) \end{aligned} \quad (C.2-1)$$

Where the frequencies ω_n are distributed densely in the interval $(0, \omega_m)$, the phase φ_n are uniformly distributed between $(0, 2\pi)$ and the amplitudes c_n are such that any small interval of frequency $d\omega$ satisfies.

$$\sum_{\omega_n \in \omega} \frac{1}{2} c_n^2 = S(\omega) d\omega \quad (C.2-2)$$

It will be shown that $X(t)$ is stationary in the wide sense ([7] p.304) with zero mean and find its autocorrelation. Equation (C.2-1) can be written

$$X(t) = \sum_{n=1}^K (a_n \cos \omega_n t + b_n \sin \omega_n t) \quad (C.2-3)$$

where

$$a_n = c_n \cos \varphi_n$$

$$b_n = c_n \sin \varphi_n$$

(for our input $c_n = \text{const} = 1$)

$$\begin{aligned} \langle X(t) \rangle &= \langle \sum_{n=1}^K (a_n \cos \omega_n t + b_n \sin \omega_n t) \rangle \\ &= \langle \sum g(a_n, b_n) \rangle \end{aligned}$$

additivity property of $\langle \rangle$.

$$\langle X(t) \rangle = \sum \langle g_n \rangle$$

but $g(a_n, b_n)$ is the sum of two random variables

$$\text{therefore } \langle g(a_n, b_n) \rangle = \langle a_n \cos \omega_n t \rangle + \langle b_n \sin \omega_n t \rangle \quad (C.2-4)$$

since $a_n, \cos \omega_n t$ are independent this average is equal to zero for $\langle a_n \rangle = \langle b_n \rangle = 0$

* Note that for the sake of convenience in notation the excitation is denoted as $X(t)$ not as $F(t)$.

$$R(t_1, t_2) = \left\langle \left[\sum (a_n \cos \omega_n t_1 + b_n \sin \omega_n t_1) \right] \left[\sum (a_n \cos \omega_n t_2 + b_n \sin \omega_n t_2) \right] \right\rangle$$

if $\langle a_n b_n \rangle = 0$ all cross terms are eliminated (C.2-5)

hence $R(t_1, t_2) = \sum \langle a_n^2 (\cos \omega_n t_1 \cos \omega_n t_2) + b_n^2 (\sin \omega_n t_1 \sin \omega_n t_2) \rangle$

$$= \sum \left\langle \frac{a_n^2}{2} [\cos \omega_n (t_1 - t_2) + \cos \omega_n (t_1 + t_2)] + \frac{b_n^2}{2} [\cos \omega_n (t_1 - t_2) - \cos \omega_n (t_1 + t_2)] \right\rangle$$

if $\langle b_n^2 \rangle = \langle a_n^2 \rangle = \sigma_n^2$

therefore $R(t_1, t_2) = \sum \langle a_n^2 \rangle \cos \omega_n \tau = \sum \sigma_n^2 \cos \omega_n \tau = R(\tau)$

where $\tau = t_1 - t_2$ (C.2-6)

Hence necessary conditions for $X(t)$ to be stationary in the wide sense with zero mean and autocorrelation

$$R(\tau) = \sum \sigma_n^2 \cos \omega_n \tau$$

is that the random variables a_n, b_n both have

- 1) zero mean $\langle a_n \rangle = \langle b_n \rangle = 0$
- 2) are uncorrelated $\langle a_n b_n \rangle = 0$
- 3) $\langle a_n^2 \rangle = \langle b_n^2 \rangle = \sigma_n^2$

These conditions are satisfied by our particular a_n, b_n .

$$\langle a_n b_n \rangle = \langle \sin \varphi_n \cos \varphi_n \rangle$$

and since the probability density $f(\varphi) = 1/2\pi$

$$g(\varphi) = \sin \varphi \cos \varphi = a b$$

$$\langle a_n b_n \rangle = \int_0^{2\pi} \sin \varphi \cos \varphi \frac{1}{2\pi} d\varphi = \frac{1}{2\pi} \left[\frac{\sin 2\varphi}{2} \right]_0^{2\pi} = 0$$

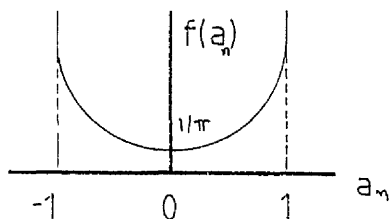
also

$$\langle a_n \rangle = \langle b_n \rangle = 0 \quad \text{and} \quad \langle a_n^2 \rangle = \langle b_n^2 \rangle = 1/2$$

Note a_n, b_n , are uncorrelated but not independent since

$$a_n = f(b_n), \quad a_n = \sqrt{1-b_n^2}$$

The probability density function of $a_n = f(a_n) = \frac{1}{\pi} \frac{1}{\sqrt{1-a_n^2}}$



$$\text{and } f(b_n) = \frac{1}{\pi} \frac{1}{\sqrt{1-b_n^2}}$$

b) The Central Limit Theorem

Consider a sequence x_1, \dots, x_n, \dots of independent random variables with respective densities $f_i(x)$. It is known from the law of large numbers that the variance of their mean $\bar{x} = (x_1 + x_2 + \dots + x_n)/K$ is small for large K . Hence (from the Tchebycheff inequality) the density $f_{\bar{x}}(\bar{x})$ is concentrated near its mean. However the law says nothing about the shape of this density ($f_{\bar{x}}(\bar{x})$). It turns out that as K increases $f_{\bar{x}}(\bar{x})$ tends to a normal curve regardless of the shape of the densities $f_i(x)$ ([7] p.266) provided that $f_i(x)$ has finite area, mean and variance. Hence what ever the probability of

$$x_n(t) = a_n \cos \omega_n t + b_n \sin \omega_n t \quad (C.2-7)$$

its mean over K values

$$\bar{x} = \sum_{n=1}^K \frac{x_n(t)}{K}$$

will have a Gaussian distribution provided K is large enough and density $f_i(x)$ has finite area, mean and variance.

The input signal equation (C.2-1) may be thought of as such an average value multiplied by a constant i.e.

$$X(t) = \sum_{n=1}^K \frac{x_n(t)}{K} \cdot K$$

It is also true that some averages approach the Gaussian distribution faster than others, depending on their original distribution e.g. [7] p.268.

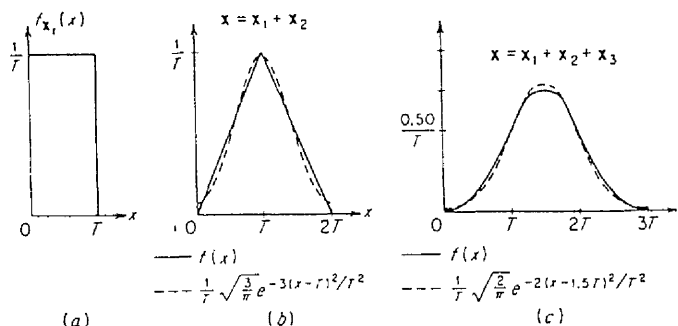


Figure C.2-1

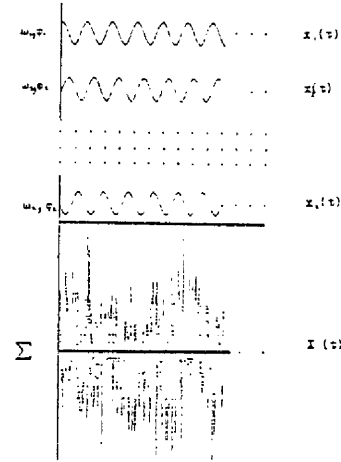
An attempt will be made to show that this is the case with the excitation $X(t)$

$$X(t) = \sum_{n=1}^K x_n(t) \quad (C.2-8)$$

$$x_n(t) = \cos(\omega_n t + \varphi_n) \quad (C.2-8)$$

If we select randomly some $x_i(t)$ from the sum then $x_i(t)$ can be regarded as a function of a random variable z_i which is the sum of the random variables φ_i, ω_i Figure (C.2-2). This way we can regard ω_i as a random variable uniformly distributed between 0, and $\omega_k = 2\psi\pi$ say.

Figure C.2-2



Hence $z_i = \varphi_i + \omega_i$, φ_i, ω_i are independent therefore

density
$$f_z(z) = \int_0^\infty f_\omega(\omega) f_\varphi(z-\omega) d\omega$$

where

$$f_\varphi(\varphi) = \begin{cases} 0 & \varphi < 0 \text{ or } \varphi > 2\pi \\ \frac{1}{\pi} & 0 \leq \varphi \leq 2\pi \end{cases}$$

$$f_\omega(\omega) = \begin{cases} 0 & \omega < 0 \text{ or } \omega > 2\psi\pi \\ \frac{1}{2\psi\pi} & 0 \leq \omega \leq 2\psi\pi \end{cases}$$

hence
$$\begin{aligned} f_z(z) &= \int_0^z \frac{1}{4\psi\pi^2} dz = z/4\psi\pi^2, \quad 0 < z < 2\pi \\ &= \int_0^{2\pi} \frac{1}{4\psi\pi^2} dz = \frac{1}{2\psi\pi}, \quad 2\pi \leq z \leq 2\psi\pi \\ &= \int_{z-2\psi\pi}^{2\psi\pi} \frac{1}{4\psi\pi^2} dz = \frac{2\pi(\psi+1)-z}{4\psi\pi^2}, \quad 2\psi\pi < z < 2\pi(\psi+1) \\ &= 0 \quad z \leq 0 \text{ or } z \geq 2\pi(\psi+1) \end{aligned}$$

$$\langle z \rangle = \langle \varphi \rangle + \langle \omega \rangle, \langle z^2 \rangle = ((2\pi)^2 + (2\psi\pi)^2)/3 - 4\psi\pi^2/2$$

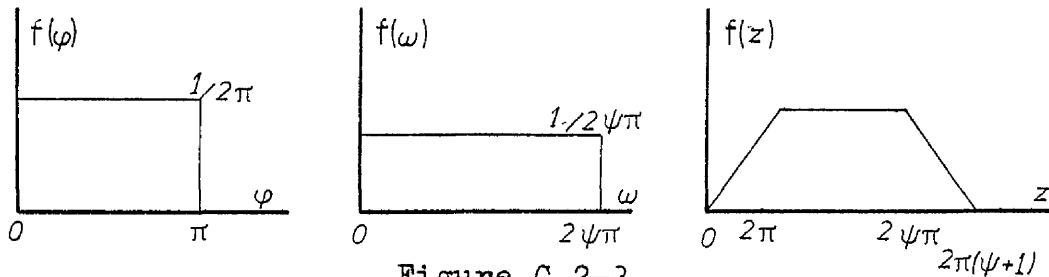


Figure C.2-3

hence $f_z(z)$ can be described in general as

$$f_z(z) \begin{cases} az & 0 \leq z \leq 2\pi \\ b & 2\pi < z \leq 2\psi\pi \\ -az + \xi & 2\psi\pi \leq z \leq 2(\psi+1)\pi \end{cases} \quad (C.2-10)$$

$x_n(t)$ is a function of the random variable z (since the process is stationary t can be ignored)

$$x_n = g(z_n) = \cos(z_n) \quad (C.2-11)$$

$$\text{density} \quad f_{x_n}(x_n) = f_g(g(z)) = \sum_n f_z(z_n)/g'(z_n)$$

where z_n is the solution to equation (C.2-11)

$$g'(z) = -\sin z = -\sqrt{1-x_n^2}$$

$$\text{therefore} \quad f_{x_n}(x_n) = \frac{-1}{\sqrt{1-x_n^2}} \sum_n f_{z_n}(z_n)$$

Equation (C.2-11) has two solutions for every 2π interval of z say z_1, z_2 for the interval $0 < z < 2\pi$ and $z_1 = 2\pi - z_2$, $z_1 = \cos^{-1} x_n$ for the interval $2\psi\pi < z < 2(\psi+1)\pi$ there exist an other two solutions say z_3, z_4 , their density equal to $f_z(z_1), f_z(z_2)$ respectively. Finally in the interval $2\pi < z < 2\psi\pi$ we have $(\psi-1)$ number of solutions.

$$\begin{aligned} f_{x_n}(x_n) &= \frac{-1}{\sqrt{1-x_n^2}} [(\psi-1)b + 2az_1 + 2az_2] \\ &= -[(\psi-1)b + 2a + (2\pi - z_1)2a] / \sqrt{1-x_n^2} \\ &= [(\psi-1)b + 4a\pi] / \sqrt{1-x_n^2} \end{aligned}$$

hence

$$\begin{aligned}\langle x_n \rangle &= \int_{-\infty}^{\infty} x_n f_{x_n}(x_n) dx_n = 0 \\ \langle x_n^2 \rangle &= \int_{-\infty}^{\infty} x_n^2 f_{x_n}(x_n) dx_n = \pi/2 \\ \text{area} &= \int_{-\infty}^{\infty} f_{x_n}(x_n) dx_n = 1\end{aligned}\quad (\text{C.2-12})$$

The shape of $f_{x_n}(x_n)$ is sketched in Figure (C.2-4)

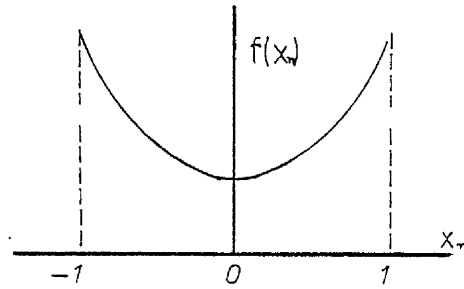


Figure C.2-4

Although the shape is far from normal, the conditions for the central limit theorem to apply are satisfied equation (C.2-12)

Proceeding as above we can select two x_i 's and form a new random variable (random selection)

$$u_i = x_n + x_m$$

the pd $f(u)$ is given by the convolution integral

$$f(u) = \int_{-\infty}^{\infty} f_{x_n}(x_n) f_{x_m}(u-x_n) dx_n \quad (\text{C.2-13})$$

for the ease of calculation we shall put

$$f(x_n) = \frac{k}{\sqrt{1-x_n^2}}, \quad f(x_m) = \frac{k}{\sqrt{1-x_m^2}}$$

if we use, the characteristic function of these densities e.g. (C.2-13) is equivalent to

$$G_u(\omega) = \Phi_{x_n}(\omega) \Phi_{x_m}(\omega) \quad (\text{C.2-14})$$

(Note : here ω is not the random variable ω_i)

where

$$\begin{aligned}\Phi_x(\omega) &= k \int_{-\infty}^{\infty} e^{j\omega x} / \sqrt{1-x^2} dx \\ &= -kj \int_{-\infty}^{\infty} \sin \omega x / \sqrt{1-x^2} dx + k \int_{-\infty}^{\infty} \cos \omega x / \sqrt{1-x^2} dx\end{aligned}$$

hence

$$\Phi_x(\omega) = k \int_{-1}^1 \cos \omega x / \sqrt{1-x^2} dx$$

This integral results a Bessel function of the first kind
[4] .

$$\text{therefore } \Phi_x(\omega) = k(\pi/2) J_0(\omega)$$

$$\text{therefore } G_u(\omega) = (\pi^2/4) k J_0(\omega) J_0(\omega)$$

The inverse fourier transform of $G_u(\omega)$ will give us the required density of $X(t) = \sum_{n=1}^2 x_n(t)$.

Proceeding as above and using the properties of convolution one can find an exact expression for the density of $X(t) = \sum_n x_n(t)$.

If we denote the convolution integral of f, g by $f * g$ and with bars the fourier transforms, then

$$\overline{f * g * h} = \bar{f} \cdot \bar{g} \cdot \bar{h} \quad \text{etc.}$$

Now in producing the excitation signal numerically K was 340^* thus to obtain the exact probability density of the signal, a convolution of 340 characteristic functions is necessary.

Figure (C.2-5) compares the density function after 60 convolutions with the normal.

* See Figure (C.3-1) for 4096 points in time domain, $K = 2048$
 $MK = 340 \quad K/6$.

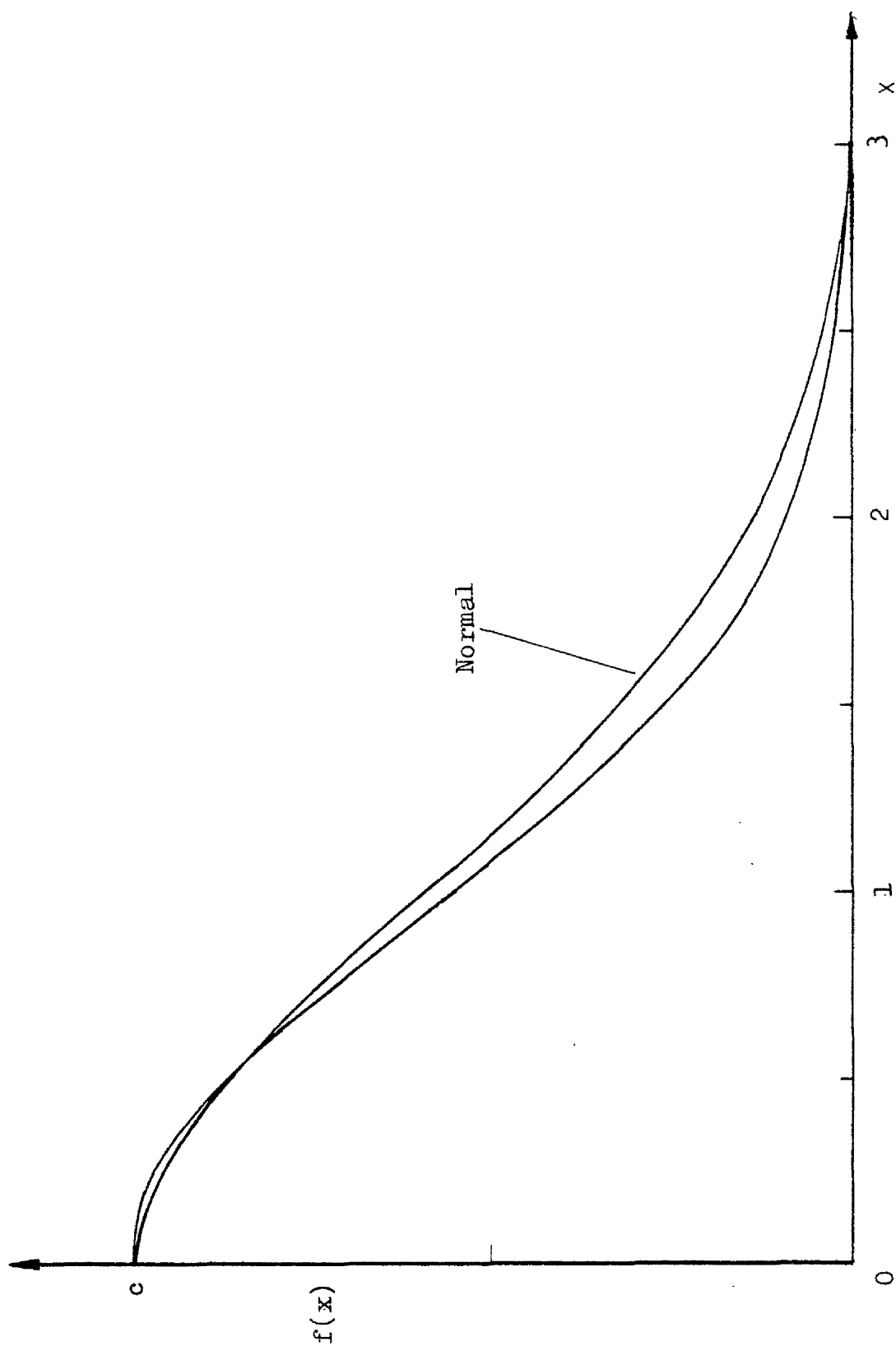


Figure C.2-5
 Probability density of $X = \sum_{60} x_n(t)$ compared with normal

C.3. Generation of the Excitation Signal

Generally speaking, if we have a large set of numbers which are assumed to be digitised from some time history, the individual values determine the probability distribution of the record, and the order in which the numbers appear defines the 'frequency composition' of the sample. If, for example, the numbers in the sample increase and then decrease periodically, the time history can be considered to be a narrow band. If, however, the numbers exhibit no periodic pattern, they will be representative of wide band random. The set however may be arranged in an infinite number of ways giving different frequency contents when each number is associated with a time co-ordinate. In particular for the input process described in Sections (3.2) and (C.2). The input signal is produced as follows.

The sine and cosine components of the signal are defined as

$$\left. \begin{aligned} A_n &= \alpha \sin(\varphi_n) \\ B_n &= \alpha \cos(\varphi_n) \end{aligned} \right\} n = 2, 3, \dots, MK$$

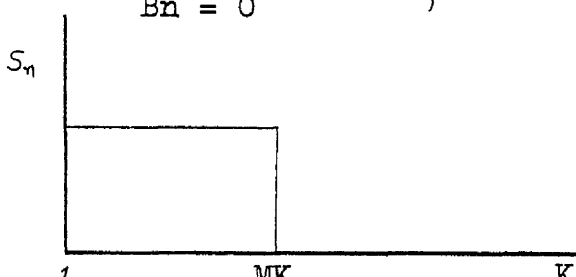
$$\left. \begin{aligned} A_n &= 0 \\ B_n &= 0 \end{aligned} \right\} n = 1, MK+1, \dots, K$$


Figure C.3-1

Where φ_n is a random angle uniformly distributed between $0 = 2\pi$. The inverse FFT of these components returns a series of numbers ($2K$) which is regarded as a digitised time history. When a time interval Δt is defined for these data the process is uniquely defined. i.e.

$$T = \Delta t \quad 2K, \quad \Delta\omega = 2\pi\Delta f$$

$$\Delta f = 1/T, \quad \omega_n = 2\pi K\Delta f, \quad \omega_{MK} = 2\pi MK\Delta f$$

$$S(\omega) = \frac{S_n T}{2\pi} = \frac{\alpha^2 T}{4\pi} = S_n \Delta\omega \quad \text{for } n\Delta\omega < \omega < (n+1)\Delta\omega \quad \text{and} \quad \sigma^2 = \frac{\alpha^2}{2} \omega_{MK}$$

It is known that the Fourier coefficient S_n at a particular frequency n is the contribution to the mean square of the signal at this frequency

$$S_n = (A_n^2 + B_n^2)/2 = [\alpha^2 \sin^2(\varphi_n) + \alpha^2 \cos^2(\varphi_n)]/2 = \alpha^2/2$$

Therefore if the data are multiplied by a constant D

$$D \quad F(t) = D \times \alpha \sum_{n=1}^{MK} \cos(\omega_n t + \varphi_n)$$

therefore

$$S_n = (D\alpha)^2/2$$

therefore

$$S_n(\omega) = D^4 \alpha^2 T/4\pi$$

therefore

$$\sigma^2 = D^2 \alpha^2 \omega_{MK}/2$$

It is obvious from the above that the same series of numbers may be used to represent signals of different frequency and energy contents but of the same probability distribution, by assigning to it different values of Δt and D . It should be noted that the number of points transformed, $2K$ must be large enough to produce dense spectral definition (small band width) and also small enough to be handled economically by a computer. This and the need for $2K$ to be equal to an even power of two for the FFT algorithm leads to values of $2K$ in the region 256-8192. At first 1024 points were chosen, but when this proved inadequate in certain circumstances it was increased to 4096. To obtain a relatively smooth spectrum and more reliable statistics forty blocks of $2K = 4096$ points were used with the phase angle continuing to be randomised between them. These are treated as forty independent events.

C.4. Listings of Simulation Programs

The complete simulation process is described in Figure(C.4-1) in the form of a flow diagram.

The excitation data are produced through the program - called INPUTUN, (the last two letters in the program name signify an unformatted program input-output) and stored in a file (usually on a demountable disc). Next the excitation data are read by program PR6UN which handles the numerical integration and stores the response in another demountable file. Program REC6ETUN accesses the response displacement and velocity data and calculates their spectra and statistical values. The spectral data are stored on line formatted this time for access by the frequency averaging program FRAV. Thus the spectral values are ready to be plotted by the appropriate program in their smoothed form.

a) The Input Program. (INPUTUN)

This program produces the input signal in the manner described in Section (C.3) One defines the spectrum of the required signal by supplying its sine and cosine components up to the cut off frequency ω_K . These we supply to an inverse FFT subroutine (supplied by NAG) with a random phase between them and which is uniformly distributed between $0 - 2\pi$ and the FFT returns the time signal. The process is repeated to produce an ensemble of M (here $M = 40$) realisations of $2K$ number of points each (here $2K = 4096$). The random phase is supplied by a NAG subroutine which produces random numbers uniformly distributed between $0 = 1$. Hence the sine and cosine components supplied to the inverse FFT (code name (C6AAF) are

$$\left. \begin{array}{l} A_n = 1 \sin(\varphi) \\ B_n = 1 \cos(\varphi) \end{array} \right\} \text{ for } n = 1, 2, 3, \dots, MK$$

$$\text{and} \quad A_n = B_n = 0 \quad \text{for} \quad MK < n \leq K$$

where $\varphi_n = 2\pi r$ and r is a random number uniformly distributed between $0 = 1$ (NAG subroutine CO5CAF). The time signals ($2K$) are stored in a file (on demountable disc) to be accessed by the numerical integration program as unformatted numbers. A flow diagram of this program is shown in Figure (C.4-2).

b) The Numerical Integration Program (PR6UN)

This program reads the data stored in the file mentioned above, one realisation at a time. Multiplies the data by a constant (to increase or decrease the energy content; see Section C.3) and using a user defined time interval and zero initial conditions, integrates the set of differential equations describing the system (subroutine FCN), according to the technique described in Section 3.1. The response data (displacement and velocity i.e. 2 x 2K points) are stored unformatted in a file and the program returns to read the next excitation record. The process is repeated until all M(= 40) excitation records are used. A flow diagram is shown in Figure (C.4-3).

c) The Response Analysis Program (REC6ETUN)

The stored response signals (2M) are read and processed by this program two at a time (displacement and velocity). The first LTR number of points of each signal are scraped to allow for the settling time. There is also an option to taper the data before obtaining the spectra. The data are processed to produce certain statistical information and then zero padded before the spectrum is obtained. The process is repeated until all signals are processed and an average value for the spectrum obtained.

The statistical data obtained are the same for displacement and velocity records. The list of the displacement statistics and the way in which they are obtained is as follows.

a) For each individual record

- 1) Mean displacement of frame j (j = 1,M)

$$\hat{x}_j = \left(\sum_{i=1}^{2K} x_i \right) \frac{1}{2K}$$

- 2) Mean square value

$$\hat{x}_j^2 = \left(\sum_{i=1}^{2K} x_i^2 \right) \frac{1}{2K}$$

3) Variance

$$\sigma_j^2 = \hat{x}^2 - (\hat{x})^2$$

4) Skewness

$$Ss_j = \left(\sum_{i=1}^{2K} (x_i - \hat{x})^3 \right) \frac{1}{2K (\sigma_j^2)^{3/2}}$$

5) Kurtosis

$$Ku_j = \left(\sum_{i=1}^{2K} (x_i - \hat{x})^4 \right) \frac{1}{2K (\sigma_j^2)^2}$$

b) Overall statistics were obtained as the average values of the above values.

e.g. for M number of records

$$\bar{x} = \left(\sum_{j=1}^M \hat{x}_j \right) \frac{1}{M}, \quad \bar{x}^2 = \left(\sum_{j=1}^M \hat{x}_j^2 \right) \frac{1}{M} \text{ etc.}$$

the variance of the overall statistics is also calculated e.g.

$$\sigma^2 \text{ of mean averages} = \left(\sum_{j=1}^M (\hat{x}_j)^2 \right) \frac{1}{M} - (\bar{x})^2$$

The power spectrum was obtained by taking the FFT of each zero padded (LTR number of zeroes to make 2K number of points again) signal which produced the sine and cosine components of the signal. These were squared and added together for each frequency (raw spectral density). The power spectrum components S_n at each frequency (ω_n) is the sum average of the above process overall M records and divided by 2. The area under the spectrum was obtained as the sum of these components

$$A = \sum_{n=1}^K S_n$$

Also the second and fourth moments were defined as

$$M_2 = \sum_{n=1}^K L_n^2 S_n, \quad M_4 = \sum_{n=1}^K L_n^4 S_n$$

where L is the lever (integer number) from the origin $\omega = 0$.
The following relations apply

$$\sigma^2 = A = \sum_{n=1}^K S_n$$

$$m_2 = (\Delta\omega)^2 M_2, \quad m_4 = (\Delta\omega)^4 M_4$$

It must also be noted that since the output is not Gaussian strictly speaking the error estimations of the spectrum based on the Chi square Pothesis do not apply. Hence such standard error estimations as $\epsilon = 1/\sqrt{B_f T}$ where B_f is the band width of analysis and T the record length, which is used to obtain an estimation of the random error involved in the spectral estimates, cannot be used confidently.

In this program there are also options for tapering the data subtracting the mean and ensemble averaging. However as discussed in Section (5.3) it was necessary to frequency average the response spectra. This was achieved through program FRAV listed here which uses a 21 point moving average technique taking into account the symmetry of the spectrum about the zero frequency. Figure (C.4-4) shows a flow diagram of program REC6ETUN.

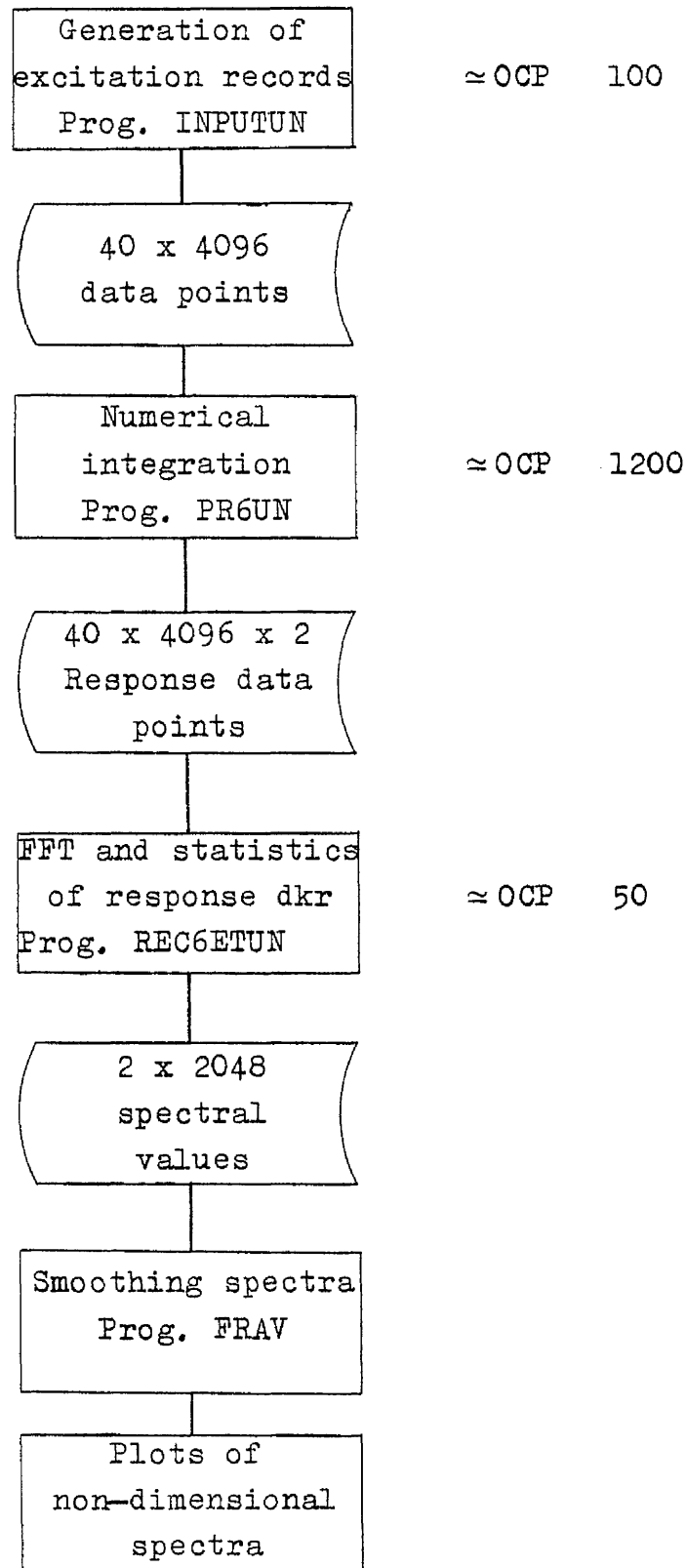


Figure C4-1

Flow Diagram of Complete Simulation

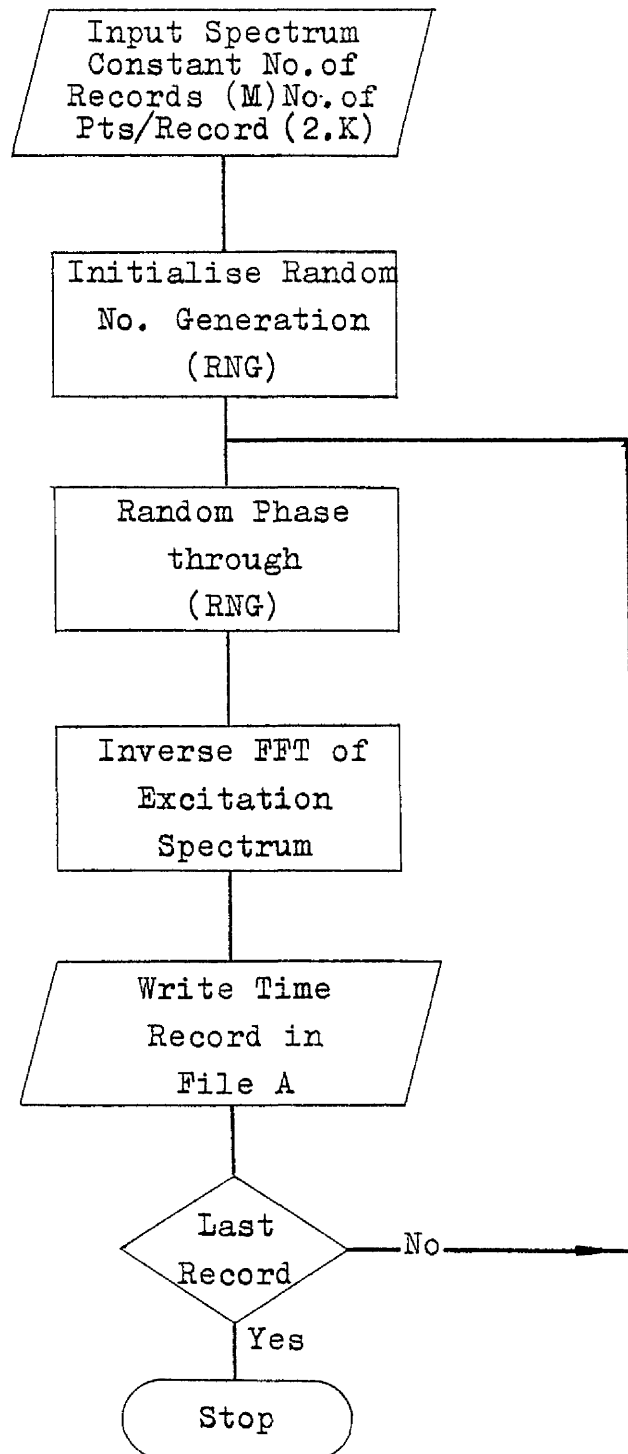


Figure C4-2

Flow Diagram of Program INPUTUN

```

      PROGRAM INPUTUN
C THIS PROGRAM PRODUCES REAL TIME DATA FROM A SQUARE SPECTRUM DEFINED BY
C AN UPPER & A LOWER FREQ. CUT OFF. MK IS THE UPPER CUT OFF FREQ. OF THE
C & MKO IS THE LOWER. NK2 IS THE MAX FREQ OF THE ANALYSIS.
      IMPLICIT REAL*7(A-H, O-Z)
      DIMENSION A(2050) ,B(2050) ,ILIST(24) ,FANG(2050)
      READ(5,*) MKO,MK,K,M1,NK1,LK
      NK2=K/2
      N1=NK2+1
      IF(LK.EQ.0) CALL G05CAF(0)
      IF(LK.EQ.0) WRITE(6,107)
C FOR THE CONTENTS OF A, B, ILIST, NK2, M1, N1
C READ NAG SUBROUTINE C06AAF
C NK1 IS THE NO OF SAMPLES GENERATED
C IF LK.EQ.0 DIFFERENT RUNS WILL PRODUCE THE SAME NOS.
      WRITE(8,108) MK,NK2
      DO 11 I1=1,NK1
      DO 5 I2=1,MKO
      A(I2)=0.0
      B(I2)=0.0
5      CONTINUE
      DO 1 I=MKO+1,MK
      FANG(I)=2*3.1415927*G05CAF(I)
C G05CAF PRODUCES RANDOM NOS UNIFORMLY
C DISTRIBUTED BETWEEN 0-1
      A(I)=COS(FANG(I))
      B(I)=SIN(FANG(I))
1      CONTINUE
      DO 2 I1=MK+1,M1
      A(I1)=0.0
      B(I1)=0.0
2      CONTINUE
      CALL C06AAF(A,B,M1,.TRUE.,M1,ILIST)
      IND=1
      JND=64
      DO 3 I3=1,32
      WRITE(8)(A(J),J=IND,JND)
      IND=IND+64
      JND=JND+64
3      CONTINUE
      INB=1
      JNB=64
      DO 4 I4=1,32
      WRITE(8)(B(J),J=INB,JNB)
      INB=INB+64
      JNB=JNB+64
4      CONTINUE
103  FORMAT(/3E15.3)
      WRITE(6,103) (A(I), I=1,8), (B(I), I=1,8)
11      CONTINUE
      WRITE(6,102) MK,NK2,NK1,K
102  FORMAT(///' PROGRAM INPUT RUN FOR'/
&20X,' CUTOFF=' ,I10,' MAX FR=' ,I10/
&10X,' PRODUCED' ,I4,' SAMPLES OF' ,I10,' PTS EACH')
108  FORMAT(1X,2I10)
107  FORMAT(///'***** COUNTER SET *****')
      STOP
      END

```

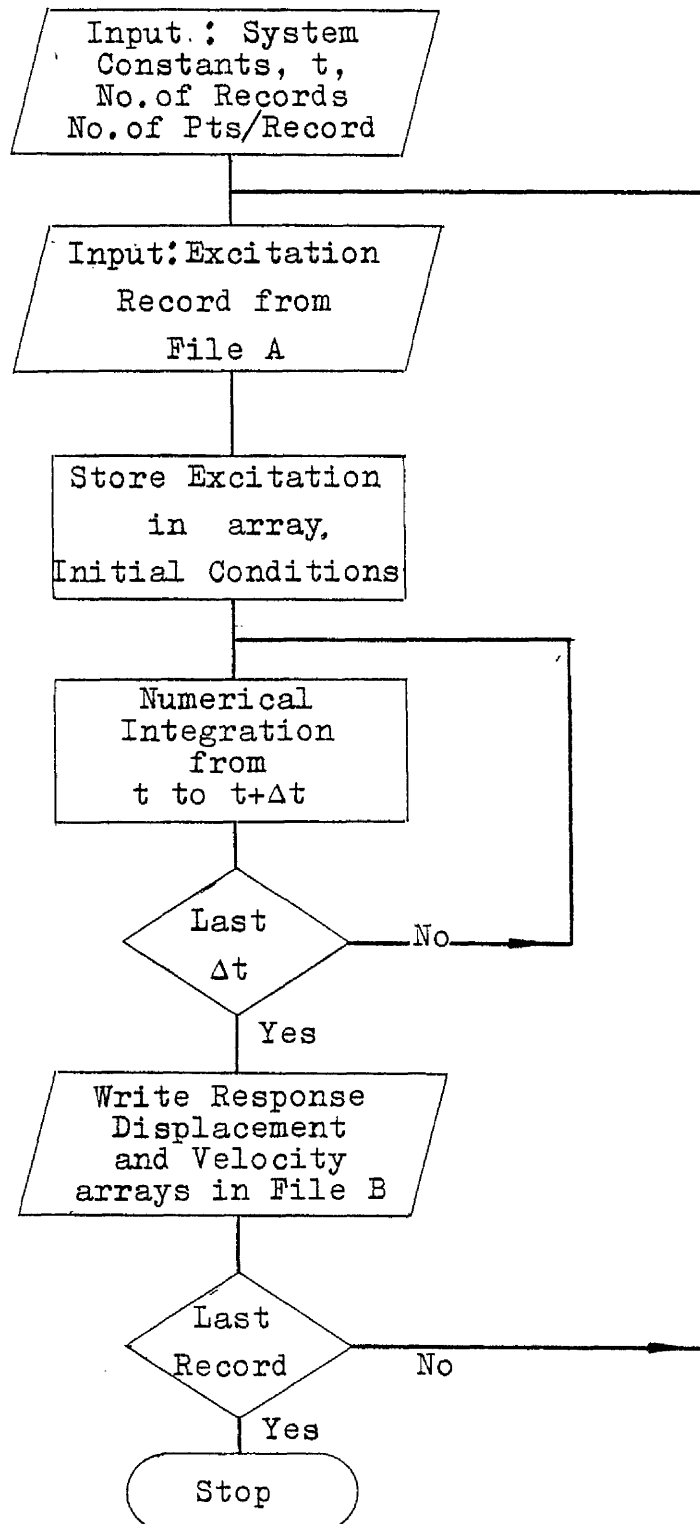


Figure C4-3

Flow Diagram of Program PR6UN

```

      PROGRAM PR6UN
C   THIS IS A NUM. INTEGRATION PROGRAM: ACCEPTS UNFORMATED DATA
C   AS INPUT TO THE SYSTEM OF D.EQ.'S, DEFINED BY F(1)&F(2) IN
C   SUBROUTINE FCN, AND STORES THE RESPONSES IN ARRAYS OUTV&OUTD
C   THE INPUT IS READ THROUGH CHANNEL 11 AND STORED IN ARRAY SNP
C   -----
C   NK1=NO OF INPUT RECORDS
C   K=NO. OF POINTS PER RECORD
C   A= AVERAGE VALUE TO BE ADDED TO INPUT VALUES
C   DAMP= DAMPING COEFF. "ZETA"
C   B= NONLINEARITY COEFF.
C   FRN= NATURAL FREQ.(RADS)/ PI
C   TINT= TIME INTERVAL BETWEEN INPUT NOS
C   D= MAGNIFICATION FACTOR FOR INPUT
C   KL1, KL3 TO BE USED BY PROG. REC6ETUN
C   SEE ALSO INPL.DOCUMENT FOR NAG SUBROUTINE D02BAF
C   -----
C
      IMPLICIT REAL*8(A-H,O-Z)
      DIMENSION Y(2), F(2), W(2,18), SNP(4100), OUTD(4100), OUTV(4100)
      &, ST(45)
      COMMON FRN, DAMP, B, GRAD, CONEW, A
      EXTERNAL FCN
      READ(5,*) NK1, K, A, DAMP, B, FRN, TOL, TINT, KL1, KL3, D
      CALL ICL9HEMASK(64, IJKL)
      PI=ATAN(1.0)*4.0
      FRN=PI*FRN
      NK2=K/2
      READ(11,108) MK, NK12
      K1=K+1
      WRITE(3,107) NK1, K, NK2, KL1, KL3
      WRITE(5,107) NK1, K, NK2, KL1, KL3
      WRITE(6,101) FRN, DAMP, B, K, TINT, TOL, A, D, MK, NK12
      N=2
      IFAIL=0
      DO 11 JJ=1, NK1
C   +++++
      IND=1
      JND=64
      DO 1 I=1, 64
      READ(11) ( SNP(JK), JK=IND, JND)
      IND=IND+64
      JND=JND+64
1      CONTINUE
C   +++++
      SNP(K+1)=0.0
      ST(JJ)=SNP(1)
      Y(1)=0.0
      Y(2)=0.0
      WRITE(6,106) (SNP(I), I=1, 3)
C   LINEAR INTERPOLATION BETWEEN INPUT DATA PTS.
C   -----
      DO 2 J=1, K
      X=(J-1)*TINT
      DIF=(SNP(J+1)-SNP(J))*D
      GRAD=DIF/TINT
      CONEW=(SNP(J))IND-GRAD*X
      XEND=J*TINT
      OUTD(J)=Y(1)
      OUTV(J)=Y(2)
      CALL D02BAF(X, XEND, N, Y, TOL, FCN, W, IFAIL)
      TOL=ABS(TOL)
      IF (TOL.LT.0.0) WRITE(6,104)
2      CONTINUE
C   +++++
      IN1=1
      IN2=64
      DO 3 ML=1, 64
      WRITE(3) (OUTD(JZ), JZ=IN1, IN2)
      IN1=IN1+64
3      CONTINUE

```

```

      IN2=IN2+64
3      CONTINUE
      IN3=1
      IN4=64
      DO 4 J3=1,64
      WRITE(2) (OUTV(JX),JX=IN3,IN4)
      IN3=IN3+64
      IN4=IN4+64
4      CONTINUE
C *****
11     CONTINUE
      WRITE(6,106)(ST(I),I=1,NK1)
101    FORMAT(/ ' NAT. FREQ=' ,F10.7, ' DAMP=' ,F10.7,2X, 'NL TERM=' ,F10.7/
      & ' NO. OF DATA PTS=' ,I5,2X, 'TIME INT=' ,F10.7,2X/
      & ' TOLERANCE=' ,F10.7,5X, 'MEAN INPUT=' ,F10.6,5X, 'FACTOR=' ,F10.6,
      & /5X, 'CUT OFF=' ,I10, 'MAX FR=' ,I10)
104    FORMAT(/ ' RANGE TOO SHORT FOR TOL')
106    FORMAT(/3E15.8)
107    FORMAT(5I4)
108    FORMAT(1X,2I10)
      STOP
      END

```

```

SUBROUTINE FCN(T,Y,F)
IMPLICIT REAL*8(A-H,O-Z)
DIMENSION F(2),Y(2)
COMMON FRN,DAMP,B,GRAD,CONEW,A
FORS=GRAD*T+CONEW
F(1)=Y(2)
F(2)=FORS-Y(2)+2*DAMP*FRN-FRN*FRN*(1+B*Y(1)+Y(1))*Y(1)
RETURN
END

```

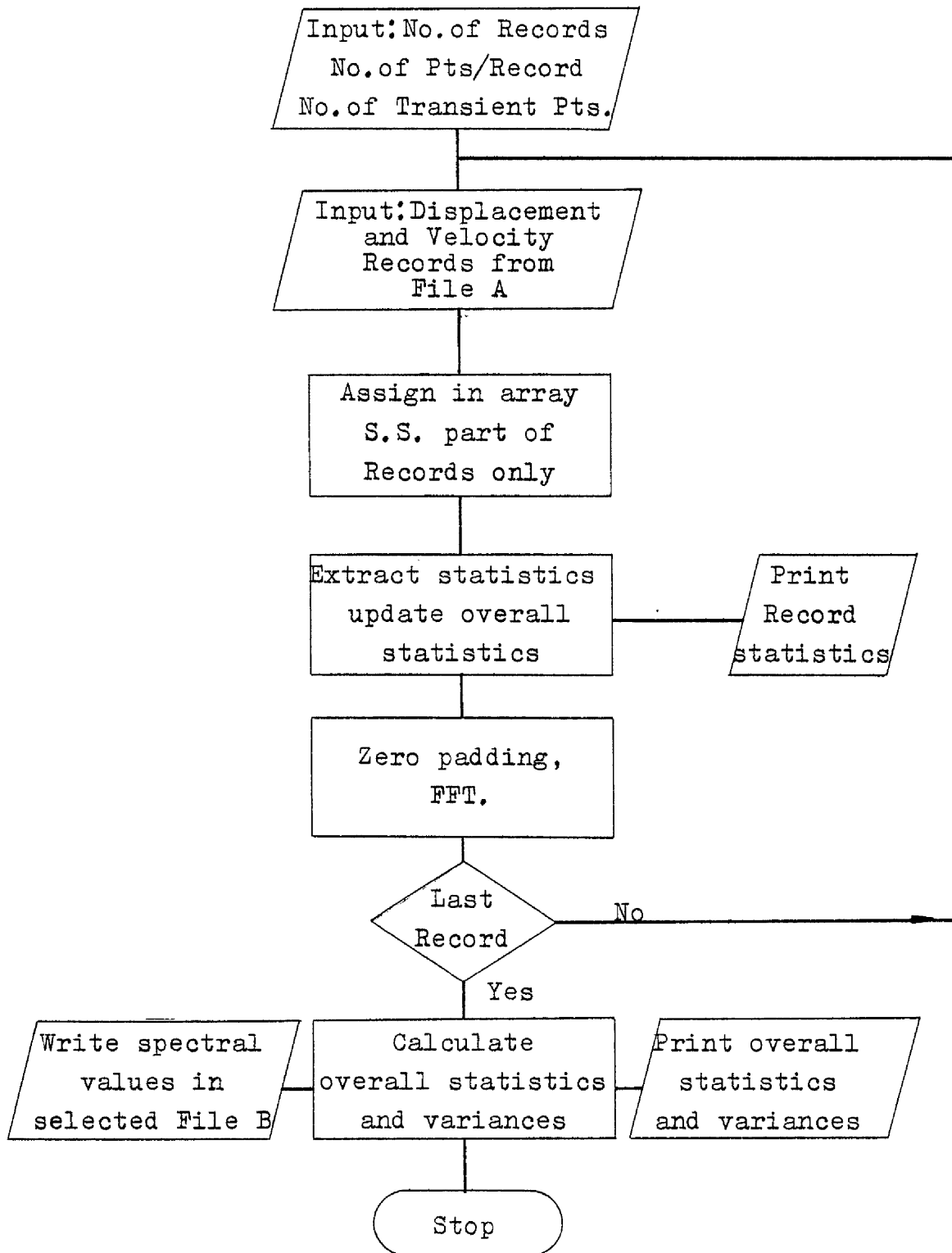


Figure C.4-4

Flow Diagram for Program REC6ETUN

```

      PROGRAM RESETUN
      IMPLICIT REAL*8(A-H,O-Z)
      DIMENSION OUTD(4100),SS2(2050),SS3(2050),ILIST(24),
      &OUTV(4100),OUTD1(2050),OUTD2(2050),OUTV1(2050),OUTV2(2050)
      &,TSS2(2050),TSS3(2050),EMEAND(4100),EMEANV(4100),TCOEF(500)
C*****
C THIS PROGRAM ACCEPTS NK1 SAMPLES , SUBTRACTS EACH TRANSIENT,
C CALCULATES STATISTICS AND OPTIONALLY TAPERS EACH TO PRODUCE
C STATISTICS ARE CALCULATED ALONG EACH RECORD AND ALSO AS
C ENSEMBLE AVERAGES DOWN THE RECORDS, VARIANCE VALUES ARE
C CALCULATED FOR MOST STATISTICAL ESTIMATIONS
C THE POWER SPECTRUM OF THE PROCESSES OUTD&OUTV..
C*****
C NK1 = NO. OF SAMPLES
C K = NO. OF POINTS IN EACH SAMPLE
C NK2 = 1/2 X K
C TAP = 1 = YES : TAP = 0 = NO
C LTR = NO. OF POINTS BEFORE SETTLING
C FOR THE CONTENTS OF ILIST,MI,ETC.,LOOK ALSO IMPL.DOCUMENT
C FOR NAG SUBROUTINE CO2AAF
C*****
      READ(11,109)NK1,K,NK2,KL1,KL3
      WRITE(6,109)NK1,K,NK2,KL1,KL3
      READ(5,*) TAP,LTR
C----- IF KL1=1 THE MEAN IS SUBTRACTED FROM THE PROCESSES
C----- IF KL3=1 OUTV IS IGNORED
      M1=24
      N1=NK2+1
      K2=K-LTR
      DO 9 IO=1,NK2
      EMEAND(IO)=0.0
      EMEAND(IO+NK2)=0.0
      EMEANV(IO)=0.0
      EMEANV(IO+NK2)=0.0
      SS2(IO)=0.0
      SS3(IO)=0.0
9      CONTINUE
C
C COSINE TAPER OVER 1/10 OF RECORD AT BOTH ENDS
C
      IF(TAP.EQ.0.0) GO TO 33
      TAPER=0.0038312
      NTAP=K/10
      DO 2 IT=1,NTAP
      KT=IT-1
      TCOS=SIN(KT*TAPER)
      TCOEF(IT)=TCOS*TCOS
2      CONTINUE
C
C
33  OVA2=0.0
      OVA3=0.0
      OVR2=0.0
      OVR3=0.0
      OVS2=0.0
      OVS3=0.0
      OVC2=0.0
      OVC3=0.0
      OVSQ2=0.0
      OVSQ3=0.0
      SOVA2=0.0
      SOVA3=0.0
      SOVR2=0.0
      SOVR3=0.0
      SOVC2=0.0
      SOVC3=0.0
      SOVS2=0.0
      SOVS3=0.0
      SOVSQ2=0.0
      SOVSQ3=0.0

```

```

TMEAND=0.0
TMEANV=0.0
EMIND=0.0
EMAXD=0.0
EMINV=0.0
EMAXV=0.0
DO 111 JJ=1,NK1
C+++++
IN2=64
IN1=1
DO 44 JN1=1,64
READ(11)(OUTD(IN),IN=IN1,IN2)
IN1=IN1+64
IN2=IN2+64
44 CONTINUE
IF(KL3.EQ.1) GO TO 56
IN3=1
IN4=64
DO 55 JN2=1,64
READ(11)(OUTV(IN),IN=IN3,IN4)
IN3=IN3+64
IN4=IN4+64
55 CONTINUE
C+++++
56 AV2=0.0
AV3=0.0
VAR2=0.0
VAR3=0.0
C
DO 13 I8=LTR,K
EMEAND(I8)=EMEAND(I8)+OUTD(I8)
IF(KL3.EQ.1) GO TO 13
EMEANV(I8)=EMEANV(I8)+OUTV(I8)
13 CONTINUE
C
DO 1 I=LTR,K
AV2=AV2+OUTD(I)
VAR2=VAR2+OUTD(I)*OUTD(I)
IF(KL3.EQ.1) GO TO 1
AV3=AV3+OUTV(I)
VAR3=VAR3+OUTV(I)*OUTV(I)
1 CONTINUE
AV2=AV2/K2
AV3=AV3/K2
SQM2=VAR2/K2
SQM3=VAR3/K2
VAR2=SQM2-AV2*AV2
VAR3=SQM3-AV3*AV3
SK2=0.0
SK3=0.0
CUR2=0.0
CUR3=0.0
XM2=0.0
XM3=0.0
XMI2=0.0
XMI3=0.0
DO 3 I2=LTR,K
OUTD(I2)=OUTD(I2)-AV2
SK2=SK2+OUTD(I2)*OUTD(I2)*OUTD(I2)
CUR2=CUR2+OUTD(I2)*OUTD(I2)*OUTD(I2)*OUTD(I2)
IF(OUTD(I2).GT.XM2) XM2=OUTD(I2)
IF(OUTD(I2).LT.XMI2) XMI2=OUTD(I2)
IF(KL3.EQ.1) GO TO 3
OUTV(I2)=OUTV(I2)-AV3
SK3=SK3+OUTV(I2)*OUTV(I2)*OUTV(I2)
CUR3=OUTV(I2)*OUTV(I2)*OUTV(I2)*OUTV(I2)+CUR3
IF(OUTV(I2).GT.XM3) XM3=OUTV(I2)
IF(OUTV(I2).LT.XMI3) XMI3=OUTV(I2)
3 CONTINUE
IF(KL1.EQ.1) GO TO 17

```



```

      DO 8 I1=LTR,K
      OUTD(I1)=OUTD(I1)+AV2
      IF(KL3.EQ.1) GO TO 8
      OUTV(I1)=OUTV(I1)+AV3
8      CONTINUE
C
17  IF(TAP.EQ.0.0) GO TO 4
C
      DO 22 ITT=1,NTAP
      ITV=K-ITT+1
      OUTD(ITT+LTR)=OUTD(ITT+LTR)*TCOEFF(ITT)
      OUTD(ITV)=OUTD(ITV)*TCOEFF(ITT)
      OUTV(ITT+LTR)=OUTV(ITT+LTR)*TCOEFF(ITT)
      OUTV2(ITV)=OUTV2(ITV)*TCOEFF(ITT)
22  CONTINUE
C
C  ZERO PEDDING TO ACCOUNT FOR LTR
C*****
4    DO 15 IM=1,NK2
      OUTD1(IM)=OUTD(IM+LTR)
      IF(KL3.EQ.1) GO TO 15
      OUTV1(IM)=OUTV(IM+LTR)
15  CONTINUE
      DO 16 IN=1,NK2-LTR
      OUTD2(IN)=OUTD(IN+NK2+LTR)
      IF(KL3.EQ.1) GO TO 16
      OUTV2(IN)=OUTV(IN+NK2+LTR)
16  CONTINUE
      DO 18 INK=NK2-LTR,NK2
      OUTD2(INK)=0.0
      IF(KL3.EQ.1) GO TO 18
      OUTV2(INK)=0.0
18  CONTINUE
C*****
C
      SK2=SK2/(K2*VAR2**(.3./2.))
      CUR2=CUR2/(K2*VAR2*VAR2)
      IF(KL3.EQ.1) GO TO 11
      CUR3=CUR3/(K2*VAR3*VAR3)
      SK3=SK3/(K2*VAR3**(.3./2.))
11  WRITE(6,104) JJ
      WRITE(6,102) AV2,VAR2,SK2,CUR2,XM2,XMI2,SQM2
      IF(KL3.EQ.1) GO TO 5
      WRITE(6,105) JJ
      WRITE(6,102) AV3,VAR3,SK3,CUR3,XM3,XMI3,SQM3
5    CALL C06AAF(OUTD1,OUTD2,N1,-FALSE-,M1,ILIST)
      IF(KL3.EQ.1) GO TO 6
      CALL C06AAF(OUTV1,OUTV2,N1,-FALSE-,M1,ILIST)
6    DO 7 I3=1,NK2
      SS2(I3)=SS2(I3)+OUTD1(I3)*OUTD1(I3)+OUTD2(I3)*OUTD2(I3)
      IF(KL3.EQ.1) GO TO 7
      SS3(I3)=SS3(I3)+OUTV1(I3)*OUTV1(I3)+OUTV2(I3)*OUTV2(I3)
7    CONTINUE
      OVA2=OVA2+AV2
      OVR2=OVR2+VAR2
      OVS2=OVS2+SK2
      OVSQ2=OVSQ2+SQM2
      OVC2=OVC2+CUR2
      SOVA2=SOVA2+AV2*AV2
      SOVR2=SOVR2+VAR2*VAR2
      SOVS2=SOVS2+SK2*SK2
      SOVC2=SOVC2+CUR2*CUR2
      SOVSQ2=SOVSQ2+SQM2*SQM2
      IF(KL3.EQ.1) GO TO 111
      OVA3=OVA3+AV3
      OVR3=OVR3+VAR3
      OVS3=OVS3+SK3
      OVC3=OVC3+CUR3
      OVSQ3=OVSQ3+SQM3
      SOVA3=SOVA3+AV3*AV3

```

```

- SOVR3=SOVR3+VAR3*VAR3
SOVS3=SOVS3+SK3*SK3
SOVC3=SOVC3+CUR3*CUR3
SOVSQ3=SOVSQ3+SQM3*SQM3
111 CONTINUE
C
C
EVARV=0.0
EVARD=0.0
DO 14 I9=LTR,K
EMEAND(I9)=EMEAND(I9)/NK1
EMEANV(I9)=EMEANV(I9)/NK1
TMEAND=TMEAND+EMEAND(I9)
TMEANV=TMEANV+EMEANV(I9)
IF(EMEAND(I9).LT.EMIND) EMIND=EMEAND(I9)
IF(EMEAND(I9).GT.EMAXD) EMAXD=EMEAND(I9)
IF(EMEANV(I9).LT.EMINV) EMINV=EMEANV(I9)
IF(EMEANV(I9).GT.EMAXV) EMAXV=EMEANV(I9)
EVARV=EVARV+EMEANV(I9)*EMEANV(I9)
EVARD=EVARD+EMEAND(I9)*EMEAND(I9)
14 CONTINUE
TMEANV=TMEANV/K2
TMEAND=TMEAND/K2
EVARV=(EVARV/K2)-TMEANV*TMEANV
EVARD=(EVARD/K2)-TMEAND*TMEAND
SPM2=0.0
SPM3=0.0
SPMI2=1.0
SPMI3=1.0
SUMS2=0.0
SUMS3=0.0
SUMS22=0.0
SUMS32=0.0
SUMS24=0.0
SUMS34=0.0
KK=NK1*2.0
C
C CALCULATION OF MOMENTS ,MAX ,MIN ,OF SPECTRA
C*****
DO 10 I4=1,NK2
F6=I4
F2=I4*I4
F4=F2*F2
TSS2(I4)=SS2(I4)/KK
SUMS2=SUMS2+TSS2(I4)
SUMS22=SUMS22+F2*TSS2(I4)
SUMS24=SUMS24+F4*TSS2(I4)
IF(I4.EQ.1) GO TO 20
IF(TSS2(I4).GT.SPM2) PT2=F6
IF(TSS2(I4).GT.SPM2) SPM2=TSS2(I4)
IF(TSS2(I4).LT.SPMI2) PTI2=F6
IF(TSS2(I4).LT.SPMI2) SPMI2=TSS2(I4)
20 IF(KL3.EQ.1) GO TO 10
TSS3(I4)=SS3(I4)/KK
SUMS3=SUMS3+TSS3(I4)
SUMS32=SUMS32+F2*TSS3(I4)
SUMS34=SUMS34+F4*TSS3(I4)
IF(I4.EQ.1) GO TO 10
IF(TSS3(I4).GT.SPM3) PT3=F6
IF(TSS3(I4).GT.SPM3) SPM3=TSS3(I4)
IF(TSS3(I4).LT.SPMI3) PTI3=F6
IF(TSS3(I4).LT.SPMI3) SPMI3=TSS3(I4)
10 CONTINUE
C*****
WRITE(8,103) (TSS2(I),I=1,NK2)
IF(KL3.LT.1) WRITE(8,103) (TSS3(I),I=1,NK2)
IF(KL3.GT.1) WRITE(8,103) (TSS3(I),I=1,NK2)
OVA2=OVA2/NK1
OVR2=OVR2/NK1
OVS2=OVS2/NK1

```

```

OVC2=OVC2/NK1
OVSQ2=OVSQ2/NK1
SOVA2=SOVA2/NK1-OVA2*OVA2
SOVR2=SOVR2/NK1-OVR2*OVR2
SOVS2=SOVS2/NK1-OVS2*OVS2
SOVC2=SOVC2/NK1-OVC2*OVC2
SOVSQ2=SOVSQ2/NK1-OVSQ2*OVSQ2
IF(KL3.EQ.1) GO TO 1101
OVA3=OVA3/NK1
OVR3=OVR3/NK1
OVS3=OVS3/NK1
OVC3=OVC3/NK1
OVSQ3=OVSQ3/NK1
SOVA3=SOVA3/NK1-OVA3*OVA3
SOVR3=SOVR3/NK1-OVR3*OVR3
SOVS3=SOVS3/NK1-OVS3*OVS3
SOVC3=SOVC3/NK1-OVC3*OVC3
SOVSQ3=SOVSQ3/NK1-OVSQ3*OVSQ3
1101 WRITE(6,1102)
WRITE(6,1103) OVA2,OVR2,OVS2,OVC2,OVSQ2,TMEAND,EMAXD,EMIND,EVARD
WRITE(6,1115) SUMS2,SUMS22,SUMS24
IF(KL3.EQ.1) GO TO 1105
WRITE(6,1104) OVA3,OVR3,OVS3,OVC3,OVSQ3,TMEANV,EMAXV,EMINV,EVARV
WRITE(6,1115) SUMS3,SUMS32,SUMS34
1105 WRITE(6,1112)
WRITE(6,1113) SOVA2,SOVR2,SOVS2,SOVC2,SOVSQ2
IF(KL3.EQ.1) GO TO 1106
WRITE(6,1114) SOVA3,SOVR3,SOVS3,SOVC3,SOVSQ3
1106 WRITE(6,107) SPM2,PT2,SPMI2,PTI2
IF(KL3.EQ.1) GO TO 12
WRITE(6,108) SPM3,PT3,SPMI3,PTI3
102 FORMAT(/'::::AVERAGE=' ,F11.7,5X,'::::VARIANCE=' ,F11.7,
&/' ::SKEWNESS=' ,F11.6,5X,' ::KURTOSIS=' ,F11.6,/' ' MAX VALUE=
& ,F11.6,5X,' MIN VALUE=' ,F11.6,11X,' EE MEAN SQ. VALUE=' ,F11.4)
103 FORMAT(/8E15.8)
104 FORMAT(/'::::::::::OUTPUT SS DISPL:::::' ,I4)
105 FORMAT(/'::::::::::OUTPUT SS VEL:::::' ,I4)
107 FORMAT(///' ---- AVERAGE DISP SP OUT ----'/' MAX=' ,E15.8,' AT = '
& ,F6.2,5X,' MIN = ' ,E15.8,' AT = ' ,F6.2)
108 FORMAT(///' ---- AVERAGE VEL SP OUT ----'/' MAX= ' ,E15.8,' AT = '
& ,F6.2,5X,' MIN = ' ,E15.8,' AT = ' ,F6.2)
1102 FORMAT(///' ***** OVERALL STATISTICS *****'//
&)
1112 FORMAT(///' ***** CORRESPONDING VARIANCES *****'//
&)
1103 FORMAT(///' ---- OUTPUT DISPLACEMENT ----'/'5X,'MEAN= ' ,F10.6,5X,
&'VARIANCE= ' ,F10.6,5X,'SKEWNESS= ' ,F10.6,5X,'KURTOSIS= ' ,F10.6,
&5X,'MEAN SQ= ' ,F10.6,/' ' ENSEMBLE MEAN' ,F10.6,5X,'MAX=' ,F10.6,
&5X,'MIN= ' ,F10.6,5X,'VARIANCE OF MEAN= ' ,F10.6)
1113 FORMAT(///' ---- OUTPUT DISPLACEMENT ----'/'5X,'MEAN= ' ,F10.6,5X,
&'VARIANCE= ' ,F10.6,5X,'SKEWNESS= ' ,F10.6,5X,'KURTOSIS= ' ,F10.6,
&5X,' MEAN SQ. = ' ,F10.6)
1104 FORMAT(///' ---- OUTPUT VELOCITY ----'/'5X,'MEAN= ' ,F10.6,5X,
&'VARIANCE= ' ,F10.6,5X,'SKEWNESS= ' ,F10.6,5X,'KURTOSIS= ' ,F10.6,
&5X,' MEAN SQ=' ,F10.6,/' ' ENSEMBLE MEAN=' ,F10.6,5X,' MAX=' ,F10.6,
&5X,' MIN= ' ,F10.6,5X,' VARIANCE OF MEAN=' ,F10.6)
1114 FORMAT(///' ---- OUTPUT VELOCITY ----'/'5X,'MEAN= ' ,F10.6,5X,
&' VARIANCE= ' ,F10.6,5X,'SKEWNESS= ' ,F10.6,5X,'KURTOSIS= ' ,F10.6,
&5X,' MEAN SQ. = ' ,F10.6)
1115 FORMAT(///' AREA UNDER SPEC(A)=' ,F20.10,4X,'A**2=' ,F20.10,4X,
&'A**4=' ,F20.10)
109 FORMAT(SI4)
12 STOP
END

```

```

      PROGRAM FRAV
C   THIS PROGRAM SMOOTHS THE SHAPE OF THE DATA IN D & V ARRAYS
C   USING MOVING AVERAGE OF 21 POINTS. ASSUMES SYMMETRY ABOUT THE
C   ORIGIN. ALSO LOCATES THE POSITION AND VALUE OF MAX AND MAX/100
C   OF THE SMOOTHED SHAPE
      DIMENSION D(2080),V(2080),D1(2080),V1(2080)
      &,D2(2080),V2(2080)
      N=2043
      N2=N-1
      N3=N+9
C
      READ(11,100) (D(I),I=1,N),(V(I),I=1,N)
      D1(10)=D(1)
      V1(10)=V(1)
      DO 11 I=2,11
        I2=I-1
        D2(I2)=D(I2-I)
        V2(I2)=V(I2-I)
11     CONTINUE
      DO 12 I1=2,N
        D2(I1+9)=D(I1)
        V2(I1+9)=V(I1)
12     CONTINUE
      DO 1 J=11,N2
        D1(J)=(D2(J-1)+D2(J+1)+D2(J)+D2(J-2)+D2(J+2)+
&+D2(J-3)+D2(J+3)+D2(J-4)+D2(J+4)+D2(J+5)+D2(J-5)+D2(J+6)+
&D2(J-6)+D2(J+7)+D2(J-7)+D2(J+8)+D2(J-8)+D2(J+9)+D2(J-9)+D2(J+10)+
&D2(J-10))/21
        V1(J)=(V2(J-1)+V2(J+1)+V2(J)+V2(J-2)+V2(J+2)+V2(J+4)+V2(J-4)+
&+V2(J+3)+V2(J-3)+V2(J+5)+V2(J-5)+V2(J+6)+V2(J-6)+V2(J+7)+
&V2(J-7)+V2(J+8)+V2(J-8)+V2(J+9)+V2(J-9)+V2(J+10)+V2(J-10))/21
1     CONTINUE
      DO 2 J1=N,N3
        D1(J1)=0
        V1(J1)=0
2     CONTINUE
      WRITE(7,100) (D1(I),I=10,N3),(V1(I),I=10,N3)
CC
CC
      DMAX=0.0
      VMAX=0.0
      SD=0.0
      SV=0.0
      DO 13 M=10,N3
        SD=SD+D1(M)
        SV=SV+V1(M)
        IF(D1(M).GT.DMAX) GO TO 14
15      IF(V1(M).GT.VMAX) GO TO 16
        GO TO 13
14      DMAX=D1(M)
        FRD=M
        GO TO 15
16      VMAX=V1(M)
        FRV=M
13      CONTINUE
      WRITE(6,99)SD,SV,DMAX,FRD,VMAX,FRV
99      FORMAT(' D AREA=',F15.5/' V AREA=',F15.5/' MAXD=',F15.5,3X,
&'AT=',F18.5/' MAXV=',F15.5,'AT=',F18.5)
      RATD=DMAX/100
      RATV=VMAX/100
      K=FRV
      DO 17 I4=K,N3
        K2=I4
        IF(D1(I4).LT.RATD) GO TO 18
17      CONTINUE
18      WRITE(6,98) D1(K2),K2
98      FORMAT('// ' LIMD=',F15.5,4X,'AT=',I5)
      DO 19 I3=K,N3
        K3=I3
        IF(V1(I3).LT.RATV) GO TO 20
19      CONTINUE
20      WRITE(6,98) V1(K3),K3
100     FORMAT(/8E15.8)
        STOP
        END

```